School of Pharmacy and Biomedical Sciences

Curtin Health Innovation Research Institute

Evaluation of Chitosan-Based Nanoparticles in Oral Delivery of Insulin

Chun Yuen Jerry Wong

This thesis is presented for the Degree of

Doctor of Philosophy

Of

Curtin University

September 2020

Declaration

To the best of my knowledge and belief this thesis contains no material previously published by any other person except where due acknowledgment has been made.

This thesis contains no material which has been accepted for the award of any other degree or diploma in any university.

Signature:

Date: 11th September 2020

Acknowledgement

Firstly, I would like to express my deep gratitude to my parents for their moral and financial support throughout my PhD. The PhD journey would not have been possible without their understanding.

I would like to express my sincerest appreciation to my principal supervisor Professor Crispin Dass and co-supervisor Dr. Hani Al-Salami for their ongoing support and guidance throughout my studies. They have provided invaluable advice and insights in my research project. They have been my role models to learn from and enabling me to strive for the best.

I would also like to express my gratitude to my thesis chair Professor Lynne Emmerton for her timely response when I was seeking information for the enrolment and completion of PhD program.

I wish to thank the administrative staff and laboratory technicians at the School of Pharmacy and Biomedical Sciences, Curtin Health Innovation Research Institute, as well as Curtin's Microscopy and Microanalysis Facility for their continual training, technical assistance and professional expertise.

Last but not least, I would like to acknowledge the Australian Government Research Training Program Scholarship and Curtin University Completion Scholarship for the support in the PhD study.

Abstract

Diabetes mellitus is a chronic health condition that is characterised by hyperglycaemia, reduced β cell functioning, systemic inflammation and imbalance in oxidative status. To improve patient compliance and alleviate the unwanted side effects that are associated with insulin injections, the aim of the project was to examine the potential of nanoparticles in oral delivery of insulin. Nanoparticles are capable of protecting the entrapped therapeutic proteins against gastrointestinal (GI) enzymes, facilitate the permeation of drugs across mucus layer, and improve the GI absorption of insulin. In the research design stage, comprehensive reviews on the experimental conditions and available technologies for physicochemical, cellular and *in vivo* characterisation of orally administered insulin-loaded nanoparticles were conducted. In the current project, the nanoparticles were prepared by natural polymer and biocompatible oligonucleotide *via* polyelectrolyte complexation. The following formulation properties, including polymer constitution, particle size, polydispersity index, surface charge, encapsulation efficiency and stability, were characterised. The insulin-loaded nanoparticles were optimised by using biocompatible excipients and cryoprotectants. These excipients protected the nanoparticles against external mechanical strength during lyophilisation, and maintained the bioactivity of the entrapped insulin. The fabricated nanoparticles were able to preserve the physicochemical properties upon storage, and induced glucose uptake in skeletal muscle cells.

Schematic diagram for the plan and structure of thesis

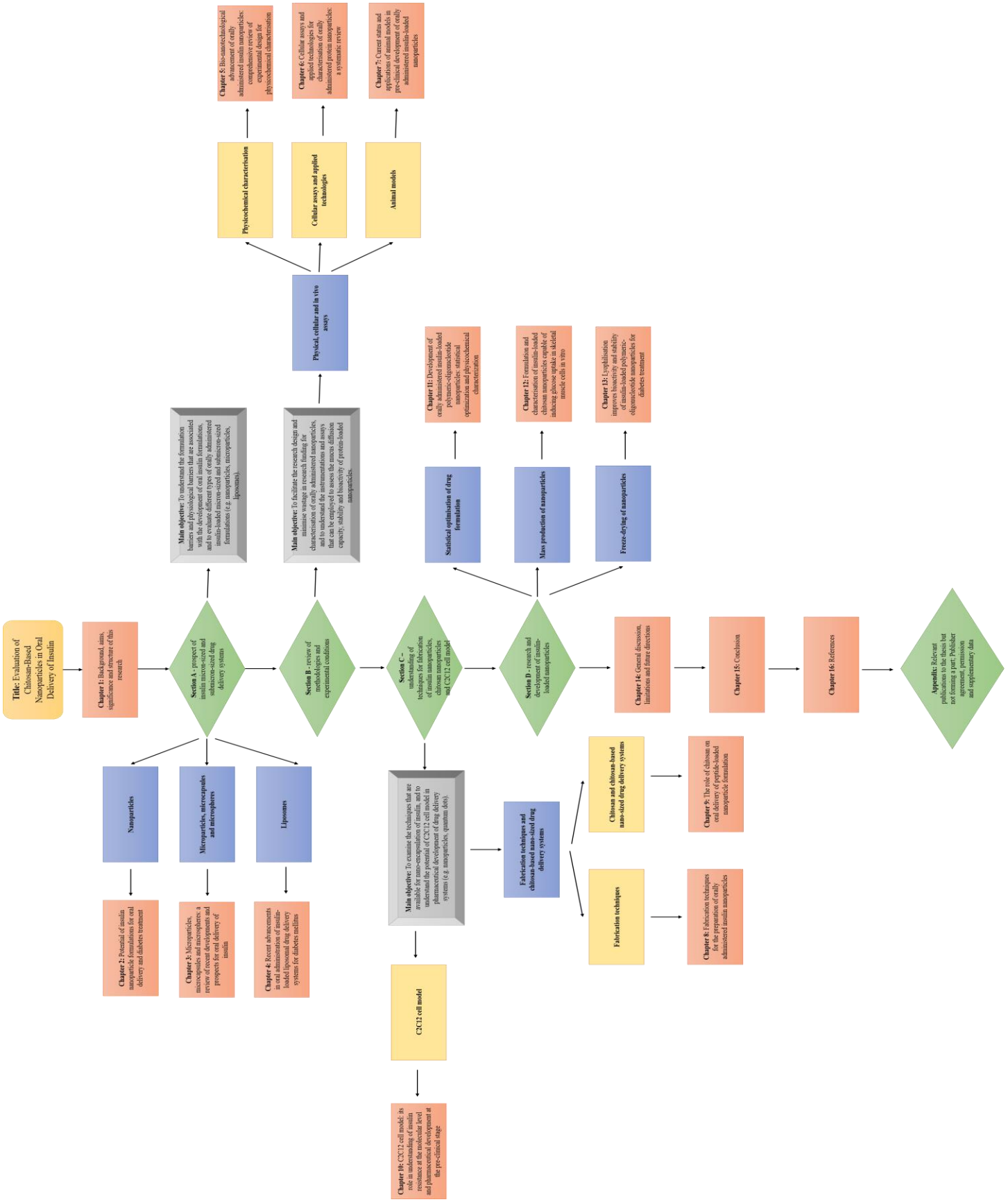

List of publications by the candidate included in the thesis

1. **Wong CY**, Al-Salami H, Dass CR (2017). Potential of insulin nanoparticle formulations for oral delivery and diabetes treatment. Journal of Controlled Release 264: 247-275.
2. **Wong CY**, Al-Salami H, Dass CR (2018). Microparticles, microcapsules and microspheres: a review of recent developments and prospects for oral delivery of insulin. International Journal of Pharmaceutics 537 (1-2): 223-244.
3. **Wong CY**, Al-Salami H, Dass CR (2018). Recent advancements in oral administration of insulin-loaded liposomal drug delivery systems for diabetes mellitus. International Journal of Pharmaceutics 549 (1-2): 201-217.
4. **Wong CY**, Al-Salami H, Dass CR (2018). The role of chitosan on oral delivery of peptide-loaded nanoparticle formulation. Journal of Drug Targeting 26 (7): 551-562.
5. **Wong CY**, Luna G, Martinez J, Al-Salami H, Dass CR (2019). Bio-nanotechnological advancement of orally administered insulin nanoparticles: Comprehensive review of experimental design for physicochemical characterization. International Journal of Pharmaceutics 572: 118720.
6. **Wong CY**, Al-Salami H, Dass CR (2020). Cellular assays and applied technologies for characterization of orally administered protein nanoparticles: A systematic review. Journal of Drug Targeting 28 (6): 585-599.
7. **Wong CY**, Al-Salami H, Dass CR (2020). Lyophilization improves bioactivity and stability of insulin-loaded polymeric-oligonucleotide nanoparticles for diabetes treatment. AAPS PharmSciTech 21 (3): 1-20.
8. **Wong CY**, Al-Salami H, Dass CR (2020). Formulation and characterisation of insulin-loaded chitosan nanoparticles capable of inducing glucose uptake in

skeletal muscle cells *in vitro*. Journal of Drug Delivery Science and Technology 57: 101738.

9. **Wong CY**, Al-Salami H, Dass CR (2020). Current status and applications of animal models in pre-clinical development of orally administered insulin-loaded nanoparticles. Journal of Drug Targeting 1-22.
10. **Wong CY**, Martinez J, Zhao J, Al-Salami H, Dass CR (2020). Development of orally administered insulin-loaded polymeric-oligonucleotide nanoparticles: statistical optimization and physicochemical characterization. Drug Development and Industrial Pharmacy 46 (8): 1238-1252.
11. **Wong CY**, Al-Salami H, Dass CR (2020). C2C12 cell model: its role in understanding of insulin resistance at the molecular level and pharmaceutical development at the pre-clinical stage. Journal of Pharmacy and Pharmacology Accepted on 25/07/2020.
12. **Wong CY**, Al-Salami H, Dass CR (2020). Fabrication techniques for the preparation of orally administered insulin nanoparticles. Journal of Drug Targeting Accepted on 26/08/2020.

Relevant publications to the thesis but not forming a part of it

1. **Wong CY**, Martinez J, Al-Salami H, Dass CR (2018). Quantification of BSA-loaded chitosan/oligonucleotide nanoparticles using reverse-phase high-performance liquid chromatography. Analytical and Bioanalytical Chemistry 410 (27): 6991-7006.

List of conferences

1. **Wong CY**, Al-Salami H, Dass CR (2018). Potential of nanoparticles and microparticles in drug encapsulation and disease management. Presented at 'The Mark Liveris Health Science Research Student Seminar', Perth/Australia. (Oral)

2. **Wong CY**, Al-Salami H, Dass CR (2019). Lyophilisation of polymeric-oligonucleotide nanoparticles for oral delivery of insulin. Presented at 'Drug Delivery Australia 2019 Conference', Brisbane/Australia. (Oral)

Statement of permission regarding copyright

I warrant that I have obtained, where necessary, permission from the copyright owners to use any third-party copyright material reproduced in the thesis (e.g. questionnaires, artwork, unpublished letters), or to use any of my own published work (e.g. journal articles) in which the copyright is held by another party (e.g. publisher, co-author).

Table of contents

Abbreviation

β-CD	Beta-cyclodextrin
γ-PGA	Poly(γ-glutamic acid)
AMPK	AMP-activated protein kinase
ATCC	American Type Culture Collection
ATR	Attenuated total reflection
BBB	Blood brain barrier
BBI	Bowman-Birk-Inhibitor
BSA	Bovine serum albumin
BSL	Blood sugar level
CD	Circular dichroism
CLDN4	Claudin-4
CLSM	Confocal laser scanning microscopy
CMCS	Carboxymethyl chitosan
Con A	Concanavalin A
CPP	Cell-penetrating peptide
CSK	CSKSSDYQC
CTB	Cell-Titre Blue
DEMC	N-diethyl methyl chitosan
DGAT1	Diacylglycerol O-acyltransferase 1
DMEC	Dimethyl-ethyl chitosan
DMEM	Dulbecco's modified Eagle medium
DMPA	Dimethoxy propyl acetophenone
DMSO	Dimethyl sulfoxide
DPP4	Dipeptidyl peptidase-4
DTPA	Diethylenetriamine pentaacetic acid
EDMA	Ethylene glycol dimethacrylate
EGDMA	Ethylene glycol dimethylacrylate
EGTA	Ethylene glycol tetraacetic acid
ELISA	Enzyme-linked immunosorbent assay
FBS	Fetal bovine serum
FcRn	Fc receptor
FoxO1	Forkhead box O1
FRET	Fluorescence resonance energy transfer
FTBA	2-formyl-3-thienylboronic acid

FTIR	Fourier transform infrared
FTS	S-farnesylthiosalicylic acid
FPBA	4-formylphenylboronic acid
G-CSF	Granulocyte colony stimulating factor
GI	Gastrointestinal
GLUT4	Glucose transporter type 4
GLP-1	Glucagon like peptide-1
HBSS	Hanks buffered salt solution
HGF	Hepatocyte growth factor
HKII	Hexokinase II
HPLC	High-performance liquid chromatography
HPMCP-55	Hydroxypropyl methylcellulose phthalate
IF	Intrinsic factor
IGF-1	Insulin-like growth factor-1
IKK	Inhibitor kappa-β kinase
IRS-1	Insulin receptor substrate-1
JAM-1	Junctional adhesion molecule
JNK	c-jun N-terminal kinase
LBL	Layer-by-layer
LC-PUFAs	Long chain polyunsaturated fatty acids
LKB1	Liver kinase B1
LMW	Low molecular weight
LMWP	Low molecular weight protamine
MCP-1	Monocyte chemotactic protein 1
$MgSO_4$	Magnesium sulphate
NAC	N-acetyl-L-cysteine
mef2a	Myocyte-enhanced factor 2A
MW	Molecular weight
nrf1	Nuclear respiratory factor 1
NVP	N-vinyl pyrrolidone
NSF	N-ethylmaleimide-sensitive factor
Omp19	Outer membrane protein
PAA	Poly(acrylic acid)
PAA	Polyallylamine
PBMAD	Poly(butadiene-maleic anhydride-co-L-DOPA)
PBS	Phosphate buffer solution
PCL	Polyester (poly(-ε-caprolactone)

PDA	Polydopamine
pdi	Polydispersity index
PEAs	Poly(ester amide)s
PEDF	Pigment epithelium-derived factor
PEG	Poly(ethylene glycol)
PEGDMA	Polyethylene glycol dimethacrylate
pHPMA	Poly(N-(2-hydroxypropyl) methacrylamide)
PI3-K	Phosphatidylinositol 3 kinase
PIP3	Phosphatidylinositol 3,4,5-trisphosphate
PLA	Poly(lactic acid)
PLGA	Poly(D, L-lactide-co-glycolide)
PMAA	Poly(methacrylic acid)
PMAP	Poly(methylaminophosphazene)
PMAPBA	Poly(3-methacrylamido phenylboronic acid)
PKB	Protein kinase B
PPAR	Peroxisome proliferator-activated receptor
PVA	Poly(vinyl alcohol)
PVCL	Poly(N-vinylcaprolactam)
rOmpA	Recombinant outer membrane protein A
ROS	Reactive oxygen species
RSM	Response surface methodology
SA	Sodium acetate
SC	Subcutaneous
SDDS	Submicron drug delivery systems
SER	Serratiopeptidase
SGF	Simulated gastric fluid
SIF	Simulated intestinal fluid
SKIP	Skeletal muscle and kidney enriched inositol polyphosphate phosphatase
SLNs	Solid lipid nanoparticles
SNAC	Sodium N-(8-[2-hydroxybenzoyl] amino)
SPC	Soybean phosphatidylcholine
SPECT	Single-photon emission computed tomography
SS	Sodium sulphate
Syn	Syntaxin
T1DM	Type 1 diabetes mellitus
T2DM	Type 2 diabetes mellitus

TAT	Trans-activating transcriptional peptide
TEER	Transepithelial-electrical-resistance
TEGDMA	Triethylene glycol dimethacrylate
TEMED	Tetramethylethylenediamine
Tf	Transferrin
TFA	Trifluoroacetic acid
TLR4	Toll-like receptor
TMC	Trimethylated chitosan
TNF	Tumour necrosis factor
TPP	Sodium tripolyphosphate
VAMP2	Vesicle-associated membrane protein 2
WGA	Wheat germ agglutinin
ZO	Zona occludens
ZrP	Zirconium phosphate

Chapter 1: Background, aims, significance and structure of this research

1. Background of research

Diabetes mellitus is a chronic health condition that is characterised by hyperglycaemia (high blood sugar level).[1] It can be classified into type 1 diabetes (T1DM) (that is, reduced functionality of β cells and limited production of endogenous insulin), type 2 diabetes mellitus (T2DM) (in essence, limited insulin-responsiveness in tissues) and gestational diabetes (that is, increased insulin resistance during pregnancy).[2,3] Most patients with diabetes mellitus are accompanied with co-morbidities such as obesity and hyperlipidaemia. It is anticipated that 9.9% of the global population (628.6 million people) will be affected by 2045.[1] In the United States of America, approximately $237 billion of revenue was spent on the direct medical costs for patients with diabetes mellitus, and $90 billion was lost due to the reduction in productivity in 2017.[4] In 2012, 1.5 million fatalities were directly attributed to diabetes mellitus worldwide.[5]

Glucose transporter type 4 (GLUT-4) is an insulin-responsive glucose transporter that localises in skeletal muscle cells, cardiac cells and adipose tissues.[6,7] In patients with diabetes mellitus, the translocation of GLUT-4 is attenuated, resulting in downregulation of insulin-stimulated glucose consumption.[6,7] When the sugar level is high in the body, insulin resistance and cellular protein degradation can occur due to the generation of excessive reactive oxygen species.[8,9] The insulin signalling pathway can be distorted due to the imbalance of oxidative balance, initiation of inflammation cascade, infiltration of macrophages, and secretion of pro-inflammatory cytokines (for instance, TNF-α, IL-6).[10] Therefore, patients with diabetes mellitus are at higher risk of a range of micro and macro complications including cardiovascular disease, renal

disease, blindness, wound healing impairment, limb amputation, cerebrovascular disease and stroke.[11-13] To date, there is no medication available that can cure T1DM and T2DM. Hence, the clinical goal is to control the blood sugar level (HbA_{1c} ~ 7%) and minimise the progressive risk of diabetes-associated complications.[14]

Insulin is a polypeptide hormone that can regulate the lipid metabolism in adipose tissue, and maintain the homeostasis of blood sugar level.[15] Subcutaneous insulin injections can mimic the physiological function of endogenous insulin.[12,14,16,17] Therefore, it remains the conventional therapy for patients with T1DM in clinical setting to control the blood sugar level. The administration of traditional insulin regimen (rapid-acting injection before meal and slow-acting injection before bed) has been confirmed to control the postprandial or basal blood glucose level in addition to lowering the occurrence of diabetes-associated complications.[18-29] However, with such intensive and invasive daily regimen, patients can experience unwanted mild or severe adverse events. These can include but is not limited to pain, topical infection, nerve damage, and hypoglycaemic episode.[30-32] In contrast, oral administration of drugs can alleviate the risk of the aforementioned adverse events, increase the patient adherence to therapy, and potentially improve the clinical outcome.

Oral administration of therapeutic proteins remains unachievable due to the presence of GI barriers, such as GI enzymes, fluctuated pH, mucus turnover and tight junctions, that can degrade and limit the GI permeability of proteins.[33-35] Nanoparticles possess favourable properties that can protect the encapsulated proteins against harsh physiological environment and GI enzymes, overcome the mucus barrier, and improve the GI absorption of proteins *via* paracellular and transcellular pathways.[36,37] As compared to other micron-sized drug delivery systems, nanoparticles possess the

smallest particle size to volume ratio, which can facilitate the GI absorption of entrapped therapeutic proteins. Multiple studies have encapsulated insulin by using nanoparticles, which include natural polymeric nanoparticles (e.g. alginate, chitosan, dextran sulfate), synthetic polymeric nanoparticles (e.g. polyallylamine, poly(lactic acid), poly(lactic-co-glycolic) acid), inorganic nanoparticles, (e.g. zirconium phosphate, gold, silica) and solid lipid nanoparticles.[33-37] However, to date, the translation of insulin-loaded nanoparticles from the laboratory to clinical setting remains unsuccessful. This suggests the need to employ novel strategies to develop the drug delivery system, enhance the entrapment efficiency of nanoparticles, and reduce the burden of drug wastage or pharmaceutical cost in the manufacturing process.

Chitosan-based nanoparticle, which can be classified as natural polymeric nanoparticle, is one of the promising drug delivery systems. Chitosan is a biocompatible and biodegradable natural polymer. It possesses positive surface charge, which can prolong the contact time and improve the mucoadhesiveness of the drug delivery systems to the GI tract.[38] It was also reported that chitosan could reduce the transepithelial-electrical-resistance reversibly, and induce transient redistribution of molecular markers in the GI tract.[39-41] Therefore, chitosan-based nanoparticles were capable of improving the oral absorption of insulin by loosening the tight junctions transiently and enhancing the paracellular absorption of therapeutic proteins.[39]

An orally administered nanoparticulate drug delivery system is deemed to be superior if it can protect the entrapped proteins against enzymatic degradation, overcome the mucus and epithelial barriers in the GI tract, maintain the biological activity of proteins in physiological environment, and improve their GI absorption. The drug encapsulation efficiency and loading capacity should also be optimised to develop a

cost-effective drug delivery system. This thesis examined the potential of polymeric-oligonucleotide nanoparticle as a drug delivery system for oral administration of insulin in diabetes treatment. Polyelectrolyte complexation was utilised to prepare insulin-loaded nanoparticles. In the presence of oppositely-charged excipients, protein-loaded nanoparticles can be formed.[42,43] These fabrication techniques possess mild conditions without the need for organic chemicals.[42,44-48] The employment of appropriate excipients could enhance the physicochemical characteristics of nanoparticles and conserve the bioactivity of proteins during the fabrication process. For instance, it was stated that β-cyclodextrin (β-CD) could effectively improve the stability of insulin in the physiological environment.[49] In the current project, the following formulation parameters, including polymer constitution, particle size, polydispersity index, zeta potential, morphology, encapsulation efficiency and stability, were optimised during nanoparticle development.

2. Aims and objectives of research

The main objective of the current research was to design a nanoparticulate drug delivery system for oral delivery of insulin. With the use of appropriate excipients, the bioactivity of the entrapped insulin should be conserved in the GI tract before reaching the blood circulation. The specific objectives of this research project are listed below:

- **Objective 1:** To identify and optimise the physicochemical characteristics (size, zeta potential, morphology, entrapment efficiency, loading efficiency and drug release behaviour) of the developed insulin-loaded nanoparticles.
- **Objective 2:** To examine the effect of preparation procedures and lyophilisation

on the physicochemical properties and bioactivity of insulin-loaded nanoparticles.

- **Objective 3:** To examine if the chosen excipients and cryoprotectants maintain the stability of insulin-loaded formulations.
- **Objective 4:** To identify if the developed insulin-loaded nanoparticles promote glucose consumption in skeletal muscle cells, and GI transportation or permeation in GI cell culture.
- **Objective 5:** To assess the stability of the developed insulin-loaded nanoparticles after storage.

3. Significance of research

According to the World Health Organization, it is anticipated that 9.9% of the global population (628.6 million people) will be diagnosed with diabetes mellitus by 2045.[1] For patients with diabetes mellitus, the deleterious effect of uncontrolled blood glucose level has been well documented.[2] Therefore, research is crucial for improving patient adherence and allay the adverse events that are associated with subcutaneous insulin injections (e.g. hypoglycaemic episode). The current research aims to develop an orally administered nanoparticulate system that can effectively manage the blood sugar level, reduce the occurrence of adverse events, and lower the pharmaceutical cost by improving the encapsulation efficiency of nanocarriers. The nanoencapsulation technology is of particular interest as it can improve the stability of the entrapped insulin in the physiological GI conditions, and enhance its GI absorption. The non-invasive and convenient route can improve the patient adherence and tolerance to the therapy. In this project, the effects of lyophilisation and cryoprotectants on the bioactivity of encapsulated insulin and stability of nanoparticles were investigated.

4. Structure of the thesis

The thesis is comprised of 4 sections, which includes the prospect of insulin micron-sized and submicron-sized drug delivery systems (**Section A; Chapter 2 - 4**), the review of methodologies and experimental conditions (**Section B; Chapter 5 - 7**), understanding of techniques for fabrication of insulin nanoparticles, chitosan nanoparticles and C2C12 cell model (**Section C; Chapter 8 - 10**), and lastly the research and development of insulin-loaded nanoparticles (**Section D; Chapter 11 - 13**).

In **chapter 11**, statistical evaluation was carried out to understand the effect of individual independent variables, main independent effects, interaction effects and quadratic effects of the examined variables (e.g. polymer concentration and oligonucleotide concentration) on the experimental response of nanoparticles. This could foster the selection of optimised formulation parameters in the developmental stage of protein-loaded nanoparticles. As mass production and clinical translation of nanotherapeutics are key challenges faced by the scientific community, the authors aimed to investigate the effect of scaling up process on the physiochemical properties and cellular responses of the developed formulation by making comparisons between the pre-scaled up nanoparticles and scaled-up nanoparticles in **chapter 12**. In **chapter 13**, lyophilisation (freeze-drying) was employed to convert the nanoformulation (in suspension form) into particles (in solid form) by removing water molecules in the presence of appropriate cryoprotectant. This technique is crucial for maintaining the physiochemical properties of nanoparticles and the bioactivity of the entrapped

proteins upon storage.

The relevant publications that are not forming a part of the thesis are attached in the appendix A. The chapters and their sub-objectives that are involved in each section are listed below:

Section	Chapters and their sub-objectives
Section A - prospect of insulin micron-sized and submicron-sized drug delivery systems	**Chapter 2:** Potential of insulin nanoparticle formulations for oral delivery and diabetes treatment • To assess the role of nanoparticles in oral administration of insulin. • To understand the formulation barriers and physiological barriers that are associated with the development of oral insulin nanoparticles. • To examine and evaluate different types of orally administered insulin-loaded nanoparticles.
	Chapter 3: Microparticles, microcapsules and microspheres: a review of recent developments and prospects for oral delivery of insulin • To assess the difference in physicochemical properties between insulin-loaded nanoparticulate systems and microparticulate systems. • To examine the current status of microparticles, hydrogel-based microparticles, microcapsules and microspheres for oral administration of insulin. • To understand the formulation barriers and physiological barriers that are associated with the development of oral insulin microparticulate systems.
	Chapter 4: Recent advancements in oral administration of insulin-loaded liposomal drug delivery systems for diabetes mellitus • To assess the difference in physicochemical properties between insulin-loaded nanoparticulate systems and liposomal systems. • To examine the *status quo* of conventional liposomal

	formulation and 7 classes of novel liposomal formulations (surface-coating liposomes, cell-specific targeting liposomes, bile salt-containing liposomes, botanic sterol-containing liposomes, double liposomes, proliposomes, archaeosomes) for oral administration of insulin. • To understand the formulation barriers and physiological barriers that are associated with the development of oral insulin liposomal systems.

Section	Chapters and their sub-objectives
Section B - review of methodologies and experimental conditions	**Chapter 5:** Bio-nanotechnological advancement of orally administered insulin nanoparticles: comprehensive review of experimental design for physicochemical characterisation • To examine and review the experimental designs and conditions for physical characterisation of orally administered protein-loaded nanoparticles. • To facilitate the research design and minimise wastage in research funding for physical characterisation of orally administered protein-loaded nanoparticles. • To understand the instrumentations and assays that can be employed to assess the mucus diffusion capacity, stability and bioactivity of protein-loaded nanoparticles.
	Chapter 6: Cellular assays and applied technologies for characterisation of orally administered protein nanoparticles: a systematic review • To examine and review the experimental designs and conditions for cellular characterisation of orally administered protein-loaded nanoparticles. • To facilitate the research design and minimise wastage in research funding for cellular characterisation of orally administered protein-loaded nanoparticles. • To understand the instrumentations and assays that can be employed to assess the cell culture condition, cytotoxicity, cellular uptake, transepithelial transport, GI permeation, integrity of nanoparticle and peptide during intracellular trafficking, endocytosis mechanism, and exocytosis mechanism of protein-loaded nanoparticles.

	Chapter 7: Current status and applications of animal models in pre-clinical development of orally administered insulin-loaded nanoparticles • To examine and review the experimental designs and conditions for *in vivo* characterisation of orally administered protein-loaded nanoparticles. • To facilitate the research design and minimise wastage in research funding for *in vivo* characterisation of orally administered protein-loaded nanoparticles. • To understand the instrumentations and assays that can be employed to assess the intestinal absorption efficacy, mucoadhesiveness capacity, biocompatibility, biodistribution, and *in vivo* efficacy of protein-loaded nanoparticles.

Section	Chapters and their sub-objectives
Section C - understanding of techniques for fabrication of insulin nanoparticles, chitosan nanoparticles and C2C12 cell model	**Chapter 8:** Fabrication techniques for the preparation of orally administered insulin nanoparticles • To examine the techniques that are available for nano-encapsulation of insulin. • To assess the characteristics of each preparation technique. • To understand the strategies that have been utilised in each technique to improve the stability and bioactivity of formulations.
	Chapter 9: The role of chitosan on oral delivery of peptide-loaded nanoparticle formulation • To examine the features of chitosan and chitosan-based nanoparticles. • To assess the potential pre-clinical applications of peptide-loaded chitosan-based nanoparticles. • To evaluate the current status and development of oral vaccination by using protein or peptide-loaded chitosan-based nanoparticles.
	Chapter 10: C2C12 cell model: its role in understanding of insulin resistance at the molecular level and pharmaceutical development at the pre-clinical stage • To examine the use of C2C12 cell model in understanding

	insulin resistance progression and pharmaceutical development. • To assess the examples of studies and therapeutic agents that utilise C2C12 cell model in the pre-clinical stage. • To understand the potential of C2C12 cell model in pharmaceutical development of drug delivery systems (e.g. nanoparticles, quantum dots).

Section	Chapters and their sub-objectives
Section D - research and development of insulin-loaded nanoparticles	**Chapter 11:** Development of orally administered insulin-loaded polymeric-oligonucleotide nanoparticles: statistical optimization and physicochemical characterization • To examine the effect of polymer and oligonucleotide concentrations on the physicochemical properties of nanoparticles by using statistical analysis. • To evaluate the stability, encapsulation efficiency and drug release behaviour of nanoparticles. • To understand the cytotoxicity of the excipients and nanoparticles.
	Chapter 12: Formulation and characterisation of insulin-loaded chitosan nanoparticles capable of inducing glucose uptake in skeletal muscle cells *in vitro* • To review and examine the potential of all existing insulin-loaded nanoparticulate formulations that were prepared by complex coacervation. • To characterise the physicochemical properties (size, polydispersity index, zeta potential, drug release) of nanoparticles that were prepared by complex coacervation. • To examine the storage stability of the optimal insulin-loaded nanoparticles. • To evaluate the metabolic effect, bioactivity, mucus permeation capacity and endocytic absorption pathways of the fabricated nanoparticles.
	Chapter 13: Lyophilisation improves bioactivity and stability of insulin-loaded polymeric-oligonucleotide nanoparticles for diabetes treatment

	• To understand the freeze-drying protocols that were employed to develop orally administered insulin-loaded nanoparticles. • To develop and examine the macroscopic stability of the lyophilised insulin-loaded nanoparticles that were prepared by complex coacervation. • To examine the effects of lyophilisation and cryoprotectant on the physicochemical characteristics (size, zeta potential, entrapment efficiency, loading efficiency, morphology) of the lyophilised insulin-loaded nanoparticles. • To investigate if the developed lyophilised formulation possesses any pH-dependent and glucose-responsive drug release behaviour. • To characterise the cytotoxicity, functionality, endocytic absorption pathways and GI cellular permeation of the developed lyophilised formulation. • To examine the effect of mucus on cellular internalisation of the developed lyophilised formulation. • To examine if the cryoprotectant maintain the chemical, physical and storage stability of the optimised lyophilised nanoparticles.

Sections	Chapters and their sub-objectives
Appendix A: Relevant publications to the thesis but not forming a part of it	**Appendix A1:** Quantification of BSA-loaded chitosan/ oligonucleotide nanoparticles using reverse-phase high-performance liquid chromatography • To develop a HPLC method to quantify the proteins including bovine serum albumin, insulin and PEDF. • To characterise the physical characteristics of BSA-loaded chitosan/oligonucleotide nanoparticles. To evaluate the drug release profile and stability of the developed nanoparticles.

5. Reference list

1. Standl E, Khunti K, Hansen TB, et al. The global epidemics of diabetes in the 21st century: current situation and perspectives. Eur J Prev Cardiol. 2019; 26:7-14.
2. Ha BG, Park JE, Shon YH. Stimulatory effect of balanced deep-sea water containing chitosan oligosaccharides on glucose uptake in C2C12 myotubes. Mar Biotechnol (NY). 2016;18:475-484.
3. Stumvoll M, Goldstein BJ, van Haeften TW. Pathogenesis of type 2 diabetes. Endocr Res. 2007;32:19-37.
4. American Diabetes Association. Economic costs of diabetes in the U.S. in 2017. Diabetes Care. 2018 ;41:917-928.
5. Roglic G. WHO global report on diabetes: a summary. Int J Infect Dis. 2016; 1:3-8.
6. Kuo YH, Lin CH, Shih CC, et al. Antcin K, a triterpenoid compound from antrodia camphorata, displays antidiabetic and antihyperlipidemic effects via glucose transporter 4 and AMP-activated protein kinase phosphorylation in muscles. Evid Based Complement Alternat Med. 2016;2016:4867092.
7. Ryder JW, Yang J, Galuska D, et al. Use of a novel impermeable biotinylated photolabeling reagent to assess insulin- and hypoxia-stimulated cell surface GLUT4 content in skeletal muscle from type 2 diabetic patients. Diabetes. 2000;49:647-654.
8. Russell ST, Rajani S, Dhadda RS, et al. Mechanism of induction of muscle protein loss by hyperglycaemia. Exp Cell Res. 2009;315:16-25.
9. Grzelkowska-Kowalczyk K, Wieteska-Skrzeczynska W, Grabiec K, Tokarska J. High glucose-mediated alterations of mechanisms important in myogenesis of mouse C2C12 myoblasts. Cell Biol Int. 2013;37:29-35.
10. Jager J, Gremeaux T, Cormont M, et al. Interleukin-1beta-induced insulin

resistance in adipocytes through down-regulation of insulin receptor substrate-1 expression. Endocrinology. 2007;148:241-251.

11. International Diabetes Federation. IDF Diabetes atlas. Brussels (Belgium): International Diabetes Federation; 2015.
12. American Diabetes Association. Diagnosis and classification of diabetes mellitus. Diabetes Care. 2013; 36:67-74.
13. Tahtat D, Mahlous M, Benamer S, et al. Oral delivery of insulin from alginate/chitosan crosslinked by glutaraldehyde. Int J Biol Macromol. 2013;58:160-168.
14. Nathan DM, Buse JB, Davidson MB, et al. Medical management of hyperglycemia in type 2 diabetes: a consensus algorithm for the initiation and adjustment of therapy. Diabetes Care. 2009; 32:193-203.
15. Jain S, Rathi VV, Jain AK, Das M, Godugu C. Folate-decorated PLGA nanoparticles as a rationally designed vehicle for the oral delivery of insulin. Nanomedicine. 2012;7:1311-1337.
16. Guariguata L, Whiting D, Weil C, et al. The International Diabetes Federation diabetes atlas methodology for estimating global and national prevalence of diabetes in adults. Diabetes Res Clin Pract. 2011; 94:322-332.
17. Hamaty M. Insulin treatment for type 2 diabetes: when to start, which to use. Cleve Clin J Med. 2011; 78:332-42.
18. Oak M, Singh J. Chitosan-zinc-insulin complex incorporated thermosensitive polymer for controlled delivery of basal insulin in vivo. J Control Release. 2012; 163:145-153.
19. Lopes MA, Abrahim-Vieira B, Oliveira C, et al. Probing insulin bioactivity in oral nanoparticles produced by ultrasonication-assisted emulsification/internal gelation. Int J Nanomedicine. 2015; 10:5865-80.
20. Raskin P, Guthrie RA, Leiter L, et al. Use of insulin aspart, a fast-acting insulin analog, as the mealtime insulin in the management of patients with type 1 diabetes.

Diabetes Care. 2000; 23:583-588.

21. Raslova K, Bogoev M, Raz I, et al. Insulin detemir and insulin aspart: a promising basal-bolus regimen for type 2 diabetes. Diabetes Res Clin Pract. 2004; 66:193-201.

Becker RH, Frick AD. Clinical pharmacokinetics and pharmacodynamics of insulin glulisine. Clin Pharmacokinet. 2008; 47:7-20.

22. Becker RH, Frick AD. Clinical pharmacokinetics and pharmacodynamics of insulin glulisine. Clin Pharmacokinet. 2008;47:7-20.

23. Garg SK, Ellis SL, Ulrich H. Insulin glulisine: a new rapid-acting insulin analogue for the treatment of diabetes. Expert Opin Pharmacother. 2005; 6:643-651.

24. Lepore M, Pampanelli S, Fanelli C, et al. Pharmacokinetics and pharmacodynamics of subcutaneous injection of long-acting human insulin analog glargine, NPH insulin, and ultralente human insulin and continuous subcutaneous infusion of insulin lispro. Diabetes. 2000; 49:2142-2148.

25. Riddle MC, Rosenstock J, Gerich J. The Treat-to-Target Trial. Randomized addition of glargine or human NPH insulin to oral therapy of type 2 diabetic patients. 2003; 26:3080-3086.

26. Heine RJ, Van Gaal LF, Johns D, et al. Exenatide versus insulin glargine in patients with suboptimally controlled type 2 diabetes: a randomized trial. Ann Intern Med. 2005; 143:559-569.

27. Havelund S, Plum A, Ribel U, et al. The mechanism of protraction of insulin detemir, a long-acting, acylated analog of human insulin. Pharm Res. 2004; 21:1498-1504.

28. Deckert T. Intermediate-acting insulin preparations: NPH and lente. Diabetes Care. 1980; 3:623-626.

29. Hurkat P, Jain A, Jain A, et al. Concanavalin A conjugated biodegradable nanoparticles for oral insulin delivery. J Nanopart Res. 2012;14:1219.

30. Zhang Z, Cai H, Liu Z, Yao P. Effective enhancement of hypoglycemic effect of insulin by liver-targeted nanoparticles containing cholic acid-modified chitosan derivative. Mol Pharm. 2016; 13:2433-2442.
31. Buzasi K, Sapi Z, Jermendy G. Acanthosis nigricans as a local cutaneous side effect of repeated human insulin injections. Diabetes Res Clin Pract. 2011; 94:34-36.
32. Richardson T, Kerr D. Skin-related complications of insulin therapy. Am J Clin Dermatol. 2003; 4:661-667.
33. Holleman F, Hoekstra JB. Insulin lispro. N Engl J Med. 1997; 337:176-183.
34. Cone RA. Barrier properties of mucus. Adv Drug Deliv Rev. 2009; 61:75-85.
35. Evans DF, Pye G, Bramley R, et al. Measurement of gastrointestinal pH profiles in normal ambulant human subjects. Gut. 1988; 29:1035-1041.
36. Lopes MA, Abrahim BA, Seica R, et al. Intestinal uptake of insulin nanoparticles: facts or myths? Curr Pharm Biotechnol. 2014; 15:629-638.
37. Hans ML, Lowman AM. Biodegradable nanoparticles for drug delivery and targeting. Curr Opin Solid State Mater Sci. 2002; 6:319-327.
38. Sarmento B, das Neves J. Chitosan-based systems for biopharmaceuticals: delivery, targeting, and polymer therapeutics. West Sussex (Chichester): John Wiley & Sons; 2011.
39. Yeh TH, Hsu LW, Tseng MT, et al. Mechanism and consequence of chitosan-mediated reversible epithelial tight junction opening. Biomaterials. 2011; 32:6164-6173.
40. Sonaje K, Chuang EY, Lin KJ, et al. Opening of epithelial tight junctions and enhancement of paracellular permeation by chitosan: microscopic, ultrastructural, and computed-tomographic observations. Mol Pharm. 2012; 9:1271-1279.
41. Hochman J, Artursson P. Mechanisms of absorption enhancement and tight junction regulation. J Control Release. 1994; 29:253-267.
42. Sadeghi AMM, Dorkoosh FA, Avadi MR, et al. Preparation, characterization and

antibacterial activities of chitosan, N-trimethyl chitosan (TMC) and N-diethylmethyl chitosan (DEMC) nanoparticles loaded with insulin using both the ionotropic gelation and polyelectrolyte complexation methods. Int J Pharm. 2008; 355:299-306.

43. Bayat A, Dorkoosh FA, Dehpour AR, et al. Nanoparticles of quaternized chitosan derivatives as a carrier for colon delivery of insulin: Ex vivo and in vivo studies. Int J Pharm. 2008; 356:259-266.
44. Su FY, Lin KJ, Sonaje K, et al. Protease inhibition and absorption enhancement by functional nanoparticles for effective oral insulin delivery. Biomaterials. 2012; 33:2801-2811.
45. Sonaje K, Lin YH, Juang JH, et al. In vivo evaluation of safety and efficacy of self-assembled nanoparticles for oral insulin delivery. Biomaterials. 2009; 30:2329-2339.
46. Lin YH, Mi FL, Chen CT, et al. Preparation and characterization of nanoparticles shelled with chitosan for oral insulin delivery. Biomacromolecules. 2007; 8:146-152.
47. Chuang EY, Lin KJ, Su FY, et al. Calcium depletion-mediated protease inhibition and apical-junctional-complex disassembly via an EGTA-conjugated carrier for oral insulin delivery. J Control Release. 2013; 169:296-305.
48. Su FY, Lin KJ, Sonaje K, et al. Protease inhibition and absorption enhancement by functional nanoparticles for effective oral insulin delivery. Biomaterials. 2012; 33:2801-2811.
49. Sajeesh S, Sharma CP. Cyclodextrin–insulin complex encapsulated polymethacrylic acid based nanoparticles for oral insulin delivery. Int J Pharm. 2006; 325:147-154.

Chapter 2: Potential of insulin nanoparticle formulations for oral delivery and diabetes treatment

Wong CY et al 2017. "Potential of insulin nanoparticle formulations for oral delivery and diabetes treatment." Journal of Controlled Release 264: 247-275.

https://doi.org/10.1016/j.jconrel.2017.09.003

https://www.sciencedirect.com/science/article/abs/pii/S0168365917308283

*This paper has been reproduced in accordance with the publisher's policy (Appendix B1).

Acknowledgement: The Version of Record of this manuscript has been published and was made available in Journal of Controlled Release on the 28th October 2017 (https://www.sciencedirect.com/science/article/abs/pii/S0168365917308283).

Contents
1 Introduction
2 Structure and physiological function of insulin
3 Nanotechnology based delivery systems for oral insulin administration
4 Barriers to oral delivery of insulin nanoparticle formulation
4.1 Physical barrier
4.2 Chemical barrier
4.3 Enzymatic barrier
5 Natural polymeric nanoparticles
5.1 Chitosan-based nanoparticles
5.1.1 Chitosan and poly(γ-glutamic acid) (γ-PGA)
5.1.2 Carboxylated, trimethylated (TMC), ethyl (DMEC), carboxymethyl (CMCS) and thiolated chitosan
5.1.3 Vitamin B12-conjugated chitosan (VitB12-Chi)
5.1.4 Chitosan and poly(ethylene glycol) (PEG)ylation
5.1.5 Chitosan-based glucose responsive system
5.2 Alginate-based nanoparticles
5.3 Dextran-based nanoparticles

6 Synthetic polymeric nanoparticles
6.1 PLGA based nanoparticles
12.6.1.1 Phospholipid conjugated PLGA nanoparticles
12.6.1.2 Optimization of PLGA nanoparticles
12.6.1.3 Active targeting PLGA nanoparticles
12.6.2 Poly(lactic acid) (PLA)-based nanoparticles
12.6.3 Polyallylamine (PAA)-based nanoparticles
12.6.4 Polymeric nanoparticles containing CPP
12.7 Inorganic nanoparticles
12.8 Nanoparticles containing Eudragit®
12.9 Solid lipid nanoparticles
12.10. Future prospects and conclusion
12.11 Reference list

1. Declaration of attribution by the candidate

I, Chun Yuen Jerry Wong, as the first author of the publication entitled "Potential of insulin nanoparticle formulations for oral delivery and diabetes treatment", declare that this work was primarily designed, experimentally executed, interpreted, and written by the first author of this manuscript.

Name	Manuscript preparation	Manuscript editing	Final Approval
Chun Yuen Jerry Wong	x	x	x
Dr Hani Al-Salami		x	x
Professor Crispin Dass		x	x

I acknowledge that these represent my contribution to the above research output.

Signature:

Date: 11th September 2020

Co-authors:

Dr Hani Al-Salami	**Professor Crispin Dass**
Signature:	Signature:
Date:	Date:

2. Summary and aims of the chapter

In this chapter, the physiological function and structure of insulin were discussed. Thereafter, the role of nanotechnology and barriers to the development of oral insulin nanoparticles were assessed. These barriers were classified into physical (mucus and epithelial layers), chemical (instability in extreme pH) and enzymatic barriers (GI enzyme degradation). In this chapter, the potential and current status of natural polymeric, synthetic polymeric, inorganic, and sold lipid nanoparticles in oral administration of insulin were evaluated. To develop a successful nanocarrier, the physicochemical properties of the nanoparticles, which include particle size, zeta potential, polydispersity index, encapsulation efficiency, morphology and stability, should be optimised. Several novel formulations including glucose-responsive nanoparticles, layer-by-layer nanoparticles and zwitterion nanoparticles have been developed to overcome the barriers that are encountered by the conventional insulin-loaded nanoparticles. The future directions for the development of orally administered insulin-loaded nanoparticles were addressed.

3. Sub-objectives of chapter 2

The first objective of the thesis is to identify and optimise the physicochemical characteristics (size, zeta potential, morphology, entrapment efficiency, loading efficiency and drug release behaviour) of the developed insulin-loaded nanoparticles. The second objective of the thesis is to examine the effect of preparation procedures and lyophilisation on the physicochemical properties and bioactivity of insulin-loaded nanoparticles. Therefore, it is crucial to understand the currently available insulin-

loaded nanoparticles in order to establish comparisons with the novel formulations, as well as drawing a conclusion and recognising the challenges that have to be addressed in future studies. The sub-objectives of chapter 2 are listed below:

- To assess the role of nanoparticles in oral administration of insulin.
- To understand the formulation barriers and physiological barriers that are associated with the development of oral insulin nanoparticles.
- To examine and evaluate different types of orally administered insulin-loaded nanoparticles.

4. Manuscript

Content is removed due to copyright restrictions. The publication can be accessed from https://www.sciencedirect.com/science/article/abs/pii/S0168365917308283.

Wong CY et al 2017. "Potential of insulin nanoparticle formulations for oral delivery and diabetes treatment." Journal of Controlled Release 264: 247-275.

Content is removed due to copyright restrictions. The publication can be accessed from https://www.sciencedirect.com/science/article/abs/pii/S0168365917308283.

Wong CY et al 2017. "Potential of insulin nanoparticle formulations for oral delivery and diabetes treatment." Journal of Controlled Release 264: 247-275.

Content is removed due to copyright restrictions. The publication can be accessed from https://www.sciencedirect.com/science/article/abs/pii/S0168365917308283.

Wong CY et al 2017. "Potential of insulin nanoparticle formulations for oral delivery and diabetes treatment." Journal of Controlled Release 264: 247-275.

Content is removed due to copyright restrictions. The publication can be accessed from https://www.sciencedirect.com/science/article/abs/pii/S0168365917308283.

Wong CY et al 2017. "Potential of insulin nanoparticle formulations for oral delivery and diabetes treatment." Journal of Controlled Release 264: 247-275.

Content is removed due to copyright restrictions. The publication can be accessed from https://www.sciencedirect.com/science/article/abs/pii/S0168365917308283.

Wong CY et al 2017. "Potential of insulin nanoparticle formulations for oral delivery and diabetes treatment." Journal of Controlled Release 264: 247-275.

Content is removed due to copyright restrictions. The publication can be accessed from https://www.sciencedirect.com/science/article/abs/pii/S0168365917308283.

Wong CY et al 2017. "Potential of insulin nanoparticle formulations for oral delivery and diabetes treatment." Journal of Controlled Release 264: 247-275.

Content is removed due to copyright restrictions. The publication can be accessed from https://www.sciencedirect.com/science/article/abs/pii/S0168365917308283.

Wong CY et al 2017. "Potential of insulin nanoparticle formulations for oral delivery and diabetes treatment." Journal of Controlled Release 264: 247-275.

Content is removed due to copyright restrictions. The publication can be accessed from https://www.sciencedirect.com/science/article/abs/pii/S0168365917308283.

Wong CY et al 2017. "Potential of insulin nanoparticle formulations for oral delivery and diabetes treatment." Journal of Controlled Release 264: 247-275.

Content is removed due to copyright restrictions. The publication can be accessed from https://www.sciencedirect.com/science/article/abs/pii/S0168365917308283.

Wong CY et al 2017. "Potential of insulin nanoparticle formulations for oral delivery and diabetes treatment." Journal of Controlled Release 264: 247-275.

Content is removed due to copyright restrictions. The publication can be accessed from https://www.sciencedirect.com/science/article/abs/pii/S0168365917308283.

Wong CY et al 2017. "Potential of insulin nanoparticle formulations for oral delivery and diabetes treatment." Journal of Controlled Release 264: 247-275.

Content is removed due to copyright restrictions. The publication can be accessed from https://www.sciencedirect.com/science/article/abs/pii/S0168365917308283.

Wong CY et al 2017. "Potential of insulin nanoparticle formulations for oral delivery and diabetes treatment." Journal of Controlled Release 264: 247-275.

Content is removed due to copyright restrictions. The publication can be accessed from https://www.sciencedirect.com/science/article/abs/pii/S0168365917308283.

Wong CY et al 2017. "Potential of insulin nanoparticle formulations for oral delivery and diabetes treatment." Journal of Controlled Release 264: 247-275.

Content is removed due to copyright restrictions. The publication can be accessed from https://www.sciencedirect.com/science/article/abs/pii/S0168365917308283.

Wong CY et al 2017. "Potential of insulin nanoparticle formulations for oral delivery and diabetes treatment." Journal of Controlled Release 264: 247-275.

Content is removed due to copyright restrictions. The publication can be accessed from https://www.sciencedirect.com/science/article/abs/pii/S0168365917308283.

Wong CY et al 2017. "Potential of insulin nanoparticle formulations for oral delivery and diabetes treatment." Journal of Controlled Release 264: 247-275.

Content is removed due to copyright restrictions. The publication can be accessed from https://www.sciencedirect.com/science/article/abs/pii/S0168365917308283.

Wong CY et al 2017. "Potential of insulin nanoparticle formulations for oral delivery and diabetes treatment." Journal of Controlled Release 264: 247-275.

Content is removed due to copyright restrictions. The publication can be accessed from https://www.sciencedirect.com/science/article/abs/pii/S0168365917308283.

Wong CY et al 2017. "Potential of insulin nanoparticle formulations for oral delivery and diabetes treatment." Journal of Controlled Release 264: 247-275.

Content is removed due to copyright restrictions. The publication can be accessed from https://www.sciencedirect.com/science/article/abs/pii/S0168365917308283.

Wong CY et al 2017. "Potential of insulin nanoparticle formulations for oral delivery and diabetes treatment." Journal of Controlled Release 264: 247-275.

Content is removed due to copyright restrictions. The publication can be accessed from https://www.sciencedirect.com/science/article/abs/pii/S0168365917308283.

Wong CY et al 2017. "Potential of insulin nanoparticle formulations for oral delivery and diabetes treatment." Journal of Controlled Release 264: 247-275.

Content is removed due to copyright restrictions. The publication can be accessed from https://www.sciencedirect.com/science/article/abs/pii/S0168365917308283.

Wong CY et al 2017. "Potential of insulin nanoparticle formulations for oral delivery and diabetes treatment." Journal of Controlled Release 264: 247-275.

Content is removed due to copyright restrictions. The publication can be accessed from https://www.sciencedirect.com/science/article/abs/pii/S0168365917308283.

Wong CY et al 2017. "Potential of insulin nanoparticle formulations for oral delivery and diabetes treatment." Journal of Controlled Release 264: 247-275.

Content is removed due to copyright restrictions. The publication can be accessed from https://www.sciencedirect.com/science/article/abs/pii/S0168365917308283.

Wong CY et al 2017. "Potential of insulin nanoparticle formulations for oral delivery and diabetes treatment." Journal of Controlled Release 264: 247-275.

Content is removed due to copyright restrictions. The publication can be accessed from https://www.sciencedirect.com/science/article/abs/pii/S0168365917308283.

Wong CY et al 2017. "Potential of insulin nanoparticle formulations for oral delivery and diabetes treatment." Journal of Controlled Release 264: 247-275.

Content is removed due to copyright restrictions. The publication can be accessed from https://www.sciencedirect.com/science/article/abs/pii/S0168365917308283.

Wong CY et al 2017. "Potential of insulin nanoparticle formulations for oral delivery and diabetes treatment." Journal of Controlled Release 264: 247-275.

Content is removed due to copyright restrictions. The publication can be accessed from https://www.sciencedirect.com/science/article/abs/pii/S0168365917308283.

Wong CY et al 2017. "Potential of insulin nanoparticle formulations for oral delivery and diabetes treatment." Journal of Controlled Release 264: 247-275.

Content is removed due to copyright restrictions. The publication can be accessed from https://www.sciencedirect.com/science/article/abs/pii/S0168365917308283.

Wong CY et al 2017. "Potential of insulin nanoparticle formulations for oral delivery and diabetes treatment." Journal of Controlled Release 264: 247-275.

Content is removed due to copyright restrictions. The publication can be accessed from https://www.sciencedirect.com/science/article/abs/pii/S0168365917308283.

Wong CY et al 2017. "Potential of insulin nanoparticle formulations for oral delivery and diabetes treatment." Journal of Controlled Release 264: 247-275.

Content is removed due to copyright restrictions. The publication can be accessed from https://www.sciencedirect.com/science/article/abs/pii/S0168365917308283.

Wong CY et al 2017. "Potential of insulin nanoparticle formulations for oral delivery and diabetes treatment." Journal of Controlled Release 264: 247-275.

Content is removed due to copyright restrictions. The publication can be accessed from https://www.sciencedirect.com/science/article/abs/pii/S0168365917308283.

Wong CY et al 2017. "Potential of insulin nanoparticle formulations for oral delivery and diabetes treatment." Journal of Controlled Release 264: 247-275.

Content is removed due to copyright restrictions. The publication can be accessed from https://www.sciencedirect.com/science/article/abs/pii/S0168365917308283.

Wong CY et al 2017. "Potential of insulin nanoparticle formulations for oral delivery and diabetes treatment." Journal of Controlled Release 264: 247-275.

Chapter 3: Microparticles, microcapsules and microspheres: a review of recent developments and prospects for oral delivery of insulin

Wong CY et al 2018. "Microparticles, microcapsules and microspheres: a review of recent developments and prospects for oral delivery of insulin." International Journal of Pharmaceutics 537 (1-2): 223-244.

https://doi.org/10.1016/j.ijpharm.2017.12.036

https://www.sciencedirect.com/science/article/pii/S0378517317311808

*This paper has been reproduced in accordance with the publisher's policy (Appendix B2).

Acknowledgement: The Version of Record of this manuscript has been published and was made available in International Journal of Pharmaceutics on thr 15th February 2018 (https://www.sciencedirect.com/science/article/pii/S0378517317311808).

Contents
1 Introduction
2 Microparticulate delivery system for oral insulin administration
2.1 Insulin-loaded natural polymeric microparticles
2.1.1 Chitosan-based insulin-loaded microparticles
2.1.2 Dextran-based insulin-loaded microparticles
2.1.3 Alginate-based insulin-loaded microparticles
2.1.4 PLGA-based insulin-loaded microparticles
2.1.5 Other insulin-loaded polymeric microparticles
3 Insulin-loaded inorganic microparticles
4 Colon-targeting bioadhesive microparticles
5 Hydrogel-based insulin-loaded microparticles
5.1 Alginate/whey insulin-loaded hydrogel microparticles
5.2 Poly(methacylic acid) (PMAA)-based insulin-loaded hydrogel microparticles
5.2.1 Poly(methacylic acid-co-N-vinyl pyrrolidone) (P(MAA-co-NVP))-based insulin-loaded hydrogel microparticles
5.2.2 Poly(N-vinylcaprolactam-co-methacrylic acid) (P(PVCL-co-MAA))-based

1. Declaration of attribution by the candidate

I, Chun Yuen Jerry Wong, as the first author of the publication entitled "Microparticles, microcapsules and microspheres: a review of recent developments and prospects for oral delivery of insulin", declare that this work was primarily designed, experimentally executed, interpreted, and written by the first author of this manuscript.

Name	Manuscript preparation	Manuscript editing	Final Approval
Chun Yuen Jerry Wong	x	x	x
Dr Hani Al-Salami		x	x
Professor Crispin Dass		x	x

I acknowledge that these represent my contribution to the above research output.

Signature:

Date: 11th September 2020

Co-authors:

Dr Hani Al-Salami	**Professor Crispin Dass**
Signature:	Signature:
Date:	Date:

2. Summary and aims of the chapter

In this chapter, the current status of microparticles, hydrogel-based microparticles, microcapsules and microspheres for oral administration of insulin were examined. The following strategies, which included layer-by-layer coating, self-polymerisation of shell, and nanocomposite microparticulate drug delivery systems have been developed to enhance the oral bioavailability of insulin. This chapter illustrates the various challenges that will have to be addressed towards optimising the properties of insulin-loaded microparticles in future. This will be crucial in enhancing the therapeutic effects of formulations.

3. Sub-objectives of chapter 3

The first objective of the thesis is to identify and optimise the physicochemical characteristics (size, zeta potential, morphology, entrapment efficiency, loading efficiency and drug release behaviour) of the developed insulin-loaded nanoparticles. Therefore, it is crucial to understand the currently available insulin-loaded micron-sized and submicron sized drug delivery systems (e.g. microparticles, liposomes) in order to make comparison with the novel formulations, as well as to draw a conclusion and recognise the challenges that have to be addressed in future studies. The sub-objectives of chapter 3 are listed below:

- To assess the difference in physicochemical properties between insulin-loaded nanoparticulate systems and microparticulate systems.

- To examine the current status of microparticles, hydrogel-based microparticles, microcapsules and microspheres for oral administration of insulin.
- To understand the formulation barriers and physiological barriers that are associated with the development of oral insulin microparticulate systems.

4. Manuscript

Content is removed due to copyright restrictions. The publication can be accessed from https://www.sciencedirect.com/science/article/pii/S0378517317311808.

Wong CY et al 2018. "Microparticles, microcapsules and microspheres: a review of recent developments and prospects for oral delivery of insulin." International Journal of Pharmaceutics 537 (1-2): 223-244.

Content is removed due to copyright restrictions. The publication can be accessed from https://www.sciencedirect.com/science/article/pii/S0378517317311808.

Wong CY et al 2018. "Microparticles, microcapsules and microspheres: a review of recent developments and prospects for oral delivery of insulin." International Journal of Pharmaceutics 537 (1-2): 223-244.

Content is removed due to copyright restrictions. The publication can be accessed from https://www.sciencedirect.com/science/article/pii/S0378517317311808.

Wong CY et al 2018. "Microparticles, microcapsules and microspheres: a review of recent developments and prospects for oral delivery of insulin." International Journal of Pharmaceutics 537 (1-2): 223-244.

Content is removed due to copyright restrictions. The publication can be accessed from https://www.sciencedirect.com/science/article/pii/S0378517317311808.

Wong CY et al 2018. "Microparticles, microcapsules and microspheres: a review of recent developments and prospects for oral delivery of insulin." International Journal of Pharmaceutics 537 (1-2): 223-244.

Content is removed due to copyright restrictions. The publication can be accessed from https://www.sciencedirect.com/science/article/pii/S0378517317311808.

Wong CY et al 2018. "Microparticles, microcapsules and microspheres: a review of recent developments and prospects for oral delivery of insulin." International Journal of Pharmaceutics 537 (1-2): 223-244.

Content is removed due to copyright restrictions. The publication can be accessed from https://www.sciencedirect.com/science/article/pii/S0378517317311808.

Wong CY et al 2018. "Microparticles, microcapsules and microspheres: a review of recent developments and prospects for oral delivery of insulin." International Journal of Pharmaceutics 537 (1-2): 223-244.

Content is removed due to copyright restrictions. The publication can be accessed from https://www.sciencedirect.com/science/article/pii/S0378517317311808.

Wong CY et al 2018. "Microparticles, microcapsules and microspheres: a review of recent developments and prospects for oral delivery of insulin." International Journal of Pharmaceutics 537 (1-2): 223-244.

Content is removed due to copyright restrictions. The publication can be accessed from https://www.sciencedirect.com/science/article/pii/S0378517317311808.

Wong CY et al 2018. "Microparticles, microcapsules and microspheres: a review of recent developments and prospects for oral delivery of insulin." International Journal of Pharmaceutics 537 (1-2): 223-244.

Content is removed due to copyright restrictions. The publication can be accessed from https://www.sciencedirect.com/science/article/pii/S0378517317311808.

Wong CY et al 2018. "Microparticles, microcapsules and microspheres: a review of recent developments and prospects for oral delivery of insulin." International Journal of Pharmaceutics 537 (1-2): 223-244.

Content is removed due to copyright restrictions. The publication can be accessed from https://www.sciencedirect.com/science/article/pii/S0378517317311808.

Wong CY et al 2018. "Microparticles, microcapsules and microspheres: a review of recent developments and prospects for oral delivery of insulin." International Journal of Pharmaceutics 537 (1-2): 223-244.

Content is removed due to copyright restrictions. The publication can be accessed from https://www.sciencedirect.com/science/article/pii/S0378517317311808.

Wong CY et al 2018. "Microparticles, microcapsules and microspheres: a review of recent developments and prospects for oral delivery of insulin." International Journal of Pharmaceutics 537 (1-2): 223-244.

Content is removed due to copyright restrictions. The publication can be accessed from https://www.sciencedirect.com/science/article/pii/S0378517317311808.

Wong CY et al 2018. "Microparticles, microcapsules and microspheres: a review of recent developments and prospects for oral delivery of insulin." International Journal of Pharmaceutics 537 (1-2): 223-244.

Content is removed due to copyright restrictions. The publication can be accessed from https://www.sciencedirect.com/science/article/pii/S0378517317311808.

Wong CY et al 2018. "Microparticles, microcapsules and microspheres: a review of recent developments and prospects for oral delivery of insulin." International Journal of Pharmaceutics 537 (1-2): 223-244.

Content is removed due to copyright restrictions. The publication can be accessed from https://www.sciencedirect.com/science/article/pii/S0378517317311808.

Wong CY et al 2018. "Microparticles, microcapsules and microspheres: a review of recent developments and prospects for oral delivery of insulin." International Journal of Pharmaceutics 537 (1-2): 223-244.

Content is removed due to copyright restrictions. The publication can be accessed from https://www.sciencedirect.com/science/article/pii/S0378517317311808.

Wong CY et al 2018. "Microparticles, microcapsules and microspheres: a review of recent developments and prospects for oral delivery of insulin." International Journal of Pharmaceutics 537 (1-2): 223-244.

Content is removed due to copyright restrictions. The publication can be accessed from https://www.sciencedirect.com/science/article/pii/S0378517317311808.

Wong CY et al 2018. "Microparticles, microcapsules and microspheres: a review of recent developments and prospects for oral delivery of insulin." International Journal of Pharmaceutics 537 (1-2): 223-244.

Content is removed due to copyright restrictions. The publication can be accessed from https://www.sciencedirect.com/science/article/pii/S0378517317311808.

Wong CY et al 2018. "Microparticles, microcapsules and microspheres: a review of recent developments and prospects for oral delivery of insulin." International Journal of Pharmaceutics 537 (1-2): 223-244.

Content is removed due to copyright restrictions. The publication can be accessed from https://www.sciencedirect.com/science/article/pii/S0378517317311808.

Wong CY et al 2018. "Microparticles, microcapsules and microspheres: a review of recent developments and prospects for oral delivery of insulin." International Journal of Pharmaceutics 537 (1-2): 223-244.

Content is removed due to copyright restrictions. The publication can be accessed from https://www.sciencedirect.com/science/article/pii/S0378517317311808.

Wong CY et al 2018. "Microparticles, microcapsules and microspheres: a review of recent developments and prospects for oral delivery of insulin." International Journal of Pharmaceutics 537 (1-2): 223-244.

Content is removed due to copyright restrictions. The publication can be accessed from https://www.sciencedirect.com/science/article/pii/S0378517317311808.

Wong CY et al 2018. "Microparticles, microcapsules and microspheres: a review of recent developments and prospects for oral delivery of insulin." International Journal of Pharmaceutics 537 (1-2): 223-244.

Content is removed due to copyright restrictions. The publication can be accessed from https://www.sciencedirect.com/science/article/pii/S0378517317311808.

Wong CY et al 2018. "Microparticles, microcapsules and microspheres: a review of recent developments and prospects for oral delivery of insulin." International Journal of Pharmaceutics 537 (1-2): 223-244.

Content is removed due to copyright restrictions. The publication can be accessed from https://www.sciencedirect.com/science/article/pii/S0378517317311808.

Wong CY et al 2018. "Microparticles, microcapsules and microspheres: a review of recent developments and prospects for oral delivery of insulin." International Journal of Pharmaceutics 537 (1-2): 223-244.

Chapter 4: Recent advancements in oral administration of insulin-loaded liposomal drug delivery systems for diabetes mellitus

Wong CY et al 2018. "Recent advancements in oral administration of insulin-loaded liposomal drug delivery systems for diabetes mellitus." International Journal of Pharmaceutics 549 (1-2): 201-217.

https://doi.org/10.1016/j.ijpharm.2018.07.041

https://www.sciencedirect.com/science/article/pii/S0378517318305167

*This paper has been reproduced in accordance with the publisher's policy (Appendix B3).

Acknowledgement: The Version of Record of this manuscript has been published and was made available in International Journal of Pharmaceutics on the 5th October 2018 (https://www.sciencedirect.com/science/article/pii/S0378517318305167).

Contents
1 Introduction
2 Insulin-loaded liposome and its composition
3 Conventional liposomes
4 Surface-coating liposomes
4.1 Natural polymeric-coated liposomes
4.2 Silica nanoparticles-coated liposomes
4.3 PEG or mucin-coated liposomes
5 Cell-specific targeting liposomes
5.1 Biotin-modified liposomes
5.2 Folic acid-modified liposomes
5.3 Lectin-modified liposomes
6 Bile salt-containing liposomes
6.1 Sodium deoxycholate
6.2 Sodium taurocholate
6.3 Sodium glycocholate
7 Botanic sterol-containing liposomes

1. Declaration of attribution by the candidate

I, Chun Yuen Jerry Wong, as the first author of the publication entitled "Recent advancements in oral administration of insulin-loaded liposomal drug delivery systems for diabetes mellitus", declare that this work was primarily designed, experimentally executed, interpreted, and written by the first author of this manuscript.

Name	Manuscript preparation	Manuscript editing	Final Approval
Chun Yuen Jerry Wong	x	x	x
Dr Hani Al-Salami		x	x
Professor Crispin Dass		x	x

I acknowledge that these represent my contribution to the above research output.

Signature:

Date: 11th September 2020

Co-authors:

Dr Hani Al-Salami	**Professor Crispin Dass**
Signature:	Signature:
Date:	Date:

2. Summary and aims of the chapter

In this chapter, the current status of liposomes for oral administration of insulin was examined. Liposomal formulations have gained attention due to their versatility, biocompatibility, protective effect against enzymatic degradation, and cell-specific targeting. The state of art of 7 classes of novel liposomal formulations and conventional liposomal formulation was assessed. The strategies and prospects for improving the oral bioavailability of insulin-loaded liposomal formulations in the future studies were discussed.

3. Sub-objectives of chapter 4

The first objective of the thesis is to identify and optimise the physicochemical characteristics (size, zeta potential, morphology, entrapment efficiency, loading efficiency and drug release behaviour) of the developed insulin-loaded nanoparticles. Therefore, it is crucial to understand the currently available insulin-loaded drug delivery systems (e.g. microparticles, liposomes) in order to make comparison with the novel formulations, as well as draw a conclusion and recognise the challenges that have to be addressed in future studies. The sub-objectives of chapter 4 are listed below:

- To assess the difference in physicochemical properties between insulin-loaded nanoparticulate systems and liposomal systems.
- To examine the *status quo* of conventional liposomal formulation and 7 classes of novel liposomal formulations (surface-coating liposomes, cell-specific targeting liposomes, bile salt-containing liposomes, botanic sterol-containing

liposomes, double liposomes, proliposomes, archaeosomes) for oral administration of insulin.

- To understand the formulation barriers and physiological barriers that are associated with the development of oral insulin liposomal systems.

4. Manuscript

Content is removed due to copyright restrictions. The publication can be accessed from https://www.sciencedirect.com/science/article/pii/S0378517318305167.

Wong CY et al 2018. "Recent advancements in oral administration of insulin-loaded liposomal drug delivery systems for diabetes mellitus." International Journal of Pharmaceutics 549 (1-2): 201-217.

Content is removed due to copyright restrictions. The publication can be accessed from https://www.sciencedirect.com/science/article/pii/S0378517318305167.

Wong CY et al 2018. "Recent advancements in oral administration of insulin-loaded liposomal drug delivery systems for diabetes mellitus." International Journal of Pharmaceutics 549 (1-2): 201-217.

Content is removed due to copyright restrictions. The publication can be accessed from https://www.sciencedirect.com/science/article/pii/S0378517318305167.

Wong CY et al 2018. "Recent advancements in oral administration of insulin-loaded liposomal drug delivery systems for diabetes mellitus." International Journal of Pharmaceutics 549 (1-2): 201-217.

Content is removed due to copyright restrictions. The publication can be accessed from https://www.sciencedirect.com/science/article/pii/S0378517318305167.

Wong CY et al 2018. "Recent advancements in oral administration of insulin-loaded liposomal drug delivery systems for diabetes mellitus." International Journal of Pharmaceutics 549 (1-2): 201-217.

Content is removed due to copyright restrictions. The publication can be accessed from https://www.sciencedirect.com/science/article/pii/S0378517318305167.

Wong CY et al 2018. "Recent advancements in oral administration of insulin-loaded liposomal drug delivery systems for diabetes mellitus." International Journal of Pharmaceutics 549 (1-2): 201-217.

Content is removed due to copyright restrictions. The publication can be accessed from https://www.sciencedirect.com/science/article/pii/S0378517318305167.

Wong CY et al 2018. "Recent advancements in oral administration of insulin-loaded liposomal drug delivery systems for diabetes mellitus." International Journal of Pharmaceutics 549 (1-2): 201-217.

Content is removed due to copyright restrictions. The publication can be accessed from https://www.sciencedirect.com/science/article/pii/S0378517318305167.

Wong CY et al 2018. "Recent advancements in oral administration of insulin-loaded liposomal drug delivery systems for diabetes mellitus." International Journal of Pharmaceutics 549 (1-2): 201-217.

Content is removed due to copyright restrictions. The publication can be accessed from https://www.sciencedirect.com/science/article/pii/S0378517318305167.

Wong CY et al 2018. "Recent advancements in oral administration of insulin-loaded liposomal drug delivery systems for diabetes mellitus." International Journal of Pharmaceutics 549 (1-2): 201-217.

Content is removed due to copyright restrictions. The publication can be accessed from https://www.sciencedirect.com/science/article/pii/S0378517318305167.

Wong CY et al 2018. "Recent advancements in oral administration of insulin-loaded liposomal drug delivery systems for diabetes mellitus." International Journal of Pharmaceutics 549 (1-2): 201-217.

Content is removed due to copyright restrictions. The publication can be accessed from https://www.sciencedirect.com/science/article/pii/S0378517318305167.

Wong CY et al 2018. "Recent advancements in oral administration of insulin-loaded liposomal drug delivery systems for diabetes mellitus." International Journal of Pharmaceutics 549 (1-2): 201-217.

Content is removed due to copyright restrictions. The publication can be accessed from https://www.sciencedirect.com/science/article/pii/S0378517318305167.

Wong CY et al 2018. "Recent advancements in oral administration of insulin-loaded liposomal drug delivery systems for diabetes mellitus." International Journal of Pharmaceutics 549 (1-2): 201-217.

Content is removed due to copyright restrictions. The publication can be accessed from https://www.sciencedirect.com/science/article/pii/S0378517318305167.

Wong CY et al 2018. "Recent advancements in oral administration of insulin-loaded liposomal drug delivery systems for diabetes mellitus." International Journal of Pharmaceutics 549 (1-2): 201-217.

Content is removed due to copyright restrictions. The publication can be accessed from https://www.sciencedirect.com/science/article/pii/S0378517318305167.

Wong CY et al 2018. "Recent advancements in oral administration of insulin-loaded liposomal drug delivery systems for diabetes mellitus." International Journal of Pharmaceutics 549 (1-2): 201-217.

Content is removed due to copyright restrictions. The publication can be accessed from https://www.sciencedirect.com/science/article/pii/S0378517318305167.

Wong CY et al 2018. "Recent advancements in oral administration of insulin-loaded liposomal drug delivery systems for diabetes mellitus." International Journal of Pharmaceutics 549 (1-2): 201-217.

Content is removed due to copyright restrictions. The publication can be accessed from https://www.sciencedirect.com/science/article/pii/S0378517318305167.

Wong CY et al 2018. "Recent advancements in oral administration of insulin-loaded liposomal drug delivery systems for diabetes mellitus." International Journal of Pharmaceutics 549 (1-2): 201-217.

Content is removed due to copyright restrictions. The publication can be accessed from https://www.sciencedirect.com/science/article/pii/S0378517318305167.

Wong CY et al 2018. "Recent advancements in oral administration of insulin-loaded liposomal drug delivery systems for diabetes mellitus." International Journal of Pharmaceutics 549 (1-2): 201-217.

Content is removed due to copyright restrictions. The publication can be accessed from https://www.sciencedirect.com/science/article/pii/S0378517318305167.

Wong CY et al 2018. "Recent advancements in oral administration of insulin-loaded liposomal drug delivery systems for diabetes mellitus." International Journal of Pharmaceutics 549 (1-2): 201-217.

Chapter 5: Bio-nanotechnological advancement of orally administered insulin nanoparticles: comprehensive review of experimental design for physicochemical characterisation

Wong CY et al 2019. "Bio-nanotechnological advancement of orally administered insulin nanoparticles: comprehensive review of experimental design for physicochemical characterization." International Journal of Pharmaceutics 572: 118720.

https://doi.org/10.1016/j.ijpharm.2019.118720

https://www.sciencedirect.com/science/article/pii/S0378517319307653

#Supplementary data is available in appendix 4.1.

*This paper has been reproduced in accordance with the publisher's policy (Appendix B4.2).

Acknowledgement: The Version of Record of this manuscript has been published and was made available in International Journal of Pharmaceutics on the 9th September 2019 (https://www.sciencedirect.com/science/article/pii/S0378517319307653).

Contents
1 Introduction
1.1 Physical examination of nanoparticles
2 Encapsulation efficiency and drug loading efficiency of nanoparticles
2.1 Measurement of encapsulation efficiency and loading capacity
3 Size of protein-based nanoparticles
3.1 Factors influencing size of protein-based nanoparticles
3.2 Size measurement of protein-based nanoparticles
3.3 Polydispersity of protein-based nanoparticles
4 Zeta potential measurement of protein-based nanoparticles
5 Morphological examination of protein-based nanoparticles
5.1 Transmission electron microscopy
5.2 Scanning electron microscopy

1. Declaration of attribution by the candidate

I, Chun Yuen Jerry Wong, as the first author of the publication entitled "Bio-nanotechnological advancement of orally administered insulin nanoparticles: Comprehensive review of experimental design for physicochemical characterization", declare that this work was primarily designed, experimentally executed, interpreted, and written by the first author of this manuscript.

Name	Manuscript preparation	Manuscript editing	Final Approval
Chun Yuen Jerry Wong	x	x	x
Mr Giuseppe Luna		x	x
Mr Jorge Martinez		x	x
Dr Hani Al-Salami		x	x
Professor Crispin Dass		x	x

I acknowledge that these represent my contribution to the above research output.

Signature:

Date: 11th September 2020

Co-authors:

Mr Giuseppe Luna

Signature:

Date:

Mr Jorge Martinez

Signature:

Date:

Dr Hani Al-Salami

Signature:

Date:

Professor Crispin Dass

Signature:

Date:

2. Summary and aims of the chapter

Although several strategies have been developed to improve the stability and oral bioavailability of protein-loaded nanoparticles, their clinical translation remain limited. A well-designed experiment can facilitate the pharmaceutical development of the nanomedicine and reduce unwanted wastage in the research funding. Therefore, a comprehensive review on the experimental designs and conditions for **physical characterisation** of oral protein-loaded and insulin-loaded nanoparticles was conducted. In 2018, a consensus was made from the leading formulation scientists in "Minimum Information Reporting in Bio-Nano Experimental Literature" (Faria et al., 2018), which outlined the essential information that should be reported for physical characterisation of nano-formulations. These included size, shape, zeta potential, synthesis, composition, drug loading, drug release, size dispersity, labelling and independently varied properties. However, the experimental conditions and protocols for characterising the above physical properties can be absent and varied in the published research articles. In this chapter, the experimental conditions that were documented in approximately 200 research articles were examined. The tables in the manuscript and the supplementary material illustrate the experimental conditions for measurement of encapsulation efficiency, size, polydispersity index, zeta potential, morphology, drug release, interaction with mucin and stability of protein-loaded nanoparticles. This chapter provides a critical review, and examines the various experimental conditions and instrumentations that were utilised to examine protein encapsulation, size, polydispersity, morphology, protein release property, *in vitro* mucin interaction, and stability of protein-based nanoparticles. The instrumentations and assays that can be employed to assess the mucus diffusion capacity, stability and bioactivity of protein-based nanoparticles were reviewed. These included circular

dichroism, fourier transform infrared spectroscopy, X-ray diffractogram, UV spectroscopy, differential scanning calorimetry, fluorescence spectrum, Förster resonance energy transfer, NMR spectroscopy, Raman spectroscopy, cellular assays and animal models.

3. Sub-objectives of chapter 5

The first objective of the thesis is to identify and optimise the physicochemical characteristics (size, zeta potential, morphology, entrapment efficiency, loading efficiency and drug release behaviour) of the developed insulin-loaded nanoparticles. Prior to the initiation of research, it is integral to understand the essential information that should be reported in research publications, and establish a well-designed protocol for physical characterisation of nanoparticles. The sub-objectives of chapter 5 are listed below:

- To examine and review the experimental designs and conditions for physical characterisation of orally administered protein-loaded nanoparticles.
- To facilitate the research design and minimise wastage in research funding for physical characterisation of orally administered protein-loaded nanoparticles.
- To understand the instrumentations and assays that can be employed to assess the mucus diffusion capacity, stability and bioactivity of protein-loaded nanoparticles.

4. Manuscript

Content is removed due to copyright restrictions. The publication can be accessed from https://www.sciencedirect.com/science/article/pii/S0378517319307653.

Wong CY et al 2019. "Bio-nanotechnological advancement of orally administered insulin nanoparticles: comprehensive review of experimental design for physicochemical characterization." International Journal of Pharmaceutics 572: 118720.

Content is removed due to copyright restrictions. The publication can be accessed from https://www.sciencedirect.com/science/article/pii/S0378517319307653.

Wong CY et al 2019. "Bio-nanotechnological advancement of orally administered insulin nanoparticles: comprehensive review of experimental design for physicochemical characterization." International Journal of Pharmaceutics 572: 118720.

Content is removed due to copyright restrictions. The publication can be accessed from https://www.sciencedirect.com/science/article/pii/S0378517319307653.

Wong CY et al 2019. "Bio-nanotechnological advancement of orally administered insulin nanoparticles: comprehensive review of experimental design for physicochemical characterization." International Journal of Pharmaceutics 572: 118720.

Content is removed due to copyright restrictions. The publication can be accessed from https://www.sciencedirect.com/science/article/pii/S0378517319307653.

Wong CY et al 2019. "Bio-nanotechnological advancement of orally administered insulin nanoparticles: comprehensive review of experimental design for physicochemical characterization." International Journal of Pharmaceutics 572: 118720.

Content is removed due to copyright restrictions. The publication can be accessed from https://www.sciencedirect.com/science/article/pii/S0378517319307653.

Wong CY et al 2019. "Bio-nanotechnological advancement of orally administered insulin nanoparticles: comprehensive review of experimental design for physicochemical characterization." International Journal of Pharmaceutics 572: 118720.

Content is removed due to copyright restrictions. The publication can be accessed from https://www.sciencedirect.com/science/article/pii/S0378517319307653.

Wong CY et al 2019. "Bio-nanotechnological advancement of orally administered insulin nanoparticles: comprehensive review of experimental design for physicochemical characterization." International Journal of Pharmaceutics 572: 118720.

Content is removed due to copyright restrictions. The publication can be accessed from https://www.sciencedirect.com/science/article/pii/S0378517319307653.

Wong CY et al 2019. "Bio-nanotechnological advancement of orally administered insulin nanoparticles: comprehensive review of experimental design for physicochemical characterization." International Journal of Pharmaceutics 572: 118720.

Content is removed due to copyright restrictions. The publication can be accessed from https://www.sciencedirect.com/science/article/pii/S0378517319307653.

Wong CY et al 2019. "Bio-nanotechnological advancement of orally administered insulin nanoparticles: comprehensive review of experimental design for physicochemical characterization." International Journal of Pharmaceutics 572: 118720.

Content is removed due to copyright restrictions. The publication can be accessed from https://www.sciencedirect.com/science/article/pii/S0378517319307653.

Wong CY et al 2019. "Bio-nanotechnological advancement of orally administered insulin nanoparticles: comprehensive review of experimental design for physicochemical characterization." International Journal of Pharmaceutics 572: 118720.

Content is removed due to copyright restrictions. The publication can be accessed from https://www.sciencedirect.com/science/article/pii/S0378517319307653.

Wong CY et al 2019. "Bio-nanotechnological advancement of orally administered insulin nanoparticles: comprehensive review of experimental design for physicochemical characterization." International Journal of Pharmaceutics 572: 118720.

Content is removed due to copyright restrictions. The publication can be accessed from https://www.sciencedirect.com/science/article/pii/S0378517319307653.

Wong CY et al 2019. "Bio-nanotechnological advancement of orally administered insulin nanoparticles: comprehensive review of experimental design for physicochemical characterization." International Journal of Pharmaceutics 572: 118720.

Content is removed due to copyright restrictions. The publication can be accessed from https://www.sciencedirect.com/science/article/pii/S0378517319307653.

Wong CY et al 2019. "Bio-nanotechnological advancement of orally administered insulin nanoparticles: comprehensive review of experimental design for physicochemical characterization." International Journal of Pharmaceutics 572: 118720.

Content is removed due to copyright restrictions. The publication can be accessed from https://www.sciencedirect.com/science/article/pii/S0378517319307653.

Wong CY et al 2019. "Bio-nanotechnological advancement of orally administered insulin nanoparticles: comprehensive review of experimental design for physicochemical characterization." International Journal of Pharmaceutics 572: 118720.

Content is removed due to copyright restrictions. The publication can be accessed from https://www.sciencedirect.com/science/article/pii/S0378517319307653.

Wong CY et al 2019. "Bio-nanotechnological advancement of orally administered insulin nanoparticles: comprehensive review of experimental design for physicochemical characterization." International Journal of Pharmaceutics 572: 118720.

Content is removed due to copyright restrictions. The publication can be accessed from https://www.sciencedirect.com/science/article/pii/S0378517319307653.

Wong CY et al 2019. "Bio-nanotechnological advancement of orally administered insulin nanoparticles: comprehensive review of experimental design for physicochemical characterization." International Journal of Pharmaceutics 572: 118720.

Content is removed due to copyright restrictions. The publication can be accessed from https://www.sciencedirect.com/science/article/pii/S0378517319307653.

Wong CY et al 2019. "Bio-nanotechnological advancement of orally administered insulin nanoparticles: comprehensive review of experimental design for physicochemical characterization." International Journal of Pharmaceutics 572: 118720.

Content is removed due to copyright restrictions. The publication can be accessed from https://www.sciencedirect.com/science/article/pii/S0378517319307653.

Wong CY et al 2019. "Bio-nanotechnological advancement of orally administered insulin nanoparticles: comprehensive review of experimental design for physicochemical characterization." International Journal of Pharmaceutics 572: 118720.

Content is removed due to copyright restrictions. The publication can be accessed from https://www.sciencedirect.com/science/article/pii/S0378517319307653.

Wong CY et al 2019. "Bio-nanotechnological advancement of orally administered insulin nanoparticles: comprehensive review of experimental design for physicochemical characterization." International Journal of Pharmaceutics 572: 118720.

Content is removed due to copyright restrictions. The publication can be accessed from https://www.sciencedirect.com/science/article/pii/S0378517319307653.

Wong CY et al 2019. "Bio-nanotechnological advancement of orally administered insulin nanoparticles: comprehensive review of experimental design for physicochemical characterization." International Journal of Pharmaceutics 572: 118720.

Content is removed due to copyright restrictions. The publication can be accessed from https://www.sciencedirect.com/science/article/pii/S0378517319307653.

Wong CY et al 2019. "Bio-nanotechnological advancement of orally administered insulin nanoparticles: comprehensive review of experimental design for physicochemical characterization." International Journal of Pharmaceutics 572: 118720.

Content is removed due to copyright restrictions. The publication can be accessed from https://www.sciencedirect.com/science/article/pii/S0378517319307653.

Wong CY et al 2019. "Bio-nanotechnological advancement of orally administered insulin nanoparticles: comprehensive review of experimental design for physicochemical characterization." International Journal of Pharmaceutics 572: 118720.

Content is removed due to copyright restrictions. The publication can be accessed from https://www.sciencedirect.com/science/article/pii/S0378517319307653.

Wong CY et al 2019. "Bio-nanotechnological advancement of orally administered insulin nanoparticles: comprehensive review of experimental design for physicochemical characterization." International Journal of Pharmaceutics 572: 118720.

Content is removed due to copyright restrictions. The publication can be accessed from https://www.sciencedirect.com/science/article/pii/S0378517319307653.

Wong CY et al 2019. "Bio-nanotechnological advancement of orally administered insulin nanoparticles: comprehensive review of experimental design for physicochemical characterization." International Journal of Pharmaceutics 572: 118720.

Content is removed due to copyright restrictions. The publication can be accessed from https://www.sciencedirect.com/science/article/pii/S0378517319307653.

Wong CY et al 2019. "Bio-nanotechnological advancement of orally administered insulin nanoparticles: comprehensive review of experimental design for physicochemical characterization." International Journal of Pharmaceutics 572: 118720.

Content is removed due to copyright restrictions. The publication can be accessed from https://www.sciencedirect.com/science/article/pii/S0378517319307653.

Wong CY et al 2019. "Bio-nanotechnological advancement of orally administered insulin nanoparticles: comprehensive review of experimental design for physicochemical characterization." International Journal of Pharmaceutics 572: 118720.

Content is removed due to copyright restrictions. The publication can be accessed from https://www.sciencedirect.com/science/article/pii/S0378517319307653.

Wong CY et al 2019. "Bio-nanotechnological advancement of orally administered insulin nanoparticles: comprehensive review of experimental design for physicochemical characterization." International Journal of Pharmaceutics 572: 118720.

Content is removed due to copyright restrictions. The publication can be accessed from https://www.sciencedirect.com/science/article/pii/S0378517319307653.

Wong CY et al 2019. "Bio-nanotechnological advancement of orally administered insulin nanoparticles: comprehensive review of experimental design for physicochemical characterization." International Journal of Pharmaceutics 572: 118720.

Content is removed due to copyright restrictions. The publication can be accessed from https://www.sciencedirect.com/science/article/pii/S0378517319307653.

Wong CY et al 2019. "Bio-nanotechnological advancement of orally administered insulin nanoparticles: comprehensive review of experimental design for physicochemical characterization." International Journal of Pharmaceutics 572: 118720.

Content is removed due to copyright restrictions. The publication can be accessed from https://www.sciencedirect.com/science/article/pii/S0378517319307653.

Wong CY et al 2019. "Bio-nanotechnological advancement of orally administered insulin nanoparticles: comprehensive review of experimental design for physicochemical characterization." International Journal of Pharmaceutics 572: 118720.

Content is removed due to copyright restrictions. The publication can be accessed from https://www.sciencedirect.com/science/article/pii/S0378517319307653.

Wong CY et al 2019. "Bio-nanotechnological advancement of orally administered insulin nanoparticles: comprehensive review of experimental design for physicochemical characterization." International Journal of Pharmaceutics 572: 118720.

Chapter 6: Cellular assays and applied technologies for characterisation of orally administered protein nanoparticles: a systematic review

Wong CY et al 2020. "Cellular assays and applied technologies for characterization of orally administered protein nanoparticles: a systematic review." Journal of Drug Targeting 28 (6): 585-599.

https://doi.org/10.1080/1061186X.2020.1726356

https://www.tandfonline.com/doi/abs/10.1080/1061186X.2020.1726356

#Supplementary data is available in appendix 5.1.

*This paper has been reproduced in accordance with the publisher's policy (Appendix B5.2).

Acknowledgement: The Version of Record of this manuscript has been published and was made available in Journal of Drug Targeting on the 12th February 2020 (https://www.tandfonline.com/doi/abs/10.1080/1061186X.2020.1726356).

Contents
1 Introduction
2 Cell culture for characterisation of protein-loaded nanoparticles
2.1 Caco-2 cells (enterocytes)
2.2 HT-29 cells (goblet cells)
2.3 Caco-2/HT-29 co-culture and Caco-2/ HT-29-MTX/Raji B cells triple co-culture
3 GI cellular uptake studies for development of protein-loaded nanoparticles
3.1 Cellular uptake pathways of NPs
3.1.1 Paracellular absorption
3.1.2 Transcellular absorption
3.2 Technologies used for GI cellular uptake study
3.2.1 Wide-field fluorescence microscopy
3.2.2 CLSM
3.2.3 Flow cytometry

1. Declaration of attribution by the candidate

I, Chun Yuen Jerry Wong, as the first author of the publication entitled "Cellular assays and applied technologies for characterization of orally administered protein nanoparticles: a systematic review", declare that this work was primarily designed, experimentally executed, interpreted, and written by the first author of this manuscript.

Name	Manuscript preparation	Manuscript editing	Final Approval
Chun Yuen Jerry Wong	x	x	x
Dr Hani Al-Salami		x	x
Professor Crispin Dass		x	x

I acknowledge that these represent my contribution to the above research output.

Signature:

Date: 11th September 2020

Co-authors:

Dr Hani Al-Salami	**Professor Crispin Dass**
Signature:	Signature:
Date:	Date:

2. Summary and aims of the chapter

According to a recent published paper "Minimum Information Reporting in Bio-Nano Experimental Literature" (Faria et al., 2018), it was stated that the minimum information that should be reported for cellular characterisation of nano-formulations can be classified into cell seeding details, cell characterisation, cell line authentication, passage number, cell background signal, cell viability and culture dimensions. However, the experimental conditions and protocols for characterising the above properties can be absent and varied in the published research articles. Currently, there is an absence of comprehensive reviews on the experimental conditions for cellular characterisation of orally administered protein-loaded nanoparticles. To facilitate the clinical translation of protein-based nanomedicine, a comprehensive review on the experimental conditions for cellular characterisation of oral protein-loaded nanoparticles was conducted. In this chapter, the cellular assays and applied technologies for pharmaceutical development of orally administered protein nanoparticles were examined. This chapter provides a critical review and examines the various cellular assays and instrumentations that have been utilised to examine cell culture condition, cytotoxicity, cellular uptake, transepithelial transport, permeability, nanoparticle and peptide integrity during intracellular trafficking, endocytosis mechanism, and exocytosis mechanism of protein-based nanoparticles. All novel instrumentations and assays that are available to examine cellular uptake of protein-based nanoparticles were reviewed. These included CLSM, flow cytometry, ELISA, fluorescence microscopy, microplate reader, and transmission electron microscopy.

3. Sub-objectives of chapter 6

The fourth objective of the thesis is to identify if the developed insulin-loaded nanoparticles promote glucose consumption in skeletal muscle cells, and GI transportation or permeation in GI cell culture. Prior to the initiation of research, it is important to understand the essential information that should be reported in research project, and establish a well-designed protocol for cellular characterisation of nanoparticles. The sub-objectives of chapter 6 are listed below:

- To examine and review the experimental designs and conditions for cellular characterisation of orally administered protein-loaded nanoparticles.
- To facilitate the research design and minimise wastage in research funding for cellular characterisation of orally administered protein-loaded nanoparticles.
- To understand the instrumentations and assays that can be employed to assess the cell culture condition, cytotoxicity, cellular uptake, transepithelial transport, GI permeation, integrity of nanoparticle and peptide during intracellular trafficking, endocytosis mechanism, and exocytosis mechanism of protein-loaded nanoparticles.

4. Manuscript

Content is removed due to copyright restrictions. The publication can be accessed from https://www.tandfonline.com/doi/abs/10.1080/1061186X.2020.1726356.

Wong CY et al 2020. "Cellular assays and applied technologies for characterization of orally administered protein nanoparticles: a systematic review." Journal of Drug Targeting 28 (6): 585-599.

Content is removed due to copyright restrictions. The publication can be accessed from https://www.tandfonline.com/doi/abs/10.1080/1061186X.2020.1726356.

Wong CY et al 2020. "Cellular assays and applied technologies for characterization of orally administered protein nanoparticles: a systematic review." Journal of Drug Targeting 28 (6): 585-599.

Content is removed due to copyright restrictions. The publication can be accessed from https://www.tandfonline.com/doi/abs/10.1080/1061186X.2020.1726356.

Wong CY et al 2020. "Cellular assays and applied technologies for characterization of orally administered protein nanoparticles: a systematic review." Journal of Drug Targeting 28 (6): 585-599.

Content is removed due to copyright restrictions. The publication can be accessed from https://www.tandfonline.com/doi/abs/10.1080/1061186X.2020.1726356.

Wong CY et al 2020. "Cellular assays and applied technologies for characterization of orally administered protein nanoparticles: a systematic review." Journal of Drug Targeting 28 (6): 585-599.

Content is removed due to copyright restrictions. The publication can be accessed from https://www.tandfonline.com/doi/abs/10.1080/1061186X.2020.1726356.

Wong CY et al 2020. "Cellular assays and applied technologies for characterization of orally administered protein nanoparticles: a systematic review." Journal of Drug Targeting 28 (6): 585-599.

Content is removed due to copyright restrictions. The publication can be accessed from https://www.tandfonline.com/doi/abs/10.1080/1061186X.2020.1726356.

Wong CY et al 2020. "Cellular assays and applied technologies for characterization of orally administered protein nanoparticles: a systematic review." Journal of Drug Targeting 28 (6): 585-599.

Content is removed due to copyright restrictions. The publication can be accessed from https://www.tandfonline.com/doi/abs/10.1080/1061186X.2020.1726356.

Wong CY et al 2020. "Cellular assays and applied technologies for characterization of orally administered protein nanoparticles: a systematic review." Journal of Drug Targeting 28 (6): 585-599.

Content is removed due to copyright restrictions. The publication can be accessed from https://www.tandfonline.com/doi/abs/10.1080/1061186X.2020.1726356.

Wong CY et al 2020. "Cellular assays and applied technologies for characterization of orally administered protein nanoparticles: a systematic review." Journal of Drug Targeting 28 (6): 585-599.

Content is removed due to copyright restrictions. The publication can be accessed from https://www.tandfonline.com/doi/abs/10.1080/1061186X.2020.1726356.

Wong CY et al 2020. "Cellular assays and applied technologies for characterization of orally administered protein nanoparticles: a systematic review." Journal of Drug Targeting 28 (6): 585-599.

Content is removed due to copyright restrictions. The publication can be accessed from https://www.tandfonline.com/doi/abs/10.1080/1061186X.2020.1726356.

Wong CY et al 2020. "Cellular assays and applied technologies for characterization of orally administered protein nanoparticles: a systematic review." Journal of Drug Targeting 28 (6): 585-599.

Content is removed due to copyright restrictions. The publication can be accessed from https://www.tandfonline.com/doi/abs/10.1080/1061186X.2020.1726356.

Wong CY et al 2020. "Cellular assays and applied technologies for characterization of orally administered protein nanoparticles: a systematic review." Journal of Drug Targeting 28 (6): 585-599.

Content is removed due to copyright restrictions. The publication can be accessed from https://www.tandfonline.com/doi/abs/10.1080/1061186X.2020.1726356.

Wong CY et al 2020. "Cellular assays and applied technologies for characterization of orally administered protein nanoparticles: a systematic review." Journal of Drug Targeting 28 (6): 585-599.

Content is removed due to copyright restrictions. The publication can be accessed from https://www.tandfonline.com/doi/abs/10.1080/1061186X.2020.1726356.

Wong CY et al 2020. "Cellular assays and applied technologies for characterization of orally administered protein nanoparticles: a systematic review." Journal of Drug Targeting 28 (6): 585-599.

Content is removed due to copyright restrictions. The publication can be accessed from https://www.tandfonline.com/doi/abs/10.1080/1061186X.2020.1726356.

Wong CY et al 2020. "Cellular assays and applied technologies for characterization of orally administered protein nanoparticles: a systematic review." Journal of Drug Targeting 28 (6): 585-599.

Content is removed due to copyright restrictions. The publication can be accessed from https://www.tandfonline.com/doi/abs/10.1080/1061186X.2020.1726356.

Wong CY et al 2020. "Cellular assays and applied technologies for characterization of orally administered protein nanoparticles: a systematic review." Journal of Drug Targeting 28 (6): 585-599.

Chapter 7: Current status and applications of animal models in pre-clinical development of orally administered insulin-loaded nanoparticles

Wong CY et al 2020. "Current status and applications of animal models in pre-clinical development of orally administered insulin-loaded nanoparticles." Journal of Drug Targeting 1-22.

https://doi.org/10.1080/1061186X.2020.1759078

https://www.tandfonline.com/doi/abs/10.1080/1061186X.2020.1759078

#Supplementary data is available in appendix 6.1.

*This paper has been reproduced in accordance with the publisher's policy (Appendix B6.2).

Acknowledgement: The Version of Record of this manuscript has been published and was made available in Journal of Drug Targeting on the 29th April 2020 (https://www.tandfonline.com/doi/abs/10.1080/1061186X.2020.1759078).

Contents
1 Introduction
2 Intestinal absorption studies for orally administered insulin-loaded nanoparticles
2.1 *Ex vivo* intestinal absorption models
2.2 Ussing chamber
2.3 Fluorescence microscopy
2.4 Transmission electron microscopy
2.5 Confocal microscopy
3. Mucoadhesiveness study
4. Biocompatibility of insulin-loaded nanoparticles
4.1 Physical symptoms
4.2 Integrity of intestinal mucosa
4.3 Histological analysis
4.4 Oxidative stress
5 Biodistribution of insulin-loaded nanoparticles

1. Declaration of attribution by the candidate

I, Chun Yuen Jerry Wong, as the first author of the manuscript entitled "Current status and applications of animal models in pre-clinical development of orally administered insulin-loaded nanoparticles", declare that this work was primarily designed, experimentally executed, interpreted, and written by the first author of this manuscript.

Name	Manuscript preparation	Manuscript editing	Final Approval
Chun Yuen Jerry Wong	x	x	x
Dr Hani Al-Salami		x	x
Professor Crispin Dass		x	x

I acknowledge that these represent my contribution to the above research output.

Signature:

Date: 11th September 2020

Co-authors:

Dr Hani Al-Salami	**Professor Crispin Dass**
Signature:	Signature:
Date:	Date:

2. Summary and aims of the chapter

As documented in "Minimum Information Reporting in Bio-Nano Experimental Literature" (Faria et al., 2018), it was stated that the minimum information that should be reported for *in vivo* characterisation of nano-formulation can be classified into toxicity, administered dose, method of administration, imaging details, tissue mass, justification of biological model, and biological fluid characterization. To foster the clinical translation of nanomedicine, there is a need to conduct a comprehensive review on the experimental conditions for insulin-loaded nanoparticles. Reliable and robust characterisation is essential to verify the physiological interactions and therapeutic potential of protein-based nanoparticles. In this chapter, the experimental conditions, which were documented in approximately 150 research articles, were examined. This chapter examines the various experimental conditions and instrumentations that have been utilised to examine intestinal absorption efficacy, mucoadhesiveness capacity, biocompatibility (e.g. integrity of intestinal mucosa, histological analysis, oxidative stress, physical symptoms), biodistribution, and *in vivo* efficacy of protein-loaded nanoparticles. All novel instrumentations and assays that are available to examine the above properties, which include Ussing chamber, fluorescence microscope, transmission electron microscopy, confocal microscopy, small animal imaging system, and single-photon emission computed tomography, were examined. The strengths and limitations of the above techniques were discussed in this chapter.

3. Sub-objectives of chapter 7

Prior to the initiation of research, it is essential to understand the essential information that should be reported, and develop a well-designed protocol for *in vivo* characterisation of nanoparticles. The sub-objectives of chapter 7 are listed below:

- To examine and review the experimental designs and conditions for *in vivo* characterisation of orally administered protein-loaded nanoparticles.
- To facilitate the research design and minimise wastage in research funding for *in vivo* characterisation of orally administered protein-loaded nanoparticles.
- To understand the instrumentations and assays that can be employed to assess the intestinal absorption efficacy, mucoadhesiveness capacity, biocompatibility, biodistribution, and *in vivo* efficacy of protein-loaded nanoparticles.

4. Manuscript

Content is removed due to copyright restrictions. The publication can be accessed from https://www.tandfonline.com/doi/abs/10.1080/1061186X.2020.1759078.

Wong CY et al 2020. "Current status and applications of animal models in pre-clinical development of orally administered insulin-loaded nanoparticles." Journal of Drug Targeting 1-22.

Content is removed due to copyright restrictions. The publication can be accessed from https://www.tandfonline.com/doi/abs/10.1080/1061186X.2020.1759078.

Wong CY et al 2020. "Current status and applications of animal models in pre-clinical development of orally administered insulin-loaded nanoparticles." Journal of Drug Targeting 1-22.

Content is removed due to copyright restrictions. The publication can be accessed from https://www.tandfonline.com/doi/abs/10.1080/1061186X.2020.1759078.

Wong CY et al 2020. "Current status and applications of animal models in pre-clinical development of orally administered insulin-loaded nanoparticles." Journal of Drug Targeting 1-22.

Content is removed due to copyright restrictions. The publication can be accessed from https://www.tandfonline.com/doi/abs/10.1080/1061186X.2020.1759078.

Wong CY et al 2020. "Current status and applications of animal models in pre-clinical development of orally administered insulin-loaded nanoparticles." Journal of Drug Targeting 1-22.

Content is removed due to copyright restrictions. The publication can be accessed from https://www.tandfonline.com/doi/abs/10.1080/1061186X.2020.1759078.

Wong CY et al 2020. "Current status and applications of animal models in pre-clinical development of orally administered insulin-loaded nanoparticles." Journal of Drug Targeting 1-22.

Content is removed due to copyright restrictions. The publication can be accessed from https://www.tandfonline.com/doi/abs/10.1080/1061186X.2020.1759078.

Wong CY et al 2020. "Current status and applications of animal models in pre-clinical development of orally administered insulin-loaded nanoparticles." Journal of Drug Targeting 1-22.

Content is removed due to copyright restrictions. The publication can be accessed from https://www.tandfonline.com/doi/abs/10.1080/1061186X.2020.1759078.

Wong CY et al 2020. "Current status and applications of animal models in pre-clinical development of orally administered insulin-loaded nanoparticles." Journal of Drug Targeting 1-22.

Content is removed due to copyright restrictions. The publication can be accessed from https://www.tandfonline.com/doi/abs/10.1080/1061186X.2020.1759078.

Wong CY et al 2020. "Current status and applications of animal models in pre-clinical development of orally administered insulin-loaded nanoparticles." Journal of Drug Targeting 1-22.

Content is removed due to copyright restrictions. The publication can be accessed from https://www.tandfonline.com/doi/abs/10.1080/1061186X.2020.1759078.

Wong CY et al 2020. "Current status and applications of animal models in pre-clinical development of orally administered insulin-loaded nanoparticles." Journal of Drug Targeting 1-22.

Content is removed due to copyright restrictions. The publication can be accessed from https://www.tandfonline.com/doi/abs/10.1080/1061186X.2020.1759078.

Wong CY et al 2020. "Current status and applications of animal models in pre-clinical development of orally administered insulin-loaded nanoparticles." Journal of Drug Targeting 1-22.

Content is removed due to copyright restrictions. The publication can be accessed from https://www.tandfonline.com/doi/abs/10.1080/1061186X.2020.1759078.

Wong CY et al 2020. "Current status and applications of animal models in pre-clinical development of orally administered insulin-loaded nanoparticles." Journal of Drug Targeting 1-22.

Content is removed due to copyright restrictions. The publication can be accessed from https://www.tandfonline.com/doi/abs/10.1080/1061186X.2020.1759078.

Wong CY et al 2020. "Current status and applications of animal models in pre-clinical development of orally administered insulin-loaded nanoparticles." Journal of Drug Targeting 1-22.

Content is removed due to copyright restrictions. The publication can be accessed from https://www.tandfonline.com/doi/abs/10.1080/1061186X.2020.1759078.

Wong CY et al 2020. "Current status and applications of animal models in pre-clinical development of orally administered insulin-loaded nanoparticles." Journal of Drug Targeting 1-22.

Content is removed due to copyright restrictions. The publication can be accessed from https://www.tandfonline.com/doi/abs/10.1080/1061186X.2020.1759078.

Wong CY et al 2020. "Current status and applications of animal models in pre-clinical development of orally administered insulin-loaded nanoparticles." Journal of Drug Targeting 1-22.

Content is removed due to copyright restrictions. The publication can be accessed from https://www.tandfonline.com/doi/abs/10.1080/1061186X.2020.1759078.

Wong CY et al 2020. "Current status and applications of animal models in pre-clinical development of orally administered insulin-loaded nanoparticles." Journal of Drug Targeting 1-22.

Content is removed due to copyright restrictions. The publication can be accessed from https://www.tandfonline.com/doi/abs/10.1080/1061186X.2020.1759078.

Wong CY et al 2020. "Current status and applications of animal models in pre-clinical development of orally administered insulin-loaded nanoparticles." Journal of Drug Targeting 1-22.

Content is removed due to copyright restrictions. The publication can be accessed from https://www.tandfonline.com/doi/abs/10.1080/1061186X.2020.1759078.

Wong CY et al 2020. "Current status and applications of animal models in pre-clinical development of orally administered insulin-loaded nanoparticles." Journal of Drug Targeting 1-22.

Content is removed due to copyright restrictions. The publication can be accessed from https://www.tandfonline.com/doi/abs/10.1080/1061186X.2020.1759078.

Wong CY et al 2020. "Current status and applications of animal models in pre-clinical development of orally administered insulin-loaded nanoparticles." Journal of Drug Targeting 1-22.

Content is removed due to copyright restrictions. The publication can be accessed from https://www.tandfonline.com/doi/abs/10.1080/1061186X.2020.1759078.

Wong CY et al 2020. "Current status and applications of animal models in pre-clinical development of orally administered insulin-loaded nanoparticles." Journal of Drug Targeting 1-22.

Content is removed due to copyright restrictions. The publication can be accessed from https://www.tandfonline.com/doi/abs/10.1080/1061186X.2020.1759078.

Wong CY et al 2020. "Current status and applications of animal models in pre-clinical development of orally administered insulin-loaded nanoparticles." Journal of Drug Targeting 1-22.

Content is removed due to copyright restrictions. The publication can be accessed from https://www.tandfonline.com/doi/abs/10.1080/1061186X.2020.1759078.

Wong CY et al 2020. "Current status and applications of animal models in pre-clinical development of orally administered insulin-loaded nanoparticles." Journal of Drug Targeting 1-22.

Content is removed due to copyright restrictions. The publication can be accessed from https://www.tandfonline.com/doi/abs/10.1080/1061186X.2020.1759078.

Wong CY et al 2020. "Current status and applications of animal models in pre-clinical development of orally administered insulin-loaded nanoparticles." Journal of Drug Targeting 1-22.

Chapter 8: Fabrication techniques for the preparation of orally administered insulin nanoparticles

Wong CY et al 2020. "Fabrication techniques for the preparation of orally administered insulin nanoparticles." Journal of Drug Targeting.
https://www.tandfonline.com/doi/full/10.1080/1061186X.2020.1817042
https://doi.org/10.1080/1061186X.2020.1817042

*This paper has been reproduced in accordance with the publisher's policy (Appendix B7).

Acknowledgement: The Version of Record of this manuscript has been published and was made available in Journal of Drug Targeting on the 2nd September 2020 (https://www.tandfonline.com/doi/full/10.1080/1061186X.2020.1817042).

Contents
1 Introduction
2 Fabrication of insulin-loaded nanoparticles
2.1 Nanoprecipitation
2.2 Hydrophobic conjugation
2.3 Flash nanocomplexation
2.4 Double emulsion
2.4.1 Micelle-double emulsion
2.4.2 Double emulsion (solvent evaporation)
2.4.3 Hydrophobic ion pairing and emulsion solvent diffusion method
2.5 Ionotropic gelation
2.6 Layer-by-layer adsorption
2.7 Reduction
2.8 Complex coacervation
2.9 Sol-gel technology
3 Conclusion
4 Reference list

1. Declaration of attribution by the candidate

I, Chun Yuen Jerry Wong, as the first author of the publication entitled " Fabrication techniques for the preparation of orally administered insulin nanoparticles ", declare that this work was primarily designed, experimentally executed, interpreted, and written by the first author of this manuscript.

Name	Manuscript preparation	Manuscript editing	Final Approval
Chun Yuen Jerry Wong	x	x	x
Dr Hani Al-Salami		x	x
Professor Crispin Dass		x	x

I acknowledge that these represent my contribution to the above research output.

Signature:

Date: 11th September 2020

Co-authors:

Dr Hani Al-Salami	**Professor Crispin Dass**
Signature:	Signature:
Date:	Date:

2. Summary and aims of the chapter

Various techniques have been used to encapsulate the fragile therapeutic proteins *via* hydrophobic bonding and electrostatic interaction. These included nanoprecipitation, hydrophobic conjugation, flash nanocomplexation, double emulsion, ionotropic gelation, layer-by-layer adsorption, reduction, complex coacervation (polyelectrolyte complexation), hydrophobic ion pairing and emulsion solvent diffusion method, and sol-gel technology. A desirable technique should involve minimal harsh conditions and encapsulate therapeutic proteins with preserved functionalities. The current chapter examines the characteristics of each preparation technique, and illustrates the examples of insulin-loaded nanoparticles that have been developed in each fabrication method. This chapter also discusses the strategies that have been utilised during the formulation process to improve the stability and bioactivity of therapeutic proteins.

3. Sub-objectives of chapter 8

The second objective of the thesis is to examine the effect of preparation procedures on the physicochemical properties and bioactivity of insulin-loaded nanoparticles. Therefore, the techniques that have been employed to encapsulate the fragile therapeutic proteins should be understood. The sub-objectives of chapter 8 are listed below:

- To examine the techniques that are available for nano-encapsulation of insulin.
- To assess the characteristics of each preparation technique.
- To understand the strategies that have been utilised in each technique to improve the stability and bioactivity of formulations.

4. Manuscript

Content is removed due to copyright restrictions. The publication can be accessed from https://www.tandfonline.com/doi/full/10.1080/1061186X.2020.1817042.

Wong CY et al 2020. "Fabrication techniques for the preparation of orally administered insulin nanoparticles." Journal of Drug Targeting.

Content is removed due to copyright restrictions. The publication can be accessed from https://www.tandfonline.com/doi/full/10.1080/1061186X.2020.1817042.

Wong CY et al 2020. "Fabrication techniques for the preparation of orally administered insulin nanoparticles." Journal of Drug Targeting.

Content is removed due to copyright restrictions. The publication can be accessed from https://www.tandfonline.com/doi/full/10.1080/1061186X.2020.1817042.

Wong CY et al 2020. “Fabrication techniques for the preparation of orally administered insulin nanoparticles.” Journal of Drug Targeting.

Content is removed due to copyright restrictions. The publication can be accessed from https://www.tandfonline.com/doi/full/10.1080/1061186X.2020.1817042.

Wong CY et al 2020. "Fabrication techniques for the preparation of orally administered insulin nanoparticles." Journal of Drug Targeting.

Content is removed due to copyright restrictions. The publication can be accessed from https://www.tandfonline.com/doi/full/10.1080/1061186X.2020.1817042.

Wong CY et al 2020. "Fabrication techniques for the preparation of orally administered insulin nanoparticles." Journal of Drug Targeting.

Content is removed due to copyright restrictions. The publication can be accessed from https://www.tandfonline.com/doi/full/10.1080/1061186X.2020.1817042.

Wong CY et al 2020. “Fabrication techniques for the preparation of orally administered insulin nanoparticles.” Journal of Drug Targeting.

Content is removed due to copyright restrictions. The publication can be accessed from https://www.tandfonline.com/doi/full/10.1080/1061186X.2020.1817042.

Wong CY et al 2020. “Fabrication techniques for the preparation of orally administered insulin nanoparticles.” Journal of Drug Targeting.

Content is removed due to copyright restrictions. The publication can be accessed from https://www.tandfonline.com/doi/full/10.1080/1061186X.2020.1817042.

Wong CY et al 2020. "Fabrication techniques for the preparation of orally administered insulin nanoparticles." Journal of Drug Targeting.

Content is removed due to copyright restrictions. The publication can be accessed from https://www.tandfonline.com/doi/full/10.1080/1061186X.2020.1817042.

Wong CY et al 2020. “Fabrication techniques for the preparation of orally administered insulin nanoparticles.” Journal of Drug Targeting.

Content is removed due to copyright restrictions. The publication can be accessed from https://www.tandfonline.com/doi/full/10.1080/1061186X.2020.1817042.

Wong CY et al 2020. “Fabrication techniques for the preparation of orally administered insulin nanoparticles.” Journal of Drug Targeting.

Content is removed due to copyright restrictions. The publication can be accessed from https://www.tandfonline.com/doi/full/10.1080/1061186X.2020.1817042.

Wong CY et al 2020. “Fabrication techniques for the preparation of orally administered insulin nanoparticles.” Journal of Drug Targeting.

Content is removed due to copyright restrictions. The publication can be accessed from https://www.tandfonline.com/doi/full/10.1080/1061186X.2020.1817042.

Wong CY et al 2020. “Fabrication techniques for the preparation of orally administered insulin nanoparticles.” Journal of Drug Targeting.

Content is removed due to copyright restrictions. The publication can be accessed from https://www.tandfonline.com/doi/full/10.1080/1061186X.2020.1817042.

Wong CY et al 2020. “Fabrication techniques for the preparation of orally administered insulin nanoparticles.” Journal of Drug Targeting.

Content is removed due to copyright restrictions. The publication can be accessed from https://www.tandfonline.com/doi/full/10.1080/1061186X.2020.1817042.

Wong CY et al 2020. “Fabrication techniques for the preparation of orally administered insulin nanoparticles.” Journal of Drug Targeting.

Content is removed due to copyright restrictions. The publication can be accessed from https://www.tandfonline.com/doi/full/10.1080/1061186X.2020.1817042.

Wong CY et al 2020. "Fabrication techniques for the preparation of orally administered insulin nanoparticles." Journal of Drug Targeting.

Content is removed due to copyright restrictions. The publication can be accessed from https://www.tandfonline.com/doi/full/10.1080/1061186X.2020.1817042.

Wong CY et al 2020. “Fabrication techniques for the preparation of orally administered insulin nanoparticles.” Journal of Drug Targeting.

Content is removed due to copyright restrictions. The publication can be accessed from https://www.tandfonline.com/doi/full/10.1080/1061186X.2020.1817042.

Wong CY et al 2020. “Fabrication techniques for the preparation of orally administered insulin nanoparticles.” Journal of Drug Targeting.

Content is removed due to copyright restrictions. The publication can be accessed from https://www.tandfonline.com/doi/full/10.1080/1061186X.2020.1817042.

Wong CY et al 2020. “Fabrication techniques for the preparation of orally administered insulin nanoparticles.” Journal of Drug Targeting.

Content is removed due to copyright restrictions. The publication can be accessed from https://www.tandfonline.com/doi/full/10.1080/1061186X.2020.1817042.

Wong CY et al 2020. "Fabrication techniques for the preparation of orally administered insulin nanoparticles." Journal of Drug Targeting.

Content is removed due to copyright restrictions. The publication can be accessed from https://www.tandfonline.com/doi/full/10.1080/1061186X.2020.1817042.

Wong CY et al 2020. “Fabrication techniques for the preparation of orally administered insulin nanoparticles.” Journal of Drug Targeting.

Content is removed due to copyright restrictions. The publication can be accessed from https://www.tandfonline.com/doi/full/10.1080/1061186X.2020.1817042.

Wong CY et al 2020. “Fabrication techniques for the preparation of orally administered insulin nanoparticles.” Journal of Drug Targeting.

Content is removed due to copyright restrictions. The publication can be accessed from https://www.tandfonline.com/doi/full/10.1080/1061186X.2020.1817042.

Wong CY et al 2020. "Fabrication techniques for the preparation of orally administered insulin nanoparticles." Journal of Drug Targeting.

Chapter 9: The role of chitosan on oral delivery of peptide-loaded nanoparticle formulation

Wong CY et al 2017. "The role of chitosan on oral delivery of peptide-loaded nanoparticle formulation." Journal of Drug Targeting 26 (7): 551-562.

https://doi.org/10.1080/1061186X.2017.1400552

https://www.tandfonline.com/doi/abs/10.1080/1061186X.2017.1400552

*This paper has been reproduced in accordance with the publisher's policy (Appendix B8).

Acknowledgement: The Version of Record of this manuscript has been published and was made available in Journal of Drug Targeting on the 2nd November 2017 (http://www.tandfonline.com/ doi/full/10.1080/10.1080/1061186X.2017.1400552).

Contents
5.1 Introduction
5.2 Features of chitosan
5.3 Chitosan-based nanoparticles
5.4 Chitosan-coated and chitosan-conjugated nanoparticles
5.5 Oral chitosan-based peptide-loaded nanoparticles for pre-clinical use
5.5.1 Diabetes
5.5.2 *Salmonella Typhimurium* infection
5.5.3 Parasitic infection, cancer and osteoarthritis
5.5.4 Neurological disease
5.5.5 Liver regeneration
5.5.6 Osteoporosis
5.5.7 Febrile neutropenia
5.5.8 Enzyme insufficiency
5.6. Oral vaccination
5.6.1 Human vaccination
5.6.2 Aquaculture
5.7 Conclusion and future direction
5.8 Reference list

1. Declaration of attribution by the candidate

I, Chun Yuen Jerry Wong, as the first author of the publication entitled "The role of chitosan on oral delivery of peptide-loaded nanoparticle formulation", declare that this work was primarily designed, experimentally executed, interpreted, and written by the first author of this manuscript.

Name	Manuscript preparation	Manuscript editing	Final Approval
Chun Yuen Jerry Wong	x	x	x
Dr Hani Al-Salami		x	x
Professor Crispin Dass		x	x

I acknowledge that these represent my contribution to the above research output.

Signature:

Date: 11th September 2020

Co-authors:

Dr Hani Al-Salami	**Professor Crispin Dass**
Signature:	Signature:
Date:	Date:

2. Summary and aims of the chapter

Chitosan-based nanoparticles have gained phenomenal attention for oral vaccination and oral administration of peptides. Chitosan-based nanoparticles possess advantages including superior biocompatibility, controlled drug release profile, and enhanced gastrointestinal absorption. When peptides are encapsulated within the nanocarrier, the formulation can withstand enzymatic degradation and extreme pH. The gastrointestinal absorption of chitosan-based nanoparticles can be further facilitated by the transcellular pathway *via* ligand conjugation of the nanoparticle surface. This chapter discusses the features of chitosan-based nanoparticles, and identifies the potential clinical applications of peptide-loaded chitosan-based nanoparticles. A thorough understanding in the physical characteristics of chitosan-based nanoparticles will be beneficial for the optimisation of formulation in the research and development stages.

3. Sub-objectives of chapter 9

The third objective of the thesis is to examine if the chosen excipients and cryoprotectant can maintain the stability of insulin-loaded formulations. Therefore, the role, features and potential application of chitosan and chitosan-based nanoparticles should be understood. The sub-objectives of chapter 9 are listed below:

- To examine the features of chitosan and chitosan-based nanoparticles.
- To assess the potential pre-clinical applications of peptide-loaded chitosan-based nanoparticles.

- To evaluate the current status and development of oral vaccination by using protein or peptide-loaded chitosan-based nanoparticles.

4. Manuscript

Content is removed due to copyright restrictions. The publication can be accessed from https://www.tandfonline.com/doi/abs/10.1080/1061186X.2017.1400552.

Wong CY et al 2017. "The role of chitosan on oral delivery of peptide-loaded nanoparticle formulation." Journal of Drug Targeting 26 (7): 551-562.

Content is removed due to copyright restrictions. The publication can be accessed from

https://www.tandfonline.com/doi/abs/10.1080/1061186X.2017.1400552.

Wong CY et al 2017. "The role of chitosan on oral delivery of peptide-loaded nanoparticle formulation." Journal of Drug Targeting 26 (7): 551-562.

Content is removed due to copyright restrictions. The publication can be accessed from

https://www.tandfonline.com/doi/abs/10.1080/1061186X.2017.1400552.

Wong CY et al 2017. "The role of chitosan on oral delivery of peptide-loaded nanoparticle formulation." Journal of Drug Targeting 26 (7): 551-562.

Content is removed due to copyright restrictions. The publication can be accessed from

https://www.tandfonline.com/doi/abs/10.1080/1061186X.2017.1400552.

Wong CY et al 2017. "The role of chitosan on oral delivery of peptide-loaded nanoparticle formulation." Journal of Drug Targeting 26 (7): 551-562.

Content is removed due to copyright restrictions. The publication can be accessed from

https://www.tandfonline.com/doi/abs/10.1080/1061186X.2017.1400552.

Wong CY et al 2017. "The role of chitosan on oral delivery of peptide-loaded nanoparticle formulation." Journal of Drug Targeting 26 (7): 551-562.

Content is removed due to copyright restrictions. The publication can be accessed from

https://www.tandfonline.com/doi/abs/10.1080/1061186X.2017.1400552.

Wong CY et al 2017. "The role of chitosan on oral delivery of peptide-loaded nanoparticle formulation." Journal of Drug Targeting 26 (7): 551-562.

Content is removed due to copyright restrictions. The publication can be accessed from

https://www.tandfonline.com/doi/abs/10.1080/1061186X.2017.1400552.

Wong CY et al 2017. "The role of chitosan on oral delivery of peptide-loaded nanoparticle formulation." Journal of Drug Targeting 26 (7): 551-562.

Content is removed due to copyright restrictions. The publication can be accessed from

https://www.tandfonline.com/doi/abs/10.1080/1061186X.2017.1400552.

Wong CY et al 2017. "The role of chitosan on oral delivery of peptide-loaded nanoparticle formulation." Journal of Drug Targeting 26 (7): 551-562.

Content is removed due to copyright restrictions. The publication can be accessed from

https://www.tandfonline.com/doi/abs/10.1080/1061186X.2017.1400552.

Wong CY et al 2017. "The role of chitosan on oral delivery of peptide-loaded nanoparticle formulation." Journal of Drug Targeting 26 (7): 551-562.

Content is removed due to copyright restrictions. The publication can be accessed from

https://www.tandfonline.com/doi/abs/10.1080/1061186X.2017.1400552.

Wong CY et al 2017. "The role of chitosan on oral delivery of peptide-loaded nanoparticle formulation." Journal of Drug Targeting 26 (7): 551-562.

Content is removed due to copyright restrictions. The publication can be accessed from

https://www.tandfonline.com/doi/abs/10.1080/1061186X.2017.1400552.

Wong CY et al 2017. "The role of chitosan on oral delivery of peptide-loaded nanoparticle formulation." Journal of Drug Targeting 26 (7): 551-562.

Content is removed due to copyright restrictions. The publication can be accessed from

https://www.tandfonline.com/doi/abs/10.1080/1061186X.2017.1400552.

Wong CY et al 2017. "The role of chitosan on oral delivery of peptide-loaded nanoparticle formulation." Journal of Drug Targeting 26 (7): 551-562.

Chapter 10: C2C12 cell model: its role in understanding of insulin resistance at the molecular level and pharmaceutical development at the pre-clinical stage

Wong CY et al 2020. "C2C12 cell model: its role in understanding of insulin resistance at the molecular level and pharmaceutical development at the pre-clinical stage." Journal of Pharmacy and Pharmacology.

https://doi.org/10.1111/jphp.13359

https://onlinelibrary.wiley.com/doi/full/10.1111/jphp.13359

*This paper has been reproduced in accordance with the publisher's policy (Appendix B9.2).

Acknowledgement: The Version of Record of this manuscript has been published and was made available in Journal of Pharmacy and Pharmacology on the 18th August 2020 (https://onlinelibrary.wiley.com/doi/full/10.1111/jphp.13359).

Contents

1. Declaration of attribution by the candidate

I, Chun Yuen Jerry Wong, as the first author of the manuscript entitled "C2C12 cell model: its role in understanding of insulin resistance at the molecular level and pharmaceutical development at the pre-clinical stage", declare that this work was primarily designed, experimentally executed, interpreted, and written by the first author of this manuscript.

Name	Manuscript preparation	Manuscript editing	Final Approval
Chun Yuen Jerry Wong	x	x	x
Dr Hani Al-Salami		x	x
Professor Crispin Dass		x	x

I acknowledge that these represent my contribution to the above research output.

Signature:

Date: 11th September 2020

Co-authors:

Dr Hani Al-Salami	**Professor Crispin Dass**
Signature:	Signature:
Date:	Date:

2. Summary and aims of the chapter

In this chapter, a comprehensive review on C2C12 cell model was conducted. C2C12 cell model has been employed in the understanding of insulin resistance progression, as well as pharmaceutical development of drug compounds and traditional herbs. The use of C2C12 cell model has strengthened our understanding in glucose metabolism, insulin signaling mechanism, insulin resistance, oxidative stress, reactive oxygen species, and glucose transporters at cellular and molecular levels. In this chapter, approximately 200 research articles were reviewed. A number of studies that utilised C2C12 cell model demonstrated that the following metabolic diseases, including diabetes mellitus, obesity, hyperlipidaemia, muscle atrophy, impaired growth, and hepatic steatosis, have close relationships in terms of disease progression, pathogenesis and therapeutic management. This chapter provides a critical review on the application of C2C12 model for the pharmaceutical development of novel therapeutic agents that can elicit therapeutic effects at both cellular (e.g. mitochondria, glucose transporter) and molecular levels (e.g. genes, signaling pathway).

3. Sub-objectives of chapter 10

The fourth objective of the thesis is to identify whether the developed insulin-loaded nanoparticles promote glucose consumption in skeletal muscle cells. Therefore, the role of C2C12 cell line on the pre-clinical development of chitosan-based nanoparticles should be understood. The sub-objectives of chapter 10 are listed below:

- To examine the use of C2C12 cell model in understanding insulin resistance

progression and pharmaceutical development.

- To assess the examples of studies and therapeutic agents that utilise C2C12 cell model in the pre-clinical stage.
- To understand the potential of C2C12 cell model in pharmaceutical development of drug delivery systems (e.g. nanoparticles, quantum dots).

4. Manuscript

Content is removed due to copyright restrictions. The publication can be accessed from https://onlinelibrary.wiley.com/doi/full/10.1111/jphp.13359.

Wong CY et al 2020. “C2C12 cell model: its role in understanding of insulin resistance at the molecular level and pharmaceutical development at the pre-clinical stage.” Journal of Pharmacy and Pharmacology.

Content is removed due to copyright restrictions. The publication can be accessed from https://onlinelibrary.wiley.com/doi/full/10.1111/jphp.13359.

Wong CY et al 2020. “C2C12 cell model: its role in understanding of insulin resistance at the molecular level and pharmaceutical development at the pre-clinical stage.” Journal of Pharmacy and Pharmacology.

Content is removed due to copyright restrictions. The publication can be accessed from https://onlinelibrary.wiley.com/doi/full/10.1111/jphp.13359.

Wong CY et al 2020. “C2C12 cell model: its role in understanding of insulin resistance at the molecular level and pharmaceutical development at the pre-clinical stage.” Journal of Pharmacy and Pharmacology.

Content is removed due to copyright restrictions. The publication can be accessed from https://onlinelibrary.wiley.com/doi/full/10.1111/jphp.13359.

Wong CY et al 2020. “C2C12 cell model: its role in understanding of insulin resistance at the molecular level and pharmaceutical development at the pre-clinical stage.” Journal of Pharmacy and Pharmacology.

Content is removed due to copyright restrictions. The publication can be accessed from https://onlinelibrary.wiley.com/doi/full/10.1111/jphp.13359.

Wong CY et al 2020. “C2C12 cell model: its role in understanding of insulin resistance at the molecular level and pharmaceutical development at the pre-clinical stage.” Journal of Pharmacy and Pharmacology.

Content is removed due to copyright restrictions. The publication can be accessed from https://onlinelibrary.wiley.com/doi/full/10.1111/jphp.13359.

Wong CY et al 2020. “C2C12 cell model: its role in understanding of insulin resistance at the molecular level and pharmaceutical development at the pre-clinical stage.” Journal of Pharmacy and Pharmacology.

Content is removed due to copyright restrictions. The publication can be accessed from https://onlinelibrary.wiley.com/doi/full/10.1111/jphp.13359.

Wong CY et al 2020. “C2C12 cell model: its role in understanding of insulin resistance at the molecular level and pharmaceutical development at the pre-clinical stage.” Journal of Pharmacy and Pharmacology.

Content is removed due to copyright restrictions. The publication can be accessed from https://onlinelibrary.wiley.com/doi/full/10.1111/jphp.13359.

Wong CY et al 2020. “C2C12 cell model: its role in understanding of insulin resistance at the molecular level and pharmaceutical development at the pre-clinical stage.” Journal of Pharmacy and Pharmacology.

Content is removed due to copyright restrictions. The publication can be accessed from https://onlinelibrary.wiley.com/doi/full/10.1111/jphp.13359.

Wong CY et al 2020. “C2C12 cell model: its role in understanding of insulin resistance at the molecular level and pharmaceutical development at the pre-clinical stage.” Journal of Pharmacy and Pharmacology.

Content is removed due to copyright restrictions. The publication can be accessed from https://onlinelibrary.wiley.com/doi/full/10.1111/jphp.13359.

Wong CY et al 2020. “C2C12 cell model: its role in understanding of insulin resistance at the molecular level and pharmaceutical development at the pre-clinical stage.” Journal of Pharmacy and Pharmacology.

Content is removed due to copyright restrictions. The publication can be accessed from https://onlinelibrary.wiley.com/doi/full/10.1111/jphp.13359.

Wong CY et al 2020. “C2C12 cell model: its role in understanding of insulin resistance at the molecular level and pharmaceutical development at the pre-clinical stage.” Journal of Pharmacy and Pharmacology.

Content is removed due to copyright restrictions. The publication can be accessed from https://onlinelibrary.wiley.com/doi/full/10.1111/jphp.13359.

Wong CY et al 2020. “C2C12 cell model: its role in understanding of insulin resistance at the molecular level and pharmaceutical development at the pre-clinical stage.” Journal of Pharmacy and Pharmacology.

Content is removed due to copyright restrictions. The publication can be accessed from https://onlinelibrary.wiley.com/doi/full/10.1111/jphp.13359.

Wong CY et al 2020. “C2C12 cell model: its role in understanding of insulin resistance at the molecular level and pharmaceutical development at the pre-clinical stage.” Journal of Pharmacy and Pharmacology.

Content is removed due to copyright restrictions. The publication can be accessed from https://onlinelibrary.wiley.com/doi/full/10.1111/jphp.13359.

Wong CY et al 2020. “C2C12 cell model: its role in understanding of insulin resistance at the molecular level and pharmaceutical development at the pre-clinical stage.” Journal of Pharmacy and Pharmacology.

Content is removed due to copyright restrictions. The publication can be accessed from https://onlinelibrary.wiley.com/doi/full/10.1111/jphp.13359.

Wong CY et al 2020. “C2C12 cell model: its role in understanding of insulin resistance at the molecular level and pharmaceutical development at the pre-clinical stage.” Journal of Pharmacy and Pharmacology.

Content is removed due to copyright restrictions. The publication can be accessed from https://onlinelibrary.wiley.com/doi/full/10.1111/jphp.13359.

Wong CY et al 2020. “C2C12 cell model: its role in understanding of insulin resistance at the molecular level and pharmaceutical development at the pre-clinical stage.” Journal of Pharmacy and Pharmacology.

Content is removed due to copyright restrictions. The publication can be accessed from https://onlinelibrary.wiley.com/doi/full/10.1111/jphp.13359.

Wong CY et al 2020. “C2C12 cell model: its role in understanding of insulin resistance at the molecular level and pharmaceutical development at the pre-clinical stage.” Journal of Pharmacy and Pharmacology.

Content is removed due to copyright restrictions. The publication can be accessed from https://onlinelibrary.wiley.com/doi/full/10.1111/jphp.13359.

Wong CY et al 2020. “C2C12 cell model: its role in understanding of insulin resistance at the molecular level and pharmaceutical development at the pre-clinical stage.” Journal of Pharmacy and Pharmacology.

Content is removed due to copyright restrictions. The publication can be accessed from https://onlinelibrary.wiley.com/doi/full/10.1111/jphp.13359.

Wong CY et al 2020. “C2C12 cell model: its role in understanding of insulin resistance at the molecular level and pharmaceutical development at the pre-clinical stage.” Journal of Pharmacy and Pharmacology.

Content is removed due to copyright restrictions. The publication can be accessed from https://onlinelibrary.wiley.com/doi/full/10.1111/jphp.13359.

Wong CY et al 2020. “C2C12 cell model: its role in understanding of insulin resistance at the molecular level and pharmaceutical development at the pre-clinical stage.” Journal of Pharmacy and Pharmacology.

Content is removed due to copyright restrictions. The publication can be accessed from https://onlinelibrary.wiley.com/doi/full/10.1111/jphp.13359.

Wong CY et al 2020. “C2C12 cell model: its role in understanding of insulin resistance at the molecular level and pharmaceutical development at the pre-clinical stage.” Journal of Pharmacy and Pharmacology.

Content is removed due to copyright restrictions. The publication can be accessed from https://onlinelibrary.wiley.com/doi/full/10.1111/jphp.13359.

Wong CY et al 2020. “C2C12 cell model: its role in understanding of insulin resistance at the molecular level and pharmaceutical development at the pre-clinical stage.” Journal of Pharmacy and Pharmacology.

Content is removed due to copyright restrictions. The publication can be accessed from https://onlinelibrary.wiley.com/doi/full/10.1111/jphp.13359.

Wong CY et al 2020. “C2C12 cell model: its role in understanding of insulin resistance at the molecular level and pharmaceutical development at the pre-clinical stage.” Journal of Pharmacy and Pharmacology.

Content is removed due to copyright restrictions. The publication can be accessed from https://onlinelibrary.wiley.com/doi/full/10.1111/jphp.13359.

Wong CY et al 2020. “C2C12 cell model: its role in understanding of insulin resistance at the molecular level and pharmaceutical development at the pre-clinical stage.” Journal of Pharmacy and Pharmacology.

Content is removed due to copyright restrictions. The publication can be accessed from https://onlinelibrary.wiley.com/doi/full/10.1111/jphp.13359.

Wong CY et al 2020. “C2C12 cell model: its role in understanding of insulin resistance at the molecular level and pharmaceutical development at the pre-clinical stage.” Journal of Pharmacy and Pharmacology.

Content is removed due to copyright restrictions. The publication can be accessed from https://onlinelibrary.wiley.com/doi/full/10.1111/jphp.13359.

Wong CY et al 2020. “C2C12 cell model: its role in understanding of insulin resistance at the molecular level and pharmaceutical development at the pre-clinical stage.” Journal of Pharmacy and Pharmacology.

Content is removed due to copyright restrictions. The publication can be accessed from https://onlinelibrary.wiley.com/doi/full/10.1111/jphp.13359.

Wong CY et al 2020. “C2C12 cell model: its role in understanding of insulin resistance at the molecular level and pharmaceutical development at the pre-clinical stage.” Journal of Pharmacy and Pharmacology.

Chapter 11: Development of orally administered insulin-loaded polymeric-oligonucleotide nanoparticles: statistical optimization and physicochemical characterization

Wong CY et al 2020. "Development of orally administered insulin-loaded polymeric-oligonucleotide nanoparticles: statistical optimization and physicochemical characterization." Drug Development and Industrial Pharmacy 46 (8): 1238-1252.

https://doi.org/10.1080/03639045.2020.1788061

https://www.tandfonline.com/doi/abs/10.1080/03639045.2020.1788061

Acknowledgement: The Version of Record of this manuscript has been published and was made available in Drug Development and Industrial Pharmacy on the 8th July 2020 (https://www.tandfonline.com/doi/abs/10.1080/03639045.2020.1788061).

Contents
1 Introduction
2. Materials and methods
2.1 Materials
2.2 RP-HPLC for insulin testing
2.3 Preparation of insulin-loaded CS-Dz13Scr nanoparticles
2.4 Physicochemical characterization of insulin-loaded nanoparticles
2.4.1 Particle size and polydispersity index measurement
2.4.2 Zeta-potential measurement
2.5 Statistical evaluation of insulin-loaded nanoparticles
2.6 Conservation of the physicochemical properties
2.7 Fourier transform infrared (FTIR) spectroscopic analysis
2.8 Morphological characterization
2.9 Encapsulation efficiency and drug release study
2.10 Cell culture
2.11 Cytotoxicity

1. Declaration of attribution by the candidate

I, Chun Yuen Jerry Wong, as the first author of the manuscript entitled " Development of orally administered insulin-loaded polymeric-oligonucleotide nanoparticles: statistical optimization and physicochemical characterization ", declare that this work was primarily designed, experimentally executed, interpreted, and written by the first author of this manuscript.

Name	Manuscript preparation	Manuscript editing	Final Approval
Chun Yuen Jerry Wong	x	x	x
Mr Jorge Martinez		x	x
Dr Jian Zhao		x	x
Dr Hani Al-Salami		x	x
Professor Crispin Dass		x	x

I acknowledge that these represent my contribution to the above research output.

Signature:

Date: 11th September 2020

Co-authors:

Mr Jorge Martinez	**Dr Jian Zhao**
Signature:	Signature:
Date:	Date:
Dr Hani Al-Salami	**Professor Crispin Dass**
Signature:	Signature:
Date:	Date:

2. Summary and aims of the chapter

The use of nanoparticles in oral delivery is a promising strategy that can overcome the GI barriers such as enzymatic degradation in the stomach, mucus layer and tight junctions in epithelial cells. In the present chapter, statistical analysis was utilised to understand the effect of excipients on the physicochemical properties of insulin-loaded chitosan-Dz13Scr nanoparticles. The individual effect, main effect and interactive significance of independent variables, including polymer concentration and oligonucleotide concentration, in influencing size, polydispersity index and zeta potential were identified. No such similar study has been reported to date for insulin-loaded chitosan-Dz13Scr nanoparticles. This chapter illustrates the potential applications of the developed nanoparticles.

3. Sub-objectives of chapter 11

The sub-objectives of chapter 11 were established to address the main objectives of the thesis. The sub-objectives are listed below:

- To examine the effect of polymer and oligonucleotide concentrations on the physicochemical properties of nanoparticles by using statistical analysis.
- To evaluate the stability, encapsulation efficiency and drug release behaviour of nanoparticles.

4. Manuscript

Content is removed due to copyright restrictions. The publication can be accessed from https://www.tandfonline.com/doi/abs/10.1080/03639045.2020.1788061.

Wong CY et al 2020. "Development of orally administered insulin-loaded polymeric-oligonucleotide nanoparticles: statistical optimization and physicochemical characterization." Drug Development and Industrial Pharmacy 46 (8): 1238-1252.

Content is removed due to copyright restrictions. The publication can be accessed from https://www.tandfonline.com/doi/abs/10.1080/03639045.2020.1788061.

Wong CY et al 2020. "Development of orally administered insulin-loaded polymeric-oligonucleotide nanoparticles: statistical optimization and physicochemical characterization." Drug Development and Industrial Pharmacy 46 (8): 1238-1252.

Content is removed due to copyright restrictions. The publication can be accessed from https://www.tandfonline.com/doi/abs/10.1080/03639045.2020.1788061.

Wong CY et al 2020. "Development of orally administered insulin-loaded polymeric-oligonucleotide nanoparticles: statistical optimization and physicochemical characterization." Drug Development and Industrial Pharmacy 46 (8): 1238-1252.

Content is removed due to copyright restrictions. The publication can be accessed from https://www.tandfonline.com/doi/abs/10.1080/03639045.2020.1788061.

Wong CY et al 2020. "Development of orally administered insulin-loaded polymeric-oligonucleotide nanoparticles: statistical optimization and physicochemical characterization." Drug Development and Industrial Pharmacy 46 (8): 1238-1252.

Content is removed due to copyright restrictions. The publication can be accessed from https://www.tandfonline.com/doi/abs/10.1080/03639045.2020.1788061.

Wong CY et al 2020. "Development of orally administered insulin-loaded polymeric-oligonucleotide nanoparticles: statistical optimization and physicochemical characterization." Drug Development and Industrial Pharmacy 46 (8): 1238-1252.

Content is removed due to copyright restrictions. The publication can be accessed from https://www.tandfonline.com/doi/abs/10.1080/03639045.2020.1788061.

Wong CY et al 2020. "Development of orally administered insulin-loaded polymeric-oligonucleotide nanoparticles: statistical optimization and physicochemical characterization." Drug Development and Industrial Pharmacy 46 (8): 1238-1252.

Content is removed due to copyright restrictions. The publication can be accessed from https://www.tandfonline.com/doi/abs/10.1080/03639045.2020.1788061.

Wong CY et al 2020. "Development of orally administered insulin-loaded polymeric-oligonucleotide nanoparticles: statistical optimization and physicochemical characterization." Drug Development and Industrial Pharmacy 46 (8): 1238-1252.

Content is removed due to copyright restrictions. The publication can be accessed from https://www.tandfonline.com/doi/abs/10.1080/03639045.2020.1788061.

Wong CY et al 2020. "Development of orally administered insulin-loaded polymeric-oligonucleotide nanoparticles: statistical optimization and physicochemical characterization." Drug Development and Industrial Pharmacy 46 (8): 1238-1252.

Content is removed due to copyright restrictions. The publication can be accessed from https://www.tandfonline.com/doi/abs/10.1080/03639045.2020.1788061.

Wong CY et al 2020. "Development of orally administered insulin-loaded polymeric-oligonucleotide nanoparticles: statistical optimization and physicochemical characterization." Drug Development and Industrial Pharmacy 46 (8): 1238-1252.

Content is removed due to copyright restrictions. The publication can be accessed from https://www.tandfonline.com/doi/abs/10.1080/03639045.2020.1788061.

Wong CY et al 2020. "Development of orally administered insulin-loaded polymeric-oligonucleotide nanoparticles: statistical optimization and physicochemical characterization." Drug Development and Industrial Pharmacy 46 (8): 1238-1252.

Content is removed due to copyright restrictions. The publication can be accessed from https://www.tandfonline.com/doi/abs/10.1080/03639045.2020.1788061.

Wong CY et al 2020. "Development of orally administered insulin-loaded polymeric-oligonucleotide nanoparticles: statistical optimization and physicochemical characterization." Drug Development and Industrial Pharmacy 46 (8): 1238-1252.

Content is removed due to copyright restrictions. The publication can be accessed from https://www.tandfonline.com/doi/abs/10.1080/03639045.2020.1788061.

Wong CY et al 2020. "Development of orally administered insulin-loaded polymeric-oligonucleotide nanoparticles: statistical optimization and physicochemical characterization." Drug Development and Industrial Pharmacy 46 (8): 1238-1252.

Content is removed due to copyright restrictions. The publication can be accessed from https://www.tandfonline.com/doi/abs/10.1080/03639045.2020.1788061.

Wong CY et al 2020. "Development of orally administered insulin-loaded polymeric-oligonucleotide nanoparticles: statistical optimization and physicochemical characterization." Drug Development and Industrial Pharmacy 46 (8): 1238-1252.

Content is removed due to copyright restrictions. The publication can be accessed from https://www.tandfonline.com/doi/abs/10.1080/03639045.2020.1788061.

Wong CY et al 2020. "Development of orally administered insulin-loaded polymeric-oligonucleotide nanoparticles: statistical optimization and physicochemical characterization." Drug Development and Industrial Pharmacy 46 (8): 1238-1252.

Content is removed due to copyright restrictions. The publication can be accessed from https://www.tandfonline.com/doi/abs/10.1080/03639045.2020.1788061.

Wong CY et al 2020. "Development of orally administered insulin-loaded polymeric-oligonucleotide nanoparticles: statistical optimization and physicochemical characterization." Drug Development and Industrial Pharmacy 46 (8): 1238-1252.

Chapter 12: Formulation and characterisation of insulin-loaded chitosan nanoparticles capable of inducing glucose uptake in skeletal muscle cells *in vitro*

Wong CY et al 2020. "Formulation and characterisation of insulin-loaded chitosan nanoparticles capable of inducing glucose uptake in skeletal muscle cells *in vitro*." Journal of Drug Delivery Science and Technology, 57: 101738.

https://doi.org/10.1016/j.jddst.2020.101738

https://www.sciencedirect.com/science/article/abs/pii/S1773224720301945

*This paper has been reproduced in accordance with the publisher's policy (Appendix B11).

Acknowledgement: The Version of Record of this manuscript has been published and was made available in Journal of Drug Delivery Science and Technology on the 10th April 2020 (https://doi.org/10.1016/j.jddst.2020.101738).

Contents
1 Introduction
2 Materials and methods
2.1 Pre-screening stage
2.1.1 Preparation of insulin-loaded nanoparticles
2.1.2 Insulin quantification
2.1.3 Encapsulation efficiency and loading content
2.2 Optimisation stage
2.2.1 Small scale production of nanoparticles
2.2.2 Particle size, polydispersity and zeta-potential
2.3 Scaled-up stage
2.3.1 Scaled-up production and characterisation of nanoparticles
2.4 Physical characterisation stage
2.4.1 *In vitro* drug release of nanoparticles
2.4.2 Insulin release kinetic analysis
2.4.3 Stability studies
2.5 Cellular characterization stage

1. Declaration of attribution by the candidate

I, Chun Yuen Jerry Wong, as the first author of the manuscript entitled "Formulation and characterisation of insulin-loaded chitosan nanoparticles capable of inducing glucose uptake in skeletal muscle cells *in vitro*", declare that this work was primarily designed, experimentally executed, interpreted, and written by the first author of this manuscript.

Name	Manuscript preparation	Manuscript editing	Final Approval
Chun Yuen Jerry Wong	x	x	x
Dr Hani Al-Salami		x	x
Professor Crispin Dass		x	x

I acknowledge that these represent my contribution to the above research output.

Signature:

Date: 11th September 2020

Co-authors:

Dr Hani Al-Salami	**Professor Crispin Dass**
Signature:	Signature:
Date:	Date:

2. Summary and aims of the chapter

Complex coacervation has been utilised to encapsulate labile therapeutic agents such as proteins, peptides and nucleic acids. Prior to initiation of research, a comprehensive review on the *status quo* was conducted, and opportunities and challenges of complex coacervation for the preparation of insulin-loaded nanoparticles were considered. As shown in Table 1 of the manuscript, recent studies revealed that nanoparticles prepared by complex coacervation could improve the colloidal stability and bioactivity of therapeutic proteins, promote sustained and controlled delivery of drugs, and protect peptides from enzymatic degradation. In this chapter, the potential of complex coacervation technique for manufacturing of insulin-loaded polymeric-oligonucleotide nanoparticles was examined. The effect of insulin nanoparticles on glucose uptake in skeletal muscle cells was investigated. The current study was divided into 4 stages, including a pre-screening stage (to understand the encapsulation potential of the novel drug delivery system), an optimisation stage (to refine the amount of encapsulated insulin and explore the physicochemical properties of pre-scaled up nanoparticles), a scaled-up stage (to explore the physicochemical properties of scaled-up nanoparticles), a physical characterisation stage (to visualise the stability and drug release kinetic), and lastly a cellular characterisation stage (to evaluate the cytotoxicity, glucose consumption capacity, permeation efficiency and endocytic absorption mechanism). The optimal combination of natural polymer (chitosan) and oligonucleotide (Dz13Scr) was chosen for the preparation of nanoparticles in the optimisation stage and scaled-up stage. The obtained results revealed that 0.5% of natural polymer (chitosan) and 10 μg of an oligonucleotide (Dz13Scr) could produce nanoparticles with desirable physicochemical characteristics. The complex coacervation technique could preserve the bioactivity of entrapped insulin and

improve the stability of the formulation. The gastrointestinal absorption of nanoparticles could be enhanced by endocytic and paracellular pathways. This work highlights the importance of achieving a balance between the mucoadhesiveness strength and muco-penetrating capacity to enhance the permeation of encapsulated insulin across the GI tract. The optimised formulation maintained its stability upon storage and induced glucose uptake in C2C12 skeletal muscle cells. This chapter provides a comprehensive discussion and result obtained to other insulin-loaded nanoparticles that were prepared by complex coacervation.

3. Sub-objectives of chapter 12

The sub-objectives of chapter 12 were established to address the main objectives of the thesis. The sub-objectives are listed below:

- To review and examine the potential of all existing insulin-loaded nanoparticulate formulations that were prepared by complex coacervation.
- To characterise the physicochemical properties (size, polydispersity index, zeta potential, drug release) of nanoparticles that were prepared by complex coacervation.
- To examine the storage stability of the optimal insulin-loaded nanoparticles.
- To evaluate the metabolic effect, bioactivity, mucus permeation capacity and endocytic absorption pathways of the fabricated nanoparticles.

4. Manuscript

Content is removed due to copyright restrictions. The publication can be accessed from https://www.sciencedirect.com/science/article/abs/pii/S1773224720301945.

Wong CY et al 2020. "Formulation and characterisation of insulin-loaded chitosan nanoparticles capable of inducing glucose uptake in skeletal muscle cells *in vitro*." Journal of Drug Delivery Science and Technology, 57: 101738.

Content is removed due to copyright restrictions. The publication can be accessed from https://www.sciencedirect.com/science/article/abs/pii/S1773224720301945.

Wong CY et al 2020. "Formulation and characterisation of insulin-loaded chitosan nanoparticles capable of inducing glucose uptake in skeletal muscle cells *in vitro*." Journal of Drug Delivery Science and Technology, 57: 101738.

Content is removed due to copyright restrictions. The publication can be accessed from https://www.sciencedirect.com/science/article/abs/pii/S1773224720301945.

Wong CY et al 2020. "Formulation and characterisation of insulin-loaded chitosan nanoparticles capable of inducing glucose uptake in skeletal muscle cells *in vitro*." Journal of Drug Delivery Science and Technology, 57: 101738.

Content is removed due to copyright restrictions. The publication can be accessed from https://www.sciencedirect.com/science/article/abs/pii/S1773224720301945.

Wong CY et al 2020. "Formulation and characterisation of insulin-loaded chitosan nanoparticles capable of inducing glucose uptake in skeletal muscle cells *in vitro*." Journal of Drug Delivery Science and Technology, 57: 101738.

Content is removed due to copyright restrictions. The publication can be accessed from https://www.sciencedirect.com/science/article/abs/pii/S1773224720301945.

Wong CY et al 2020. "Formulation and characterisation of insulin-loaded chitosan nanoparticles capable of inducing glucose uptake in skeletal muscle cells *in vitro*." Journal of Drug Delivery Science and Technology, 57: 101738.

Content is removed due to copyright restrictions. The publication can be accessed from https://www.sciencedirect.com/science/article/abs/pii/S1773224720301945.

Wong CY et al 2020. "Formulation and characterisation of insulin-loaded chitosan nanoparticles capable of inducing glucose uptake in skeletal muscle cells *in vitro*." Journal of Drug Delivery Science and Technology, 57: 101738.

Content is removed due to copyright restrictions. The publication can be accessed from https://www.sciencedirect.com/science/article/abs/pii/S1773224720301945.

Wong CY et al 2020. "Formulation and characterisation of insulin-loaded chitosan nanoparticles capable of inducing glucose uptake in skeletal muscle cells *in vitro*." Journal of Drug Delivery Science and Technology, 57: 101738.

Content is removed due to copyright restrictions. The publication can be accessed from https://www.sciencedirect.com/science/article/abs/pii/S1773224720301945.

Wong CY et al 2020. "Formulation and characterisation of insulin-loaded chitosan nanoparticles capable of inducing glucose uptake in skeletal muscle cells *in vitro*." Journal of Drug Delivery Science and Technology, 57: 101738.

Content is removed due to copyright restrictions. The publication can be accessed from https://www.sciencedirect.com/science/article/abs/pii/S1773224720301945.

Wong CY et al 2020. "Formulation and characterisation of insulin-loaded chitosan nanoparticles capable of inducing glucose uptake in skeletal muscle cells *in vitro*." Journal of Drug Delivery Science and Technology, 57: 101738.

Content is removed due to copyright restrictions. The publication can be accessed from https://www.sciencedirect.com/science/article/abs/pii/S1773224720301945.

Wong CY et al 2020. "Formulation and characterisation of insulin-loaded chitosan nanoparticles capable of inducing glucose uptake in skeletal muscle cells *in vitro*." Journal of Drug Delivery Science and Technology, 57: 101738.

Content is removed due to copyright restrictions. The publication can be accessed from https://www.sciencedirect.com/science/article/abs/pii/S1773224720301945.

Wong CY et al 2020. "Formulation and characterisation of insulin-loaded chitosan nanoparticles capable of inducing glucose uptake in skeletal muscle cells *in vitro*." Journal of Drug Delivery Science and Technology, 57: 101738.

Content is removed due to copyright restrictions. The publication can be accessed from https://www.sciencedirect.com/science/article/abs/pii/S1773224720301945.

Wong CY et al 2020. "Formulation and characterisation of insulin-loaded chitosan nanoparticles capable of inducing glucose uptake in skeletal muscle cells *in vitro*." Journal of Drug Delivery Science and Technology, 57: 101738.

Content is removed due to copyright restrictions. The publication can be accessed from https://www.sciencedirect.com/science/article/abs/pii/S1773224720301945.

Wong CY et al 2020. "Formulation and characterisation of insulin-loaded chitosan nanoparticles capable of inducing glucose uptake in skeletal muscle cells *in vitro*." Journal of Drug Delivery Science and Technology, 57: 101738.

Chapter 13: Lyophilisation improves bioactivity and stability of insulin-loaded polymeric-oligonucleotide nanoparticles for diabetes treatment

Wong CY et al 2020. "Lyophilisation improves bioactivity and stability of insulin-loaded polymeric-oligonucleotide nanoparticles for diabetes treatment." AAPS PharmSciTech 21 (3): 1-20.

https://doi.org/10.1208/s12249-020-01648-6

https://link.springer.com/article/10.1208/s12249-020-01648-6

*This paper has been reproduced in accordance with the publisher's policy (Appendix B12).

Acknowledgement: The Version of Record of this manuscript has been published and was made available in AAPS PharmSciTech on the 25th March 2020 (https://link.springer.com/article/10.1208/s12249-020-01648-6).

Contents

1. Declaration of attribution by the candidate

I, Chun Yuen Jerry Wong, as the first author of the manuscript entitled "Lyophilisation improves bioactivity and stability of insulin-loaded polymeric-oligonucleotide nanoparticles for diabetes treatment", declare that this work was primarily designed, experimentally executed, interpreted, and written by the first author of this manuscript.

Name	Manuscript preparation	Manuscript editing	Final Approval
Chun Yuen Jerry Wong	x	x	x
Dr Hani Al-Salami		x	x
Professor Crispin Dass		x	x

I acknowledge that these represent my contribution to the above research output.

Signature:

Date: 11th September 2020

Co-authors:

Dr Hani Al-Salami	**Professor Crispin Dass**
Signature:	Signature:
Date:	Date:

2. Summary and aims of the chapter

In order to improve the physical and chemical stability of nanoparticles upon storage, lyophilisation has been used to remove water molecules from the nanoparticle suspensions in the previous two decades. In recent studies, the addition of cryoprotectant was found to improve the stability and bioactivity of protein formulations by forming a protective matrix in the freezing stage. Prior to initiation of research, a comprehensive review on the experimental protocols for lyophilised oral insulin-loaded nanoparticles was conducted. The experimental conditions of freeze-drying were summarised in brief in Table 1. It is noted that research on the effect of cryoprotectant types (mannitol, sorbitol, sucrose and trehalose) and their concentrations (1, 3, 5, 7, 10% w/v) on physicochemical properties of nanoparticles is limited. Therefore, there is a compelling need to examine the effect of cryoprotectants on lyophilised nanoparticles.

In this chapter, the optimal cryoprotectant combination was chosen for characterisation in terms of drug release profile and stability. Cellular assays were performed to investigate the impact of selected cryoprotectant and lyophilisation on cytotoxicity, glucose consumption, oral absorption mechanism, and gastrointestinal permeability, of lyophilised nanoparticles. The obtained results revealed that mannitol (7% w/v) could produce nanoparticles with slight positive charge and reasonable encapsulation efficiency. As compared to freeze-dried nanoparticles without cryoprotectant, the addition of cryoprotectant could preserve the bioactivity of entrapped insulin and improve the stability of nanoparticles against mechanical stress during lyophilisation. The uptake of lyophilised nanoparticles by the HT-29 human colorectal adenocarcinoma cells was found to be an energy-dependent process, and the

gastrointestinal absorption of nanoparticles was associated with both endocytic and paracellular pathways. With the use of 7% mannitol as cryoprotectant, lyophilised nanoparticles (containing 10, 55, 100 nM insulin) induced a significant glucose uptake in C2C12 mouse myoblast. Lastly, freeze-drying could improve the physical and chemical stability of nanoparticles upon storage. This work visualises the importance of selecting appropriate cryoprotectant type and concentration in conserving the physicochemical properties, structural integrity and bioactivity of formulations. This chapter provides a thorough discussion and compares the obtained result with other lyophilised insulin-loaded nanoparticles.

3. Sub-objectives of chapter 13

The sub-objectives of chapter 13 were established to address the main objectives of the thesis. The sub-objectives are listed below:

- To understand the freeze-drying protocols that were employed to develop orally administered insulin-loaded nanoparticles.
- To develop and examine the macroscopic stability of the lyophilised insulin-loaded nanoparticles that were prepared by complex coacervation.
- To examine the effects of lyophilisation and cryoprotectant on the physicochemical characteristics (size, zeta potential, entrapment efficiency, loading efficiency, morphology) of the lyophilised insulin-loaded nanoparticles.
- To investigate if the developed lyophilised formulation possesses any pH-dependent and glucose-responsive drug release behaviour.
- To characterise the cytotoxicity, functionality, endocytic absorption pathways and

GI cellular permeation of the developed lyophilised formulation.

- To examine the effect of mucus on cellular internalisation of the developed lyophilised formulation.
- To examine if the cryoprotectant maintain the chemical, physical and storage stability of the optimised lyophilised nanoparticles.

4. Manuscript

Content is removed due to copyright restrictions. The publication can be accessed from https://link.springer.com/article/10.1208/s12249-020-01648-6.

Wong CY et al 2020. "Lyophilisation improves bioactivity and stability of insulin-loaded polymeric-oligonucleotide nanoparticles for diabetes treatment." AAPS PharmSciTech 21 (3): 1-20.

Content is removed due to copyright restrictions. The publication can be accessed from https://link.springer.com/article/10.1208/s12249-020-01648-6.

Wong CY et al 2020. "Lyophilisation improves bioactivity and stability of insulin-loaded polymeric-oligonucleotide nanoparticles for diabetes treatment." AAPS PharmSciTech 21 (3): 1-20.

Content is removed due to copyright restrictions. The publication can be accessed from https://link.springer.com/article/10.1208/s12249-020-01648-6.

Wong CY et al 2020. "Lyophilisation improves bioactivity and stability of insulin-loaded polymeric-oligonucleotide nanoparticles for diabetes treatment." AAPS PharmSciTech 21 (3): 1-20.

Content is removed due to copyright restrictions. The publication can be accessed from https://link.springer.com/article/10.1208/s12249-020-01648-6.

Wong CY et al 2020. "Lyophilisation improves bioactivity and stability of insulin-loaded polymeric-oligonucleotide nanoparticles for diabetes treatment." AAPS PharmSciTech 21 (3): 1-20.

Content is removed due to copyright restrictions. The publication can be accessed from https://link.springer.com/article/10.1208/s12249-020-01648-6.

Wong CY et al 2020. "Lyophilisation improves bioactivity and stability of insulin-loaded polymeric-oligonucleotide nanoparticles for diabetes treatment." AAPS PharmSciTech 21 (3): 1-20.

Content is removed due to copyright restrictions. The publication can be accessed from https://link.springer.com/article/10.1208/s12249-020-01648-6.

Wong CY et al 2020. "Lyophilisation improves bioactivity and stability of insulin-loaded polymeric-oligonucleotide nanoparticles for diabetes treatment." AAPS PharmSciTech 21 (3): 1-20.

Content is removed due to copyright restrictions. The publication can be accessed from https://link.springer.com/article/10.1208/s12249-020-01648-6.

Wong CY et al 2020. "Lyophilisation improves bioactivity and stability of insulin-loaded polymeric-oligonucleotide nanoparticles for diabetes treatment." AAPS PharmSciTech 21 (3): 1-20.

Content is removed due to copyright restrictions. The publication can be accessed from https://link.springer.com/article/10.1208/s12249-020-01648-6.

Wong CY et al 2020. "Lyophilisation improves bioactivity and stability of insulin-loaded polymeric-oligonucleotide nanoparticles for diabetes treatment." AAPS PharmSciTech 21 (3): 1-20.

Content is removed due to copyright restrictions. The publication can be accessed from https://link.springer.com/article/10.1208/s12249-020-01648-6.

Wong CY et al 2020. "Lyophilisation improves bioactivity and stability of insulin-loaded polymeric-oligonucleotide nanoparticles for diabetes treatment." AAPS PharmSciTech 21 (3): 1-20.

Content is removed due to copyright restrictions. The publication can be accessed from https://link.springer.com/article/10.1208/s12249-020-01648-6.

Wong CY et al 2020. "Lyophilisation improves bioactivity and stability of insulin-loaded polymeric-oligonucleotide nanoparticles for diabetes treatment." AAPS PharmSciTech 21 (3): 1-20.

Content is removed due to copyright restrictions. The publication can be accessed from https://link.springer.com/article/10.1208/s12249-020-01648-6.

Wong CY et al 2020. "Lyophilisation improves bioactivity and stability of insulin-loaded polymeric-oligonucleotide nanoparticles for diabetes treatment." AAPS PharmSciTech 21 (3): 1-20.

Content is removed due to copyright restrictions. The publication can be accessed from https://link.springer.com/article/10.1208/s12249-020-01648-6.

Wong CY et al 2020. "Lyophilisation improves bioactivity and stability of insulin-loaded polymeric-oligonucleotide nanoparticles for diabetes treatment." AAPS PharmSciTech 21 (3): 1-20.

Content is removed due to copyright restrictions. The publication can be accessed from https://link.springer.com/article/10.1208/s12249-020-01648-6.

Wong CY et al 2020. "Lyophilisation improves bioactivity and stability of insulin-loaded polymeric-oligonucleotide nanoparticles for diabetes treatment." AAPS PharmSciTech 21 (3): 1-20.

Content is removed due to copyright restrictions. The publication can be accessed from https://link.springer.com/article/10.1208/s12249-020-01648-6.

Wong CY et al 2020. "Lyophilisation improves bioactivity and stability of insulin-loaded polymeric-oligonucleotide nanoparticles for diabetes treatment." AAPS PharmSciTech 21 (3): 1-20.

Content is removed due to copyright restrictions. The publication can be accessed from https://link.springer.com/article/10.1208/s12249-020-01648-6.

Wong CY et al 2020. "Lyophilisation improves bioactivity and stability of insulin-loaded polymeric-oligonucleotide nanoparticles for diabetes treatment." AAPS PharmSciTech 21 (3): 1-20.

Content is removed due to copyright restrictions. The publication can be accessed from https://link.springer.com/article/10.1208/s12249-020-01648-6.

Wong CY et al 2020. "Lyophilisation improves bioactivity and stability of insulin-loaded polymeric-oligonucleotide nanoparticles for diabetes treatment." AAPS PharmSciTech 21 (3): 1-20.

Content is removed due to copyright restrictions. The publication can be accessed from https://link.springer.com/article/10.1208/s12249-020-01648-6.

Wong CY et al 2020. "Lyophilisation improves bioactivity and stability of insulin-loaded polymeric-oligonucleotide nanoparticles for diabetes treatment." AAPS PharmSciTech 21 (3): 1-20.

Content is removed due to copyright restrictions. The publication can be accessed from https://link.springer.com/article/10.1208/s12249-020-01648-6.

Wong CY et al 2020. "Lyophilisation improves bioactivity and stability of insulin-loaded polymeric-oligonucleotide nanoparticles for diabetes treatment." AAPS PharmSciTech 21 (3): 1-20.

Content is removed due to copyright restrictions. The publication can be accessed from https://link.springer.com/article/10.1208/s12249-020-01648-6.

Wong CY et al 2020. "Lyophilisation improves bioactivity and stability of insulin-loaded polymeric-oligonucleotide nanoparticles for diabetes treatment." AAPS PharmSciTech 21 (3): 1-20.

Content is removed due to copyright restrictions. The publication can be accessed from https://link.springer.com/article/10.1208/s12249-020-01648-6.

Wong CY et al 2020. "Lyophilisation improves bioactivity and stability of insulin-loaded polymeric-oligonucleotide nanoparticles for diabetes treatment." AAPS PharmSciTech 21 (3): 1-20.

Chapter 14: General discussion, limitations and future directions

14.1 General discussion

This chapter provides a summary for the research project that was conducted to evaluate the insulin-loaded nanoparticles. Overall, this thesis examined the potential of polymeric-oligonucleotide nanoparticles as carriers for the oral administration of insulin. Oral delivery of therapeutic proteins is challenging due to the existence of formulation barriers and physiological barriers. In terms of formulation barriers, therapeutic proteins are liable macromolecules, hence they are susceptible to chemical degradation and mechanical stress in harsh manufacturing conditions. In addition, therapeutic proteins possess a number of inherent unfavourable features.[1,2] The chemical structure of proteins can be unstable in enzymatic and acidic environment, and their permeation across the GI tract are limited due to large molecular size.[3-6] Therefore, therapeutic proteins such as insulin are mostly administered to patients *via* subcutaneous injections. Such an invasive administration route can lead to occasional overdose, adverse effects (e.g. skin necrosis, nerve pain) and poor patient compliance.[7-9] Conversely, administration of therapeutic proteins *via* oral route can improve patient acceptability and their compliance to therapy.[10-13]

In the past decade, a range of protein-loaded nanomedicine has been developed.[1,14-16] Nanoparticle is one of the drug delivery systems that has been used to improve the stability and oral bioavailability of therapeutic proteins.[14] Nanoparticles have demonstrated a decent safety profile, controlled drug release pattern and can proffer protection for the therapeutic proteins against enzymatic degradation.[8,17-22] The nanoparticles effectively enhance the GI retention time and transportation of entrapped

insulin across the GI cells both *in vitro* and *in vivo*.[3,18, 23-27] Upon prolonged storage, the insulin-loaded nanoparticles demonstrated stability in terms of particle size and physicochemical characteristics.[21,28-31] Although success has been reported for numerous insulin-loaded nanoparticulate formulations, their translation from the pre-clinical stage to the clinical setting remains unattainable. The Food and Drug Administration has not approved any orally-administered protein- or insulin-loaded nanoparticles.[32] Currently, only two protein-based nanoformulations (RSV-F protein nanoparticle vaccine and albumin-bound rapamycin) have been examined in clinical settings, but these formulations were approved to be administered *via* the intramuscular or intravenous route.

To foster the pre-clinical evaluation and clinical translation of orally administered insulin-loaded nanoparticles, comprehensive reviews on the experimental conditions and available technologies for physical, cellular and *in vivo* characterisation were conducted in the thesis (Section B). The chosen assays and protocol for characterisation of insulin-loaded nanoparticles should reflect the physiological conditions in humans. In chapter 5, the assays for physical characterisation of nanoparticles, including the particle size, polydispersity index, zeta potential, morphology, drug release, mucus diffusion capacity and stability, were examined. This chapter is crucial to facilitate the understanding of the research design, minimise inter-rater variability for physical assays, minimise variations in research design, and reduce the number of *in vivo* experiments. In chapter 6, the available assays and technologies for cellular characterisation of orally administered insulin-loaded nanoparticles were investigated. A well-rounded understanding of cell culture conditions, cytotoxicity and cellular uptake mechanism is critical in obtaining reliable *in vitro* results prior to animal studies.[33] In chapter 7, the *in vivo* studies for characterising the absorption

mechanism, GI mucoadhesiveness, biodistribution and pharmacokinetics of the insulin-loaded nanoparticles were reviewed. This chapter can facilitate the evaluation of the *in vivo* physiological properties of nanoparticles prior to clinical trials, as well as minimising unwanted wastage of research funding.

The physicochemical properties of the nanocarriers can influence the GI absorption efficacy of therapeutic proteins. In comparison to other micron-sized and submicron-sized drug delivery systems, nanoparticles can enhance the cellular uptake of entrapped insulin in the GI tract.[34-37] The GI cellular uptake of insulin-loaded nanoparticles is dependent on the particle size.[8,37-41] Particles with smaller size tend to be absorbed more efficiently into enterocytes.[42] Therefore, the following parameters, which includes protein to polymer ratio[8, 43], polymer to polymer ratio[22,31] and polymer concentration[44], should be optimised in the developmental stage of nanoparticles as they can influence the particle size. The particle size can determine the dominant absorption mechanisms of the insulin-loaded nanoparticles, which can be classified into paracellular, transcellular, transcytosis through enterocytes and receptor-mediated transcytosis.[7,15] In chapter 11 of this thesis, statistical analysis was carried out to examine the effect of polymer concentration and oligonucleotide concentration on the physicochemical properties (particle size, polydispersity index and zeta potential) of insulin-loaded nanoparticles. The individual and interactive effects of the above parameters in influencing the physicochemical properties were revealed. The results obtained indicated that the concentration of chitosan was a significant factor that affects the size and polydispersity index of the particles.

Zeta potential influences the colloidal stability[43-45], biocompatibility and GI absorption of insulin-loaded nanoparticles.[41,46] The concentrations of added insulin and polymer

can influence the overall surface charge of the nanoparticles.[35,43,47] The optimal zeta potential of nanoparticles for oral absorption of insulin remains controversial. A study reported that negatively-charged nanoparticles could facilitate the interaction between drug delivery system and enterocytes.[48] In addition, nanoparticles that possessed negatively-charged polymers could form hydrogen bonds with mucin and improve the mucoadhesiveness of drug delivery systems.[49] However, other studies stated that nanoparticles with negative charge had difficulties in diffusing across the mucin barrier due to electrostatic repulsion.[50] Although positively-charged nanoparticles were suggested to promote mucoadhesiveness *via* electrostatic force[51], a study indicated that excessive interaction could reduce the GI permeability of the encapsulated insulin.[41] Therefore, the effect of zeta potential on the performance of insulin-loaded nanoparticles warrant further thorough investigation.

Encapsulation efficiency of the nanoparticles should be optimised to diminish wastage of costly therapeutic agents in the manufacturing process and amplify the efficacy of the formulation. An optimised ratio of excipient concentrations could strengthen the electrostatic interactions between the polyelectrolytes.[18] An imbalance in the ratio of polyelectrolytes could destabilise the nanoparticles due to the presence of unreacted excipients in the drug delivery system.[8] The encapsulation efficiency of nanoparticles follows the saturation kinetic, in which excessive insulin molecules are unable to be encapsulated.[2,52] In the current research project, such a phenomenon was also noted in the developed formulations.

Initial burst release of insulin in the simulated GI medium is one of the significant issues faced by insulin-loaded nanoparticulate formulations.[1,9,21,25,36,40,46,50,53-63] As a consequence of the loosely adsorbed and non-entrapped insulin over the surface of

nanoparticles, the GI absorption and oral bioavailability of therapeutic proteins were negatively impacted.[9,40,55,64] In the current project, the nanoparticles demonstrated pH-responsive drug release behaviour. At alkaline pH, burst release of insulin was observed in the prepared insulin-loaded nanoparticles due to protein desorption from the surface. Preferably, the entrapped insulin is released from the core of the nanoparticles in a controlled manner. To achieve a desirable formulation, the destabilisation of nanoparticles and repulsive forces between the entrapped insulin and nanoparticle components should only occur at the targeted site of absorption, which enables the entry of water molecules to neutralise the overall charge of the nanoparticles. This can promote the release of insulin from the destabilised nanocomposite.[40] Therefore, strategies should be developed to optimise the drug release behaviour of the nanoparticles.

The mucus layer has been confirmed to limit the oral bioavailability of insulin-loaded nanoparticles.[62,65-73] Mucus can trap 3% to 60% of insulin-loaded nanoparticles within the layer[3,26,74], resulting in wastage of costly therapeutic proteins.[3,73] Firstly, nanoparticles with excessive bio-adhesiveness could prolong the retention time of the drug delivery systems, but their diffusion capacity across the mucus layer could be limited. Secondly, nanoparticles with sub-optimal surface characteristics have limited capability in diffusing across the mucus layer.[18,47,75] Mucus clearance can lead to poor mucus permeation of the insulin-loaded nanoparticles.[18] Thirdly, mucus could lead to changes in nanoparticle size and zeta potential.[65,68] A few studies revealed that protein-loaded nanoparticles could form aggregates with the mucin solution.[29,69,73] Therefore, insulin-loaded nanoparticles should be developed with optimised mucoadhesiveness and mucus penetrating features.[3]

Nanoparticles that are fabricated by mild preparation techniques, such as complex coacervation/polyelectrolyte complexation[36,45] and ionotropic gelation[57,76,77], can improve the colloidal stability of labile therapeutic proteins. These techniques do not require organic solvents and sonication.[78] Hence, they have been employed to encapsulate proteins, peptides and nucleic acids[31,46], which can preserve the structure and bioactivity of the active ingredients.[11,15,16,21,43,44,79] The favourable fabrication conditions include constant temperature, little agitation, minimal organic solvents, mild pH and low shear homogenisation.[1,80] Nanoparticles that were prepared by mild techniques could fabricate formulations with uniform particle size, high encapsulation efficiency, and improved GI cellular uptake.[43,46] Referring to the aforementioned favourable features, complex coacervation was employed to fabricate the insulin-loaded nanoparticles by using oppositely charged chitosan and Dz13Scr (34-mer oligonucleotide) in Section D of the thesis (research and development of insulin-loaded nanoparticles). These polyelectrolytes are known to be biocompatible and have no known detrimental effects on healthy cells.[81-83] In the current project, the developed formulations presented negligible cytotoxicity. FTIR analysis confirmed that the characteristic amide I and amide II peaks of insulin can be obtained in the spectra. In contrast, other reported techniques such as emulsification evaporation[84] and emulsion polymerisation[35,44] can involve harsh procedures that can damage the integrity of sensitive proteins.[11,15,16,43,79]

Biocompatible and biodegradable natural polymers, such as chitosan, alginate and dextran sulphate, can be used to fabricate nanoparticles with high tolerability. In Section D of the research project, positively charged chitosan was used as the principle natural polymer to fabricate nanoparticles. In terms of chitosan, it is the second most abundant polymeric polysaccharide (from crustacean shell, fungi and yeast) and can

be obtained from chitin deacetylation.[2,56] Its lethal dose is 16 g/kg in mice[35], thereby it is a safe excipient for producing protein-loaded nanoparticles.[85-87] The safety profile of chitosan was verified in a phase IV randomised clinical trial, in which a total daily dose of 2500 mg chitosan did not induce any toxicity in 64 overweight subjects.[88] The role of chitosan in oral delivery of protein-loaded nanoparticles was elucidated in detail in chapter 9. Other favourable features of chitosan include mucoadhesivess and tight junctions opening[2,31,36,40,43,57,66,89-91], which are ideal to facilitate the paracellular absorption of insulin-loaded nanoparticles.[35,44,92-97] Therefore, natural polymers are desirable excipients to generate nanoparticles and encapsulate therapeutic proteins for the management of diseases.

In chapter 12, positively-charged chitosan and negatively-charged Dz13Scr were utilised to fabricate self-assembled insulin-loaded nanoparticles by complex coacervation. In this chapter, five stages (pre-screening stage, optimisation stage, scaled-up stage, physical characterisation stage, cellular characterisation stage) were carried out to understand the encapsulation potential, refine the amount of encapsulated insulin, and characterise the physicochemical/cellular properties of insulin-loaded nanoparticles. The concentrations of polyelectrolytes should be optimised to maximise the encapsulation efficiency of insulin. Moreover, the encapsulation potential of the nanocarrier should be calculated to minimise the wastage of drugs in the preparation stage. The developed nanoparticles in this chapter demonstrated acceptable particle size, high encapsulation efficiency and positive surface charge. The fabricated nanoparticles could facilitate the transportation of insulin across the GI cells, promote glucose uptake in C2C12 skeletal muscle cells, and were stable after being stored for 2 months at 4 ^{o}C.

Although lyophilisation can improve the storage stability of nanoparticles, the freezing and dehydration stages can induce mechanical stress to the drug delivery systems, resulting in irreversible changes in particle size and aggregation.[1,98] The addition of mannitol[67], trehalose[1,98], sorbitol[29] and xylitol[67] to insulin-loaded nanoparticles prior to lyophilisation could preserve the stability, secondary structure, and bioactivity of the entrapped proteins.[39] A number of studies revealed that cryoprotectants could reduce the aggregation of insulin-loaded nanoparticles and maintain the physicochemical properties of the nanocarriers.[1,29,68,99] The storage temperature[1,100], cryoprotectant type[67] and its concentration[99] should all be taken into consideration to maintain the initial features of the lyophilised drug delivery systems upon reconstitution. In chapter 13, nanoparticles were lyophilised to improve the storage stability of nanoparticles by removing water molecules from the drug delivery system. Cryoprotectants were added to protect the nanocarriers against external stress and aggregation in the frozen stage. After lyophilisation, the effect of cryoprotectants and their concentrations on the physicochemical properties of nanoparticles were determined. It was found that sub-optimal cryoprotectant combination could lead to particle aggregation or collapse. When 7% mannitol was used to freeze dry nanoparticles, the bioactivity of the entrapped insulin was improved and made evident by the increment in glucose consumption in C2C12 cells. This thesis has clearly demonstrated that the addition of cryoprotectant could conserve the particle size, maintain the structure and bioactivity of the formulation, and prevent leakage of insulin during lyophilisation.

β-CD has been used to improve the bioactivity of nanoformulation.[77,101] Such an excipient has been confirmed to enhance the colloidal stability and storage stability of the developed formulation.[77,102,103] β-CD could also exert a protective effect for

insulin-loaded formulations against enzymatic degradation and improve their formulation in extreme pH.[77,80,101,103] To overcome the mucus and epithelial barriers of the GI tract, insulin-loaded nanoparticles have been coated with dissociable hydrophilic neutral layer such as N-(2-hydroxypropyl) methacrylamide copolymer in previous studies.[73] It was been reported that coating could reduce the level of aggregation between insulin-loaded nanoparticles and mucin. Other coating agents, such as hyaluronic acid[29] and phosphoserine[69], could also prevent excessive interaction between the drug delivery systems and the mucus layer. Zwitterion nanoparticles, which possessed the charge-reversible capability, were also reported to overcome both mucus and epithelial barriers.[104] The above strategies can potentially facilitate the diffusion of the nanoparticles across the mucus layer as well as the transportation of drug delivery systems across the GI tract. Nanoparticles with desirable surface properties (e.g. hydrophilic shell, densely charged surface) that avoid excessive electrostatic interaction between the drug delivery systems and mucus layer are deemed to be favourable to expedite mucus permeation.[18,26,69,74,105] Other strategies, such as PEG conjugation[106], ligand modification[71,107,108], and protamine-insulin conjugates[3], were also reported to overcome the mucus barriers, but the fabricated nanoparticles may have limited capacity in penetrating the epithelial barriers. The effect of the aforementioned strategies on the cellular internalisation of insulin-loaded nanoparticles should be investigated in future studies.

14.2 Limitations and future directions

To further minimise the initial burst release of insulin from the nanoparticles, strategies should be developed to optimise the drug release behaviour of the formulation. GI enzymes (trypsin, pepsin, chymotrypsin, and pancreatin) can disrupt the integrity and

unfold the structure of insulin.[109-111] Enteric-coated gelatin capsules or tablets[7,90,112] have been used to protect the nanoparticles against the penetration of GI enzymes, which are crucial in preventing the dissociation of formulations in the acidic environment and conserving the encapsulated proteins within the core of nanoparticles.[7,22,90,112] When insulin-loaded nanoparticles were filled in enteric-coated capsules, the duration of therapeutic effect was extended.[113] Therefore, future studies may examine the potential of enteric-coated coatings or drug delivery systems to achieve controlled release of insulin from the nanoparticles.

Coating of the nanoparticles can potentially improve the pH stability of the drug delivery system.[50,61,114] Coating over the nanoparticles can be achieved by the formation of electrostatic interactions between polymers and nanoparticle surface.[115] It was reported that chitosan and albumin coatings could preserve the morphology of nanoparticles for 3 hours at pH 5.5.[50] These coatings could be destabilised at pH 7.4, hence maximising the amount of intact therapeutic proteins to reach the targeted GI absorption site. Such pH-responsive nature is essential to avoid pre-mature denaturation of proteins in the gastric environment.[41] Other potential strategies, including polymer modification[43,91] and cross-linking salt incorporation[116], have also been reported to minimise the initial burst release of therapeutic proteins. Insulin-loaded nanoparticles with coatings, such as hyaluronic acid[29,67], polyvinyl alcohol[28], sodium dodecyl sulfate[28], trimethyl chitosan[25], and chitosan[28], could also conserve the size of nanoparticles in physiological conditions. The use of coating agents such as wheat germ agglutinin[117] and bovine serum albumin[118] can further improve the stability of nanoparticles against GI enzymatic degradation. The insulin release profile should be addressed in future formulations to reduce burst release, and maximise the amount of the entrapped insulin being absorbed in the GI tract.

Furthermore, the use of chitosan derivatives in producing nanoparticles has attracted significant attention. Several chitosan derivatives, such as trimethylated chitosan, thiolated chitosan, ethylated chitosan, carboxymethylated and carboxylated chitosan, have been examined for the preparation of water soluble nanoparticles.[26,119-122] It was previously suggested that nanoparticles prepared with chitosan derivatives were more stable in acidic pH.[121] In addition, in the jejunum and ileum, the amine groups of chitosan derivatives can protonate, hence the encapsulated drug can be released from the drug delivery systems.[120] The co-formulation of chitosan derivative-based nanoparticle and free chitosan could further improve the GI absorption of insulin in the colon. As the colon region possesses minimal enzymatic activity, the oral bioavailability of insulin could be promoted.[123]

Also, the employment of cell-penetrating peptides, such as low molecular weight protamine (LMWP), TAT and penetratin, is of particular interest. These cell-penetrating peptides can enhance GI absorption of insulin energy-independent transduction *via* energy-dependent endocytosis across the epithelial layer.[3,124] When LMWP was employed in the nanocarriers, it improved the absorption rate of insulin-loaded TMC-coated PLGA nanoparticles *via* both transcellular and paracellular pathways, and therefore the rate of insulin degradation in the GI tract can be reduced.[3]

In recent times, researchers have also expressed interest in glucose-sensitive biomaterials. For instance, boronic acid can regulates the release of insulin from the matrix of nanoparticles by sensing the concentration of surrounding glucose.[125-130] At high concentrations of glucose, it has been reported that insulin could be released from the chitosan-based glucose-responsive nanoparticulate systems at a faster rate than

medium with low glucose concentrations. However, further release of insulin in medium containing high glucose concentration could be restricted due to the formation of external crosslinking between boronic acid and glucose.[127,129-131] Further research is required to improve the selectivity and specificity of boronic acid-based chitosan drug delivery systems to glucose instead of fructose.[132,133]

Apart from GI enzymes, insulin-loaded nanoparticles were reported to be susceptible to degradation by bile acids [109], chitosanase and lysozyme.[134] Therefore, the effect of the aforementioned agents on the bioactivity and stability of the developed formulation may be assessed in future. In recent years, the intracellular barriers, including P-glycoprotein drug efflux, intracellular endosome and lysosome degradation, were observed to destabilise and limit the cellular uptake of insulin-loaded nanoparticles. Intracellular retrograde transport and lysosomal degradation can limit the amount of intact insulin being transported across the GI tract.[72] The impact of the above intracellular barriers on the integrity and bioactivity of the developed formulations were not examined in the current project, hence future studies may assess the effect of the above barriers on the intracellular trafficking of nanoparticles. This may extend to the development of strategies to overcome the intracellular barriers, and maximise the payload of the encapsulated insulin to reach the blood circulation.

A holistic *in vivo* research comprising of mammalian animal models should be conducted to examine the biodistribution, biocompatibility and pharmacokinetics of the developed insulin-loaded nanoparticles after GI absorption. This is crucial in understanding the *in vivo* performance and systemic effect of the nanocarriers on individual organs and tissues. As shown in chapter 7, Bama minipig was the only animal model being used to examine the Eudragit S100-coated RKKRRQRRR peptide

(Tat)-modified chitosan nanoparticles[13], hence large animal models should be utilised to examine the *in vivo* characteristic of the insulin-loaded nanoparticles. A prolonged *in vivo* study is warranted to examine the effect of the developed formulation on the integrity of intestinal mucosa as acute inflammation can last for 7 to 14 days.[135]

In the current project, Dz13Scr was used as the anionic component to fabricate nanoparticles. Previous studies found that Dz13 could reduce the generation of reactive oxygen species (ROS).[136] As diabetes mellitus is characterised by an elevation in ROS,[137,138] the effect of the developed insulin-loaded nanoparticles on the oxidative status should be investigated. Future studies may consider examining the antioxidant potential of the developed nanoparticle by measuring the activity of superoxide dismutase, vitamin E and glutathione (GSH). These biomarkers can suppress the progression of secondary diabetic complications.[139] A holistic measurement of both pro- and antioxidant reaction will be essential in evaluating the effect of insulin-loaded nanoparticles on the antioxidant status and ROS in diabetes.

Oral administration of insulin-loaded nanoparticles demonstrated negligible to little impact on the integrity of intestinal membrane.[112,140,141] When insulin-loaded nanoparticles are administered orally, it has been extensively reported that the nano-sized drug delivery systems can manage the blood sugar level in animal studies.[116-117,140-141] In recent studies, insulin-loaded nanoparticles could elicit cardio-protective effects (e.g. reduction in myocardial infarct size, attenuation of apoptosis in myocardial cells)[142], and suppress inflammation in adipose tissue (e.g. reduction in pro-inflammatory cytokines, macrophage infiltration).[143] Insulin-loaded nanoparticles were also reported to relieve nephropathy and kidney lesions in diabetic rats, which are common complications in diabetes.[68] In GK diabetic rats, insulin-loaded

nanoparticles could effectively reduce the malondialdehyde level and improve the oxidative status.[144] When insulin-loaded nanoparticles were formulated in topical cream[145] and spray-based formulations[146], the wound healing rate of diabetic ulcers was enhanced.[147] As insulin molecules are responsible in bone remodelling[148,149], the effect of insulin-loaded nanoparticles on bone cell proliferation[150] and osteoblast differentiation[151] should be examined in the future. As the amount of pre-existing results is limited, the potential beneficial effects of insulin-loaded nanoparticles warrant further investigation.

Chapter 15: Conclusion

In the present thesis, comprehensive reviews on the experimental conditions and available technologies for physical, cellular and *in vivo* characterisation of orally administered insulin-loaded nanoparticles were conducted. A well-rounded understanding of the research design is essential in evaluating the performance of the nanocarriers in the pre-clinical setting. The present thesis demonstrated the individual and interactive effects of polymer concentration and oligonucleotide concentration on the physicochemical properties of polymeric-oligonucleotide nanoparticles. The use of compatible cryoprotectant could improve the stability of the nanocarrier, and maintain the bioactivity of the entrapped insulin. Overall, the fabricated nanoparticles could facilitate the permeation of the entrapped insulin across the GI cells. In summary, the generated nanoparticles could preserve the physicochemical properties upon storage, and promote glucose consumption in skeletal muscle cells. Future direction which emphasises enteric-coated capsules, polymeric coatings, polymeric derivatives, cell-penetrating peptides and glucose-responsive sensors may be considered to improve the stability and oral bioavailability of insulin-loaded nanoparticles. Other crucial aspects, including the intracellular barriers, *in vivo* models, antioxidant capacities, and other potential beneficial effects (that is, cardio-protection, inflammation suppression, nephropathy relief), should be considered for the developed insulin-loaded nanoparticles.

Chapter 16: References

1. Jain S, Rathi VV, Jain AK, et al. Folate-decorated PLGA nanoparticles as a rationally designed vehicle for the oral delivery of insulin. Nanomedicine. 2012; 7:1311-1337.

2. Prusty Ak, Sahu SK. Development and evaluation of insulin incorporated nanoparticles for oral administration. ISRN Nanotechnology. 2013; 2013:1-6.

3. Sheng J, He H, Han L, et al. Enhancing insulin oral absorption by using mucoadhesive nanoparticles loaded with LMWP-linked insulin conjugates. J Control Release. 2016; 233:181-190.

4. Bai X, Kong M, Xia G, et al. Systematic investigation of fabrication conditions of nanocarrier based on carboxymethyl chitosan for sustained release of insulin. Int J Biol Macromol. 2017; 102:468-474.

5. Ma Z, Lim TM, Lim LY. Pharmacological activity of peroral chitosan-insulin nanoparticles in diabetic rats. Int J Pharm. 2005; 293:271-80.

6. Hurkat P, Jain A, Jain A, et al. Concanavalin A conjugated biodegradable nanoparticles for oral insulin delivery. J Nanopart Res. 2012; 14:1219.

7. Wong CY, Martinez J, Dass CR. Oral delivery of insulin for treatment of diabetes: status quo, challenges and opportunities. J Pharm Pharmacol. 2016; 68:1093-108.

8. Ibie CO, Knott RM, Thompson CJ. Complexation of novel thiomers and insulin to protect against in vitro enzymatic degradation - towards oral insulin delivery. Drug Dev Ind Pharm. 2018:1-9.

9. Chalasani KB, Russell-Jones GJ, Yandrapu SK, et al. A novel vitamin B12-nanosphere conjugate carrier system for peroral delivery of insulin. J Control Release. 2007; 117:421-429.

10. Zhang Z, Cai H, Liu Z, et al. Effective enhancement of hypoglycemic effect of

insulin by liver-targeted nanoparticles containing cholic acid-modified chitosan derivative. Mol Pharm. 2016; 13:2433-42.

11. Diop M, Auberval N, Viciglio A, et al. Design, characterisation, and bioefficiency of insulin-chitosan nanoparticles after stabilisation by freeze-drying or cross-linking. Int J Pharm. 2015; 491:402-408.

12. Tahtat D, Mahlous M, Benamer S, et al. Oral delivery of insulin from alginate/chitosan crosslinked by glutaraldehyde. Int J Biol Macromol. 2013; 58:160-168.

13. Chen S, Guo F, Deng T, et al. Eudragit S100-coated chitosan nanoparticles co-loading Tat for enhanced oral colon absorption of insulin. AAPS PharmSciTech. 2017; 18:1277-1287.

14. Wong CY, Al-Salami H, Dass CR. Potential of insulin nanoparticle formulations for oral delivery and diabetes treatment. J Control Release. 2017; 264:247-275.

15. Wong CY, Al-Salami H, Dass CR. Microparticles, microcapsules and microspheres: A review of recent developments and prospects for oral delivery of insulin. Int J Pharm. 2018; 537:223-244.

16. Wong CY, Al-Salami H, Dass CR. Recent advancements in oral administration of insulin-loaded liposomal drug delivery systems for diabetes mellitus. Int J Pharm. 2018; 549:201-217.

17. Sahu SK, Prusty AK. Design and evaluation of a nanoparticulate system prepared by biodegradable polymers for oral administration of protein drugs. Pharmazie. 2010; 65:824-829.

18. Liu C, Kou Y, Zhang X, et al. Enhanced oral insulin delivery via surface hydrophilic modification of chitosan copolymer based self-assembly polyelectrolyte nanocomplex. Int J Pharm. 2019; 554:36-47.

19. Burova TV, Grinberg NV, Tur DR, et al. Ternary interpolyelectrolyte complexes

insulin-poly(methylaminophosphazene)-dextran sulfate for oral delivery of insulin. Langmuir. 2013; 29:2273-2281.

20. Salvioni L, Fiandra L, Del Curto MD, et al. Oral delivery of insulin via polyethylene imine-based nanoparticles for colonic release allows glycemic control in diabetic rats. Pharmacol Res. 2016; 110:122-130.

21. Elsayed A, Remawi MA, Qinna N, et al. Formulation and characterization of an oily-based system for oral delivery of insulin. Eur J Pharm Biopharm. 2009; 73:269-279.

22. Makhlof A, Tozuka Y, Takeuchi H. Design and evaluation of novel pH-sensitive chitosan nanoparticles for oral insulin delivery. Eur J Pharm Sci. 2011; 42:445-451.

23. Woitiski CB, Sarmento B, Carvalho RA, et al. Facilitated nanoscale delivery of insulin across intestinal membrane models. Int J Pharm. 2011; 412:123-131.

24. Tan X, Liu X, Zhang Y, et al. Silica nanoparticles on the oral delivery of insulin. Expert Opin Drug Deliv. 2018; 15:805-820.

25. Sheng J, Han L, Qin J, et al. N-trimethyl chitosan chloride-coated PLGA nanoparticles overcoming multiple barriers to oral insulin absorption. ACS Appl Mater Interfaces. 2015; 7:15430-15441.

26. Liu M, Zhang J, Zhu X, et al. Efficient mucus permeation and tight junction opening by dissociable "mucus-inert" agent coated trimethyl chitosan nanoparticles for oral insulin delivery. J Control Release. 2016; 222:67-77.

27. Onoue S, Yamada S, Chan HK. Nanodrugs: Pharmacokinetics and safety. Int J Nanomedicine. 2014; 9:1025-1037.

28. Czuba E, Diop M, Mura C, et al. Oral insulin delivery, the challenge to increase insulin bioavailability: Influence of surface charge in nanoparticle system. Int J Pharm. 2018; 542:47-55.

29. He Z, Liu Z, Tian H, et al. Scalable production of core-shell nanoparticles by flash

nanocomplexation to enhance mucosal transport for oral delivery of insulin. Nanoscale. 2018; 10:3307-3319.

30. Li H, Zhang Z, Bao X, et al. Fatty acid and quaternary ammonium modified chitosan nanoparticles for insulin delivery. Colloids Surf B Biointerfaces. 2018; 170:136-143.

31. Sarmento B, Ribeiro A, Veiga F, et al. Development and characterization of new insulin containing polysaccharide nanoparticles. Colloids Surf B Biointerfaces. 2006; 53:193-202.

32. Reinholz J, Landfester K, Mailänder V. The challenges of oral drug delivery via nanocarriers. Drug Deliv. 2018; 25:1694-1705.

33. Ganeshkumar M, Ponrasu T, Sathishkumar M, et al. Preparation of amphiphilic hollow carbon nanosphere loaded insulin for oral delivery. Colloids Surf B Biointerfaces. 2013; 103:238-243.

34. Bhumkar DR, Joshi HM, Sastry M, et al. Chitosan reduced gold nanoparticles as novel carriers for transmucosal delivery of insulin. Pharm Res. 2007; 24:1415-1426.

35. Mukhopadhyay P, Sarkar K, Chakraborty M, et al. Oral insulin delivery by self-assembled chitosan nanoparticles: In vitro and in vivo studies in diabetic animal model. Mater Sci Eng C Mater Biol Appl. 2013; 33:376-382.

36. Mahjub R, Radmehr M, Dorkoosh FA, et al. Lyophilized insulin nanoparticles prepared from quaternized N-aryl derivatives of chitosan as a new strategy for oral delivery of insulin: In vitro, ex vivo and in vivo characterizations. Drug Dev Ind Pharm. 2014; 40:1645-1659.

37. Hecq J, Siepmann F, Siepmann J, et al. Development and evaluation of chitosan and chitosan derivative nanoparticles containing insulin for oral administration. Drug Dev Ind Pharm. 2015; 41:2037-2044.

38. He CB, Yin LC, Tang C, Yin CH. Size-dependent absorption mechanism of

polymeric nanoparticles for oral delivery of protein drugs. Biomaterials. 2012; 33:8569-8578.

39. Fonte P, Lino PR, Seabra V, et al. Annealing as a tool for the optimization of lyophilization and ensuring of the stability of protein-loaded PLGA nanoparticles. Int J Pharm. 2016; 503:163-173.

40. Du X, Zhang J, Zhang Y, et al. Decanoic acid grafted oligochitosan nanoparticles as a carrier for insulin transport in the gastrointestinal tract. Carbohydr Polym. 2014; 111:433-441.

41. Andreani T, de Souza AL, Kiill CP, et al. Preparation and characterization of PEG-coated silica nanoparticles for oral insulin delivery. Int J Pharm. 2014; 473:627-635.

42. Mesiha MS, Sidhom MB, Fasipe B. Oral and subcutaneous absorption of insulin poly(isobutylcyanoacrylate) nanoparticles. Int J Pharm. 2005; 288:289-293.

43. Mahjub R, Dorkoosh FA, Amini M, et al. Preparation, statistical optimization, and in vitro characterization of insulin nanoparticles composed of quaternized aromatic derivatives of chitosan. AAPS PharmSciTech. 2011; 12:1407-1419.

44. Shamsa ES, Mahjub R, Mansoorpour M, et al. Nanoparticles prepared from N,N-dimethyl-N-octyl chitosan as the novel approach for oral delivery of insulin: Preparation, statistical optimization and in-vitro characterization. Iran J Pharm Res. 2018; 17:442-459.

45. Jelvehgari M, Zakeri-Milani P, Siahi-Shadbad MR, et al. Development of pH-sensitive insulin nanoparticles using Eudragit L100-55 and chitosan with different molecular weights. AAPS PharmSciTech. 2010; 11:1237-1242.

46. Bayat A, Dorkoosh FA, Dehpour AR, et al. Nanoparticles of quaternized chitosan derivatives as a carrier for colon delivery of insulin: Ex vivo and in vivo studies. Int J Pharm. 2008; 356:259-266.

47. Jintapattanakit A, Junyaprasert VB, Kissel T. The role of mucoadhesion of

trimethyl chitosan and PEGylated trimethyl chitosan nanocomplexes in insulin uptake. J Pharm Sci. 2009; 98:4818-4830.

48. des Rieux A, Ragnarsson EG, Gullberg E, et al. Transport of nanoparticles across an in vitro model of the human intestinal follicle associated epithelium. Eur J Pharm Sci. 2005; 25:455-465.

49. Chickering DE, Mathiowitz E. Bioadhesive microspheres: I. A novel electrobalance-based method to study adhesive interactions between individual microspheres and intestinal mucosa. J Control Release. 1995; 34:251-262.

50. Lopes M, Shrestha N, Correia A, et al. Dual chitosan/albumin-coated alginate/dextran sulfate nanoparticles for enhanced oral delivery of insulin. J Control Release. 2016; 232:29-41.

51. Bernkop-Schnurch A. Chitosan and its derivatives: Potential excipients for peroral peptide delivery systems. Int J Pharm. 2000; 194:1-13.

52. Nam JP, Choi C, Jang MK, et al. Insulin-incorporated chitosan nanoparticles based on polyelectrolyte complex formation. Macromol Res. 2010; 18:630-635.

53. Cui F, Shi K, Zhang L, et al. Biodegradable nanoparticles loaded with insulin-phospholipid complex for oral delivery: Preparation, in vitro characterization and in vivo evaluation. J Control Release. 2006; 114:242-250.

54. Liu J, Gong T, Wang C, et al. Solid lipid nanoparticles loaded with insulin by sodium cholate-phosphatidylcholine-based mixed micelles: Preparation and characterization. Int J Pharm. 2007; 340:153-162.

55. Liu J, Zhang SM, Chen PP, et al. Controlled release of insulin from PLGA nanoparticles embedded within PVA hydrogels. J Mater Sci Mater Med. 2007; 18:2205-2210.

56. Avadi MR, Sadeghi AMM, Mohamadpour Dounighi N, et al. Ex vivo evaluation of insulin nanoparticles using chitosan and arabic gum. ISRN Pharmaceutics. 2011;

2011:860109.

57. Ji N, Hong Y, Gu Z, et al. Fabrication and characterization of complex nanoparticles based on carboxymethyl short chain amylose and chitosan by ionic gelation. Food Funct. 2018; 9:2902-2912.

58. Qian F, Cui F, Ding J, et al. Chitosan graft copolymer nanoparticles for oral protein drug delivery: Preparation and characterization. Biomacromolecules. 2006; 7:2722-2727.

59. Lin YH, Chen CT, Liang HF, et al. Novel nanoparticles for oral insulin delivery via the paracellular pathway. Nanotechnology. 2007; 18:105102.

60. Reix N, Parat A, Seyfritz E, et al. In vitro uptake evaluation in Caco-2 cells and in vivo results in diabetic rats of insulin-loaded PLGA nanoparticles. Int J Pharm. 2012; 437:213-220.

61. Zhang X, Sun M, Zheng A, et al. Preparation and characterization of insulin-loaded bioadhesive PLGA nanoparticles for oral administration. Eur J Pharm Sci. 2012; 45:632-638.

62. Tian H, He Z, Sun C, et al. Uniform core-shell nanoparticles with thiolated hyaluronic acid coating to enhance oral delivery of insulin. Adv Healthc Mater. 2018; 7:e1800285.

63. Wu ZM, Zhou L, Guo XD, et al. HP55-coated capsule containing PLGA/RS nanoparticles for oral delivery of insulin. Int J Pharm. 2012; 425:1-8.

64. Bayrami S, Esmaili Z, SeyedAlinaghi S, et al. Fabrication of long-acting insulin formulation based on poly (3-hydroxybutyrate-co-3-hydroxyvalerate) (PHBV) nanoparticles: Preparation, optimization, characterization, and in-vitro evaluation. Pharm Dev Technol. 2019; 24:176-188.

65. Andreani T, Miziara L, Lorenzon EN, et al. Effect of mucoadhesive polymers on the in vitro performance of insulin-loaded silica nanoparticles: Interactions with mucin

and biomembrane models. Eur J Pharm Biopharm. 2015; 93:118-126.

66. Li X, Guo S, Zhu C, et al. Intestinal mucosa permeability following oral insulin delivery using core shell corona nanolipoparticles. Biomaterials. 2013; 34:9678-9687.

67. Zeng Z, Dong C, Zhao P, et al. Scalable production of therapeutic protein nanoparticles using flash nanoprecipitation. Adv Healthc Mater. 2019; 8:e1801010.

68. Liu L, Zhang Y, Yu S, et al. Dual stimuli-responsive nanoparticle-incorporated hydrogels as an oral insulin carrier for intestine-targeted delivery and enhanced paracellular permeation. ACS Biomater Sci Eng. 2018; 4: 2889-2902.

69. Wu J, Zheng Y, Liu M, et al. Biomimetic viruslike and charge reversible nanoparticles to sequentially overcome mucus and epithelial barriers for oral insulin delivery. ACS Appl Mater Interfaces. 2018; 10:9916-9928.

70. Sgorla D, Lechanteur A, Almeida A, et al. Development and characterization of lipid-polymeric nanoparticles for oral insulin delivery. Expert Opin Drug Deliv. 2018; 15:213-222.

71. Liu M, Wu L, Shan W, et al. Iron-mimic peptide converts transferrin from foe to friend for orally targeting insulin delivery. J Mater Chem B. 2018; 6:593-601.

72. Zheng Y, Wu J, Shan W, et al. Multifunctional nanoparticles enable efficient oral delivery of biomacromolecules via improving payload stability and regulating the transcytosis pathway. ACS Appl Mater Interfaces. 2018; 10:34039-34049.

73. Shan W, Zhu X, Liu M, et al. Overcoming the diffusion barrier of mucus and absorption barrier of epithelium by self-assembled nanoparticles for oral delivery of insulin. ACS Nano. 2015; 9:2345-2356.

74. Shan W, Zhu X, Tao W, et al. Enhanced oral delivery of protein drugs using zwitterion-functionalized nanoparticles to overcome both the diffusion and absorption barriers. ACS Appl Mater Interfaces. 2016; 8:25444-25453.

75. Fiebrig I, Harding SE, Rowe AJ, et al. Transmission electron microscopy studies

on pig gastric mucin and its interactions with chitosan. Carbohydr Polym. 1995; 28:239-244.

76. Sarmento B, Ferreira DC, Jorgensen L, et al. Probing insulin's secondary structure after entrapment into alginate/chitosan nanoparticles. Eur J Pharm Biopharm. 2007; 65:10-17.

77. Sajeesh S, Sharma CP. Cyclodextrin-insulin complex encapsulated polymethacrylic acid based nanoparticles for oral insulin delivery. Int J Pharm. 2006; 325:147-154.

78. Lin YH, Sonaje K, Lin KM, et al. Multi-ion-crosslinked nanoparticles with pH-responsive characteristics for oral delivery of protein drugs. J Control Release. 2008; 132:141-149.

79. Tiyaboonchai W, Woiszwillo J, Sims RC, et al. Insulin containing polyethylenimine-dextran sulfate nanoparticles. Int J Pharm. 2003; 255:139-151.

80. Zhang N, Li J, Jiang W, et al. Effective protection and controlled release of insulin by cationic beta-cyclodextrin polymers from alginate/chitosan nanoparticles. Int J Pharm. 2010; 393:212-218.

81. Tan ML, Friedhuber AM, Dass CR. Co-nanoencapsulated doxorubicin and Dz13 control osteosarcoma progression in a murine model. J Pharm Pharmacol. 2013; 65:35-43.

82. Dass CR, Friedhuber AM, Khachigian LM, et al. Biocompatible chitosan-DNAzyme nanoparticle exhibits enhanced biological activity. J Microencapsul. 2008; 25:421-425.

83. Wong CY, Martinez J, Al-Salami H, et al. Quantification of BSA-loaded chitosan/oligonucleotide nanoparticles using reverse-phase high-performance liquid chromatography. Anal Bioanal Chem. 2018; 410:6991-7006.

84. Sarmento B, Martins S, Ferreira D, et al. Oral insulin delivery by means of solid

lipid nanoparticles. Int J Nanomedicine. 2007; 2:743-749.

85. George M, Abraham TE. Polyionic hydrocolloids for the intestinal delivery of protein drugs: Alginate and chitosan - a review. J Control Release. 2006; 114:1-14.

86. Baldrick P. The safety of chitosan as a pharmaceutical excipient. Regul Toxicol Pharmacol. 2010; 56: 290-299.

87. Kean T, Thanou M. Biodegradation, biodistribution and toxicity of chitosan. Adv Drug Deliv Rev. 2010; 62: 3-11.

88. Trivedi VR, Satia MC, Deschamps A, et al. Single-blind, placebo controlled randomised clinical study of chitosan for body weight reduction. Nutr J. 2016; 15: 3.

89. Wong CY, Al-Salami H, Dass CR. The role of chitosan on oral delivery of peptide-loaded nanoparticle formulation. J Drug Target. 2018; 26:551-562.

90. Wong CY, Martinez J, Carnagarin R, et al. In-vitro evaluation of enteric coated insulin tablets containing absorption enhancer and enzyme inhibitor. J Pharm Pharmacol. 2017; 69(3):285-294.

91. Barbari GR, Dorkoosh F, Amini M, et al. Synthesis and characterization of a novel peptide-grafted Cs and evaluation of its nanoparticles for the oral delivery of insulin, in vitro, and in vivo study. Int J Nanomedicine. 2018; 13:5127-5138.

92. Wong CY, Al-Salami H, Dass CR. The role of chitosan on oral delivery of peptide-loaded nanoparticle formulation. J Drug Target. 2018; 26(7):551-562.

93. Sonaje K, Chuang EY, Lin KJ, et al. Opening of epithelial tight junctions and enhancement of paracellular permeation by chitosan: Microscopic, ultrastructural, and computed-tomographic observations. Mol Pharm. 2012; 9:1271-1279.

94. Dyawanapelly S, Koli U, Dharamdasani V, et al. Improved mucoadhesion and cell uptake of chitosan and chitosan oligosaccharide surface-modified polymer nanoparticles for mucosal delivery of proteins. Drug Deliv Transl Res. 2016; 6:365-379.

95. Lopes M, Shrestha N, Correia A, et al. Dual chitosan/albumin-coated alginate/dextran sulfate nanoparticles for enhanced oral delivery of insulin. J Control Release. 2016; 232:29-41.

96. Ilium L. Chitosan and its use as a pharmaceutical excipient. Pharm Res. 1998; 15:1326-1331.

97. Mao S, Sun W, Kissel T. Chitosan-based formulations for delivery of DNA and siRNA. Adv Drug Deliv Rev. 2010; 62:12-27.

98. Sonaje K, Chen YJ, Chen HL, et al. Enteric-coated capsules filled with freeze-dried chitosan/poly(gamma-glutamic acid) nanoparticles for oral insulin delivery. Biomaterials. 2010; 31:3384-3394.

99. Chopra S, Bertrand N, Lim J-M, et al. Design of insulin-loaded nanoparticles enabled by multistep control of nanoprecipitation and zinc chelation. ACS Appl Mater Interfaces. 2017; 9:11440-11450.

100. Boushra M, Tous S, Fetih G, et al. Development and evaluation of viscosity-enhanced nanocarrier (VEN) for oral insulin delivery. Int J Pharm. 2016; 511:462-472.

101. Zhu X, Shan W, Zhang P, et al. Penetratin derivative-based nanocomplexes for enhanced intestinal insulin delivery. Mol Pharm. 2014; 11:317-328.

102. Moses LR, Dileep KJ, Sharma CP. Beta cyclodextrin–insulin-encapsulated chitosan/alginate matrix: Oral delivery system. J Appl Polym Sci. 2000; 75:1089-1096.

103. Sonaje K, Lin YH, Juang JH, et al. In vivo evaluation of safety and efficacy of self-assembled nanoparticles for oral insulin delivery. Biomaterials. 2009; 30:2329-2339.

104. Wu J, Zheng Y, Liu M, et al. Biomimetic viruslike and charge reversible nanoparticles to sequentially overcome mucus and epithelial barriers for oral insulin delivery. ACS Appl Mater Interfaces. 2018; 10:9916-9928.

105. Pereira de Sousa I, Moser T, Steiner C, et al. Insulin loaded mucus permeating

nanoparticles: Addressing the surface characteristics as feature to improve mucus permeation. Int J Pharm. 2016; 500:236-244.

106. Yang M, Lai SK, Wang YY, et al. Biodegradable nanoparticles composed entirely of safe materials that rapidly penetrate human mucus. Angew Chem Int Ed Engl. 2011; 50:2597-2600.

107. Zhang P, Xu Y, Zhu X, et al. Goblet cell targeting nanoparticle containing drug-loaded micelle cores for oral delivery of insulin. Int J Pharm. 2015; 496:993-1005.

108. Yang L, Li M, Sun Y, et al. A cell-penetrating peptide conjugated carboxymethyl-β-cyclodextrin to improve intestinal absorption of insulin. Int J Biol Macromol. 2018; 111:685-695.

109. Lowe PJ, Temple CS. Calcitonin and insulin in isobutylcyanoacrylate nanocapsules: Protection against proteases and effect on intestinal absorption in rats. J Pharm Pharmacol. 1994; 46:547-552.

110. Boushra M, Tous S, Fetih G, et al. Methocel-lipid hybrid nanocarrier for efficient oral insulin delivery. J Pharm Sci. 2016; 105:1733-1740.

111. Thompson CJ, Tetley L, Uchegbu IF, et al. The complexation between novel comb shaped amphiphilic polyallylamine and insulin: towards oral insulin delivery. Int J Pharm. 2009; 376:46-55.

112. Xu Y, Zheng Y, Wu L, et al. Novel solid lipid nanoparticle with endosomal escape function for oral delivery of insulin. ACS Appl Mater Interfaces. 2018; 21: 9315-9324.

113. Jain A, Jain SK. L-Valine appended PLGA nanoparticles for oral insulin delivery. Acta Diabetol. 2015; 52:663-676.

114. Cui FD, Tao AJ, Cun DM, et al. Preparation of insulin loaded PLGA-Hp55 nanoparticles for oral delivery. J Pharm Sci. 2007; 96:421-427.

115. Garcia-Fuentes M, Prego C, Torres D, et al. A comparative study of the potential of solid triglyceride nanostructures coated with chitosan or poly(ethylene glycol) as

carriers for oral calcitonin delivery. Eur J Pharm Sci. 2005; 25:133-143.

116. Gupta R, Mohanty S. Controlled release of insulin from folic acid-insulin complex nanoparticles. Colloids Surf B Biointerfaces. 2017; 154:48-54.

117. Zhang N, Ping Q, Huang G, et al. Lectin-modified solid lipid nanoparticles as carriers for oral administration of insulin. Int J Pharm. 2006; 327:153-159.

118. Reis CP, Ribeiro AJ, Veiga F, et al. Polyelectrolyte biomaterial interactions provide nanoparticulate carrier for oral insulin delivery. Drug Deliv. 2008; 15:127-139.

119. Cui F, Qian F, Zhao Z, et al. Preparation, characterization, and oral delivery of insulin loaded carboxylated chitosan grafted poly(methyl methacrylate) nanoparticles. Biomacromolecules. 2009; 10:1253-1258.

120. Thanou M, Verhoef JC, Junginger HE. Oral drug absorption enhancement by chitosan and its derivatives. Adv Drug Deliv Rev. 2001; 52:117-126.

121. Mi FL, Wu YY, Lin YH, et al. Oral delivery of peptide drugs using nanoparticles self-assembled by poly(gamma-glutamic acid) and a chitosan derivative functionalized by trimethylation. Bioconjug Chem. 2008; 19:1248-1255.

122. Wang J, Kong M, Zhou Z, et al. Mechanism of surface charge triggered intestinal epithelial tight junction opening upon chitosan nanoparticles for insulin oral delivery. Carbohydr Polym. 2017; 157:596-602.

123. Bayat A, Dorkoosh FA, Dehpour AR, et al. Nanoparticles of quaternized chitosan derivatives as a carrier for colon delivery of insulin: Ex vivo and in vivo studies. Int J Pharm. 2008; 356:259-266.

124. Daimon Y, Kamei N, Kawakami K, et al. Dependence of intestinal absorption profile of insulin on carrier morphology composed of beta-cyclodextrin-grafted chitosan. Mol Pharm. 2016; 13:4034-4042.

125. Wu H, Wang J, Kang X, et al. Glucose biosensor based on immobilization of glucose oxidase in platinum nanoparticles/graphene/chitosan nanocomposite film.

Talanta. 2009; 80:403-406.

126. Wu Z, Zhang S, Zhang X, et al. Phenylboronic acid grafted chitosan as a glucose-sensitive vehicle for controlled insulin release. J Pharm Sci. 2011; 100:2278-2286.

127. Siddiqui NA, Billa N, Roberts CJ, et al. Cross-linked dependency of boronic acid-conjugated chitosan nanoparticles by diols for sustained insulin release. Pharmaceutics. 2016; 8: 30.

128. Asantewaa Y, Aylott J, Burley JC, et al. Correlating physicochemical properties of boronic acid-chitosan conjugates to glucose adsorption sensitivity. Pharmaceutics. 2012; 5:69-80.

129. Wang Y, Huang F, Sun Y, Gao M, Chai Z. Development of shell cross-linked nanoparticles based on boronic acid-related reactions for self-regulated insulin delivery. J Biomater Sci Polym Ed. 2017; 28:93-106.

130. Siddiqui NA, Billa N, Roberts CJ. Multiboronic acid-conjugated chitosan scaffolds with glucose selectivity to insulin release. J Biomater Sci Polym Ed. 2017; 28:1-30.

131. Springsteen G, Wang B. A detailed examination of boronic acid–diol complexation. Tetrahedron. 2002; 58:5291-5300.

132. Veiseh O, Tang BC, Whitehead KA, et al. Managing diabetes with nanomedicine: challenges and opportunities. Nat Rev Drug Discov. 2015; 14:45-57.

133. Wu X, Li Z, Chen XX, et al. Selective sensing of saccharides using simple boronic acids and their aggregates. Chem Soc Rev. 2013; 42:8032-8048.

134. Ma Z, Yeoh HH, Lim LY. Formulation pH modulates the interaction of insulin with chitosan nanoparticles. J Pharm Sci. 2002; 91:1396-1404.

135. Sattar SBA, Singh S. Bacterial Gastroenteritis. In: StatPearls. Florida: StatPearls Publishing; 2020. Available from: https://www.ncbi.nlm.nih.gov/books/NBK513295/

136. Xiao L, Hong C, Jun N, et al. c-Jun DNAzymes inhibit myocardial inflammation,

ROS generation, infarct size, and improve cardiac function after ischemia-reperfusion injury. Arterioscler Thromb Vasc Biol. 2009; 29:1836-1842.

137. Ayeleso TB, Ramachela K, Mukwevho E. Aqueous-methanol extracts of orange-fleshed sweet potato (Ipomoeabatatas) ameliorate oxidative stress and modulate type 2 diabetes associated genes in insulin resistant C2C12 cells. Molecules. 2018; 23:2058.

138. Grzelkowska-Kowalczyk K, Wieteska-Skrzeczynska W, Grabiec K, et al. High glucose-mediated alterations of mechanisms important in myogenesis of mouse C2C12 myoblasts. Cell Biol Int. 2013; 37:29-35.

139. Matough FA, Budin SB, Hamid ZA, et al. The role of oxidative stress and antioxidants in diabetic complications. Sultan Qaboos Univ Med J. 2012; 12:5-18.

140. Zhang Y, Wu X, Meng L, et al. Thiolated Eudragit nanoparticles for oral insulin delivery: Preparation, characterization and in vivo evaluation. Int J Pharm. 2012; 436:341-350.

141. Liu X, Liu C, Zhang W, et al. Oligoarginine-modified biodegradable nanoparticles improve the intestinal absorption of insulin. Int J Pharm. 2013; 448:159-167.

142. Tong F, Liu S, Yan B, et al. Endogenous ornithine decarboxylase/polyamine system mediated the antagonist role of insulin/PEG-CMCS preconditioning against heart ischemia/reperfusion injury in diabetes mellitus. Int J Nanomedicine. 2018; 13:2507-2520.

143. Rho JG, Han HS, Han JH, et al. Self-assembled hyaluronic acid nanoparticles: Implications as a nanomedicine for treatment of type 2 diabetes. J Control Release. 2018; 279:89-98.

144. Deng W, Xie Q, Wang H, et al. Selenium nanoparticles as versatile carriers for oral delivery of insulin: Insight into the synergic antidiabetic effect and mechanism.

Nanomedicine. 2017; 13:1965-1974.

145. Lima MHM, Caricilli AM, de Abreu LL, et al. Topical insulin accelerates wound healing in diabetes by enhancing the AKT and ERK pathways: A double-blind placebo-controlled clinical trial. PLOS ONE. 2012; 7:e36974.

146. Wang E, Zhao M, Forrester JV, et al. Electric fields and MAP kinase signaling can regulate early wound healing in lens epithelium. Invest Ophthalmol Vis Sci. 2003; 44:244-249.

147.Abdelkader DH, Osman MA, El-Gizawy SA, et al. Effect of poly(ethylene glycol) on insulin stability and cutaneous cell proliferation in vitro following cytoplasmic delivery of insulin-loaded nanoparticulate carriers - A potential topical wound management approach. Eur J Pharm Sci. 2018; 114:372-384.

148. Ferron M, Wei J, Yoshizawa T, et al. Insulin signaling in osteoblasts integrates bone remodeling and energy metabolism. Cell. 2010; 142:296-308.

149. Capilla E, Teles-Garcia A, Acerete L, et al. Insulin and IGF-I effects on the proliferation of an osteoblast primary culture from sea bream (Sparus aurata). Gen Comp Endocrinol. 2011; 172:107-114.

150. Luginbuehl V, Wenk E, Koch A, et al. Insulin-like growth factor I-releasing alginate-tricalciumphosphate composites for bone regeneration. Pharm Res. 2005; 22:940-950.

151. Zhang W, Shen X, Wan C, et al. Effects of insulin and insulin-like growth factor 1 on osteoblast proliferation and differentiation: Differential signalling via Akt and ERK. Cell Biochem Funct. 2012; 30:297-302.

Appendix A:

Relevant publications to the thesis but not forming a part of it

Appendix Part A1:

1st relevant publications to the thesis but not forming a part of it

Wong CY et al 2018. "Quantification of BSA-loaded chitosan/oligonucleotide nanoparticles using reverse-phase high-performance liquid chromatography." Analytical and Bioanalytical Chemistry 410 (27): 6991-7006.

https://doi.org/10.1007/s00216-018-1319-9

https://link.springer.com/article/10.1007/s00216-018-1319-9

*This paper has been reproduced in accordance with the publisher's policy (Appendix 10).

Acknowledgement: The Version of Record of this manuscript has been published and were made available in Analytical and Bioanalytical Chemistry on the 11th September 2018 (https://doi.org/10.1007/s00216-018-1319-9).

Appendix Part A1: Declaration of attribution by the candidate

I, Chun Yuen Jerry Wong, as the first author of the publication entitled "Quantification of BSA-loaded chitosan/oligonucleotide nanoparticles using reverse-phase high-performance liquid chromatography", declare that this work was primarily designed, experimentally executed, interpreted, and written by the first author of this manuscript. I acknowledge that these represent my contribution to the above research output.

Signature:

Date: 11th September 2020

Co-authors:

Mr Jorge Martinez	**Dr Hani Al-Salami**
Signature:	Signature:
Date:	Date:

Professor Crispin Dass

Signature:

Date:

Appendix Part A1: Summary and aims

The use of HPLC has been largely shunned previously due to high cost and lack of sensitivity when analysing proteins. This chapter reports on the use of HPLC as a quantitative tool for the quantification of the model protein drug (plus two other actual protein drugs - insulin and PEDF). The objectives were to develop a HPLC method to quantify the proteins (that is, bovine serum albumin, insulin and PEDF), to characterise the physical characteristics of BSA-loaded chitosan/oligonucleotide nanoparticles, and lastly to evaluate the drug release profile and stability of the developed nanoparticles. No such similar study has been reported to date.

Appendix Part A1: Manuscript

Wong CY et al 2018. "Quantification of BSA-loaded chitosan/oligonucleotide nanoparticles using reverse-phase high-performance liquid chromatography." Analytical and Bioanalytical Chemistry 410 (27): 6991-7006.

Content is removed due to copyright restrictions. The publication can be accessed from https://link.springer.com/article/10.1007/s00216-018-1319-9.

Wong CY et al 2018. "Quantification of BSA-loaded chitosan/oligonucleotide nanoparticles using reverse-phase high-performance liquid chromatography." Analytical and Bioanalytical Chemistry 410 (27): 6991-7006.

Content is removed due to copyright restrictions. The publication can be accessed from https://link.springer.com/article/10.1007/s00216-018-1319-9.

Wong CY et al 2018. "Quantification of BSA-loaded chitosan/oligonucleotide nanoparticles using reverse-phase high-performance liquid chromatography." Analytical and Bioanalytical Chemistry 410 (27): 6991-7006.

Content is removed due to copyright restrictions. The publication can be accessed from https://link.springer.com/article/10.1007/s00216-018-1319-9.

Wong CY et al 2018. "Quantification of BSA-loaded chitosan/oligonucleotide nanoparticles using reverse-phase high-performance liquid chromatography." Analytical and Bioanalytical Chemistry 410 (27): 6991-7006.

Content is removed due to copyright restrictions. The publication can be accessed from https://link.springer.com/article/10.1007/s00216-018-1319-9.

Wong CY et al 2018. "Quantification of BSA-loaded chitosan/oligonucleotide nanoparticles using reverse-phase high-performance liquid chromatography." Analytical and Bioanalytical Chemistry 410 (27): 6991-7006.

Content is removed due to copyright restrictions. The publication can be accessed from https://link.springer.com/article/10.1007/s00216-018-1319-9.

Wong CY et al 2018. "Quantification of BSA-loaded chitosan/oligonucleotide nanoparticles using reverse-phase high-performance liquid chromatography." Analytical and Bioanalytical Chemistry 410 (27): 6991-7006.

Content is removed due to copyright restrictions. The publication can be accessed from https://link.springer.com/article/10.1007/s00216-018-1319-9.

Wong CY et al 2018. "Quantification of BSA-loaded chitosan/oligonucleotide nanoparticles using reverse-phase high-performance liquid chromatography." Analytical and Bioanalytical Chemistry 410 (27): 6991-7006.

Content is removed due to copyright restrictions. The publication can be accessed from https://link.springer.com/article/10.1007/s00216-018-1319-9.

Wong CY et al 2018. "Quantification of BSA-loaded chitosan/oligonucleotide nanoparticles using reverse-phase high-performance liquid chromatography." Analytical and Bioanalytical Chemistry 410 (27): 6991-7006.

Content is removed due to copyright restrictions. The publication can be accessed from https://link.springer.com/article/10.1007/s00216-018-1319-9.

Wong CY et al 2018. "Quantification of BSA-loaded chitosan/oligonucleotide nanoparticles using reverse-phase high-performance liquid chromatography." Analytical and Bioanalytical Chemistry 410 (27): 6991-7006.

Content is removed due to copyright restrictions. The publication can be accessed from https://link.springer.com/article/10.1007/s00216-018-1319-9.

Wong CY et al 2018. "Quantification of BSA-loaded chitosan/oligonucleotide nanoparticles using reverse-phase high-performance liquid chromatography." Analytical and Bioanalytical Chemistry 410 (27): 6991-7006.

Content is removed due to copyright restrictions. The publication can be accessed from https://link.springer.com/article/10.1007/s00216-018-1319-9.

Wong CY et al 2018. "Quantification of BSA-loaded chitosan/oligonucleotide nanoparticles using reverse-phase high-performance liquid chromatography." Analytical and Bioanalytical Chemistry 410 (27): 6991-7006.

Content is removed due to copyright restrictions. The publication can be accessed from https://link.springer.com/article/10.1007/s00216-018-1319-9.

Wong CY et al 2018. "Quantification of BSA-loaded chitosan/oligonucleotide nanoparticles using reverse-phase high-performance liquid chromatography." Analytical and Bioanalytical Chemistry 410 (27): 6991-7006.

Content is removed due to copyright restrictions. The publication can be accessed from https://link.springer.com/article/10.1007/s00216-018-1319-9.

Wong CY et al 2018. "Quantification of BSA-loaded chitosan/oligonucleotide nanoparticles using reverse-phase high-performance liquid chromatography." Analytical and Bioanalytical Chemistry 410 (27): 6991-7006.

Content is removed due to copyright restrictions. The publication can be accessed from https://link.springer.com/article/10.1007/s00216-018-1319-9.

Wong CY et al 2018. "Quantification of BSA-loaded chitosan/oligonucleotide nanoparticles using reverse-phase high-performance liquid chromatography." Analytical and Bioanalytical Chemistry 410 (27): 6991-7006.

Content is removed due to copyright restrictions. The publication can be accessed from https://link.springer.com/article/10.1007/s00216-018-1319-9.

Wong CY et al 2018. "Quantification of BSA-loaded chitosan/oligonucleotide nanoparticles using reverse-phase high-performance liquid chromatography." Analytical and Bioanalytical Chemistry 410 (27): 6991-7006.

Content is removed due to copyright restrictions. The publication can be accessed from https://link.springer.com/article/10.1007/s00216-018-1319-9.

Wong CY et al 2018. "Quantification of BSA-loaded chitosan/oligonucleotide nanoparticles using reverse-phase high-performance liquid chromatography." Analytical and Bioanalytical Chemistry 410 (27): 6991-7006.

Appendix Part A1: Publisher agreement and permission

Wong CY et al 2018. "Quantification of BSA-loaded chitosan/oligonucleotide nanoparticles using reverse-phase high-performance liquid chromatography." Analytical and Bioanalytical Bhemistry 410 (27): 6991-7006.

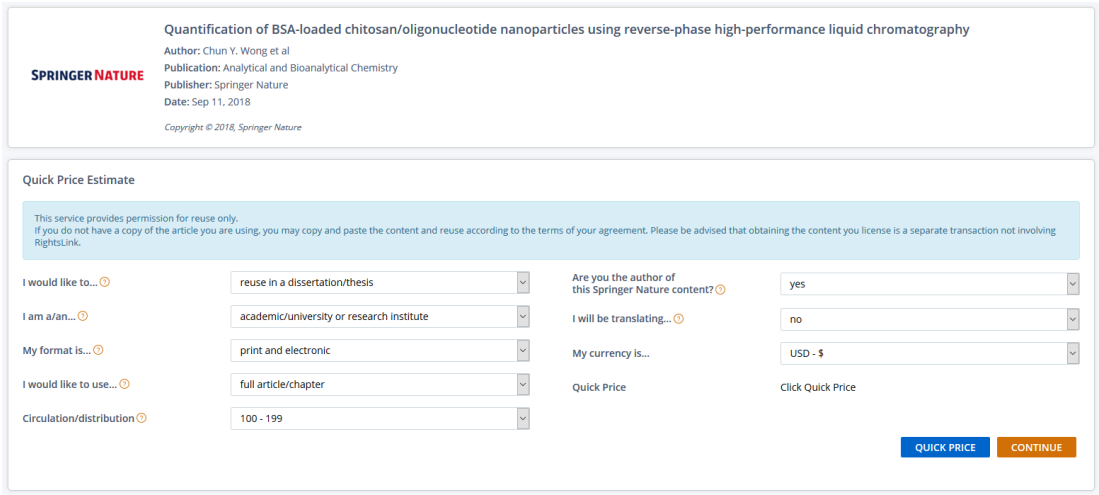

SPRINGER NATURE

Quantification of BSA-loaded chitosan/oligonucleotide nanoparticles using reverse-phase high-performance liquid chromatography

Author: Chun Y. Wong et al
Publication: Analytical and Bioanalytical Chemistry
Publisher: Springer Nature
Date: Sep 11, 2018

Copyright © 2018, Springer Nature

Quick Price Estimate

This service provides permission for reuse only.
If you do not have a copy of the article you are using, you may copy and paste the content and reuse according to the terms of your agreement. Please be advised that obtaining the content you license is a separate transaction not involving RightsLink.

I would like to...	reuse in a dissertation/thesis	Are you the author of this Springer Nature content?	yes
I am a/an...	academic/university or research institute	I will be translating...	no
My format is...	print and electronic	My currency is...	USD - $
I would like to use...	full article/chapter	Quick Price	Click Quick Price
Circulation/distribution	100 - 199		

QUICK PRICE CONTINUE

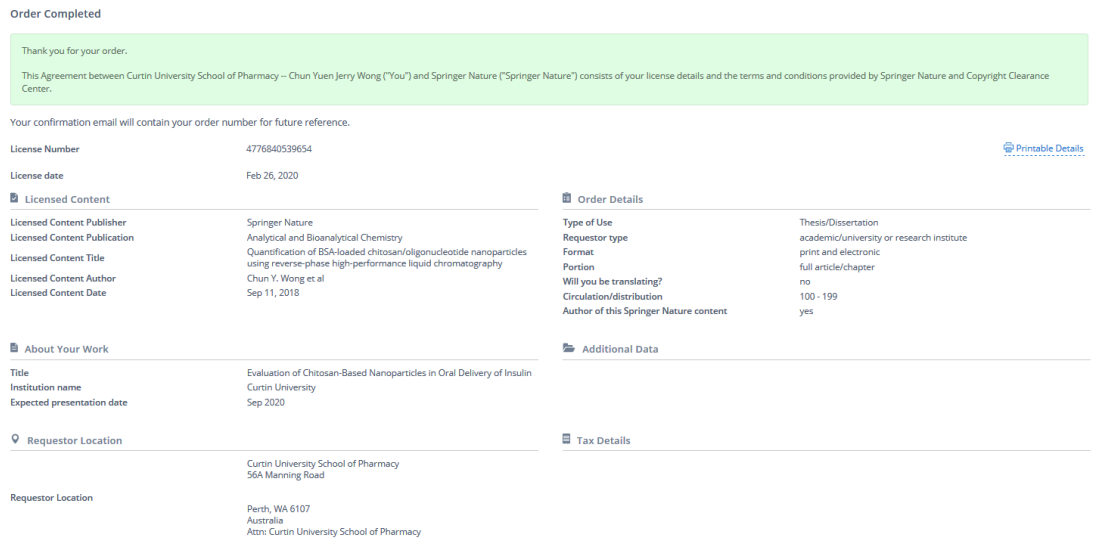

Order Completed

Thank you for your order.

This Agreement between Curtin University School of Pharmacy -- Chun Yuen Jerry Wong ("You") and Springer Nature ("Springer Nature") consists of your license details and the terms and conditions provided by Springer Nature and Copyright Clearance Center.

Your confirmation email will contain your order number for future reference.

Printable Details

License Number	4776840539654
License date	Feb 26, 2020

Licensed Content

Licensed Content Publisher	Springer Nature
Licensed Content Publication	Analytical and Bioanalytical Chemistry
Licensed Content Title	Quantification of BSA-loaded chitosan/oligonucleotide nanoparticles using reverse-phase high-performance liquid chromatography
Licensed Content Author	Chun Y. Wong et al
Licensed Content Date	Sep 11, 2018

Order Details

Type of Use	Thesis/Dissertation
Requestor type	academic/university or research institute
Format	print and electronic
Portion	full article/chapter
Will you be translating?	no
Circulation/distribution	100 - 199
Author of this Springer Nature content	yes

About Your Work

Title	Evaluation of Chitosan-Based Nanoparticles in Oral Delivery of Insulin
Institution name	Curtin University
Expected presentation date	Sep 2020

Additional Data

Requestor Location

Requestor Location	Curtin University School of Pharmacy 56A Manning Road Perth, WA 6107 Australia Attn: Curtin University School of Pharmacy

Tax Details

From: no-reply@copyright.com
To: Chun Yuen Wong
Subject: Thank you for your order with RightsLink / Springer Nature
Date: Thursday, 27 February 2020 12:26:07 PM

Thank you for your order!

Dear Mr. Chun Yuen Jerry Wong,

Thank you for placing your order through Copyright Clearance Center's RightsLink® service.

Order Summary

Licensee:	Curtin University School of Pharmacy
Order Date:	Feb 26, 2020
Order Number:	4776840539654
Publication:	Analytical and Bioanalytical Chemistry
Title:	Quantification of BSA-loaded chitosan/oligonucleotide nanoparticles using reverse-phase high-performance liquid chromatography
Type of Use:	Thesis/Dissertation
Order Total:	0.00 AUD

View or print complete details of your order and the publisher's terms and conditions.

Sincerely,

Copyright Clearance Center

Appendix B:

Publisher agreement, permission and supplementary data

Appendix B1: Publisher agreement and permission for chapter 2 - Potential of insulin nanoparticle formulations for oral delivery and diabetes treatment

Wong CY et al 2017. "Potential of insulin nanoparticle formulations for oral delivery and diabetes treatment." Journal of Controlled Release 264: 247-275.

Appendix B2: Publisher agreement and permission for chapter 3 - Microparticles, microcapsules and microspheres: a review of recent developments and prospects for oral delivery of insulin

Wong CY et al 2018. "Microparticles, microcapsules and microspheres: a review of recent developments and prospects for oral delivery of insulin." International Journal of Pharmaceutics 537 (1-2): 223-244.

Appendix B3: Publisher agreement and permission for chapter 4 - Recent advancements in oral administration of insulin-loaded liposomal drug delivery systems for diabetes mellitus

Wong CY et al 2018. "Recent advancements in oral administration of insulin-loaded liposomal drug delivery systems for diabetes mellitus." International Journal of Pharmaceutics 549 (1-2): 201-217.

Appendix B4.1: Supplementary data for chapter 5 - Bio-nanotechnological advancement of orally administered insulin nanoparticles: Comprehensive review of experimental design for physicochemical characterization.

Wong CY et al 2019. "Bio-nanotechnological advancement of orally administered insulin nanoparticles: Comprehensive review of experimental design for physicochemical characterization." International Journal of Pharmaceutics 572: 118720.

The following supplementary data is available from https://doi.org/10.1016/j.ijpharm.2019.118720 and https://www.sciencedirect.com/science/article/pii/S0378517319307653

Supplementary table 1. Experimental conditions for examination of encapsulation efficiency and drug loading efficiency for insulin nanoparticles

Supplementary table 2. Experimental condition for size measurement and polydispersity index of insulin nanoparticles

Supplementary table 3. Experimental conditions for zeta potential measurement of insulin nanoparticles

Supplementary table 4. Experimental conditions for morphological examination of insulin nanoparticles

Supplementary table 5. Experimental conditions for *in vitro* release of insulin from the nanoparticles

Supplementary table 6. Experimental conditions to examine interaction between mucin and insulin nanoparticles *in vitro*

Supplementary table 7. Experimental conditions to examine size, protein release, freeze-drying and enzymatic stability of insulin nanoparticles *in vitro*

Supplementary table 8. Experimental conditions to examine stability and bioactivity of insulin nanoparticles

Supplementary table 1. Experimental conditions for examination of encapsulation efficiency and drug loading efficiency for insulin nanoparticles

Method	System	Sample treatment	Column	Detection λ	Flow rate; injection	Mobile phase	Ref
RP-HPLC	Agilent 1260 infinity	Insulin lyophilized NPs dissolved in phosphate buffered (pH 7.4) for 3 hr then centrifuged	Supelco Discovery C18 (150 × 4.6 mm, 5 µm)	214 nm	1 mL/min; 75 µL	Acetonitrile and 0.1% trifluoroacetic acid in water from 30:70 to 40:60 over 5 min	(Lopes et al., 2016)
		Insulin NPs dissolved in 1 N HCl for 7 min	ODS3 (150 × 4.6 mm, 5 µm)	214 nm	0.8 mL/min	Buffer (containing 0.1 M monobasic potassium phosphate and 5% triethylamine, pH adjusted to 2.7 with orthophosphoric acid) and acetonitrile at ratio of 7.:30	(Mahjub et al., 2014)
		Centrifuged at 15000 rpm for 30 min at 4 °C	MZ analytical Perfect Sil Target ODS-3 (150 × 4.6 mm, 5 µm) at ambient temperature	214 nm	50 µL	Acetonitrile and 0.1% trifluoroacetic acid in water at ratio of 30:70	(Mahjub et al., 2011)
	Agilent 1200	Insulin NPs (10 mg/mL) dispersed in 0.01 M HCl at 1000 rpm and 25°C for 1 h; Centrifuged at 40000 rpm for 7 h at 4 °C; Filter with poly(vinylidene fluoride) membrane filter (0.45 µm)	Agilent Zorbax SB-C18 (250 x 4.6 mm, 300 nm) at 25 °C	215 nm	0.5 mL/min; 20 µL	Mobile phase A (0.03% trifluoroacetic acid in 90% H_2O and 10% acetonitrile); Mobile phase B (0.03% trifluoroacetic acid in 10% H_2O and 90% acetonitrile) at 20:80 for 5 min, then 80:20 for 10 min	(Alfatama et al., 2018)
		Centrifuged at 15000 rpm for 30 min at 4 °C	Dikma Bio-Bond HPLC C18 (250 × 4.6 mm, 5 µm)	214 nm	1 mL/min; 20 µL	Water, acetonitrile and trifluoroacetic acid at ratio of 67:33:0.1	(Sheng et al., 2016)
		Centrifuged at 17000 g for 50 min at 4 °C	Diamonsil C18 (150 × 4.6 mm, 5 µm) at 35 °C	214 nm	n/a	Acetonitrile-water solution (28:72, containing 0.2 M sodium sulfate, pH adjusted to 2.3 with phosphoric acid)	(Shan et al., 2016)
		Insulin NPs dissolved in pH 7.4 PBS and 1% Triton X100; 1 mL samples centrifuged at 4000 rpm for 20 min in Amicon Ultra-4 centrifugal devices (MWCO 100 kDa)	Agilent 300 SB-C8 (250 × 4.6 mm, 5 µm) at 40 °C	214 nm	1 mL/min; 20 µL	0.1 M sulfate buffer and acetonitrile at ratio of 73:27, pH adjusted to 2.3 with 0.1 M sulfate buffer containing 0.1 M sodium sulfate and trifluoroacetic acid	(Liu et al., 2016a)
		Insulin NPs dialysed by a dialysis membrane (MWCO: 8000–14,000)	n/a	n/a	n/a	n/a	(Zhang et al., 2015)
		n/a	Zorbax 300 SB-C18 (150 x 4.6 mm, 5 µm) at 30 °C	214 nm	0.8 mL/min	Acetonitrile and 0.2M sodium sulfate anhydrous solution at ratio of 27:73, pH adjusted to 2.3 with phosphoric acid	(Yu et al., 2015)
		Centrifuged at 14000 g for 20 min at 4 °C	n/a	n/a	n/a		(Shan et al., 2015)

		30 mg NPs dissolved in 10 mL of 1N chlorhydric acid; centrifuged by Ultracel regenerated cellulose (10 kDa)	Zorbax 300 SB-C18 (250 x 4.6 mm, 5 µm) at 40 °C	214 nm	1 mL/min	Water and acetonitrile at ratio of 73:27 completed with 0.138 mol/l of sodium sulfate and 2.7 mL of 85% phosphoric acid, pH adjusted to 2.3 with1N sodium hydroxide	(Hecq et al., 2015)
		Centrifuged at 16000 g for 15 min at 4 °C	n/a	n/a	n/a	n/a	(Zhu et al., 2014)
		200 µL insulin NPs in ultrapure water were lyophilized, then dissolved in 50 µL acetone and 150 µL HCl (100 mM)	n/a	n/a	n/a	n/a	(Liu et al., 2013)
		n/a	Zorbax 300 SB-C18 (150 x 4.6 mm, 5 µm) at 30 °C	n/a	0.8 mL/min; 20 µL	Isocratic mixture of acetonitrile and 0.2M sodium sulfate anhydrous solution at ratio of 27:73, pH adjusted to 2.3 with phosphoric acid	(Wu et al., 2012)
	Agilent 1100	Centrifuged at 40000 g for 30 min at 10 °C	Hypersil ODS C18 (200 x 4.6 mm, 5 µm)	210 nm	1 mL/min; 20 µl	Water, acetonitrile and trifluoroacetic acid at ratio of 82:18:0.3	(Zhang et al., 2012a)
	Agilent	Insulin standard calibration curve (1 - 100 µg/mL in 0.01 M HCl); centrifuged at 14000 rpm for 45 min	Zorbax 300 SB-C18 (250 x 4.6 mm, 5 µm) at 30 °C	214 nm	1 mL/min	0.1% trifluoroacetic acid and 0.1% trifluoroacetic acid in acetonitrile from 75:25 to 40:60 over 7 min	(Siddiqui et al., 2017)
		Insulin standard calibration curve (0.625 - 100 µg/mL in 0.01 M HCl); centrifuged at 14000 rpm for 45 min	Zorbax 300 SB-C18 (250 x 4.6 mm, 5 µm) at 30 °C	214 nm	1 mL/min; 20 µL	0.1% trifluoroacetic acid and 0.1% trifluoroacetic acid in acetonitrile from 75:25 to 40:60 over 8 min	(Siddiqui et al., 2016)
	Shimadzu LC-20AD pump	Insulin standard calibration curve (10–1000 µg/mL)	Gemini C18 (25 × 4.6 mm) at 25 °C	Ex/Em = 276/600 nm	1 mL/min	Water and acetonitrile at ratio of 68.5:31.5, pH adjusted to 2 with trifluoroacetic acid	(Thompson et al., 2009; Thompson et al., 2010)
	Shimadzu LC-2010 HT	NPs dissolved in sodium citrate (55 mM) prepared in phosphate buffer solution (pH 7.4) for 1; centrifuged at 12500 g for 10 min at 4°C	Waters X-Terra RP 18 (250 x 4.6 mm, 5 µm) and Merck Purospher STAR RP-18 precolumn (4 x 4 mm, 5 µm)	214 nm	1 mL/min; 20 µL	Acetonitrile and 0.1% trifluoroacetic acid aqueous solution from 30:70 to 40:60 over 5 min until 10 min	(Lopes et al., 2015)
		Centrifuged at 20000 g for 60 min at 4°C	Waters X-Terra RP 18 (250 x 4.6 mm, 5 µm) and Merck Purospher STAR RP-18 precolumn (4 x 4 mm, 5 µm)	214 nm	1 mL/min	Acetonitrile and 0.1% trifluoroacetic acid aqueous solution from 30:70 to 40:60 over 5 min, then changed to 30:70 in 1 min	(Woitiski et al., 2009a; Woitiski et al., 2009b; Woitiski et al., 2010)

Shimadzu SPD-M20A 230	NPs (containing 3.6 mg insulin) centrifuged at 58800 g for 1 hr at 4 °C; dissolved in 200 µL acetonitrile and 800 µL 0.01 M HCl, then centrifuged at 58800 g for 20 min at 4 °C	Luna C18 (250 x 4.6 mm) at 40 °C	214 nm	0.8 mL/min; 20 µL	0.2 M sodium sulfate anhydrous solution (adjusted to pH 2.3 with phosphoric acid) and acetonitrile at ratio of 73:27, filtered through 0.22 µm membrane filter.	(Hurkat et al., 2012)
	Centrifuged at 20000 rpm for 10 min	Princeton SPHER-300 C18 (250 x 4.6 mm, 5 µm)	214 nm	1 mL/min; 30 µl	Acetonitrile and water (containing 0.1% trifluoro acetic acid) at ratio of 30:70	(Jain et al., 2012)
Shimadzu LC-2010	15 mg NPs dissolved in 10 mL of sodium citrate (55 mM) prepared in phosphate buffer (pH 7.4) for 1 hr at 100 rpm	Waters X-Terra RP 18 (250 x 4.6 mm, 5 µm) and Merck Purospher STAR RP-18 precolumn (4 x 4 mm, 5 µm) at 25°C	n/a	1.2 mL/min	Water and acetonitrile with 0.04% trifluoroacetic acid from 70:30 to 60:40 over 5 min	(Reis et al., 2008)
Shimadzu LC-10A	NPs centrifuged at 15000 rpm for 15 min at 4°C	Phenomenex gemini-C18 at 40°C	n/a	1 mL/min	Acetonitrile, 0.1M monosodium dihydrogen orthophosphate and 0.05M sodium sulfate at ratio of 30:35:35, pH adjusted to 3 with phosphoric acid	(Prusty and Sahu, 2013)
	NPs centrifuged at 40000 rpm for 30 min at 10°C	Kromasil C-18, (200 x 4.6 mm, 5 µm) at 35°C	214 nm	1 mL/min; 20 µL	Acetonitrile, 0.1M monosodium dihydrogen orthophosphate and 0.05M sodium sulfate at ratio of 30:35:35, pH adjusted to 2.5 with phosphoric acid	(Pan et al., 2002a)
	NPs centrifuged at 10000 rpm for 30 min	Kromasil C-18, (200 x 4.6 mm, 5 µm) at 35°C	214 nm	1 ml/min; 20 µL	Acetonitrile, 0.1M monosodium dihydrogen orthophosphate and 0.05M sodium sulfate at ratio of 30:35:35, pH adjusted to 2.5 with phosphoric acid	(Pan et al., 2002b)
Shimadzu LC-10ATVP	Centrifuged at 74200 g for 30 min at 20◦°C	Waters Spherisorb ODS1 S10 (200 x 4.6 mm)	214 nm	1.5 mL/min	Acetonitrile and phosphate buffer (0.1 M monobasic sodium phosphate adjusted to pH 2.0 with phosphoric acid) from 76:26 to 68:32 in 30 min.	(Ma et al., 2005)
Shimadzu SCL-6B	Centrifuged at 74200 g for 30 min at 20◦°C	Waters Spherisorb ODS1 S10 (250 x 4.6 mm)	214 nm	1.5 mL/min; 20 µL	Acetonitrile and phosphate buffer (0.1 M monobasic sodium phosphate adjusted to pH 2.0 with phosphoric acid) from 76:26 to 68:32 in 30 min.	(Ma et al., 2002)
	Insulin standard calibration curve (0.1-0.5 mg/mL in 0.01 N HCl); lyophilized NPs (20 mg) dissolved in 0.5 mL HCl (0.05 N), and NPs (containing 200 µg insulin) dissolved in	Vydac C4 (250 x 4.6 mm, 5 µm)	230 nm	1 mL/min	50 mM phosphate buffer (pH 2.4) and acetonitrile at ratio of 73:27	(Tiyaboonchai et al., 2003)

		1 mL HCl (0.05 N); centrifuged at 12000 g for 20 min					
	UHPLC Dionex Ultimate 3000	Centrifuged at 10000 g for 10 min at room temperature	C18 (250 × 4.6 mm, 5 µm)	215 nm	0.8 mL/min	Acetonitrile (containing 0.1% trifluoroacetic acid) and water at ratio of 15:85, gradually increase to 60:40 in 7.5 min, reduce to 15:85 at 8 min and maintain until 11.5 min	(Gupta and Mohanty, 2017)
		Centrifuged at 10000g in Amicon® centrifugal filtering device (MWCO 50 kDa) for 10 min	Zorbax RX-C8 (250 × 4.6 mm, 5 µm) guarded with a precolumn at 30 °C	220 nm	1 mL/min	0.57% phosphoric acid solution (pH 2.25 with triethylamine) and acetonitrile at ratio of 73:27	(Deng et al., 2017)
	Prominence LC-20AD	Filter samples through a 0.2 µm membrane filter	Phenomenex C18 250 × 4.6 mm, 5 µm) at room temperature	214 nm	1 mL/min; 20 µL	Acetonitrile and 0.2 M sodium sulfate buffer at ratio of 30:70, pH adjusted to 2.8	(Guha et al., 2016)
	Merck Hitachi Elite La Chrome	Centrifuged at 40000 g for 30 min at 4 °C after lyophilization	LiChrospher 100 RP-18 guard column (5 µm), XTerra RP-18 (250 x 4.6 mm, 5 µm)	n/a	n/a	n/a	(Fonte et al., 2016)
		50 mg lyophilized insulin NPs in 2 mL PBS (100 mM) in addition of 5 mM EDTA, 5 mM Tris-HCl and 10% DMSO at 700 rpm and 37 °C for 24 hr	Multi High Bio RP 18 (150 x 4.6 mm)	254 nm.	1 mL/min; 100 µL	Acetonitrile and 0.1% trifluoroacetic acid in distilled water from 91:9 to 39:61 over 22 min	(Deutel et al., 2016)
	Hitachi L-7110 pump	Centrifuged at 40000 rpm for 2 hr at 4 °C	Phenomenex Prodigy ODS3 (250 x 4.6 mm, 5 µm)	214 nm	1 mL/min	0.2 M sulfate buffer (add 2 mL phosphoric acid and pH adjusted to 2.3 with ethanolamine) and acetonitrile at ratio of 73:27	(Du et al., 2014)
		n/a	ODS C18 (150 x 4.6 mm, 5 µm) at 35 °C	214 nm	1 mL/min; 20 µL	0.1 moL/L monosodium dihydrogen orthophosphate aqueous solution, 0.05 mol/L sodium sulfate aqueous solution and acetonitrile at ratio of 35:35:30, pH adjusted to 3 with H_3PO_4 solution	(Avadi et al., 2011)
		Freeze-dried NPs dissolved in acetone and 0.1 M HCl; centrifuged at 45000 g for 2 hr at 4 °C	ODS C18 (200 x 4.6 mm, 5 µm)	214 nm	1 mL/min; 20 µL	0.1 moL/L monosodium dihydrogen orthophosphate aqueous solution, 0.05 mol/L sodium sulfate aqueous solution and acetonitrile at ratio of 35:35:30, pH adjusted to 3 with H_3PO_4 solution	(Cui et al., 2007)

Merck Hitachi F-1050	Centrifuged at 14000 rpm for 30 min at room temperature	LiChrospher 100 RP-18 (250 x 4.6 mm, 5 µm)	Em/Ex = 600/280 nm	1 mL/min; 20 µL	Ultra-pure water with 0.1% trifluoroacetic acid and eluent B (containing acetonitrile: water: trifluoroacetic acid at ratio of 89.9:10:0.1) at final ratio of 65:35	(Mao et al., 2006)
Two Prostar 210 solvent delivery systems	Insulin standard calibration curve (1-200 µg/mL); centrifuged at 20000 g for 1 hr at 4 °C	Symmetry C18 (250 x 4.6 mm, 5 µm) at 40 °C	214 nm	1 mL/min	0.2 M sodium sulfate in water (pH 2.3) and 0.05M sodium sulfate in water (pH 2.3)/Acetonitrile (55:45) in final ratio of 42:58	(Diop et al., 2015)
	Centrifuged at 20000 g for 1 hr at 4 °C	Symmetry 300 C18 (250 x 4.6 mm, 5 µm) at 25 °C	214 nm	1 mL/min	0.2 M sodium sulfate in water with 0.23% phosphoric acid and 0.2 M sodium sulfate in water with 0.23% phosphoric acid /Acetonitrile (55:45) in final ratio of 42:58	(Reix et al., 2012)
TSP 1000 pump system	Insulin standard calibration curve (0.9-10 mg/mL); centrifuged at 14000 g for 30 min	C18 (150 x 4.6 mm, 5 µm) at 40 °C	214 nm	1 mL/min; 20 µL	Sulphate buffer (pH 2.3) and acetonitrile at ratio of 73:27	(Al-Kurdi et al., 2015)
Waters 2695	n/a	Symmetry 300 C4 (150 x 3.9 mm, 5 µm)	n/a	20 µL	70% water (containing 0.1% trifluoroacetic acid) and 30% acetonitrile (containing 0.08% trifluoroacetic acid)	(Carr and Peppas, 2010)
	Indirect method: centrifuged at 15000 rpm for 30 min at 4°C **Direct method:** NPs dissolved in 1N HCl then filtered through 0.1 µm syringe filter	Chrompack C8 column (250 x 4.6 mm, 5 µm)	214 nm	1.5 mL/min; 20 µL	27% acetonitrile and 73% buffer (0.1 M potassium dihydrogen phosphate and 1% triethylamine), adjusted to pH 3 with phosphoric acid	(Bayat et al., 2008)
Waters UPLC	Centrifuged at 15000 g for 30 min at 4 °C	Acquity UPLC BEH C18 column (50 × 2.1 mm, 1.7 µm)	214 nm	0.3 mL/min; 1 µL	Water, acetonitrile and trifluoroacetic acid at ratio of 68.5:31.5:0.1	(Sheng et al., 2015)
Waters 1525 pump system	Insulin standard calibration curve (2, 5, 10, 25, 50, 75, 100 µg/mL) in buffers (HCl/KCl, PBS or TC-199)	Phenomenex C18 (250 x 4.6 mm, 5 µm)	220 nm	1 mL/min; 100 µL	Acetonitrile and water with 0.1% trifluoroacetic acid at ratio of 40:60	(Andreani et al., 2014)
Waters 600 pump	n/a	Symmetry C18 (150 x 4.6 mm, 5 µm)	214 nm	1 mL/min	Acetonitrile and 0.1% trifluoroacetic acid aqueous solution at ratio of 30:70	(Zhang et al., 2010)
Waters bus SAT/IN	NPs dissolved in pH 7.4; centrifuged at 50000 rpm for 30 min	Phenomenex C18 column	214 nm	0.5 mL/min; 20 mL	Potassium hydrogen phosphate solution (adjusted to pH 3 with phosphoric acid) and acetonitrile at ratio of 70 : 30	(Davaran et al., 2008)
Waters 2690	0.6 mL NPs (containing 60 µg insulin) dissolved in 0.4 mL HCl (0.1 M); centrifuged at 14000 rpm for 15 min at 4°C; washed by distilled water (adjusted to pH 3	Inertsil ODS-3 (150 x 4.6 mm, 5 µm)	214 nm	1.0 mL/min; 20 µL	0.2 M sodium sulfate anhydrous solution (adjusted to pH 2.3 with phosphoric acid) and acetonitrile at ratio of 72:28	(Liu et al., 2007a)

		with HCl) and dissolved in 200 µL mobile phase					
	Kontron Instruments	Centrifuged at 18000 g for 40 min	LiChrosper 100 RP-18 (5 µm)	214 nm	1 mL/min; 20 µL	n/a	(Viehof et al., 2013)
	LC-10 Avp pump	Insulin standard calibration curve (10-200 µg/mL) NPs dissolved in 50% ethanol at 70°C for 10 min; centrifuged at 14000 rpm in ultimate filtration tube (MWCO 10000) for 10 min at 4°C	Shim-pack CLC-ODS (150 x 6 mm, 5 µm) at 30°C	220 nm	20 µL	Acetonitrile and water at ratio of 51:49	(Zhang et al., 2012c)
	Jasco 1580 pump	Centrifuged at 15000 rpm for 30 min at 4°C	RP-Kromasil 100-5C18 (250 x 4.6 mm) at 40°C	214 nm	1.0 mL/min	Acetonitrile and 0.2 M sulfate buffer solution (adjusted to pH 2.3 with ethanolamine) at ratio of 27:73	(Zhang et al., 2012b)
	Jusco 875	n/a	Thermo Quest C18 (250 x 4.6 mm, 5 µm)	n/a	n/a	n/a	(Lin et al., 2007a)
	Anyang SDV 505	Centrifuged at 14,000 rpm for 15 min at 4°C	Chrompack C8 (150 x 6 mm, 5 µm)	210 nm	1.2 mL/min	Acetonitrile and phosphate buffer solution at ratio of 28:72 with 1% triethylamine, adjusted to pH 3.0 with phosphoric acid	(Avadi et al., 2010)
	Thermospectra TSP 1000 pump	Insulin standard calibration curve (0.5, 1, 1.5, 2 IU/mL)	ACE (250 x 5 mm, 5 µm)	214 nm	1 mL/min	Acetonitrile and 0.2 M sodium sulfate aqueous solution at ratio of 27:73, pH adjusted to 2.3 with concentrated phosphoric acid	(Elsayed et al., 2009)
	Varian 9012	Insulin standard calibration curve (1-100 µg/mL)	Waters XTerra RP 18 (250 x 4.6 mm, 5 µm) and LiChrospher 100 RP-18 guard column (5 µm)	214 nm	1 mL/min	Acetonitrile and 0.1% trifluoroacetic acid aqueous solution from 30:70 to 40:60 in 5 min until 10 min	(Sarmento et al., 2006b; Sarmento et al., 2007a; Sarmento et al., 2007d)
		Centrifuged at 20000 g for 30 min	XTerra RP 18	214 nm	n/a	0.1% trifluoroacetic acid aqueous solution and acetonitrile from 70:30 to 60:40 over 5 min until 10 min	(Sarmento et al., 2007c)
	LC-5A pump	Centrifuged at 20000 g for 30 min then gel filtration through Sephadex	GL-PACK Nucleosil 100-5 C18 column (150 x 4.6 mm)	220 nm	1.2 mL/min	Acetonitrile, 0.1% trifluoroacetic acid and sodium chloride at ratio of 31:69:0.58	(Barichello et al., 1999)
	n/a	Centrifuged at 50000 rpm for 1 hr at 4 °C; pellets were dissolved in 0.01 M HCl and methanol then centrifuged again at 15000 rpm for 10 min	C18	214 nm	1 mL/min; 20 µL	3.9% tetramethylammonium hydroxide solution in water and acetonitrile at ratio of 70:30, pH adjusted to 2.5 with phosphoric acid, filtered through a 0.22 µm membrane filter and degassed	(Boushra et al., 2016b)

	n/a	GL-Pack Nucleosil 100-5 C18 (150 x 4.6 mm, 5 µm)	220 nm	1.0 mL/min; 20 µL	Acetonitrile, 0.1% trifluoroacetic acid, and sodium chloride at ratio of 31:69:0.58		(Daimon et al., 2016)
	30 µg/mL insulin NPs and centrifuged at 12000 rpm for 20 min	n/a	n/a	n/a	n/a		(Salvioni et al., 2016)
	Centrifuged at 50000 rpm for 1 hr at 4 °C; pellets were dissolved in 0.01 M HCl and methanol then centrifuged again at 15000 rpm for 10 min	Waters C18 (300 x 3.9 mm, 15-20 µm)	214 nm	1 mL/min; 20 µL	3.9% tetramethylammonium hydroxide solution in water and acetonitrile at ratio of 70:30, pH adjusted to 2.5 with phosphoric acid, filtered through a 0.22 µm membrane filter and degassed		(Boushra et al., 2016a)
	1 mL NPs in water (containing 100 IU or 3.6 mg insulin) centrifuged at 50000 rpm for 1 hr at 4 °C; pellets were dissolved in 200 µL acetonitrile and 800 µL 0.01 M HCl, then centrifuged at 15000 rpm for 20 min at 4 °C	C18 (250 x 4.6 mm, 5 µm)	214 nm	1.2 mL/min; 20 µL	0.2 M sodium sulphate anhydrous (adjusted to pH 2.3 with orthophosphoric acid) and acetonitrile at ratio of 74:26, filtered through 0.45 µm nylon membrane filter and degassed		(Jain and Jain, 2015)
	Centrifuged at 12000 rpm for 5 min	Diamonsil C18 (250 x 4.6 mm, 5 µm) at 35 °C	214 nm	1 mL/min; 10 µL	0.1 mol/L sodium dihydrogen phosphate, 0.05 mol/L sodium sulfate and acetonitrile at ratio of 35:35:30 (adjusted to pH 3 with phosphoric acid)		(Zhao et al., 2013)
	n/a	35°C	214 nm	1 ml/min; 20 µL	0.1 mol/L sodium dihydrogen phosphate, 0.05 mol/L Na_2SO_4 and acetonitrile at ratio of 35:35:30 (adjusted to pH 3 with phosphoric acid)		(Sun et al., 2011)
	Insulin standard calibration curve (3, 6, 12.5, 25, and 100 µg/mL in USP XXVI acetate buffer pH 4.7); centrifuged at 50000 rpm for 45 min	Waters XTerra RP 18 (250 x 4.6 mm, 5 µm) and LiChrospher 100 RP-18 guard column (5 µm)	n/a	1 mL/min; 20 µL	Acetonitrile and 0.1% trifluoroacetic acid aqueous solution from 30:70 to 40:60 over 5 min until 10 min		(Sarmento et al., 2011)
	NPs suspended in mobile phase and vortexed for 30 min	n/a	n/a	n/a	0.1 M sodium dihydrogen phosphate, 0.05 M sodium sulfate and acetonitrile at ratio of 35:35:30		(Sonaje et al., 2010a)
	NPs dissolved in 50% ethanol at 70°C for 10 min; centrifuged at 14000 rpm for 15 min at 4°C	VP-ODS (150 x 4.6 mm, 5 µm)	214 nm	1 mL/min	0.2 mol/L sodium sulfate (pH adjusted to 2.3 with ethanolamine) and acetonitrile at ratio of 72:27		(Zhang et al., 2009)
	Centrifuged at 32000 rpm for 50 min at 4°C	n/a	210 nm	1.3 mL/min; 100 µL	33.5% acetonitrile and water containing 1.5% triethylamine, adjusted to pH 2.5 with trifluoroacetic acid		(Lin et al., 2007b)

		Centrifuged at 100000 rpm for 15 min at 4°C	C8 (250 x 4.6 mm, 5 µm)	n/a	n/a	n/a	(Chalasani et al., 2007a)
		15 mg NPs dispersed in 300 µL of distilled water; centrifuged at 1000000 rpm for 15 min 4 °C	Merck LiChrospher C8 (250 × 4 mm, 5 µm)	210 nm	1.3 mL/min; 100 µL	33.5% acetonitrile and water containing 1.5% triethylamine, adjusted to pH 2.5 with trifluoroacetic acid	(Chalasani et al., 2007b)
		Method 1: NPs dissolved in methanol (adjusted to pH 2 by H_3PO_4) at 65 ◦C for 10 min; centrifuged at 4000 rpm for 15 min **Method 2:** 4 mL NPs centrifuged at 40000 rpm for 1 hr at 10°C, then washed with distilled water	Inertsil ODS-3 (250 x 4.6 mm)	n/a	1 mL/min	0.025 mol/L sodium dihydrogen phosphate, 0.05 mol/L sodium sulfate and hydrocyanic ether at ratio of 36:36:28, adjusted to pH 2 by phosphoric acid	(Zhang et al., 2006)
BCA assay	Microplate reader (MCC340)	Centrifuged at 15000 rpm for 30 min at 4°C	n/a	562 nm	n/a	n/a	(Bai et al., 2017)
	TECAN UV spectrophotometer	NPs (1 mg/mL) dissolved at 60°C for 2 h, then mix 125 µL NPs with 125 µL BCA reagents, followed by incubation at 60°C for 30 min; prepare blank NPs and blank buffer (pH 7.4) as controls	n/a	562 nm	n/a	n/a	(Chopra et al., 2017)
	n/a	Centrifuged at 6500 g for 30 min for 4 hr in presence of 10µL glycerol, then washed with 5 mM HCl; mix 150 µL supernatants with 150 BCA reagents for 2 hr at 37°C	n/a	562 nm	n/a	n/a	(Pereira de Sousa et al., 2016)
	n/a	Ultrafiltration of NPs by Amicon Ultra centrifugal filter (MWCO 100 kDa)	n/a		n/a	n/a	(Zhang et al., 2016)
	Shimadzu 1601 UV spectrophotometer	NPs dispersed in 1 mL distilled water; centrifuged at 22000 rpm for 20 min at 4-8°C, then dilute with PBS	n/a	562 nm	n/a	n/a	(Sharma et al., 2015)
	Shimadzu UV-1601 UV spectrophotometer	5 mg NPs dissolved in 1 mL HCl (1 N); mix 0.1 mL supernatants with BCA reagents for 30 min at 37°C	n/a	562 nm	n/a	n/a	(Nam et al., 2010)
UV and fluorescent detection assay	Shimadzu UV-2550 spectrometer	NPs dialysed against water in dialysis bag (MWCO 3.5 kDa); centrifuged at 11000 rpm for 30 min; Bradford method	n/a	595 nm	n/a	n/a	(Wang et al., 2017b)
	TECAN infinite M1000 plate reader	FITC-insulin standard calibration curve	n/a	400-700 nm	n/a	n/a	(Hosseini-Nassab et al., 2017)
	PerkinElmer LS55 spectrofluorometer	n/a	n/a	Ex/Em = 490/516 nm	n/a	n/a	(Chen et al., 2017)
	Jasco V-550 UV spectrophotometer	NPs dissolved in phosphate buffer (pH 7.8) for 10 hr at 4°C, then filtered through Whatman filter paper (grade 41)	n/a	275 nm	n/a	n/a	(Guha et al., 2016)

Varioskan flash multimode reader	FITC-insulin standard calibration curve	n/a	Ex/Em = 488/516 nm	n/a	n/a		(Shan et al., 2015)
Shimadzu fluoro-spectrophotometer	FITC-insulin standard calibration curve	n/a	Ex/Em = 488/516 nm	n/a	n/a		(Ke et al., 2015)
Fluorescence spectrometry	n/a	n/a	Ex/Em = 488/518 nm	n/a	n/a		(Zhu et al., 2014)
Genesys 10S UV spectrophotometer	BSA standard calibration curve (100-500 µg/mL); centrifuged for 5 min in PBS (pH 6.8), then Bradford method	n/a	595 nm	n/a	n/a		(Andreani et al., 2015)
	30 mg lyophilized NPs dissolved in 3 mL PBS (pH 6.8) at 150 rpm for 30 min; centrifuged at 5000 rpm for 5 min	n/a	595 nm	n/a	n/a		(Andreani et al., 2014)
n/a	20 mg NPs dissolved in in 10 mL PBS (pH 7.4) at room temperature; prepare blank nanoparticles as control	n/a	272 nm	n/a	n/a		(Tahtat et al., 2013)
LAMBDA-25 UV spectrophotometer	Centrifuged at 14000 rpm for 30 min at room temperature	n/a		n/a	n/a		(Mukhopadhyay et al., 2013)
VersaFluor fluorometer	400 µL FITC-insulin in 2 mL PVA (2.5 %) or 10 mL PVA (0.15%)	n/a	Ex/Em = 490/520 nm	n/a	n/a		(Reix et al., 2012)
Shimadzu UV-2550 spectrometer	Centrifuged at 8600 g for 30 min at 15°C; Bradford method	n/a	595 nm	n/a	n/a		(Wu et al., 2011)
UV spectrophotometry	10 mg lyophilized NPs dissolved in 0.1 mol/L NaOH solutions, adjusted to pH 7.4 using 0.1 mol/ L HCl; centrifuged at 16000 g or 87000 g for 30 min	n/a	274 nm	n/a	n/a		(Jelvehgari et al., 2010)
Thermomax plate reader	Mix insulin supernatant and Bradford reagent at 1:1 for 15 min at room temperature; modified Bradford assay	n/a	595 nm	n/a	n/a		(Sarmento et al., 2007b)
Thermomax plate reader	Centrifuged at 14000 rpm/ 20000g for 45 min; Coomassie Plus modified Bradford assay and mix insulin supernatants with Bradford reagent at 1:1 for 15 min at room temperature	n/a	595 nm	n/a	n/a		(Sarmento et al., 2006c)
UV spectrophotometer	n/a	n/a	276 nm	n/a	n/a		(Liu et al., 2007b)
Shimadzu RF-5301 PC spectrofluorometer	FITC-insulin standard calibration curve (0-1.2 µg/mL) 10 mL FITC-insulin NPs centrifuged at 120000 g for 30 min	n/a	Ex/Em = 494/517 nm	n/a	n/a		(Li et al., 2007)

	Shimadzu UV-160 A spectrophotometer	100 mg NPs dissolved in 20 mL phosphate buffer for 24 hr under stirring; Lowry's method	n/a	750 nm	n/a	n/a	(Sajeesh and Sharma, 2006)
	Jobin Yvon spectrofluo JY3D spectrofluorometer	Centrifuged at 112000 g for 90 min	n/a	Ex/Em = 583/603 nm	n/a	n/a	(Aboubakar et al., 2000)
Gel chromatography	UV-762 spectrophotometer	NPs dissolved in PBS (pH 7.4) at 70 rpm and 37°C	Sephadex G-50 (30 × 2.6 cm)	280 nm	n/a	n/a	(Fan et al., 2006)
ELISA	BioRad plate reader	Centrifuged at 30000 g for 15 min at 4°C	n/a	520 nm	n/a	n/a	(Verma et al., 2016)
	Shimadzu UV-1800 spectrophotometer	Centrifuged at 15000 rpm for 30 min	n/a	405 nm	n/a	n/a	(Cho et al., 2014)
	BioRad plate reader	n/a	n/a	450 nm	n/a	n/a	(Elsayed et al., 2009)

Supplementary table 2. Experimental condition for size measurement and polydispersity index of insulin nanoparticles

Method	System	Pre-treatment	Dispersion	Quantification parameter	Temperature	Ref
Dynamic light scattering	ZetaSizer Nano ZS90	n/a	n/a	n/a	25 °C	(Wang et al., 2017b)
		Sonication for 30 s	96% ethanol	Quartz cell at 90° scattering	25 °C	(Alfatama et al., 2018)
		Dilution of 5 µL of PPy NPs	2 mL water	1 mL of resultant solution	n/a	(Hosseini-Nassab et al., 2017)
		Dilution of 200 µL NPs, centrifugation at 10000 rpm for 10 min, sonication for 10 min	2 mL deionised water	90° scattering, refractive index 1.33	n/a	(Gupta and Mohanty, 2017)
		Dilution of NPs by 10-fold	Distilled water	633 nm laser, 90° angle	n/a	(Chen et al., 2017)
		Dilution of blank NPs and insulin NPs at appropriate concentrations	Deionised water	670 nm laser, 90° angle	25 °C	(Bai et al., 2017)
		Addition of 5 mM NaCl	n/a	90° scattering	25 °C	(Zhang et al., 2016)
		Dispersion of lyophilized NPs	Distilled water	n/a	25 °C	(Sun et al., 2015)
		n/a	n/a	90° scattering, 15 s acquisition time	25°C	(Ke et al., 2015)
		Dilution	10 mM KCl	90° scattering	25°C	(Jain and Jain, 2015)
		n/a	n/a	n/a	25 °C	(Sun et al., 2011)
		Preparation of NPs before and after lyophilisation	Distilled water	n/a	n/a	(Sun et al., 2010)
		Dilution of 0.2 mL NPs	1 mL water	50 mV laser, 90° scattering, 2 min acquisition time, 10 subruns	25 °C	(Liu et al., 2007a)
	ZetaSizer Nano ZS	n/a	n/a	4 mW He–Ne laser (633 nm)	25 °C	(Siddiqui et al., 2017)
		Dilution of NPs by 20-folds	Deionised water	n/a	25 °C	(Deng et al., 2017)
		n/a	n/a	4 mW He-Ne laser (633 nm)	25 °C	(Siddiqui et al., 2016)
		Dilution of NPs to reach 0.4 mg/mL	Milli-Q water	n/a	n/a	(Lopes et al., 2016)
		Filtration through 22 µm filter	n/a	He-Ne laser (632.8 nm), 173° scattering, 1 cm cuvette, 10 min acquisition time, 5 subruns with 10-16 scans	25 °C	(Burova et al., 2013)
		n/a	50 mM PBS (pH 7)	n/a	n/a	(Hecq et al., 2015)

		Dilution of NPs by 500-folds	Distilled water	n/a	25 °C	(Diop et al., 2015)
		n/a	n/a	90° scattering	25 °C	(Al-Kurdi et al., 2015)
		Dissolving NPs by vortexing	Ultrapure water	n/a	n/a	(Andreani et al., 2014)
		n/a	n/a	Disposable polystyrene cuvettes, 90° scattering, viscosity 0.8872 cP, refractive index 1.33	25 °C	(Prusty and Sahu, 2013)
		Filtration through 0.5 µm filter	n/a	10 mm diameter cylindrical cell, 173° scattering,	37 °C	(Mukhopadhyay et al., 2013)
		n/a	Deionised water	n/a	n/a	(Su et al., 2012)
		Dilution of NPs to suitable concentration	Milli-Q water	n/a	n/a	(Sarmento et al., 2011)
		Preparation of polymer, insulin complex and insulin	Tris buffer (pH 7.4)	n/a	25 °C	(Thompson et al., 2010)
		Preparation of polymer, insulin complex and insulin	Tris buffer (pH 7.4)	n/a	25 °C	(Thompson et al., 2009)
		n/a	n/a	13 subruns, 173° scattering	25 °C	(Elsayed et al., 2009)
	Brookhaven BIC 90 plus	Dilution of lyophilised NPs to suitable concentration	Milli-Q water	n/a	n/a	(Fonte et al., 2016)
		Dilution of NPs by 3-folds and filtration through 0.45 mm filters	Deionised water	677 nm laser	n/a	(Ma et al., 2002)
	Malvern 300 HS	Dilution of NPs by 10-folds, filtration through 0.22 µm filter	n/a	n/a	n/a	(Mahjub et al., 2011)
	Nicomp 380 ZLS	Filtration through 0.22 µm membrane	Distilled water	90° scattering	n/a	(Liu et al., 2016a)
		n/a	n/a	90° scattering, 10 min acquisition time	n/a	(Pereira de Sousa et al., 2016)
		Suspended freshly prepared NPs and freeze-dried NPs	Ultrapure water	n/a	n/a	(Zhang et al., 2012b)
		Suspended lyophilised NPs at 1 mg/mL	Deionised water	He-Ne laser (632.8 nm), 90° scattering	25 °C	(Nam et al., 2010)
	Nicomp ZPW 388	Centrifuged NPs at 15000 rpm for 20 min at 4 °C	Distilled water	90° scattering, 15 min acquisition time	Room temperature	(Deutel et al., 2016)
	ZetaSizer 3000 HS	Dilution to achieve 50-200 kilo counts/second	Distilled water	n/a	n/a	(Boushra et al., 2016a)
		n/a	Deionised water	Polystyrene cuvettes, 90° scattering	n/a	(Sharma et al., 2015)
		Centrifuged NPs at 15000 rpm for 20 min at 4 °C	Distilled water	n/a	25 °C	(Mahjub et al., 2014)

		Preparation of NPs before and after freeze-drying	n/a	n/a	n/a	n/a	(Sonaje et al., 2010a)
		Dilution	Purified water	90° scattering	25 °C		(Bayat et al., 2008)
		n/a	Distinct GI pH	n/a	n/a		(Mi et al., 2008)
		Washing for three times, centrifuged at 32000 rpm for 50 min		n/a	n/a		(Lin et al., 2007a)
		n/a	pH 1.2 (0.1 N HCl), pH 2.5 (0.01 N HCl), and pH 6.6 or 7.4 (10 mM PBS)	n/a	n/a		(Lin et al., 2007b)
		Calibrated instrument with standard reference latex particles	Distilled water	10 mW He–Ne laser (633 nm), 90° scattering, viscosity 0.88 cP, refractive index 1.33	25 °C		(Mao et al., 2006)
	ZetaSizer ZEN 3600	Dilution to achieve 7-9 attenuator values	Milli-Q water and1 mM sodium chloride	633 nm laser, 173° scattering, refractive index 1.524	n/a		(Salvioni et al., 2016)
		Dilution	Water	180 s acquisition time	n/a		(Zhang et al., 2012a)
	ZetaSizer	Dilution to achieve 50-200 kilo counts/second	Distilled water	Disposable polystyrene cells	25 °C		(Boushra et al., 2016b)
		n/a	n/a	90° scattering	25 °C		(Avadi et al., 2010)
		Preparation of 5 mL NPs	n/a	90° scattering, 10 subruns	25 °C		(Sarmento et al., 2006a)
	Beckman coulter LS 230	n/a	n/a	6 subruns	n/a		(Cui et al., 2007)
	Beckman Coulter Delsa Nano C	Calibrated instrument with standard reference latex particles	n/a	60° scattering,	25 °C		(Lopes et al., 2015)
	Beckman Coulter LS 13 320	Ultrasonication of NPs	n/a	refractive index 1.36, 90 s acquisition time	n/a		(Lopes et al., 2015)
	BI-200SM goniometer version 2	Dilution to achieve 20 kHz count rate, filtration through 0.22 µm filter unit	Water	30 mW He-Ne laser, 90° scattering	n/a		(Ganeshkumar et al., 2013)
		n/a	n/a	30 mW He-Ne laser, 5 subruns	n/a		(Wu et al., 2011)
	ZetaSizer DTS 4.1	Dilution of NPs by 9-folds	Deionised water	n/a	n/a		(Hurkat et al., 2012)
	ZetaSizer and particle analyzer 5000	Dilution of NPs to suitable concentration	Milli-Q water	n/a	n/a		(Fonte et al., 2011)
		Preparation of 5 mL NPs	n/a	90° scattering	25 °C		(Zhang et al., 2010)
		Dilution of NPs to suitable concentration	n/a	90° scattering	25 °C		(Sarmento et al., 2007b;

		n/a	n/a		90° scattering, 10 subruns	25 °C		Sarmento et al., 2007c)
		5 mL NPs	n/a		90° scattering	25 °C		(Sarmento et al., 2007d)
		n/a	n/a		90° scattering	25 °C		(Sarmento et al., 2007a)
		n/a	n/a		90° scattering, 10 subruns	25 °C		(Sarmento et al., 2006c)
	ZetaSizer II	Dilution	n/a		90° scattering	25 °C		(Sarmento et al., 2006b)
	Beckman coulter N5 particle analyzer	Calibrated instrument with standard reference latex particles	n/a		90° scattering	25 °C		(Wu et al., 2012)
	Shimadzu SALD 2101	n/a	Distilled water		n/a	n/a		(Woitiski et al., 2009a; Woitiski et al., 2009b)
	Autosizer Lo-C	n/a			10 mW He-Ne laser (633 nm), 90° scattering	25 °C		(Jelvehgari et al., 2010)
	Beckman coulter LS130	n/a	Acetate buffer (pH 4.5)		n/a	n/a		(Jintapattanakit et al., 2007)
	Mastersizer 2000	n/a			90° scattering	Room temperature		(Reis et al., 2008)
	Brookhaven BI 90	Dilution of 0.5 mL NPs	20 mL		n/a	25 °C		(Bhumkar et al., 2007)
	ZetaSizer HSA	Dilution of NPs to suitable concentration	Distilled water		n/a	n/a		(Qian et al., 2006)
			PBS (pH 7.4)		n/a	n/a		(Zhang et al., 2009)
	Brookhaven BI-200SM goniometer	Preparation of NPs before and after lyophilisation	Nanopure water		50 mW He-Ne laser (532 nm), 90° scattering, 3 min acquisition time	n/a		(Sajeesh and Sharma, 2006)
	Otsuka Electronics	n/a	n/a		n/a	25 °C		(Tiyaboonchai et al., 2003)
	Malvern 4700 laser spectrometer	Dilution, filtration through 0.2 µm filters	Water or 0.1% acetic acid		632.8 nm laser, 90° scattering	25 °C		(Barichello et al., 1999)
Atomic force microscopy	Nanoscope IV bioscopet	1-2 µL NPs on split untreated mica sheet, dried at room temperature	n/a		Nitride tip in tapping mode, scan speed at 1 Hz	n/a		(Lowe and Temple, 1994)
Scanning electron microscopy	Hitachi 3400N	10-12 µL NPs on glass slide, dried at room temperature on the stub, sputter coated with gold under vacuum	n/a		20 KV acceleration voltage	n/a		(Mukhopadhyay et al., 2013)

	Zeiss Sigma FESEM	Aluminium stub, dried overnight, sputter coated with Au/Pd under vacuum	n/a	n/a	n/a	(Hosseini-Nassab et al., 2017)
	Hillsboro FEI Quanta 400 FEG	Metal stubs, coated with gold or palladium under vacuum	n/a	15 mA current for 60 s	n/a	(Fonte et al., 2016)
	Philips XL-30 ESEM	n/a	n/a	Measuring size of 100 particles	n/a	(Fan et al., 2006)
Transmission electron microscopy	FEI Tecnai G20	Carbon coated copper grid, 2% phosphotungstate solution for staining, dried at room temperature	n/a	n/a	n/a	(Sheng et al., 2016)
	Hitachi H-600A	A drop of NPs (20 mg/mL) on Formvar-coated copper grid, 2% phosphotungstate solution staining for 3 min, dried completely	n/a	n/a	n/a	(Qian et al., 2006)

Supplementary table 3. Experimental conditions for zeta potential measurement of insulin nanoparticles

System	Pre-treatment	Dispersion	Quantification parameter	Temperature	Ref
ZetaSizer Nano ZS90	Sonication for 30 s	96% ethanol	Quartz cell, 90° scattering	25 °C	(Alfatama et al., 2017)
	Dilution of NPs by 10-folds	n/a	633 nm laser, 90° scattering	n/a	(Chen et al., 2017)
	Preparation of blank NPs and insulin NPs	Deionised water	670 nm laser, 90° scattering	25 °C	(Bai et al., 2017)
	Preparation of lyophilized NPs	5 mM NaCl	90° scattering	25 °C	(Zhang et al., 2016)
	n/a	n/a	n/a	25 °C	(Sun et al., 2015)
	n/a	n/a	90° scattering, 15s acquisition time	25 °C	(Ke et al., 2015)
	n/a	n/a	n/a	25 °C	(Sun et al., 2011)
	Dilution of NPs by 5-folds	n/a	n/a	n/a	(Liu et al., 2007a)
Brookhaven ZetaPALS	Dilution of lyophilized NPs to suitable concentration	Milli-Q water	Calculation of lyophilisation ratio	n/a	(Fonte et al., 2016)
	Dilution of NPs by 40-folds	Demineralized water	n/a	20 °C	(Qian et al., 2006)
	Dispersion of 4 mg lyophilized NPs	1.3 mL water	25 mW solid state laser (676 nm), 15° scattering, 10 subruns	n/a	(Tiyaboonchai et al., 2003)
Nicomp ZPW 388	Dipping electrodes into NPs suspension	n/a	1 V/cm electric field strength, 0.4 cm electrode spacing	Room temperature	(Deutel et al., 2016)
Nicomp 380 ZLS	n/a	n/a	Doppler electrophoretic laser shift at 28°C	-14 °C	(Liu et al., 2016a)
	n/a	n/a	5 V/cm electric field strength for 3 min		(Pereira de Sousa et al., 2016)
	Preparation of fresh NPs and freeze-dried NPs	Ultrapure water	n/a	n/a	(Zhang et al., 2012b)
	n/a	NaCl	n/a	n/a	(Cui et al., 2009)
Beckman coulter Delsa Nano C	Calibration with mobility standard	pH 4.5	n/a	25 °C	(Lopes et al., 2015)
ZetaSizer 3000 HS	Dilution of NPs to 50-200 kilo counts/ second	Distilled water	n/a	n/a	(Boushra et al., 2016a)
		Deionised water	Electrophoretic cell, 15.24 V/cm electric field	n/a	(Sharma et al., 2015)

	Dilution of NPs by 10-folds, filtration through 0.22 µm filter	Purified water	n/a	n/a	(Mahjub et al., 2011)
	n/a	n/a	Electrophoretic cell, 150 mV potential	n/a	(Wu et al., 2011)
	Preparation of freeze-dried NPs	n/a	n/a	n/a	(Sonaje et al., 2010a)
	Dilution of NPs	Purified water	Electrophoretic cell, 150 mV potential	n/a	(Bayat et al., 2008)
	n/a	pH 1.2 (0.1 N HCl), pH 2.5 (0.01 N HCl), pH 6.6 or 7.4 (10 mM PBS)	n/a	n/a	(Lin et al., 2007b)
	Washing of NPs trice, ultracentrifuged at 32000 rpm for 50 min	n/a	n/a	n/a	(Lin et al., 2007a)
	n/a	0.01 M Tris buffer (pH 6.8, 7.4)	Electrophoretic cell	25 °C	(Mao et al., 2006)
	n/a	n/a	4 mW He-Ne laser (633 nm) laser	25 °C	(Siddiqui et al., 2017)
	Dilution of NPs to 0.1 mg/mL	Water	Folded capillary cell	n/a	(Chopra et al., 2017)
	Dilution of NPs by 20-folds	Deionised water		25 °C	(Deng et al., 2017)
	n/a	n/a	4 mW He-Ne laser (633 nm) laser	25 °C	(Siddiqui et al., 2017)
	n/a	n/a	4 mW He-Ne laser (633 nm) laser	25 °C	(Siddiqui et al., 2016)
	Dilution of NPs to 0.4 mg/mL	Milli-Q water	n/a	n/a	(Lopes et al., 2016)
	n/a	50 mM PBS (pH 7)	n/a	n/a	(Hecq et al., 2015)
	n/a	Purified water with 0.9% sodium chloride solution	50 µs conductivity	n/a	(Andreani et al., 2015)
	n/a	Purified water with 0.9% sodium chloride solution	50 µs conductivity	n/a	(Andreani et al., 2014)
	n/a	n/a	90° scattering	25 °C	(Al-Kurdi et al., 2015)
	n/a	Deionised water	n/a	n/a	(Su et al., 2012)
	Dilution of NPs	Purified water with 0.9% sodium chloride solution	50 µs conductivity	n/a	(Sarmento et al., 2011)
	n/a	Deionized water	Folded capillary electrophoresis cell	25 °C	(Woitiski et al., 2010)
	Calibration with standards (-50 mV)	n/a	n/a	n/a	(Thompson et al., 2010)
ZetaSizer Nano ZS					

	Dilution of NPs to appropriate concentration	Distilled water	n/a	n/a	(Zhang et al., 2009)
	Dilution of NPs to appropriate concentration	Ultrapure water	Folded capillary electrophoresis cell	25 °C	(Woitiski et al., 2009a)
	Dilution of NPs to appropriate concentration	Ultrapure water	Folded capillary electrophoresis cell	25 °C	(Woitiski et al., 2009b)
	Calibration with standards (-50 mV)	n/a	n/a	n/a	(Thompson et al., 2009)
	n/a	10 mM Tris buffer (pH 7.4)	n/a	25 °C	(Jintapattanakit et al., 2007)
	n/a		Folded capillary cells with gold electrodes	25 °C	(Elsayed et al., 2009)
ZetaSizer	Dilution of NPs to appropriate concentration	Water	n/a	n/a	(Boushra et al., 2016b)
	Dilution of NPs	Deionized water	n/a	n/a	(Jelvehgari et al., 2010)
	Dilution of NPs	Double distilled water	n/a	n/a	(Avadi et al., 2010)
ZetaSizer DTS 4.10	Dilution of NPs by 9-folds	Deionized water	n/a	n/a	(Hurkat et al., 2012)
ZetaSizer and particle analyzer 5000	Dilution of NPs	n/a	n/a	n/a	(Sarmento et al., 2007b; Sarmento et al., 2007c)
ZetaSizer ZEN 3600	Dilution of NPs	Milli-Q water with sodium chloride (1 mM)	633 nm laser, 173° scattering, sample concentration kept at 7-9 attenuator value, 1.524 refractive index	n/a	(Salvioni et al., 2016)
	Dilution of NPs	0.1 mM KCl	Automatic mode	n/a	(Zhang et al., 2012a)
ZetaSizer II	Dilution of NPs	n/a	n/a	25 °C	(Wu et al., 2012)
ZetaSizer III	n/a	KCl (0.1 mol/L)	Electrophoretic cell, 150 mV potential	n/a	(Pan et al., 2002a)
ZetaSizer 3000 HSA	Without dilution	n/a	60 s acquisition time	n/a	(Bhumkar et al., 2007)
	Dispersion of a drop of NPs	Twice-distilled water (adjusted to pH 4 with 1 mM HCl or 1 mM NaOH)		n/a	(Fan et al., 2006)

Supplementary table 4. Experimental conditions for morphological examination of insulin nanoparticles

Method	System	Sampling grid	Sample treatment	Staining	Drying	Microscopic parameters	Ref
Transmission electron microscopy	FEI Tecnai G20	Copper grid coated with carbon	n/a	2% phosphotungstate solution	Dried at room temperature	n/a	(Sheng et al., 2016)
	Hitachi H-7650	n/a	Diluted NPs with distilled water	2% phosphotungstic acid	n/a	n/a	(Zhang et al., 2009)
	Hitachi H-600	Copper grid coated with Formvar	Removed surface water by filter paper	2% phosphotungstate solution (pH 6.5) for 2 min	Air dried	75 kV acceleration voltage	(Liu et al., 2016b)
		Copper grid	Diluted a droplet of NPs with deionised water, removed excess fluid	1% phosphotungstic acid	n/a	n/a	(Zhang et al., 2015)
		Copper grid with films	Diluted NPs by 2-folds	2% phosphotungstic acid for 30 s	n/a	n/a	(Liu et al., 2007a)
	LEO 912	Glow discharged copper grid coated with Formvar (200 mesh)	n/a	1% aqueous methylamine vanadate stain	Air dried	120 kV acceleration voltage	(Thompson et al., 2010)
		Glow discharged copper grid coated with Formvar/ carbon (200 mesh)	n/a	1% aqueous methylamine vanadate stain	Dried on hydrophilic support film.	80/100 kV acceleration voltage	(Thompson et al., 2009)
	JEM-1200 EX	Copper grid coated with carbon	Dripped drops of NPs, remove extra solution by blotting paper.	n/a	Dried for 1 min	120 kV acceleration voltage	(Bhumkar et al., 2007)
		n/a	PBS (pH 7.4), reconstituted gastric and intestinal media at 37 °C for 0, 30 min, and 5 h	2% sodium phosphotungstate solution, pH 7.4	n/a	n/a	(Aboubakar et al., 2000)
	FEI Tecnai TF20	Copper grid	n/a	n/a	n/a	200 kV acceleration voltage, low dose mode for imaging	(Gupta and Mohanty, 2017)
	JEOL JEM-1230	Copper grid coated with carbon	Diluted 0.05 mL NPs with 1 mL distilled water	n/a	Evaporated residual water	100 kV acceleration voltage	(Deng et al., 2017)
	100 CX II	Copper grid	n/a	No staining	Dried at room temperature	n/a	(Wang et al., 2017a)
		Copper grid	n/a	Phosphotungstic acid	Dried at room temperature	n/a	(Bai et al., 2017)
		Copper grid coated with nitrocellulose	n/a	No staining	Dried at room temperature	n/a	(Bayat et al., 2008)
	FEI Tecnai G2 TWIN	Copper grid coated with carbon (200 mesh)	Dispersed one drop in acetone	n/a	Dried at 25 °C	200 kV acceleration voltage	(Alfatama et al., 2018)
	JEOL JEM-1400	Copper grid coated with carbon	Dispersed NPs in Milli-Q water, HBSS-MES (pH 5.5), HBSS-HEPES (pH 7.4)	n/a	Air dried overnight at room temperature	120 kV acceleration voltage	(Lopes et al., 2016)

	Copper grid coated with carbon (300 mesh)	n/a	n/a	Dried at room temperature	120 kV acceleration voltage	(Boushra et al., 2016a)
FEI Tecnai F30Ò	n/a	n/a	n/a	n/a	150 kV acceleration voltage	(Verma et al., 2016)
Tecnai G2 Spirit Bio TWIN	n/a	n/a	n/a	n/a	80 kV acceleration voltage	(Shan et al., 2016)
Philips Tecnai 20	Polycarbonate grids	n/a	n/a	Cooled with liquid nitrogen	n/a	(Liu et al., 2016a)
JEOL	Copper grid coated with carbon	Dispersed NPs in ethanol then ultrasonication	n/a	n/a	200 kV acceleration voltage	(Guha et al., 2016)
Zeiss 902	Copper grid coated with graphite	Dripped 10 µL NPs	n/a	Dried under red light for 30 min	n/a	(Deutel et al., 2016)
Hillsboro FEI Quanta 400 FEG	Metal stubs	NPs coated with gold/palladium with 15 mA current for 60s	n/a	n/a	n/a	(Fonte et al., 2016)
JEOL JEM 2100	Copper screen	Diluted NPs by 10-folds with distilled water, removed excess fluid by filter paper	3% phosphotungstic acid	Dried for 20 min	n/a	(Chen et al., 2017)
	Copper grid coated with carbon (300 mesh)	n/a	3% uranyl acetate	Dried at room temperature	120 kV acceleration voltage	(Boushra et al., 2016b)
	Copper grid coated with carbon	n/a	1% phosphotungstic acid, then washed twice with distilled water	Dried at room temperature	n/a	(Zhang et al., 2014)
Philips Morgagni 268	n/a	Dripped 10 µL NPs for 90 s at room temperature	1% phosphotungstic acid	n/a	100 kV acceleration voltage	(Sharma et al., 2015)
JEOL JEM 200 CX	n/a	Removed excess solution by filter paper	2% phosphotungstic acid for 10 s	Air dried	n/a	(Jain and Jain, 2015)
Tecnai G2 Sphera	Mica slice coated with carbon under vacuum	Dripped 2 µL NPs for 1 min, removed excess suspension	1% uranyl acetate for 1 min	n/a	n/a	(Diop et al., 2015)
JEOL JEM 1010	Copper grid coated with ultrathin (200 mesh)	Dripped 2 µL NPs	2% uranyl acetate	Air dried	120 kV acceleration voltage	(Salvioni et al., 2016)
	Copper grid with films	n/a	2% phosphotungstic acid	Dried for 10 min	100 nm scale bar	(Cho et al., 2014)
Philips CM-200	n/a	n/a	1% phosphotungstic acid	n/a	160 kV acceleration voltage	(Li et al., 2013)
Hitachi JEM-100 CXII	Copper grid supported with microgrid carbon polymer	Dispersed few drops of NPs in n-hexane, held in vacuum-transfer sample holder	n/a	Dried under ambient conditions	n/a	(Zhao et al., 2013)
	Copper grid	n/a	2% phosphotungstic acid	Dried at room temperature	n/a	(Wu et al., 2012)
Zeiss CEM 902A	Copper grid coated with carbon	Dispersed lyophilized NPs in distilled water, dripped	n/a	Dried for 5 min	n/a	(Mahjub et al., 2011)

			drops of lyophilized and re-dispersed NPs				
		n/a	n/a	Uranil acetate	n/a	n/a	(Sarmento et al., 2007b)
	JEM 1200	Copper grid coated with carbon	Dripped 10 µL NPs	1% phosphotungstic acid, then washed with distilled water twice	Dried completely	300 kV acceleration voltage	(Zhang et al., 2012b)
	JEOL JEM-2000 FX	Copper grid coated with carbon	Dripped a drop of NPs	n/a	n/a	80 kV acceleration voltage	(Nam et al., 2010)
	JEOL 2010	Copper grid	n/a	n/a	n/a	200 kV acceleration voltage, colour manipulated by ImageJ	(Diaz et al., 2010)
	Zeiss EM 10 CR	Formvar coated grid	Centrifuged 0.5 mL NPs in 10 mL acetone at 4000 rpm for10 min, then rinsed and redispersed in water: acetone (1:1; 10 mL)	n/a	Dried at room temperature	n/a	(Elsayed et al., 2009)
	Hitachi	Copper grid	n/a	Phosphothungstic acid	Dried at room temperature	n/a	(Cui et al., 2009)
	Zeiss LEO 906	Copper grid coated with carbon	Dispersed one drop of NPs in aqueous solution	n/a	Freeze-dried	80 kV acceleration voltage	(Davaran et al., 2008)
	Zeiss EM 902A	Carbon grid	n/a	Uranyl acetate	Dried at room temperature	n/a	(Reis et al., 2007)
		n/a	n/a	Uranyl acetate	n/a	n/a	(Sarmento et al., 2006b)
	JEOL JEM-1200EXII	Copper grid coated with carbon/ Formvar membrane (300 mesh)	Dispersed lyophilized NPs in 1 mL nanopore water, then dialyzed for 24 hr (MWCO 15000), removed excess solvent by Whatman no. 1 filter paper	2% sodium phosphotungstate solution (5 µL)	Stored in desiccator overnight	n/a	(Tiyaboonchai et al., 2003)
	n/a	Copper grid coated with carbon	Dripped one drop of NPs	Osmium tetroxide	Dried completely	n/a	(Du et al., 2014)
		Copper grid coated with carbon (400 mesh)	Dripped one drop of NPs for 2 min, removed surface water by filter paper	Alkaline bismuth solution	n/a	n/a	(Lin et al., 2007a)
Scanning electron microscopy	n/a	Glass slide	Dripped 10-12 µL of NPs, sputter-coated with gold under vacuum	n/a	Dried at room temperature	20 kV acceleration voltage	(Mukhopadhyay et al., 2013)
	FEI FESEM Quanta 400F	Stub	Diluted NPs by 10-folds, dripped on drop of NPs	n/a	Air-dried at room temperature for 24 hr	20 kV acceleration voltage under low vacuum	(Siddiqui et al., 2017)

	Stub	Diluted NPs by 10-folds, dripped on drop of NPs	n/a	Air-dried at room temperature for 24 hr	20 kV acceleration voltage under low vacuum	(Siddiqui et al., 2016)
Phenom G2 Pure	n/a	Diluted NPs in deionized water by 10-folds, sublimated at -90°C for 4 min, sputter coated with gold/palladium for 40 s	Phosphotungstic acid, frozen using liquid nitrogen slush (-210 °C) under vacuum	Dried in desiccator for 24 hr	n/a	(Lopes et al., 2015)
Oxford EDSJEOL JSM 6301 F	n/a	Sublimated at -90°C for 4 min, sputter coated with gold/palladium for 40 s	Phosphotungstic acid, frozen using liquid nitrogen slush (-210 °C) under vacuum	n/a	n/a	(Lopes et al., 2015)
Philips XL 30	n/a	Sputter-coated with gold–palladium alloy (150-250 A)	n/a	n/a	n/a	(Jain and Jain, 2015)
JEOL JSM 5600 LV	Metallic studs with double-sided conductive tape	Sputter coated with platinum for 40 s under vacuum at 40 mA	n/a	n/a	n/a	(Sun et al., 2015)
	Metallic studs with double-sided conductive tape	Sputter coated with platinum for 40 s under vacuum at 40 mA	n/a	n/a	n/a	(Sun et al., 2011)
	Metallic studs with double-sided conductive tape	Sputter coated with platinum for 40 s under vacuum at 40 mA	n/a	n/a	n/a	(Sun et al., 2010)
	Conductive paper mounted with adhesive on a cuprum stud	Dripped a drop of NPs, coated with platinum	n/a	n/a	7 kV acceleration voltage, 17000 magnification	(Ma et al., 2002)
Variable press Leo 435 VP	n/a	n/a	n/a	n/a	30 kV acceleration voltage	(Sharma et al., 2015)
	Double adhesive tape on aluminium stub	Sputter-coated with gold of 300 A°	n/a	n/a	30 kV acceleration voltage	(Hurkat et al., 2012)
Hitachi S-2460N	n/a	Sputter coated with gold	n/a	Dried completely	25 kV acceleration voltage	(Viehof et al., 2013)
Philips XL 30 ESEM	n/a	Coated with gold	n/a	Dried at room temperature	n/a	(Tahtat et al., 2013)
JEOL JSM-6510 LV	n/a	Coated with platinum	n/a	n/a	n/a	(Makhlof et al., 2011)
LEO 1530 VP	Aluminium stub	Coated with gold	n/a	n/a	10 kV acceleration voltage, 20,000× magnification	(Wu et al., 2012)
JEOL JSM 6330 F	Aluminium sampler holder	Sputter coated with gold	n/a	Dried under vacuum	5 kV acceleration voltage	(Woitiski et al., 2011)
	Aluminium sampler holder	Sputter coated with carbon	n/a	Dried under vacuum	5 kV acceleration voltage	(Woitiski et al., 2010)
JEOL JSM-840	Metal stubs using adhesive tape	Coated with gold	n/a	n/a	n/a	(Fonte et al., 2011)

	Metal grids using double-faced adhesive	Spray dried NPs, coated with gold	n/a	n/a	n/a		(Reis et al., 2008)
	Metal stubs using adhesive tape	Coated with gold under vacuum	n/a	n/a	n/a		(Sarmento et al., 2007d)
	Metal stubs	Coated with gold under vacuum	n/a	n/a	10 kV voltage	acceleration	(Sarmento et al., 2006b)
	Metal stubs	Coated with gold under vacuum	n/a	n/a	10 kV voltage	acceleration	(Sarmento et al., 2006a)
Hitachi S-4700	n/a	Sputter coated with platinum with 6 nm thickness, 6 pa vacuum rate and 15 mA discharge current	n/a	n/a	30 kV voltage	acceleration	(Nam et al., 2010)
LEO 440i	Metal stubs with double adhesive tape	Coated with platinum/palladium alloy under vacuum	n/a	n/a	15 kV voltage	acceleration	(Jelvehgari et al., 2010)
Hitachi S-450	Metal stubs	NPs were lyophilized, coated with gold under vacuum	n/a	n/a	20 kV voltage	acceleration	(Zhang et al., 2010)
Leo Electron Microscopy	Double stick tape over aluminium stubs	NPs were lyophilized, sputter coated with gold under argon atmosphere then cooled over liquid nitrogen	n/a	n/a	n/a		(Davaran et al., 2008)
JEOL JSM-5900LV	n/a	Placed on graphite surface, sputter coated with gold	n/a	Oven-drying	20 kV voltage	acceleration	(Liu et al., 2007a)
JEOL SM-T20	n/a	Sprinkled the freeze-dried NPs	n/a	n/a	n/a		(Cui et al., 2007)
Philips XL-30 ESEM	Glass slide	NPs rinsed with 95% ethanol or 0.1 mM HCl, ultrasonicated for 2 min at 10 °C, coated with gold	n/a	Air-dried	n/a		(Fan et al., 2006)
Hitachi S-570	Conductive tab on stud	Sprinkled the lyophilized NPs, coated with 20 nm gold-palladium (60:40) in cathode evaporator	n/a	n/a	n/a		(Tiyaboonchai et al., 2003)
n/a	Conductive tape	Dripped freeze-dried powder, sprayed with gold	n/a	n/a	n/a		(Du et al., 2014)
Atomic force microscopy	APE Research	n/a	n/a	n/a	Non-contact mode, NSC15/AIBS cantilever (125 µm length x 35 µm width, tip radius <10 nm)		(Verma et al., 2016)
Nanoscope III	n/a	n/a	n/a	n/a	Collected in air operating in tapping mode		(Ke et al., 2015)

	Dual-Scope	n/a	Dispersed NPs in Milli-Q water	n/a	n/a	Topographical images (10 mm x 10 mm scan area)	(Mahjub et al., 2014)
	Nanoscope IIIa	n/a	Dispersed NPs in ultra-purified water, then dripped 5 µL NPs	n/a	n/a	Tapping mode at 25 °C	(Andreani et al., 2014)
	Nanoscope IV Bioscope	Untreated mica sheet	Dripped 1-2 µL NPs	n/a	Dried at room temperature	Silicon nitride tip in tapping mode (1 Hz scan speed at ambient condition)	(Mukhopadhyay et al., 2013)
		n/a	n/a	n/a	n/a	Contact mode (5 µm scanner)	(Zhang et al., 2012c)
		n/a	n/a	n/a	n/a	Tapping mode (1 Hz scan rate, 512 × 512 pixels)	(Reix et al., 2012)
		n/a	Diluted NPs in Milli-Q water (pH 5.5)	n/a	n/a	Silicon chip for 10 min, I-tape cantilever (125 µm length, 220 kHz frequency, 36 N/m nominal force), tapping mode	(Mao et al., 2006)
	Nano Wizard JPK	Cleaved mica surface	Diluted NPs with ultra-pure water, dripped 10 µL NPs for few min	n/a	Air dried for 10 min	Silicon tips attached to I-type silicon cantilevers (230 µm length, 170 kHz resonance frequency, 0.8-1.1 scan frequency), tapping mode	(Jintapattanakit et al., 2007)

Supplementary table 5. Experimental conditions for *in vitro* release of insulin from the nanoparticles

Method	Drug amount	Material and sample treatment	Dissolution medium	Time intervals	Sample withdrawn	Ref
Dialysis method	10 mL insulin NPs	Cellulose membrane dialysis tube (MWCO 8000-10000 Da)	49 mL SGF (pH 1.2) for 2 hr, then SIF (pH 7) for another 4 hr	n/a	n/a	(Wang et al., 2017a)
	1.25 mL Ins-Zn NPs (1 mg/mL)	Dialysis bag (MWCO 10000 Da) soaked by 15% ethanol for 20 min and distilled water for 30 min	PBS (pH 7.4) at 37°C and continuous stirring	n/a	n/a	(Chopra et al., 2017)
	5 mL NPs	Cellulose membrane dialysis tube (MWCO 8000-10000 Da)	45 mL PBS (pH 1.2, pH 6.8) at 37 °C and shaking (100 rpm)	0-4 h	1 mL	(Bai et al., 2017)
	NPs (containing 2mg insulin)	Dialysis bag (MWCO 12000 Da)	SGF with enzymes (pH 1.2) for 2 hr, then replaced to SIF with enzymes (pH 6.8) for remaining time at 37 °C and shaking (100 rpm)	n/a	500 µL	(Verma et al., 2016)
	n/a	Dialysis bag (MWCO 10000 Da)	SGF (without pepsin, pH 2.5) for 2 hr, then replaced by SIF (without trypsin, pH 6.8) at 37 °C	n/a	200 µL	(Shan et al., 2016)
	10 mg insulin NPs (sink conditions)	Dialysis bag (MWCO 10000 Da)	50 mL SGF (USP 34) at pH 1.2 for 2 hr, then replaced by SIF (USP 34) at pH 5.5 and pH 7.4 under 37 °C and 100 rpm	n/a	100 µL	(Lopes et al., 2016)
	1 mL Insulin/HTCC-CA NPs	Dialysis bag (MWCO 10000 Da)	9 mL PBS (10 mM pH 7.4 containing 0.15 M NaCl) at 37 °C with shaking	n/a	1 mL	(Zhang et al., 2016)
	0.5 mL insulin NPs	Dialysis bag (MWCO 8000-14000 Da)	4.5 mL artificial gastric juice (pH 2.5, 0.02 M) and artificial intestinal liquid (pH 7.4, 0.02 M) at 37 °C for 8 hr	n/a	200 µL	(Zhang et al., 2015)
	5 mL insulin PLGA and PPC NPs (sink conditions)	Dialysis bag (MWCO 12000 Da)	40 mL dissolution medium	n/a		(Sharma et al., 2015)
	Capsule filled with insulin NPs or conjugated NPs (5 mL)	Dialysis bag (MWCO 12000 Da) and heated in distilled water at 60 °C for 1 hr	100 mL 0.1 N HCl (pH 1.2) for 2 hr, followed by pH 5.5 for 1 hr, pH 6.8 for 2 hr and pH 7.5 until the end	n/a	1 mL	(Jain and Jain, 2015)
	F-insulin NPs (0.5 mL) or free F-insulin	Dialysis bag	20 mL PBS (pH 6.8)	n/a	n/a	(Zhu et al., 2014)
	Insulin NPs and adhesive NPs (containing 0.5 mg insulin)	Dialysis bag (MWCO 10000 Da, 8 cm length, 2.5 cm diameter)	5 mL PBS (pH 7.4) at 37 °C with shaking (60 rpm)	0, 0.5, 1, 2, 3, 5, 7, 10, 12, 15, 20 hr	200 µL	(Zhang et al., 2012a)
	Insulin NPs and Con A NPs (containing 2 mg insulin)	Dialysis bag (MWCO 12000-14000 Da)	50 mL SGF (pH 1.2) at 37 °C with continuous stirring for 2 hr, then replaced with SIF (pH 6.8) for another 4 hr, and eventually replaced by SIF (pH 7.4) up to 24 h.	0.5, 1, 2 hr in SGF	0.5 mL	(Hurkat et al., 2012)
	1 µL NPs (containing 100 µg insulin)	Dialysis device (MWCO 20000 Da)	20 mL SGF without enzymes (0.1M HCl) in shaking bath(60 rpm, 37 °C)	n/a	1 mL	(Makhlof et al., 2011)
	10 mg insulin-NPs or 10 mg LMWSC dispersed in 5 mL of PBS (0.1 M, pH 7.4)	Dialysis bag (MWCO 8000 Da)	45 mL PBS (0.1M, pH 7.4)	n/a	0.1 mL	(Nam et al., 2010)

	15 mg NPs (1 mL)	Dialysis bag	20 mL PBS pH 7.4	0, 0.5, 1, 2, 4, 6, 8, 10, 12, 24, 48 hr	100 µL	(Chalasani et al., 2007b)
	NPs (15 mg)	Dialysis bag	20 mL PBS (pH 7.4)	n/a	100 µL	(Chalasani et al., 2007a)
	n/a	Ultrafiltration centrifuge filter (MWCO 10000 Da)	SGF (USP-NF XXIV, pH 1.2) and SIF (USP-NF XXIV, pH 6.8) without enzymes at 37 °C with continuous stirring (50 rpm)	0, 0.5, 1, 2, 4, 6, 8, 12, 24 hr	0.5 mL	(Cui et al., 2006)
Dissolution study	100 µL FPBAINP and FTBAINP	Centrifuged tested samples at 14000 g for 5 min	1 mL deionised water, glucose (1, 2 and 3 mg/mL), fructose (0.002 mg/mL) and a mixture of glucose (2 mg/mL) and fructose (0.002 mg/mL) at 37 °C with horizontal shaking at 100 rpm	n/a	20 µL	(Siddiqui et al., 2017)
	Insulin NPs (5 mg; sink conditions)	Simulated intestinal samples were acidified with 1 mL of 0.01 M HCl. All aliquots were filtered through 0.45 µm PVDF membrane and assayed for insulin content by HPLC.	5 mL of HCl/KCl buffer (pH 1.2), PBS (pH 6.8) at 37 °C and 50 rpm	0.5, 1, 2 hr (pH 1.2) and 4, 6 hr (pH 6.8)	0.4 mL	(Alfatama et al., 2018)
	Lyophilisation of insulin pellet	Centrifuged tested samples at 10000 rpm for 10 min, released samples stored at 2 °C in the absence of light	10 mL PBS	1, 4, 12, 24 hr	n/a	(Gupta and Mohanty, 2017)
	2 mL insulin-SeNPs	n/a	250 mL HCl (pH 1.2), PBS (pH 6.8, 7.4) with 80 µM H_2O_2 at 37 °C for 12 hr under stirring (100 rpm)	n/a	1 mL	(Deng et al., 2017)
	n/a	Centrifuged tested samples by ultrafiltration device (MWCO 10000 Da) at 3000 rpm for 5 min	10 mL HCl (pH 1.2), PBS (pH 6.8, 7.4) at 37 °C under stirring (75 rpm)	n/a	1 mL	(Chen et al., 2017)
	100 µL F3PN	Centrifuged tested samples at 14000 rpm for 15 min	1 mL glucose and fructose concentrations (1, 3, 5 mg/mL) at 37 °C with shaking (100 rpm)	n/a	20 µL	(Siddiqui et al., 2016)
	2 mg ^{125}I-insulin-LMWP MNPs (containing 0.027 µmoL conjugates)	Radioactive counts of the supernatant	1 mL SGF, SIF, SGF-sp and SIF-sp	n/a	n/a	(Sheng et al., 2016)
	Insulin NPs (containing 0.35 mg of insulin)	0.2% bovine albumin added to medium to avoid non-specific adsorption of protein, filtered tested samples with 0.2 µM polyethersulfone membrane and acidified by 40 µL HCl (1 M)	10 mL SIF (0.095 M PBS, pH 6.8), at 37 °C under stirring (600 rpm)	n/a	1 mL	(Salvioni et al., 2016)
	300 µL ChS-PEG C/CS/insulin NPs (0.8 mg/mL)	Centrifuged tested samples at 13400 rpm for 15 min	Stirring at 800 rpm for 16 hr at 37 °C	n/a	n/a	(Pereira de Sousa et al., 2016)
	n/a	Centrifuged tested samples at 17465 g for 20 min at 4 °C	pH 2.0, 6.0 and 7.4 at 37 °C with shaking (100 rpm)	n/a	200 µL	(Liu et al., 2016b)
	Insulin-BCC NPs (pH 6.0, containing 62.6 µM BCC and 10 IU/mL insulin)	Filtered tested samples by syringe filter (0.2 µm pore size)	PBS or intestinal fluid from male Sprague-Dawley rats at 37 °C	5, 15, 30, 60 min	100 µL	(Daimon et al., 2016)

1.0 mL insulin L/C NPs (containing 0.1 mg/mL insulin)	Obtained pellets by centrifugation at 4000 rpm for 20 min, centrifuged tested samples at 3000 rpm for 20 min	10 mL PBS (pH 1.2, pH 6.8) at 37 °C and 50 rpm	n/a	500 µL		(Liu et al., 2016a)
Insulin APB NPs	Centrifuged tested samples at 10000 g for 5 min	PBS (pH 7.4) containing glucose at concentrations of 0-15 mM	10, 30, 60, 90, 180 min	1 mL		(Hsieh et al., 2016)
200 µL PAA100-Cys/PVP/insulin, PAA100/ PVP/insulin NPs	Filtered NPs with 100 nm cutoff and washed for five times with 10 mL demineralized water at pH 3.7, centrifuged tested samples at 7200 g for 10 min at 4 °C	2 mL of 100 mM PBS (pH 7.4 in addition of 5 mM EDTA, 5 mM Tris–HCl and 10% DMSO) at 37 °C	0, 5, 10, 15, 30, 60, 90, 120, 180, 240, 300, 360 min	80 µL		(Deutel et al., 2016)
Insulin PLGA-lipid-PEG NPs and MPs	Centrifuged tested samples at 20000 rpm for 30 min	PBS (pH 7.4) at 37 C under agitation (100 rpm)	n/a	2 mL		(Yu et al., 2015)
^{125}I-labeled insulin NPs (0.2 mg/mL insulin)	Radioactivity of ^{125}I-Ins in the supernatant was counted	SGF-sp, SIF-sp, SGF and SIF at 37 °C with agitation (100 rpm)	n/a	n/a		(Sheng et al., 2015)
5 mL insulin NPs	Centrifuged tested samples at 12500 rpm for 10 min at 4 °C	10 mL SGF without pepsin at 37°C for 2 hr and shaking (100 strokes/minute) then replaced with 10 mL of SIF without pancreatin for other 6 hr	n/a	n/a		(Lopes et al., 2015)
n/a	Centrifuged tested samples at 20000 rpm for 30 min at 4 °C	Gradual pH changing buffers (pH 1.2 for 2 hr, pH 6.8 for another 4 hr, and pH 7.4 up to 24 hr) with oscillating (100 rpm) at 37 °C	0, 0.5, 1, 2, 4, 6, 8, 12, 24 hr	100 µL		(Sun et al., 2015)
75 mg dry NPs	Filtered tested samples with 0.1 mm polyvinylidene fluoride membrane	500 mL PBS (pH 7.0, 0.05 M containing 0.05% polysorbate 20) with stirring (70 rpm) at 37 °C	0, 30, 90, 150, 210 min	2 mL		(Hecq et al., 2015)
n/a	n/a	PBS at 37 °C with gentle stirring	0, 0.25, 0.5, 1, 2, 4 h	n/a		(Diop et al., 2015)
10 mg of insulin Eul-cys and Eul-cys/GSH NPs	n/a	5 mL HCl (pH 1.2) for 2 hr, then centrifuged at 15000 rpm for 20 min and replaced with PBS (pH 7.4) at 37 °C under shaking (100 rpm)	0.5, 1, 2, 2.5, 3, 4, 5, 6 hr	200 µL		(Zhang et al., 2014)
Lyophilized and non-lyophilized NPs (containing 200 mg of insulin)	Centrifuged tested samples at 15000 rpm for 20 min at 4 °C	100 mL SIF (pH 6.8) and PBS (pH 7.4) at 37 °C with 100 rpm	n/a	1 mL		(Mahjub et al., 2014)
10 mg freeze-dried NPs	Centrifuged tested samples at 40000 rpm for 30 min	5 ml phosphate buffer (pH = 1.2, 7.4) with mild stirring	0.5, 1, 2, 4, 6 hr	n/a		(Du et al., 2014)
20 mg Insulin-SiO2-HP55 NPs	n/a	20 mL SGF (pH 1.2) and SIF (pH 7.4) and shaking (100 rpm) at 37 °C	10, 30, 60, 120, 180, 240 min	n/a		(Zhao et al., 2013)
10 mL insulin NPs (1 mg/mL)	Centrifuged tested samples at 18000 g for 10 min	50 mL buffers (pH 1.2, 3.0, 5.4, 7.4) at 37 °C and 60 rpm.	n/a	1 mL		(Viehof et al., 2013)
100 mg insulin beads	n/a	20 mL SGF (pH 1.2) for 2 hr, then SIF (pH 6.5) for 4 hr at 37 °C	n/a	2 mL		(Tahtat et al., 2013)
n/a	Centrifuged tested samples at 20000 g for 30 min	HCl (pH 1.2) and PBS (pH 6.8)	n/a	0.4 mL		(Prusty and Sahu, 2013)

	n/a	n/a	pH 1.2, pH 6.8 and pH 7.4 with mild agitation	0, 2, 4, 6, 8, 10, 12 hr		(Mukhopadhyay et al., 2013)
	20 mg freeze-dried insulin NPs	Centrifuged tested samples at 12500 rpm for 10 min	Buffer (10 mL medium at pH 1.2 for 2 hr, then replaced with 20 mL buffer at pH 6.8 for another 4 hr and pH 7.4 for 18 hr) at 37 °C and 100 rpm	n/a	0.5 mL	(Jain et al., 2012)
	10% ^{125}I-insulin NPs	Centrifuged tested samples at 8000 g for 15 min	SGF (35 mM NaCl, 80 mM HCl, 0.3% pepsin, pH 1.2) and SIF (50 mM KH2PO4, 15 mM NaOH, 1.0% pancreatin, pH 6.8.) with or without enzymes in FBS at 37 °C and 50 rpm	n/a	n/a	(Reix et al., 2012)
	Insulin NPs (10 mg)	n/a	5 mL HCl (pH 1.2) under continuous oscillation (100 rpm) for 2 hr at 37 °C, then centrifuged at 12500 g for 10 min and replaced with 5mL PBS (pH 6.8)	2.5, 3, 4, 5, 6 hr	0.2 mL	(Zhang et al., 2012b)
	n/a	n/a	2 mL PBS at 37 °C with horizontal shaking.	n/a	n/a	(Wu et al., 2011)
	Insulin NPs (5 mg) with or without HP55-coated capsules	n/a	5 mL SGF (pH 1.2) and SIF (pH 7.4) at 37 °C and 100 rpm	0, 30, 60, 120, 240 min	n/a	(Wu et al., 2012)
	Lyophilized NPs (200 mg insulin; sink conditions	Centrifuged tested samples at 20000 rpm for 30 min	80 mL pre-heated PBS (pH 6.8) at 37 °C with gentle stirring (100 rpm)	n/a	1 mL	(Mahjub et al., 2011)
	n/a	Filtered tested samples through 0.1 µm filter	25 mL HCl (0.1 N), PBS (pH 6.5, 7.2) at 37 °C and 75 rpm	n/a	n/a	(Avadi et al., 2011)
	n/a	n/a	20 mL HCl (pH 1.2) for 2 hr, then replaced with 20 mL phosphate (pH 6.8) for 4 hr, under stirring 100rpm at 37 °C	n/a	n/a	(Zhang et al., 2010)
	5 mg insulin NPs	Centrifuged tested samples at 20000 rpm for 10 min	10 mL SGF (free of pepsin and pancreatin) at 37 °C under 100 rpm for 120 min, then centrifuged at 20000 g for 30 min and SIF for 180 min	n/a	100	(Woitiski et al., 2010)
	Enteric-coated capsules and freeze-dried NPs	n/a	Distinct pH at 37 °C under agitation (100 rpm)	n/a	n/a	(Sonaje et al., 2010a)
	Insulin (0.03%) intercalated ZrP	Centrifuged tested samples 1 min	PBS (pH 7.4 and 8.2, 0.1 M)	Between 1-5 hr	10 mL	(Diaz et al., 2010)
	50 mg freeze-dried insulin NPs	n/a	20 mL of saline PBS (pH 7.4, containing 0.1% Tween 80) at 37 °C under stirring (300 rpm)	5, 15, 30, 45 min, 1, 2, 3, 4, 6, 8, 24 h	1 mL	(Damge et al., 2010)
	Physical mixture or purified nanoparticles (1.5 mg insulin)	Centrifuged tested samples at 22000 rpm for 30 min	3 mL of 0.2 N HCl (containing 0.1 mg methyl cellulose) at 37 °C for 2 h, then 0.1 mL of concentrated PBS (pH 7.4) at 37°C and 100 strokes/minutes	0.5, 1, 2, 4, 6, 8 hr	n/a	(Jelvehgari et al., 2010)
	Freeze-dried NPs (containing 4 mg insulin; sink conditions)	n/a	25 mL of pH 1.2 (0.1 N HCl), pH 6.5 (PBS), pH 7.2 (PBS) at 37°C and 75 rpm	n/a	n/a	(Avadi et al., 2010)
	R8-Ins-SLNs or Ins-SLNs	Centrifuged tested samples at 14000 rpm for 15 min at 4 °C	50 mL SIF without enzymes containing 1.5% glycine as stabilizer at 37°C and 150 rpm	n/a	0.5 mL	(Zhang et al., 2009)

	n/a	Centrifuged tested samples at 14000 rpm for 30 min	100 mL mucin solution in 900 mL NC at 37°C	n/a	n/a	n/a	(Jintapattana kit et al., 2009)
	2 g insulin NPs	n/a	5 mL SGF (pH 1.2) with and without pepsin (800 U/mg) for 1 hr at 37 °C (100 strokes/min)	n/a	3 mL		(Elsayed et al., 2009)
	Mixture of insulin and CCGN (1 mL)	Centrifuged tested samples at 12000 rpm for 30 min	1 mL of pH 7.4 PBS, pH 6.8 PBS, and pH 2.0 HCl at 37 °C and 100 rpm.	n/a	n/a		(Cui et al., 2009)
	Lyophilized insulin NPs (10 mg)	n/a	10 mL HCl at pH 1.2 with stirring (100 rpm) for 2 hr at 37 °C, then centrifuged at 12500 g for 10 min and replaced with 10 mL of PBS (pH 6.8) for 6 hr	n/a	n/a		(Reis et al., 2008)
	n/a	n/a	Distinct media (pH 2.5, 6.4, 7.0, 7.4) at 37 °C under agitation (100 rpm)	n/a	n/a		(Mi et al., 2008)
	Insulin NPs (sink condition)	Filtered tested samples through 0.1µm filter	20 mL of PBS (pH 6.8) at 37 °C	0, 1, 2, 3, 4, 5 hr	n/a		(Bayat et al., 2008)
	n/a	n/a	20 mL HCl (pH 1.2) and 20 mL PBS (pH 6.8) with stirring (100 rpm)	n/a	n/a		(Sarmento et al., 2007a)
	Lyophilized insulin NPs (10 mg)	n/a	10 mL HCl (pH 1.2) with magnetic stirring (100 rpm) for 2 hr at 37 °C, then centrifuged at 12500 g for 10 min and replaced with 10 mL PBS (pH 6.8) for 6 hr	n/a	1.5 mL		(Reis et al., 2007)
	n/a	n/a	20 mL of HCl (pH 1.2), acetate (pH 4.5), acetate (pH 5.2), and phosphate (pH 6.8) at 37 °C	n/a	n/a		(Sarmento et al., 2007d)
	n/a	n/a	Dissolution media (pH 2.5, 6.6, 7.4) at 37 °C under agitation (100 rpm)	n/a	n/a		(Lin et al., 2007b)
	n/a	n/a	pH 2.5 for 2 hr, pH 6.6 for 2 hr, then pH 7.4 for 20 hr at 37 °C under agitation (100 rpm)	n/a	n/a		(Lin et al., 2007a)
	Insulin NPs (200 mg)	n/a	20 mL HCl (pH 1.2) for 2 hr, then centrifuged at 20000 g for 15 min and replaced with 20 mL of PBS (pH 6.8) for other 4 hr under magnetic stirring (100 rpm)	0, 0.25, 0.5, 1, 2, 2.25, 2.5, 3, 4, 5, 6 hr	0.4 mL		(Sarmento et al., 2007b; Sarmento et al., 2007c)
	5 mg insulin NPs	n/a	5 mL SGF and SIF at 50 rpm and 37 °C	0, 0.25, 0.5, 1, 2, 4, 6, 8, 10, 12, 16, 24 hr	n/a		(Cui et al., 2007)
	12 mg dried insulin NPs	Centrifuged tested samples at 7000 rpm for 5 min	1 mL of 0.01 M PBS (pH 7.4) at 37 °C	n/a	1 mL		(Liu et al., 2007b)
	Lyophilized nanoparticles (equivalent to 0.1 mg drug)	Centrifuged tested samples at 14000 rpm for 15 min at 4 °C	1.2 mL PBS (pH 7.4) with 1.5% glycine at 60 rpm and 37 °C	0, 1, 2, 3, 4, 5, 6, 7, 8, 12, 14, 16, 24, 48, 72, 96, 120, 144 hr	1.2 mL		(Liu et al., 2007a)
	Freeze-dried Ins-MM-SLNs (containing 1 mg insulin)	Centrifuged tested samples at 14000 rpm for 15 min at 4 °C	1.2 mL PBS (pH 7.4) with 1.5% glycine at 60 rpm and 37 °C	0, 1, 2, 3, 4, 5, 6, 7, 8, 12, 14, 16, 24, 48, 72, 96, 120, 144 hr	0.6 mL		(Liu et al., 2007a)

	Purified FITC-insulin NPs (1 mg/mL; 0.3 mL)	Centrifuged tested samples at 16000 rpm for 30 min at 4 °C	3 mL SGF (pH 2, without enzymes) and SIF (pH 6.8, without enzymes) at 100 rpm and 37 °C	0.5, 1, 2, 4, 6 hr	n/a	(Li et al., 2007)
	n/a	n/a	20 mL of HCl (pH 1.2) for 120 min, and PBS (pH 6.8) for 120 min at 100 rpm	n/a	n/a	(Sarmento et al., 2006b)
	5 mg lyophilized NPs	Centrifuged tested samples at 5000 rpm for 3 min	5 mL of PBS (pH 7.4) under stirring (70 rpm) at 37 °C	10, 30 min, 1, 2, 4, 8, 24 hr	n/a	(Fan et al., 2006)
	n/a	Centrifuged tested samples at 30000 g for 15 min	SGF (pH 1.2) and SIF (pH 6.8) without enzymes at 37 °C with continuous mixing (50 rpm)	0, 0.5, 1, 2, 4, 6, 8, 12, 24 hr	0.5 mL	(Cui et al., 2006)
	Insulin NPs (10 mg/mL; sink condition)	n/a	1 mL PBS (pH 7.4) at 37 °C	n/a	n/a	(Qian et al., 2006)
	Freeze-dried NPs	n/a	20 mL buffers (pH 1.2, 7.4)	n/a	n/a	(Sajeesh and Sharma, 2006)
	Freeze-dried NPs (100 mg)	Centrifuged tested samples at 40000 g for 30 min	20 mL of saline PBS (0.01 M, NaCl 0.15M, pH 7.4) containing Tween 80 (0.1%) at 37 °C and magnetic stirring (150 rpm)	n/a	n/a	(Attivi et al., 2005)
	Insulin NPs (15 µg)	Filtered tested samples through 0.2 µm filter	20 mL PBS (5, 10, 50 mM containing 0.15 M NaCl and 0.2% albumin) at 37 °C and 200 rpm.	n/a	1 mL	(Tiyaboonchai et al., 2003)
	Insulin NPs (sink conditions)	n/a	5 mL PBS (pH 5.8, 7.4P) and acetate (pH 4) at 37 °C	n/a	n/a	(Pan et al., 2002a)
	Insulin NPs (sink conditions)	Centrifuged tested samples at 10000 g for 30 min	5 mL PBS (pH 7.4) at 37 °C and 50 rpm.	n/a	n/a	(Pan et al., 2002b)
	n/a	Centrifuged tested samples at 25000 rpm for 30 min at 20 °C	5 mL of HCl (0.1 M) PBS (pH 5.5, 6.8, 7.4) at 37 °C under agitation (100 rpm)	0, 0.5, 1, 2, 4, 6 hr	20 µL	(Ma et al., 2002)
	n/a	n/a	PBS (pH 7.4) and continuously stirred at 37 °C	5, 10, 30, 60, 120, 180, 240, 300 min	n/a	(Aboubakar et al., 2000)

Supplementary table 6. Experimental conditions to examine interaction between mucin and insulin nanoparticles *in vitro*

Assays	System	Objective	Condition	Ref
Mucin-nanoparticle interaction models	Varioskan flash multimode reader.	Nanoparticle affinity to mucus by aggregates and fluorescence intensity measurement	Vaginal cervicovaginal mucus (0.1, 1, 2%) incubated with protein NPs for 30 min at 100 rpm and 37 °C	(Shan et al., 2016)
Fluorescence recovery after photobleaching	Olympus FV1000 confocal laser scanning microscopy	Nanoparticle mobility in mucus by fluorescence intensity measurement	10 µL Dil-protein NPs incubated with 20 µL vaginal cervicovaginal mucus	(Shan et al., 2016)
Transwell system	Varioskan flash multimode reader.	Nanoparticle diffusion across mucus by fluorescence intensity measurement	Protein NPs (containing 600 µg/mL PLA) in PBS diffused across 40 µL vaginal cervicovaginal mucus in polycarbonate membrane filters (2 µm) at 37 °C	(Shan et al., 2016)
Rotating tube technique	n/a	Nanoparticle diffusion across mucus by fluorescence intensity measurement	Porcine intestinal mucus incubated with 100 µL with fluorescent-labeled protein NPs in a plastic tube (30 mm length, 4 mm diameter) for 4 hr at 50 rpm and 37 °C	(Pereira de Sousa et al., 2016)
Multiple particle tracking	Nikon TiE Inverted fluorescence microscope	Nanoparticle mobility in mucus by Brownian motion measurement	Protein NPs incubated with human mucus in microscopy chambers for 30 min at 37 °C	(Liu et al., 2016b)
Ussing chamber system	Varioskan flash multimode reader.	Nanoparticle diffusion across mucus by fluorescence intensity measurement	0.5 mL fluorescently-labeled protein NPs diffused across 50 µL human mucus in polycarbonate filters (2 µm), oxygenated with 95% O_2 and 5% CO_2 at 37 °C in 2 mL Krebs-Ringer buffer	(Liu et al., 2016b)
Mucin-nanoparticle interaction models	Varioskan flash multimode reader.	Nanoparticle interaction with mucus by aggregates and fluorescence intensity measurement	Mucin solution (0.1, 0.3, 0.5 %) incubated with protein NPs for 30 min at 37 °C	(Shan et al., 2015)
Ussing chamber system	Varioskan flash multimode reader.	Nanoparticle diffusion across mucus by fluorescence intensity measurement	FITC-insulin NPs (0.05 mg/mL insulin) diffused across 10 µL mucus in membrane filters (2 µm), oxygenated with 95% O_2 and 5% CO_2 at 37 °C in 3 mL Krebs-Ringer buffer	(Shan et al., 2015)
Multiple particle tracking	Nikon TiE Inverted fluorescence microscope	Nanoparticle mobility in mucus by Brownian motion measurement	Protein NPs incubated with mucus in microwells for 30 min at 37 °C	(Shan et al., 2015)
Mucin-nanoparticle interaction models	ZetaSizer Nano ZS	Nanoparticle affinity to mucus by zeta potential measurement	Mucin solution (100, 250, 500 µg/mL) in HCl/KCl buffer (pH 2.0) and PBS (pH 6.8) and incubated with 286 µL protein nanoparticles for 30 min at 37 °C	(Andreani et al., 2015)
Bio-membrane models	TA nano-differential scanning calorimetry	Nanoparticle mucoadhesiveness by measurement thermographic property	DPPC liposomes (2.2 mg/mL) incubated with 25 µL NPs	(Andreani et al., 2015)

Supplementary table 7. Experimental conditions to examine size, protein release, freeze-drying and enzymatic stability of insulin nanoparticles *in vitro*

Objective	System	Conditions	Time/time interval	Ref
Assessing nanoparticle size changes	Dynamic light scattering	Water at room temperature	One week	(Chopra et al., 2017)
	Dynamic light scattering	SGF, SIF	6 hr	(Verma et al., 2016)
	Nanoparticle tracking analysis	1 mL glucose or fructose (1, 3, 5 mg/mL)	60 min	(Siddiqui et al., 2016)
	Dynamic light scattering	1 mL SGF (pH 1.2 with or without pepsin), SIF (pH 6.8 with or without pancreatin) at 37 °C and 100 rpm	2 hr	(Sheng et al., 2016)
	Dynamic light scattering	10 or 40 mM phosphate buffer (pH 2.5, 6,6.8,7.4), 2% ovomucoid solution, SGF, SIF at room temperature	n/a	(Shan et al., 2016)
	Dynamic light scattering	pH 2.5, pH 6.8 at 37 °C and 100 rpm	4 hr	(Boushra et al., 2016b)
	Dynamic light scattering	pH 2.5, pH 6.8 at 37 °C and 100 rpm	4 hr	(Boushra et al., 2016a)
	Dynamic light scattering	PBS (pH 7.4) at 37 °C	48 hr	(Yu et al., 2015)
	Dynamic light scattering	Different temperatures	n/a	(Sharma et al., 2015)
	Dynamic light scattering	SGF, SIF	2 hr	(Li et al., 2013)
	Dynamic light scattering	4 °C	12 weeks	(Viehof et al., 2013)
	Dynamic light scattering	HCl (pH 1.2, 2, 2.5), PBS (pH 6, 6.6, 7, 7.2)	n/a	(Wu et al., 2012)
	Dynamic light scattering	Different pH	n/a	(Sonaje et al., 2010a)
	Dynamic light scattering	4 and 25 °C	1 month	(Elsayed et al., 2009)
	Dynamic light scattering	SGF (pH 1.2), SIF (pH 6.8)	n/a	(Jintapattanakit et al., 2007)
	Dynamic light scattering	4 °C	0, 10, 30, 60, 90, 120, 180 days	(Liu et al., 2007a)
	Dynamic light scattering	4 °C	0, 7, 14, 28, 42, 60 days	(Sarmento et al., 2006c)
Assessing nanoparticle drug release performance and changes in encapsulation	HPLC	Peak comparison between insulin NPs, fresh insulin and A21-desamido insulin (0.01 M HCl at 40 °C for 48 hr)	n/a	(Boushra et al., 2016a; Salvioni et al., 2016)
	ELISA kit (450 nm)	4 °C	12 weeks	(Viehof et al., 2013)

	HPLC	5 mL PBS (pH 7.4) at room temperature and observe residual peak desamido A21 or B3 insulin)	24 hr	(Jain et al., 2012)
	HPLC	Different pH values	n/a	(Sonaje et al., 2010b)
	Dynamic light scattering	Obtained melting temperature in tris buffer (1 mg/mL, pH 7)	n/a	(Elsayed et al., 2009)
	HPLC	55 °C and 100 rpm	0, 12, 24, 48 hr	(Elsayed et al., 2009)
	HPLC	4 and 25 °C	30 days	(Elsayed et al., 2009)
	HPLC	5 mL 0.01 M HCl to extract rh-insulin (2g) at 400 rpm centrifugation for 15 min	n/a	(Elsayed et al., 2009)
	HPLC	50 µL 0.25% acetic acid to extract 2 mg NPs (500 µg/mL insulin) at 37 and 50 °C, followed by dilution with 10 mM Tris buffer	0, 15,60, 145, 360 min	(Jintapattanakit et al., 2007)
	HPLC	1 g NPs centrifuged at 10000 rpm for 20 min, then incubated at 60 °C, followed by extraction of insulin with 1 mL PBS at 48 °C for 24 hr	1, 2, 4, 8, 10 hr	(Davaran et al., 2008)
	HPLC	4 °C	0, 10, 30, 60, 90, 120, 180 days	(Liu et al., 2007a)
	ELISA Kit, HPLC	Diluted NPs to insulin concentration (1-200 mM/L)	n/a	(Sarmento et al., 2006c)
	ELISA Kit (450 nm)	Dispersed 100 mg insulin NPs in PBS (pH 7.4)	12 hr	(Sajeesh and Sharma, 2006)
Reconstitution of freeze-dried NPs	Dynamic light scattering, HPLC	Filtered and washed NPs by polycarbonate membrane (50 nm), then incubated at -20, 4 and 25 °C	1 month	(Boushra et al., 2016a)
	Dynamic light scattering	4 °C and room temperature (relative humidity 50 ± 5%)	3 months	(Jain et al., 2012)
Assessing enzymatic stability of nanoparticle	HPLC	SGF (pH 1.2, 0.32% pepsin), SIF (pH 6.8, 1% trypsin) at 37 °C with shaking, followed by adding 0.1 M NaOH or 0.1 M HCl respectively to inactivate enzymes	n/a	(Deng et al., 2017)
	ELISA kit	1 mL of 0.1% trypsin and chymotrypsin at 37 °C, 200 µL of rat mucus	2 hr	(Verma et al., 2016)
	HPLC	SIF with trypsin at 37 °C	n/a	(Shan et al., 2016)
	HPLC	1 mL trypsin (50 IU/mL) at 37 °C, followed by adding 0.1 M HCl to inactivate enzymes	n/a	(Liu et al., 2016b)
	HPLC	1.5 mL bovine pancreas chymotrypsin (40 units/mg) in PBS (pH 7.4) at 37 °C, followed by adding 0.1 N HCl to inactivate enzymes	n/a	(Boushra et al., 2016b)
	HPLC:	1.5 mL of pepsin (pH 2.5) and chymotrypsin (7.4) at 37 °C, followed by adding 0.1 N NaOH and 0.1 N HCl respectively to inactivate enzymes	n/a	(Boushra et al., 2016a)
	HPLC	1 mL trypsin (pH 7.4, 0.3%) at 37 °C, followed by adding 50 µL of 0.1 M ice-cold HCl to inactivate enzymes	n/a	(Zhang et al., 2015)
	Dynamic light scattering	SGF (35 mM NaCl, 80 mM HCl with or without 0.3% pepsin, pH 1.2), SIF (50 mM KH_2PO_4,15 mM NaOH, with or without 1% pancreatin, pH 6.8) at 37 °C and 100 rpm	2 hr	(Sheng et al., 2015)

	HPLC	100 µL trypsin solution (pH 7.4, 225 µg/mL), followed by 400 µL of cold water containing 0.1% trifluoroacetic acid to inactivate enzymes	n/a		(Zhu et al., 2014)
	HPLC:	50 µL of trypsin (2500 IU/mg) and chymotrypsin (800 IU/mg) in Tris buffer (pH 8) containing 1 mM $CaCl_2$ at 37 °C, followed by adding 50 µL of cold acetonitrile solution containing 0.1% trifluoroacetic acid to inactivate enzymes and Triton X-100 to extract insulin	n/a		(Li et al., 2013)
	UV spectrophotometer	40 µL of pig pepsin (0.5 mg/mL) in 0.01 M HCl and 0.15M NaCl at pH 2 at 37 °C, followed by adding 1 M NaOH (pH 8.3) to inactivate enzymes	1 hr		(Burova et al., 2013)
	HPLC	SGF (pH 1.2, pepsin), SIF (pH 6.8, trypsin) at 37 °C, followed by adding 0.05 mol/L NaOH and 0.1 mol/L HCl respectively to inactivate enzymes	n/a		(Zhang et al., 2012c)
	HPLC	SGF (pH 1.2, pepsin), SIF (pH 6.8, pancreatin) at 37 °C, followed by adding 0.5 M NaOH and 0.5 M HCl respectively to inactivate enzymes, then extracted insulin by 1 mL acetonitrile: 0.5 M HCl	2 hr		(Jain et al., 2012)
	HPLC	0.08 M HCl (pH 2, 3.2 mg/mL pepsin) at 37 °C, followed by adding 100 µL of 0.1 M NaOH to inactivate enzymes, then extracted insulin by 500 µL of hexafluoro-2-propanol	n/a		(Makhlof et al., 2011)
	HPLC	1.5 mL pepsin solution in Tris-HCl buffer (0.05 mg/mL, pH 2) at 37 °C, followed by adding 100 µL of 0.05 mol/L NaOH to inactivate enzymes	n/a		(Zhang et al., 2010)
	ELISA kit	Pepsin (300 U/mL) in 0.01 M HCl at 37 °C and 100 rpm, followed by adding PBS (pH 7.4) to inactivate enzymes	2 hr		(Woitiski et al., 2010)
	HPLC	0.05 mL trypsin (6.4 mg/mL, 2.7×10^{-4} M) in pH 8 Tris buffer, chymotrypsin (5 mg/mL, 2×10^{-4} M) in pH 8 Tris buffer, pepsin (0.1 mg/mL, 2.8×10^{-6}) in 0.01 M pH 2HCl at 37 °C, followed by adding 0.015 mL TFA (0.1%) or 0.15 mL cold Tris base (0.1 M) to inactivate enzymes	4 hr		(Thompson et al., 2010; Thompson et al., 2009)
	HPLC	100 µL trypsin in 10 mM Tris buffer (pH 7.4) at 37 °C, followed by adding 1 mL acetonitrile: purified water mixture containing 0.1% trifluoroacetic acid	30 min		(Jintapattanakit et al., 2007)
	HPLC	SGF (pH 1.2) at 37 °C and 100 rpm, then transferred to PBS (pH 7.4) for 1 hr to inactivate enzyme	2 hr		(Reis et al., 2008)
	HPLC	100 µL of trypsin and chymotrypsin (7500 IU/mg) in PBS (pH 7.4, 0.1 M $CaCl_2$), pepsin (3000 IU/mg) in glycine HCl buffer (pH 1.34), then extracted insulin with amylase (10 IU) in 0.01 M NaOH	30 min		(Chalasani et al., 2007b)
	HPLC	1.5 mL pepsin (0.05mg/mL, pH 2) in Tris-HCl buffer, trypsin (0.36 mg/mL, pH 7.4) in PBS at 37 °C, followed by adding 100 µL of 0.05 mol/L NaOH or 0.1 mol/L HCl to inactivate enzymes	n/a		(Zhang et al., 2006)
	UV spectrophotometer	50 mM MES/KOH buffer (pH 6.8) with BAEE (20 mM) in 0.067 M PBS (pH 7.6) and 1 mL trypsin (30 U/mL) at 37 °C, followed by adding 5% trichloroacetic acid solution (1 mL) to inactivate enzymes	10 min		(Sajeesh and Sharma, 2006)
	HPLC	Chitosanase-RD (0.15-0.35 U/mL) and lysozyme (5,000 U/mL) in 50 mM acetate buffer (pH 5.5) at 37 °C and 100 rpm	n/a		(Ma et al., 2002)
	Radioactivity	PBS (pH 7.4, 1 mg/mL pancreatin, 5 mg/mL bile extract) at 37 °C	n/a		(Lowe and Temple, 1994)

Supplementary table 8. Experimental conditions to examine stability and bioactivity of insulin nanoparticles

Assay	System model	Objective	Conditions	Quantification parameters	Key findings	Ref
Circular dichroism	Jasco J-815	Investigate protein secondary structure	Dispersed insulin NPs in chloroform and 0.01 M HCl	0.1 cm cell, 1.5 nm bandwidth, 5 s averaging time, 0.5 nm step size, scan over 190-250 nm at 25 °C, 5 consecutive scans	n/a	(Fonte et al., 2016)
		Investigate protein integrity, secondary structure and endothermic peak	Dispersed NPs (10 mM) in PBS, then extracted insulin in acetonitrile	50 nm/min scanning speed	Maxima (223 nm), diminished endothermic peak	(Jain and Jain, 2015)
		Investigate protein secondary structure after drug release	Dispersed NPs at pH 2.0 and pH 6.8	0.1 cm cell, scan over 250-190 nm at 25 °C, 6 consecutive scans	n/a	(Andreani et al., 2014)
		Investigate protein integrity and conformation stability after encapsulation	Dispersed NPs in PBS (pH 7.4)	0.5 ditch pitch, 50 nm/min scanning speed, scan over 260-190 nm, 3 consecutive scans	Molecular ellipticity (222 and 208 nm)	(Jain et al., 2012)
		Investigate protein secondary structure and bioactivity after drug release	Dispersed insulin NPs (10 mM) in isotonic PBS, then extracted insulin in acetonitrile	Scan at room temperature, 50 nm/min scanning speed	Maxima (220 and 223 nm)	(Hurkat et al., 2012)
	Jasco J-1500	Investigate protein integrity after drug release and freeze-drying	n/a	0.5 nm data speed, scan over 260-190 nm, 50 nm/min scanning speed	n/a	(Chopra et al., 2017)
	Jasco J-810	Investigate protein stability after encapsulation	Extracted insulin in 2 mL of methanol and 7 mL of HCl (pH 2), then centrifuged at 13000 g for 10 min	Scanned over 200-260 nm	n/a	(Deng et al., 2017)
		Investigate protein secondary structure after drug release and freeze-drying	n/a	Scan at room temperature	α-helix (209 and 222 nm)	(Mahjub et al., 2014)
		Investigate protein conformation	Dispersed insulin NPs (0.5 mg/mL) in PBS (pH 7.4)	n/a	n/a	(Zhang et al., 2012b)
		Investigate protein conformation	Dispersed insulin NPs (0.1 mg/mL) in 0.1 mol/L NaOH, then centrifuged at 16000 g for 30 min	0.2 cm cuvette, scan over 200-250 nm at 20 °C, 2 nm resolution, 200 nm/min scanning speed, 1s response time	n/a	(Jelvehgari et al., 2010)
	Chirascan	Investigate protein secondary structure	Dispersed NPs in phosphoric acid solution (pH 2.0, 0.1 mg/mL)	1 nm step size, scan over 190-250 nm at 25 °C, 3 s acquisition/point, 3 consecutive scans	n/a	(Zhang et al., 2015)
	Olis DSM 20 CD	Investigate protein stability after encapsulation,	Dispersed NPs in PBS (pH 7.4)	0.1 cm cell, scan over 200-260 nm at 37 °C, 7 nm/min scanning	α-helix (210 and 220 nm)	(Lopes et al., 2015)

Jasco J-720	rotoevaporation and ultrasonication	Investigate protein secondary structure	n/a	0.1 cm cell, scan over 200-260 nm at 25 °C, 0.2 nm resolution, 50 nm/min scanning speed, 3 consecutive scans	Minima (208 and 223 nm)	(Ganeshkumar et al., 2013)
		Investigate protein secondary structure	Dialyzed insulin NPs (0.1 mg/mL) against 5 mM PBS (pH 7) at 4 °C	0.1 cm cell, scan over 190-270 nm at 20 °C, 0.1 nm resolution, 10 nm/min scanning speed, 2 s response time, 3 consecutive scans	Minima (209 and 222 nm)	(Tiyaboonchai et al., 2003)
Jasco J-715	Investigate protein stability after drug release	Insulin NPs (0.2 mg/mL)	1 nm cell length, scan over 190-250 nm at 25 °C, 10 consecutive scans	α-helix (208 nm), β-structure (223 nm)	(Wang et al., 2017b)
	Investigate protein conformation after drug release	Insulin NPs (0.1 mg/mL)	n/a	α-helix (223 and 208 nm)	(Wu et al., 2011)
	Investigate protein secondary structure after drug release	Disperse insulin NPs in SGF (pH 1.2) and SIF (pH 6.8)	0.01 cm cell, 0.5 nm step size, 1.5 nm bandwidth, 5 s averaging time, scan over 230-200 nm at room temperature, 5 consecutive scans	α-helix (209 and 222 nm)	(Zhang et al., 2010)
	Investigate protein secondary structure	Dispersed insulin NPs in PBS (137 mM NaCl, 2.7 mM KCl, 4.3 mM Na_2HPO_4, 1.4 mM KH_2PO_4, pH 7.2-7.4)	0.1 cm quartz cell, scan over 300-200 nm at 25 °C	α-helix (209 and 222 nm)	(Fan et al., 2006)
Olis DSM-10	Investigate protein secondary structure after 6 months storage	Dispersed insulin NPs in PBS (pH 7.4, 10 mM)	1 cm quartz cell, scan over 260-310 nm, 2 nm resolution, 5 consecutive scans	n/a	(Diaz et al., 2010)
	Investigate protein secondary structure after drug release	Disperse insulin NPs (0.2 mg/mL) in SGF (pH 1.2) and SIF	0.01 cm cell, 0.5 nm step size, 1.5 nm bandwidth, scan over 250-190 nm at room temperature, 5 s averaging time, 5 consecutive scans	α-helix (205 and 222 nm)	(Sarmento et al., 2007a)
Jasco	Investigate protein secondary structure	n/a	1 cm cell, 200 nm/min speed, 0.25 response time, 1 nm bandwidth	212, 217 and 222 nm	(Cui et al., 2009)
Aviv 202	Investigate protein secondary structure after drug release	n/a	Scan over 300-200 nm	n/a	(Lin et al., 2007a)
	Investigate protein secondary structure after drug release	Dispersed insulin NPs at pH 7.4	Scan over 300-200 nm	n/a	(Lin et al., 2007b)

Fourier transform infrared spectroscopy	Nicolet 380	Investigate interaction of NPs	KBr pellets method with NPs (1%)	4 cm^{-1} resolution, 256 scans	n/a	(Tahtat et al., 2013)
	PerkinElmer Spectrum RX1	Investigate interaction of NPs	Compressed 2 mg NPs with 78 mg KBr into a disc	4 cm^{-1} resolution, scan over 450-4000 cm^{-1}	n/a	(Alfatama et al., 2018)
		Investigate peak variation and interaction of NPs at different pH	NPs at pH 6 and pH 6.6	n/a	1543 cm^{-1} ($-NH3^{+}$), 1595 cm^{-1} (-COO-), 1709-1724 cm^{-1} (-COOH)	(Lin et al., 2007b)
	Nicolet 5700	Investigate dissociation and interaction between protein and freeze-dried NPs	n/a	Scan over 4000-400 cm^{-1} at 20 °C	1660 cm^{-1} (CO), 1520 cm^{-1} (NH), 1235.5 cm^{-1} (P=O)	(Liu et al., 2016a)
		Investigate interaction between protein and freeze-dried NPs	KBr pellet method	n/a	1654 cm^{-1} (amides I), 1541 cm^{-1} (amide II), 3349 cm^{-1} (OH), 1643 cm^{-1} (aromatic), 1650 and 1537 cm^{-1}(complex formation)	(Sajeesh and Sharma, 2006)
	Shimadzu IR-Prestige	Investigate interaction between protein and NPs	n/a	Scan over 4000-400 cm^{-1}	1300-400 cm^{-1} (Si-O-Si), 1630 cm^{-1}(Si-OH), 1730 cm^{-1} (C-O-C), 1340-1460 cm^{-1} (Si-C), 2970, 2934 and 2880 cm^{-1} (C(sp3)-H stretch), 1650 cm^{-1} (amide I), 1540 cm^{-1} (amide II)	(Guha et al., 2016)
	ABB MB3000 with ATR	Investigate secondary structure and area of overlap of protein (30 mg/mL in 0.1 M HCl) and NPs	Double subtraction method, followed by SavitzkyGolay second derivative of 15 points, and 3-4 point baseline correction in amide I region, all spectra were area-normalized	Scan over 4000-600 cm^{-1}, 256 scans, 4 cm^{-1} resolution	n/a	(Fonte et al., 2016)
	n/a	Investigate interaction and area of overlap between protein and NPs after ultrasonication	Double subtraction method, followed by SavitzkyGolay second derivative of 15 points, and 3-4 point baseline correction in amide I region, all spectra were area-normalized	Scan over 4000-600 cm^{-1}, 256 scans, 4 cm^{-1} resolution	1655 cm^{-1} (amide I α-helix), 1682 cm^{-1} (high- frequency β-sheet), 1614 cm^{-1} (low-frequency β-sheet), 1700 cm^{-1} (unordered structural change)	(Lopes et al., 2015)
	PerkinElmer Pyrogon 1000	Investigate interaction between protein and NPs	KBr pellet method	n/a	3217-3396 cm^{-1} (N-H stretching), 1718-1749 cm^{-1} (C=O stretching), 1402.7-1538.3 cm^{-1} (N-H bending), 1185-1211 cm^{-1} (C-O stretch)	(Jain and Jain, 2015)
	Shimadzu Affinity-1	Investigate interaction between protein and NPs	KBr pellet method	Transmission mode, scan over 4000-600 cm^{-1} at room temperature, 4 cm^{-1} resolution	1653 cm^{-1} (C=O stretching), 1512 cm^{-1} (N-H bending with C-N stretching), 3449 cm^{-1} (OH stretching), 1093 cm^{-1} (Si-O-Si anti-symmetrical stretching), 799 cm^{-1} and 467	(Zhao et al., 2013)

	Shimadzu 8400S	Investigate interaction between protein and NPs	n/a	n/a		1664 cm^{-1} (amide I), 1531.63 cm^{-1} (amide II C=O stretching)	(Prusty and Sahu, 2013)
	Nicolet AVATAR 360	Investigate surface composition of freeze-dried NPs	n/a	n/a		1638.3 cm^{-1} (CO stretch), 3200-3700 cm^{-1} (NH stretch)	(Liu et al., 2013)
	Alpha ATR-FTIR	Investigate interaction between protein and NPs	n/a	Scan over 4000-500 cm^{-1} at room temperature, 42 scans		3427.73 cm^{-1} (OH stretch and NH stretch), 1652.90 cm^{-1} (NH_2 deformation) , 1154.09 cm^{-1} (bridge O stretch), 1092.74 cm^{-1} (CO stretch), 1641.13-1656.33 cm^{-1} (amide I C=O stretch), 1537.81 cm^{-1} (amide II C-N stretch coupled with N-H bend)	Mukhopadhyay et al., 2013)
	Perkin Elmer	Investigate encapsulation of protein	KBr pellet method	Scan over 4000-400 cm^{-1}		1654 cm^{-1} and 1537 cm^{-1}	(Ganeshkumar et al., 2013)
	Nicolet Magna 750	Investigate interaction between protein and NPs	KBr pellet method	n/a		1500 cm^{-1} (amide)	(Diaz et al., 2010)
		Investigate interaction between protein and NPs	n/a	Scan over 2000-600 cm^{-1}, 164 scans, 4 cm^{-1} resolution		1633 cm^{-1} (N-H bending), 1527 cm^{-1} (symmetrical bending), 1400 cm^{-1} (carboxylate), 1646 cm^{-1} (amide II)	(Woitiski et al., 2009a)
	Bruker IFS-55	Investigate interaction between protein and NPs	KBr pellet method	n/a		1747 cm^{-1} (–CO stretch carbonyl group), 1650.8 cm^{-1} (-NH bend of amines)	(Hurkat et al., 2012)
		Investigate interaction between protein and NPs	KBr pellet method	n/a		3398.9 cm^{-1} (amide A), 1658.3 cm^{-1} (amide I), 1516.4 cm^{-1} (amide II), 1240.6 cm^{-1} (amide III), 2938.1 and 2864.3 cm^{-1} (CH stretch), 1564 cm^{-1} (carboxylic stretch)	(Sun et al., 2011)
		Investigate interaction between protein and NPs	KBr pellet method	n/a		1726 cm^{-1} and 1645 cm^{-1}	(Cui et al., 2006)
	Jasco FT/IR-420	Investigate interaction between protein and NPs	n/a	Scan over 4000-600 cm^{-1}, 4 cm^{-1} resolution		1643-1645 cm^{-1} (amides I), 1534-1547 cm^{-1} (amides II), 1544-1563 cm^{-1}, 1455-1458 cm^{-1}	(Reis et al., 2008)
	Bomem IR	Investigate interaction and area of overlap between	Compressed 2 mg sample with 300 mg KBr by 10 kN tablet press,	256 scans at room temperature, 4 cm^{-1} resolution		1654 cm^{-1} (a-helix), 1684 and 1632 cm^{-1} (β-sheet and β-turn)	(Sarmento et al., 2007a)

		protein and NPs at different pH	double subtraction procedure, obtained second-derivative spectra with seven-point Savitsky–Golay derivative, 3–4 point baseline adjustment., area-normalized in amide I region			
		Investigate interaction between protein and NPs	Compressed NPs with 300 mg KBr by 10 kN tablet press	256 scans at room temperature, 4 cm^{-1} resolution	1640-1650 cm^{-1} (amide I), 1540-1562 cm^{-1} (amide II)	(Sarmento et al., 2006c)
		Investigate interaction between protein and NPs	Compressed NPs with 300 mg micronized KBr by 10 kN tablet press	Scan over 4000-600 cm^{-1} at room temperature, 256 scans, 4 cm^{-1} resolution	1650 cm^{-1}(amide I), 1540 cm^{-1} (amide II)	(Sarmento et al., 2006a; Sarmento et al., 2006b)
Polyacrylamide gel electrophoresis	n/a	Investigate protein integrity	Incubated NPs with 0.5% SDS and 0.1 M NaOH at room temperature for 1 hr, then centrifuged at 22000 rpm for 25 min at 4-8 °C	n/a	n/a	(Sharma et al., 2015)
	n/a	Investigate protein integrity and mobility	Centrifuged NPs at 13000 g for 15 min, then boiled samples for 5 min in 16% SDS and mercaptoethanol for 1 hr at 200 V	Silver nitrate staining	Obtained band below 26 kDa molecular weight	(Jain and Jain, 2015)
	n/a	Investigate protein integrity after fabrication	Loaded 8 µL NPs onto 5% stacking gel and separated with 17.5% resolving gel in tris-glycine electrophoretic buffer (pH 8.3), run polyacrylamide gels for 3 hr at 80V	Coomassie brilliant blue for 2 hr	n/a	(Ke et al., 2015)
	n/a	Investigate protein chemical stability	Diluted NPs with native gel sample buffer by 2 times and loaded into 4-20% polyacrylamide gel	Coomassie brilliant blue, protein standard (4 kD)	n/a	(Jain et al., 2012)
	n/a	Investigate protein integrity and mobility	NPs centrifuged at 58800 g for 15 min, then boiled samples (10-100 µg insulin) for 5 min in 16% SDS and mercaptoethanol for 1 hr at 200 V	Silver nitrate staining	n/a	(Hurkat et al., 2012)
	n/a	Investigate protein integrity after freeze-drying		Coomassie blue staining, protein standards to estimate the molecular weights	n/a	2010: (Sonaje et al., 2010a)
	n/a	Investigate protein integrity after lyophilization	Loaded NPs onto vertical slab gel consisting of 8% separating gel and 5% stacking gel	Electrophoresis at 100 mV and stained with 0.1% Coomassie brilliant Blue	n/a	(Liu et al., 2007a)
Western blotting technique	Gel Doc XR densitometer	Investigate bioactivity of proteins	Dispersed NPs in PBS (pH 7.4 with 0.1 M EDTA), stimulated rat L6 myoblasts with insulin NPs, then incubated with antibodies (PKB, phosphoPKB (Ser473), actin) in 1%	Immunoblots placed in photocartridge Hypercassette and exposed to Hyperfilm ECL High Performance Chemiluminescence Film protected from light	n/a	(Woitiski et al., 2009a)

			non-fat dry milk in TBST overnight at 4 °C			
	Densitometer	Investigate bioactivity of proteins and ratio of phosphoAkt/Akt intensities	Stimulated rat L6 myoblasts with insulin NPs, lysed cells with 1% RIPA lysis buffer and centrifuged at 4 °C	Immunoblots developed in a Kodak M35A X-OMAT processor and exposed to Kodak X-OMAT Blue XB-1 film, scanned as black and white transmissive photos at 300 dpi	n/a	(Reis et al., 2007)
X-ray diffractogram	XPERT-PRO, PANalytical	Investigate crystallographic structure of NPs	n/a	Scanned from 5-80°(2°θ), 40 kV and 30 mA, 0.02°step size	θ=21.31° due to coating of HP55	(Zhao et al., 2013)
	Rigaku UltimaIII	Investigate crystallographic structure of NPs	n/a	Scanned by CuKa (λ = 1.5404 Å) at 40 kV and 36 mA	Amorphous nature (silica matrix)	(Guha et al., 2016)
	Shimadzu AXIS UltraDLD	Investigate surface composition of lyophilised NPs	n/a	n/a	n/a	(Liu et al., 2013)
	Siemens D5000	Investigate crystallographic structure of NPs	n/a	Scanned by CuKa (λ = 1.5406 Å), scanned from 2-40°(2°θ)	n/a	(Diaz et al., 2010)
	MXP18	Investigate crystallographic structure of NPs	n/a	Scanned from 5-40°(2°θ)	2θ at 10.4° and 21.8° decreased (electrostatic interactions)	(Lin et al., 2007b)
	Kratos AXIS 165	Investigate ligands and surface composition of lyophilised NPs	Applied NPs on aluminium substrate and kept under vacuum	Dual anode (Mg and Al) apparatus using the Mg Kα anode.	n/a	(Chalasani et al., 2007b)
	D/max-r A	Investigate crystallographic structure of NPs		Scanned from 5-50°(2°θ), 0.04° step angle, 1 s count time	n/a	(Cui et al., 2006)
	Rigakudmax	Investigate crystallographic structure of lyophilised NPs	Rinsed NPs with 95% ethanol to remove residual NaCl	Scanned by CuKa (λ = 1.5406 Å), scanned from 3-80°(2°θ)	2θ at 9.2°, 19.7°, 21.2° and 40.1° decreased (electrostatic interactions)	(Fan et al., 2006)
Differential scanning calorimetry	Perkin Elmer Pyris 6	Investigate characteristic peak temperature and endotherm/exotherm enthalpies of NPs	3 mg NPs weighed into aluminium pans	10 °C/min rate from 30 to 380 °C under nitrogen purging (40 mL/min)	n/a	(Alfatama et al., 2018)
	Shimadzu DSC-50	Investigate thermal behaviour of NPs	2 mg lyophilised NPs weighed into aluminium pans	10 °C/min rate from 20 to 350 °C under nitrogen purging (20 mL/min)	70 °C (endothermic peak of insulin)	(Jain and Jain, 2015)
		Investigate thermal behaviour (endotherm, exotherm) of NPs	2 mg dehydrated NPs weighed into aluminium pans	10 °C/min rate from 20 to 350 °C under nitrogen purging (20 mL/min)	n/a	(Reis et al., 2008)
		Investigate thermal behaviour of NPs	Lyophilised NPs	10 °C/min rate from 20 to 350 °C under nitrogen purging (20 mL/min)	62.3 and 83 (insulin endothermic peaks), shifting of exothermic peak to higher temperature	(Sarmento et al., 2006c)

		Investigate thermal behaviour of NPs	Lyophilised NPs	10 °C/min rate from 20 to 350 °C under nitrogen purging (20 mL/min)	Delay of endothermic peak (62-78 °C) after encapsulation	(Sarmento et al., 2006b)
		Investigate thermal behaviour of NPs at different pH	2 mg lyophilised NPs weighed into aluminium pans	10 °C/min rate from 20 to 350 °C under nitrogen purging (20 mL/min)	Reached endothermic and exothermic condition at lower temperature compared to unloaded NPs	(Sarmento et al., 2006a)
	TA nDSC	Investigate thermal behaviour of NPs	n/a	Heated from 25 to 100 °C , 1 °C/min scan rate	n/a	(Andreani et al., 2015)
	TA DSC 204	Investigate thermal behaviour and decomposition temperature of NPs	5 mg NPs	10 °C/min rate from 35 to 300 °C under nitrogen purging	n/a	(Zhao et al., 2013)
	BIOPRIBO DASM-4	Investigate thermal behaviour, denaturation temperature, denaturation enthalpy of NPs	NPs at pH 2 and pH 8.3	2 K/min rate from 10 to 130 °C under nitrogen purging	n/a	(Burova et al., 2013)
	Thermogravimeter	Investigate thermal behaviour of NPs	40 mg dried beads weighed into aluminium pans	10 °C/min rate from 30 to 400 °C under nitrogen purging (20 mL/min)	n/a	(Tahtat et al., 2013)
	TA TGA Q500	Investigate thermal behaviour of NPs	n/a	5 °C/min rate up to 800 °C under nitrogen purging	n/a	(Diaz et al., 2010)
	TA Q100	Investigate thermal behaviour, melting point, glass transition temperature of freeze-dried NPs	2-6 mg lyophilised NPs weighed into aluminium pans	20 °C/min rate from -90 to 350 °C under nitrogen purging (20 mL/min)	Reduction in endothermic peak size	(Thompson et al., 2010; Thompson et al., 2009)
	EXSTAR 6000	Investigate thermal behaviour and recrystallization index of NPs	10 mg lyophilised NPs weighed into aluminium pans	5 °C/min rate		(Liu et al., 2007a)
Fluorescence spectrum	Jasco FP6500 spectrofluorometer	Investigate the encapsulation of protein within NPs	Extracted insulin from NPs by chloroform and 0.01 M HCl, incubated with thioflavin T at 25 °C	Scan over 290 to 450 nm at 25 °C and record at excitation wavelength of 280 nm, 0.1 s integration time per data point, 5 scans	n/a	(Fonte et al., 2016)
	UV spectrofluorometer	n/a	NPs incubated with SGF (35 mM NaCl, 80 mM HCl, pH 1.2) and SIF (50 mM KH2PO4, 15 mM NaOH, pH 6.8) at room temperature	Measured optical density at 1500nm (Abs) at 0.5, 1, 1.5, 2, 4, 7 hr	n/a	(Diop et al., 2015)
	Hitachi spectrofluorometer	Investigate the encapsulation of protein within NPs	Prepare endogenous and extrinsic fluorescence spectroscopy	Scan over 200 to 400 nm (endogenous) or 470-600 (extrinsic) and record at excitation wavelength of 282 and 488 nm respectively	n/a	(Cui et al., 2009)

	Shimadzu RF-5301 PC spectrofluorometer	Investigate the encapsulation of protein within NPs	n/a	Scan over 250 to 650 nm and record at excitation wavelength of 250 nm, 5 nm bandwidths	n/a	(Liu et al., 2007a)
		Investigate secondary structure of protein after encapsulation	n/a	n/a	n/a	(Bhumkar et al., 2007)
	Varian Cary Eclipse spectrophotometer	Inclusion of protein to NPs	Diluted insulin (1 IU/mL) PBS (pH 7) and incubated with cyclodextrin (1, 3, 5, 10 mg)	Scan over 290 to 350 nm and record at excitation wavelength of 280 nm	n/a	(Sajeesh and Sharma, 2006)
Förster resonance energy transfer	Fluorescence spectrum	Investigate NPs coating and interaction between protein and polymer	Labeled insulin NPs (10 µg/mL) with TRITC (Ex./Em = 553/576 nm) and FITC ()Ex./Em = 495/520 nm	Measured fluorescence intensity at excitation wavelength of 440 or 520 nm and emission spectrum from 490 to 610 nm	n/a	(Liu et al., 2016b)
	Shimadzu RF-5301 fluorescence spectrophotometer	Investigate interaction between protein and polymer	Labeled NPs with TRITC and FITC	Measured fluorescence intensity at excitation wavelength of 440 nm and emission spectrum from 500 to 60 nm	n/a	(Shan et al., 2015)
	Horiba Jobin Yvon fluorescence spectrophotometer	Investigate protein degradation and conformation	Labeled NPs with Cy3 and Cy5	Measured fluorescence intensity at excitation wavelength of 535 nm	n/a	(Chuang et al., 2013)
^{1}H Nuclear magnetic resonance	Varian proton	Investigate conjugation of ligands to NPs	Dispersed NPs in deuterated chloroform	n/a	PLGA peaks 4.8 and 5.2 ppm, PEG peaks at 3.6 ppm	(Liu et al., 2013)
	Bruker Avance 400 FT	n/a	Dispersed NPs in distilled water or D2O/DCl (d-form)	400 MHz	n/a	(Nam et al., 2010)
Small angle X-ray scattering	End station BL23A1	Investigate internal structures of NPs after freeze-drying	Dispersed NPs in deionised water, corrected SAXS profiles with background scattering, sample transmission, empty cell transmission, empty cell scattering and detector sensitivity	14 keV beam energy (0.2 mm in diameter), 512 x 512 pixel resolution, 0.316 mm^2 pixel size, calibrated sample-to-detector distance and absolute intensity by silver behenate and polyethylene standards	n/a	(Sonaje et al., 2010a)
Animal model	8-week-old Swiss Webster mice	Investigate bioactivity by measuring BSL	Fasted animal for 6 hr then injected NPs (1.4 and 2 IU/kg)	Glucometer before and after injection up to 1 hr	n/a	(Hosseini-Nassab et al., 2017)
	Sprague-Dawley rats (180-220 g)	Investigate bioactivity after encapsulation by measuring BSL	Extracted insulin at 37 °C for 2 hr, animal fasted with free access to water overnight, injected 2 IU/kg insulin NPs	JPS-6 blood glucose monitoring system	n/a	(Shan et al., 2016)
	Rats	Investigate protein conformation after enzymatic incubation by measuring BSL	Incubated NPs with pepsin or chymotrypsin for 15 min, then extracted insulin by 99% ethanol and 1% 0.1 N HCl. Followed by		n/a	(Boushra et al., 2016a)

			dilution with sterile saline, injected 2 IU/kg insulin NPs			
Normal rats	Investigate protein bioactivity after lyophilization	Dissolved NPs in normal saline, injected 5 IU/kg insulin NPs	ACCU-CHEK glucometer	n/a		(Du et al., 2014)
Normal rats	Investigate bioactivity by measuring BSL after freeze-drying	Dissolved 100 mg NPs in 10 mL acetonitrile, centrifuged samples at 20000 rpm for 15 min and dissolved in 0.5 mL DMSO, determined protein concentration by RP-HPLC, injected 1 IU/kg insulin NPs	Collected blood from retro-orbital plexus and centrifuged at 4000 rpm for 5 min, measured glucose level by glucose oxidase method	n/a		(Sun et al., 2011)
Diabetic rats	Investigate bioactivity by measuring BSL	Extracted insulin in PBS (pH 7.4) , injected 1 IU/kg insulin NPs	ACCU-CHEK Aviva to measure plasma glucose, took blood from tail vein for 8 hr	n/a		(Woitiski et al., 2010)
Normal rats (200 g)	Investigate bioactivity by measuring BSL after freeze-drying	Animal fasted overnight with free access to water, dissolved 100 mg NPs in 10 mL acetonitrile then centrifuged at20000 rpm for 15 min, determined protein concentration by RP-HPLC, injected 1 IU/kg insulin NPs	Collected blood from retro-orbital plexus up to 1 hr and centrifuged at 4000 rpm for 5 min, measured glucose level by glucose oxidase method	n/a		(Sun et al., 2010)
Fasted diabetic adult male Wistar rats	Investigate bioactivity by measuring BSL	Injected 10 IU/kg insulin NPs, animal was fasted during experiment	Collected blood from tail vein and measured glucose at 0.5, 1, 2, 3, 4, 6, 8, 12, 24 hr by glucometer	n/a		(Damge et al., 2010)
Normal Rats	Investigate bioactivity by measuring BSL	Injected 1 IU/kg insulin NPs	Collected blood from tail vein and determined glucose by glucose-oxidase kit	n/a		(Cui et al., 2009)
Diabetic male Wistar rats (250 g)	Investigate bioactivity by measuring BSL	Extracted insulin by PBS (pH 7.4) then centrifuged	n/a	n/a		(Reis et al., 2007)
Diabetic rats	Investigate bioactivity by measuring BSL	Injected 10 IU/kg insulin NPs, animal was fasted during experiment	Collected blood from tail vein and measured glucose at 0.25, 0.5, 1, 2, 3, 4, 8, 10, 12, 24 hr by glucometer	n/a		(Damge et al., 2007)

Reference list

Aboubakar, M., Couvreur, P., Pinto-Alphandary, H., Gouritin, B., Lacour, B., Farinotti, R., Puisieux, F., Vauthier, C., 2000. Insulin-loaded nanocapsules for oral administration: In vitro and in vivo investigation. Drug Develop Res. 49, 109-117.

Al-Kurdi, Z.I., Chowdhry, B.Z., Leharne, S.A., Qinna, N.A., Al Omari, M.M., Badwan, A.A., 2015. Influence of glucosamine on the bioactivity of insulin delivered subcutaneously and in an oral nanodelivery system. Drug Des. Devel. Ther. 9, 6167-6176.

Alfatama, M., Lim, L.Y., Wong, T.W., 2018. Alginate-C18 conjugate nanoparticles loaded in tripolyphosphate-cross-linked chitosan-Oleic acid conjugate-coated calcium alginate beads as oral insulin carrier. Mol. Pharm. 15, 3369-3382.

Andreani, T., de Souza, A.L., Kiill, C.P., Lorenzon, E.N., Fangueiro, J.F., Calpena, A.C., Chaud, M.V., Garcia, M.L., Gremiao, M.P., Silva, A.M., Souto, E.B., 2014. Preparation and characterization of PEG-coated silica nanoparticles for oral insulin delivery. Int. J. Pharm. 473, 627-635.

Andreani, T., Miziara, L., Lorenzon, E.N., de Souza, A.L.R., Kiill, C.P., Fangueiro, J.F., Garcia, M.L., Gremiao, P.D., Silva, A.M., Souto, E.B., 2015. Effect of mucoadhesive polymers on the in vitro performance of insulin-loaded silica nanoparticles: Interactions with mucin and biomembrane models. Eur. J. Pharm. Biopharm.93, 118-126.

Attivi, D., Wehrle, P., Ubrich, N., Damge, C., Hoffman, M., Maincent, P., 2005. Formulation of insulin-loaded polymeric nanoparticles using response surface methodology. Drug Dev. Ind. Pharm. 31, 179-189.

Avadi, M.R., Sadeghi, A.M., Mohammadpour, N., Abedin, S., Atyabi, F., Dinarvand, R., Rafiee-Tehrani, M., 2010. Preparation and characterization of insulin nanoparticles using chitosan and Arabic gum with ionic gelation method. Nanomedicine 6, 58-63.

Avadi, M.R., Sadeghi, A.M.M., Mohamadpour Dounighi, N., Dinarvand, R., Atyabi, F., Rafiee-Tehrani, M., 2011. Ex vivo evaluation of insulin nanoparticles using chitosan and arabic gum. ISRN Pharma. 2011, 860109.

Bai, X., Kong, M., Xia, G., Bi, S., Zhou, Z., Feng, C., Cheng, X., Chen, X., 2017. Systematic investigation of fabrication conditions of nanocarrier based on carboxymethyl chitosan for sustained release of insulin. Int. J. Biol. Macromol. 102, 468-474.

Barichello, J.M., Morishita, M., Takayama, K., Nagai, T., 1999. Encapsulation of hydrophilic and lipophilic drugs in PLGA nanoparticles by the nanoprecipitation method. Drug Dev. Ind. Pharm. 25, 471-476.

Bayat, A., Dorkoosh, F.A., Dehpour, A.R., Moezi, L., Larijani, B., Junginger, H.E., Rafiee-Tehrani, M., 2008. Nanoparticles of quaternized chitosan derivatives as a carrier for colon delivery of insulin: ex vivo and in vivo studies. Int. J. Pharm. 356, 259-266.

Bhumkar, D.R., Joshi, H.M., Sastry, M., Pokharkar, V.B., 2007. Chitosan reduced gold nanoparticles as novel carriers for transmucosal delivery of insulin. Pharm. Res. 24, 1415-1426.

Boushra, M., Tous, S., Fetih, G., Korzekwa, K., Lebo, D.B., Xue, H.Y., Wong, H.L., 2016a. Development and evaluation of viscosity-enhanced nanocarrier (VEN) for oral insulin delivery. Int. J. Pharm. 511, 462-472.

Boushra, M., Tous, S., Fetih, G., Xue, H.Y., Tran, N.T., Wong, H.L., 2016b. Methocel-lipid hybrid nanocarrier for efficient oral insulin delivery. J. Pharm. Sci. 105, 1733-1740.

Burova, T.V., Grinberg, N.V., Tur, D.R., Papkov, V.S., Dubovik, A.S., Shibanova, E.D., Bairamashvili, D.I., Grinberg, V.Y., Khokhlov, A.R., 2013. Ternary interpolyelectrolyte complexes insulin-poly(methylaminophosphazene)-dextran sulfate for oral delivery of insulin. Langmuir 29, 2273-2281.

Carr, D.A., Peppas, N.A., 2010. Assessment of poly (methacrylic acid-co-N-vinyl pyrrolidone) as a carrier for the oral delivery of therapeutic proteins using Caco-2 and HT29-MTX cell lines. J. Biomed. Mater. Res. A 92, 504-512.

Chalasani, K.B., Russell-Jones, G.J., Jain, A.K., Diwan, P.V., Jain, S.K., 2007a. Effective oral delivery of insulin in animal models using vitamin B12-coated dextran nanoparticles. J. Control. Release 122, 141-150.

Chalasani, K.B., Russell-Jones, G.J., Yandrapu, S.K., Diwan, P.V., Jain, S.K., 2007b. A novel vitamin B12-nanosphere conjugate carrier system for peroral delivery of insulin. J. Control. Release 117, 421-429.

Chen, S., Guo, F., Deng, T., Zhu, S., Liu, W., Zhong, H., Yu, H., Luo, R., Deng, Z., 2017. Eudragit S100-coated chitosan nanoparticles co-loading Tat for enhanced oral colon absorption of insulin. AAPS PharmSciTech 18, 1277-1287.

Cho, H.J., Oh, J., Choo, M.K., Ha, J.I., Park, Y., Maeng, H.J., 2014. Chondroitin sulfate-capped gold nanoparticles for the oral delivery of insulin. Int J Biol Macromol 63, 15-20.

Chopra, S., Bertrand, N., Lim, J. M., Wang, A., Farokhzad, O.C., Karnik, R., 2017. Design of insulin-loaded nanoparticles enabled by multistep control of nanoprecipitation and zinc chelation. Acs Appl. Mater. Inter. 9, 11440-11450.

Chuang, E.Y., Lin, K.J., Su, F.Y., Mi, F.L., Maiti, B., Chen, C.T., Wey, S.P., Yen, T.C., Juang, J.H., Sung, H.W., 2013. Noninvasive imaging oral absorption of insulin delivered by nanoparticles and its stimulated glucose utilization in controlling postprandial hyperglycemia during OGTT in diabetic rats. J. Control. Release 172, 513-522.

Cui, F., Qian, F., Zhao, Z., Yin, L., Tang, C., Yin, C., 2009. Preparation, characterization, and oral delivery of insulin loaded carboxylated chitosan grafted poly(methyl methacrylate) nanoparticles. Biomacromolecules 10, 1253-1258.

Cui, F., Shi, K., Zhang, L., Tao, A., Kawashima, Y., 2006. Biodegradable nanoparticles loaded with insulin-phospholipid complex for oral delivery: Preparation, in vitro characterization and in vivo evaluation. J. Control. Release 114, 242-250.

Cui, F.D., Tao, A.J., Cun, D.M., Zhang, L.Q., Shi, K., 2007. Preparation of insulin loaded PLGA-Hp55 nanoparticles for oral delivery. J. Pharm. Sci. 96, 421-427.

Daimon, Y., Kamei, N., Kawakami, K., Takeda-Morishita, M., Izawa, H., Takechi-Haraya, Y., Saito, H., Sakai, H., Abe, M., Ariga, K., 2016. Dependence of intestinal absorption profile of insulin on carrier morphology composed of beta-cyclodextrin-grafted chitosan. Mol. Pharm. 13, 4034-4042.

Damge, C., Maincent, P., Ubrich, N., 2007. Oral delivery of insulin associated to polymeric nanoparticles in diabetic rats. J. Control. Release 117, 163-170.

Damge, C., Socha, M., Ubrich, N., Maincent, P., 2010. Poly(epsilon-caprolactone)/eudragit nanoparticles for oral delivery of aspart-insulin in the treatment of diabetes. J. Pharm. Sci. 99, 879-889.

Davaran, S., Omidi, Y., Rashidi, M.R., Anzabi, M., Shayanfar, A., Ghyasvand, S., Vesal, N., Davaran, F., 2008. Preparation and in vitro evaluation of linear and star-branched PLGA nanoparticles for insulin delivery. J. Bioact. Compat. Polym. 23, 115-131.

Deng, W., Xie, Q., Wang, H., Ma, Z., Wu, B., Zhang, X., 2017. Selenium nanoparticles as versatile carriers for oral delivery of insulin: Insight into the synergic antidiabetic effect and mechanism. Nanomedicine 13, 1965-1974.

Deutel, B., Laffleur, F., Thaurer, M., Thaler, M., Bernkop-Schnurch, A., 2016. Assembly and in vitro characterization of thiomeric nanoparticles. Drug Dev. Ind. Pharm. 42, 730-736.

Diaz, A., David, A., Perez, R., Gonzalez, M.L., Baez, A., Wark, S.E., Zhang, P., Clearfield, A., Colon, J.L., 2010. Nanoencapsulation of insulin into zirconium phosphate for oral delivery applications. Biomacromolecules 11, 2465-2470.

Diop, M., Auberval, N., Viciglio, A., Langlois, A., Bietiger, W., Mura, C., Peronet, C., Bekel, A., Julien David, D., Zhao, M., Pinget, M., Jeandidier, N., Vauthier, C., Marchioni, E., Frere, Y., Sigrist, S., 2015. Design, characterisation, and bioefficiency of insulin-chitosan nanoparticles after stabilisation by freeze-drying or cross-linking. Int. J. Pharm. 491, 402-408.

Du, X., Zhang, J., Zhang, Y., Li, S., Lin, X., Tang, X., Zhang, Y., Wang, Y., 2014. Decanoic acid grafted oligochitosan nanoparticles as a carrier for insulin transport in the gastrointestinal tract. Carbohydr. Polym. 111, 433-441.

Elsayed, A., Remawi, M.A., Qinna, N., Farouk, A., Badwan, A., 2009. Formulation and characterization of an oily-based system for oral delivery of insulin. Eur. J. Pharm. Biopharm. 73, 269-279.

Fan, Y.F., Wang, Y.N., Fan, Y.G., Ma, J.B., 2006. Preparation of insulin nanoparticles and their encapsulation with biodegradable polyelectrolytes via the layer-by-layer adsorption. Int. J. Pharm. 324, 158-167.

Fonte, P., Lino, P.R., Seabra, V., Almeida, A.J., Reis, S., Sarmento, B., 2016. Annealing as a tool for the optimization of lyophilization and ensuring of the stability of protein-loaded PLGA nanoparticles. Int. J. Pharm. 503, 163-173.

Fonte, P., Nogueira, T., Gehm, C., Ferreira, D., Sarmento, B., 2011. Chitosan-coated solid lipid nanoparticles enhance the oral absorption of insulin. Drug Deliv. Transl. Res. 1, 299-308.

Ganeshkumar, M., Ponrasu, T., Sathishkumar, M., Suguna, L., 2013. Preparation of amphiphilic hollow carbon nanosphere loaded insulin for oral delivery. Colloids Surf. B Biointerfaces 103, 238-243.

Guha, A., Biswas, N., Bhattacharjee, K., Sahoo, N., Kuotsu, K., 2016. pH responsive cylindrical MSN for oral delivery of insulin-design, fabrication and evaluation. Drug Deliv. 23, 3552-3561.

Gupta, R., Mohanty, S., 2017. Controlled release of insulin from folic acid-insulin complex nanoparticles. Colloids Surf. B Biointerfaces 154, 48-54.

Hecq, J., Siepmann, F., Siepmann, J., Amighi, K., Goole, J., 2015. Development and evaluation of chitosan and chitosan derivative nanoparticles containing insulin for oral administration. Drug Dev. Ind. Pharm. 41, 2037-2044.

Hosseini-Nassab, N., Samanta, D., Abdolazimi, Y., Annes, J.P., Zare, R.N., 2017. Electrically controlled release of insulin using polypyrrole nanoparticles. Nanoscale 9, 143-149.

Hsieh, H.H., Ho, L.C., Chang, H.T., 2016. Aminophenylboronic acid polymer nanoparticles for quantitation of glucose and for insulin release. Anal. Bioanal. Chem. 408, 6557-6565.

Hurkat, P., Jain, A., Jain, A., Shilpi, S., Gulbake, A., Jain, S.K., 2012. Concanavalin A conjugated biodegradable nanoparticles for oral insulin delivery. J. Nanopart. Res. 14, 1219.

Jain, A., Jain, S.K., 2015. L-Valine appended PLGA nanoparticles for oral insulin delivery. Acta Diabetol. 52, 663-676.

Jain, S., Rathi, V.V., Jain, A.K., Das, M., Godugu, C., 2012. Folate-decorated PLGA nanoparticles as a rationally designed vehicle for the oral delivery of insulin. Nanomedicine 7, 1311-1337.

Jelvehgari, M., Zakeri-Milani, P., Siahi-Shadbad, M.R., Loveymi, B.D., Nokhodchi, A., Azari, Z., Valizadeh, H., 2010. Development of pH-sensitive insulin nanoparticles using Eudragit L100-55 and chitosan with different molecular weights. AAPS PharmSciTech 11, 1237-1242.

Jintapattanakit, A., Junyaprasert, V.B., Kissel, T., 2009. The role of mucoadhesion of trimethyl chitosan and PEGylated trimethyl chitosan nanocomplexes in insulin uptake. J. Pharm. Sci. 98, 4818-4830.

Jintapattanakit, A., Junyaprasert, V.B., Mao, S., Sitterberg, J., Bakowsky, U., Kissel, T., 2007. Peroral delivery of insulin using chitosan derivatives: A comparative study of polyelectrolyte nanocomplexes and nanoparticles. Int. J. Pharm. 342, 240-249.

Ke, Z., Guo, H., Zhu, X., Jin, Y., Huang, Y., 2015. Efficient peroral delivery of insulin via vitamin B12 modified trimethyl chitosan nanoparticles. J. Pharm. Pharm. Sci. 18, 155-170.

Li, M.G., Lu, W.L., Wang, J.C., Zhang, X., Wang, X.Q., Zheng, A.P., Zhang, Q., 2007. Distribution, transition, adhesion and release of insulin loaded nanoparticles in the gut of rats. Int. J. Pharm. 329, 182-191.

Li, X., Guo, S., Zhu, C., Zhu, Q., Gan, Y., Rantanen, J., Rahbek, U.L., Hovgaard, L., Yang, M., 2013. Intestinal mucosa permeability following oral insulin delivery using core shell corona nanolipoparticles. Biomaterials 34, 9678-9687.

Lin, Y.H., Chen, C.T., Liang, H.F., Kulkarni, A.R., Lee, P.W., Chen, C.H., Sung, H.W., 2007a. Novel nanoparticles for oral insulin delivery via the paracellular pathway. Nanotechnology 18.

Lin, Y.H., Mi, F.L., Chen, C.T., Chang, W.C., Peng, S.F., Liang, H.F., Sung, H.W., 2007b. Preparation and characterization of nanoparticles shelled with chitosan for oral insulin delivery. Biomacromolecules 8, 146-152.

Liu, J., Gong, T., Wang, C., Zhong, Z., Zhang, Z., 2007a. Solid lipid nanoparticles loaded with insulin by sodium cholate-phosphatidylcholine-based mixed micelles: Preparation and characterization. Int. J. Pharm. 340, 153-162.

Liu, J., Zhang, S.M., Chen, P.P., Cheng, L., Zhou, W., Tang, W.X., Chen, Z.W., Ke, C.M., 2007b. Controlled release of insulin from PLGA nanoparticles embedded within PVA hydrogels. J. Mater. Sci. 18, 2205-2210.

Liu, L., Zhou, C., Xia, X., Liu, Y., 2016a. Self-assembled lecithin/chitosan nanoparticles for oral insulin delivery: preparation and functional evaluation. Int. J. Nanomedicine 11, 761-769.

Liu, M., Zhang, J., Zhu, X., Shan, W., Li, L., Zhong, J., Zhang, Z., Huang, Y., 2016b. Efficient mucus permeation and tight junction opening by dissociable "mucus-inert" agent coated trimethyl chitosan nanoparticles for oral insulin delivery. J. Control. Release 222, 67-77.

Liu, X., Liu, C., Zhang, W., Xie, C., Wei, G., Lu, W., 2013. Oligoarginine-modified biodegradable nanoparticles improve the intestinal absorption of insulin. Int. J. Pharm. 448, 159-167.

Lopes, M., Shrestha, N., Correia, A., Shahbazi, M.A., Sarmento, B., Hirvonen, J., Veiga, F., Seica, R., Ribeiro, A., Santos, H.A., 2016. Dual chitosan/albumin-coated alginate/dextran sulfate nanoparticles for enhanced oral delivery of insulin. J. Control. Release 232, 29-41.

Lopes, M.A., Abrahim-Vieira, B., Oliveira, C., Fonte, P., Souza, A.M., Lira, T., Sequeira, J.A., Rodrigues, C.R., Cabral, L.M., Sarmento, B., Seica, R., Veiga, F., Ribeiro, A.J., 2015. Probing insulin bioactivity in oral nanoparticles produced by ultrasonication-assisted emulsification/internal gelation. Int. J. Nanomedicine 10, 5865-5880.

Lowe, P.J., Temple, C.S., 1994. Calcitonin and insulin in isobutylcyanoacrylate nanocapsules: protection against proteases and effect on intestinal absorption in rats. J. Pharm. Pharmacol. 46, 547-552.

Ma, Z., Lim, T.M., Lim, L.Y., 2005. Pharmacological activity of peroral chitosan-insulin nanoparticles in diabetic rats. Int. J. Pharm. 293, 271-280.

Ma, Z., Yeoh, H.H., Lim, L.Y., 2002. Formulation pH modulates the interaction of insulin with chitosan nanoparticles. J. Pharm. Sci. 91, 1396-1404.

Mahjub, R., Dorkoosh, F.A., Amini, M., Khoshayand, M.R., Rafiee-Tehrani, M., 2011. Preparation, statistical optimization, and in vitro characterization of insulin nanoparticles composed of quaternized aromatic derivatives of chitosan. AAPS PharmSciTech 12, 1407-1419.

Mahjub, R., Radmehr, M., Dorkoosh, F.A., Ostad, S.N., Rafiee-Tehrani, M., 2014. Lyophilized insulin nanoparticles prepared from quaternized N-aryl derivatives of chitosan as a new strategy for oral delivery of insulin: In vitro, ex vivo and in vivo characterizations. Drug Dev. Ind. Pharm. 40, 1645-1659.

Makhlof, A., Tozuka, Y., Takeuchi, H., 2011. Design and evaluation of novel pH-sensitive chitosan nanoparticles for oral insulin delivery. Eur. J. Pharm. Sci. 42, 445-451.

Mao, S., Bakowsky, U., Jintapattanakit, A., Kissel, T., 2006. Self-assembled polyelectrolyte nanocomplexes between chitosan derivatives and insulin. J. Pharm. Sci. 95, 1035-1048.

Mi, F.L., Wu, Y.Y., Lin, Y.H., Sonaje, K., Ho, Y.C., Chen, C.T., Juang, J.H., Sung, H.W., 2008. Oral delivery of peptide drugs using nanoparticles self-assembled by poly(gamma-glutamic acid) and a chitosan derivative functionalized by trimethylation. Bioconjug. Chem. 19, 1248-1255.

Mukhopadhyay, P., Sarkar, K., Chakraborty, M., Bhattacharya, S., Mishra, R., Kundu, P.P., 2013. Oral insulin delivery by self-assembled chitosan nanoparticles: in vitro and in vivo studies in diabetic animal model. Mater. Sci Eng C Mater Biol Appl 33, 376-382.

Nam, J.P., Choi, C., Jang, M.K., Jeong, Y.I., Nah, J.W., Kim, S.H., Park, Y., 2010. Insulin-incorporated chitosan nanoparticles based on polyelectrolyte complex formation. Macromol. Res. 18, 630-635.

Pan, Y., Li, Y.J., Zhao, H.Y., Zheng, J.M., Xu, H., Wei, G., Hao, J.S., Cui, F.D., 2002a. Bioadhesive polysaccharide in protein delivery system: Chitosan nanoparticles improve the intestinal absorption of insulin in vivo. Int. J. Pharm. 249, 139-147.

Pan, Y., Zheng, J.M., Zhao, H.Y., Li, Y.J., Xu, H., Wei, G., 2002b. Relationship between drug effects and particle size of insulin-loaded bioadhesive microspheres. Acta Pharmacol. Sin. 23, 1051-1056.

Pereira de Sousa, I., Moser, T., Steiner, C., Fichtl, B., Bernkop-Schnurch, A., 2016. Insulin loaded mucus permeating nanoparticles: Addressing the surface characteristics as feature to improve mucus permeation. Int. J. Pharm. 500, 236-244.

Prusty, A.k., Sahu, S.K., 2013. Development and evaluation of insulin incorporated nanoparticles for oral administration. ISRN Nanotechnology 2013, 1-6.

Qian, F., Cui, F., Ding, J., Tang, C., Yin, C., 2006. Chitosan graft copolymer nanoparticles for oral protein drug delivery: preparation and characterization. Biomacromolecules 7, 2722-2727.

Reis, C.P., Ribeiro, A.J., Houng, S., Veiga, F., Neufeld, R.J., 2007. Nanoparticulate delivery system for insulin: design, characterization and in vitro/in vivo bioactivity. Eur. J. Pharm. Sci. 30, 392-397.

Reis, C.P., Ribeiro, A.J., Veiga, F., Neufeld, R.J., Damge, C., 2008. Polyelectrolyte biomaterial interactions provide nanoparticulate carrier for oral insulin delivery. Drug Deliv. 15, 127-139.

Reix, N., Parat, A., Seyfritz, E., Van der Werf, R., Epure, V., Ebel, N., Danicher, L., Marchioni, E., Jeandidier, N., Pinget, M., Frere, Y., Sigrist, S., 2012. In vitro uptake evaluation in Caco-2 cells and in vivo results in diabetic rats of insulin-loaded PLGA nanoparticles. Int. J. Pharm. 437, 213-220.

Sajeesh, S., Sharma, C.P., 2006. Cyclodextrin-insulin complex encapsulated polymethacrylic acid based nanoparticles for oral insulin delivery. Int. J. Pharm. 325, 147-154.

Salvioni, L., Fiandra, L., Del Curto, M.D., Mazzucchelli, S., Allevi, R., Truffi, M., Sorrentino, L., Santini, B., Cerea, M., Palugan, L., Corsi, F., Colombo, M., 2016. Oral delivery of insulin via polyethylene imine-based nanoparticles for colonic release allows glycemic control in diabetic rats. Pharmacol. Res. 110, 122-130.

Sarmento, B., Ferreira, D., Veiga, F., Ribeiro, A., 2006a. Characterization of insulin-loaded alginate nanoparticles produced by ionotropic pre-gelation through DSC and FTIR studies. Carbohyd. Polym. 66, 1-7.

Sarmento, B., Ferreira, D.C., Jorgensen, L., van de Weert, M., 2007a. Probing insulin's secondary structure after entrapment into alginate/chitosan nanoparticles. Eur J Pharm Biopharm. 65, 10-17.

Sarmento, B., Martins, S., Ribeiro, A., Veiga, F., Neufeld, R., Ferreira, D., 2006b. Development and comparison of different nanoparticulate polyelectrolyte complexes as insulin carriers. Int. J. Pept. Res. Ther. 12, 131-138.

Sarmento, B., Mazzaglia, D., Bonferoni, M.C., Neto, A.P., Monteiro, M.D., Seabra, V., 2011. Effect of chitosan coating in overcoming the phagocytosis of insulin loaded solid lipid nanoparticles by mononuclear phagocyte system. Carbohyd. Polym. 84, 919-925.

Sarmento, B., Ribeiro, A., Veiga, F., Ferreira, D., 2006c. Development and characterization of new insulin containing polysaccharide nanoparticles. Colloids Surf. B Biointerfaces 53, 193-202.

Sarmento, B., Ribeiro, A., Veiga, F., Ferreira, D., Neufeld, R., 2007b. Oral bioavailability of insulin contained in polysaccharide nanoparticles. Biomacromolecules 8, 3054-3060.

Sarmento, B., Ribeiro, A., Veiga, F., Sampaio, P., Neufeld, R., Ferreira, D., 2007c. Alginate/chitosan nanoparticles are effective for oral insulin delivery. Pharm. Res. 24, 2198-2206.

Sarmento, B., Ribeiro, A.J., Veiga, F., Ferreira, D.C., Neufeld, R.J., 2007d. Insulin-loaded nanoparticles are prepared by alginate ionotropic pre-gelation followed by chitosan polyelectrolyte complexation. J. Nanosci. Nanotechnol. 7, 2833-2841.

Shan, W., Zhu, X., Liu, M., Li, L., Zhong, J., Sun, W., Zhang, Z., Huang, Y., 2015. Overcoming the diffusion barrier of mucus and absorption barrier of epithelium by self-assembled nanoparticles for oral delivery of insulin. ACS Nano 9, 2345-2356.

Shan, W., Zhu, X., Tao, W., Cui, Y., Liu, M., Wu, L., Li, L., Zheng, Y., Huang, Y., 2016. Enhanced oral delivery of protein drugs using zwitterion-functionalized nanoparticles to overcome both the diffusion and absorption barriers. ACS Appl. Mater. Interfaces 8, 25444-25453.

Sharma, R., Gupta, U., Garg, N.K., Tyagi, R.K., Jain, N.K., 2015. Surface engineered and ligand anchored nanobioconjugate: Sn effective therapeutic approach for oral insulin delivery in experimental diabetic rats. Colloids Surf. B Biointerfaces 127, 172-181.

Sheng, J., Han, L., Qin, J., Ru, G., Li, R., Wu, L., Cui, D., Yang, P., He, Y., Wang, J., 2015. N-trimethyl chitosan chloride-coated PLGA nanoparticles overcoming multiple barriers to oral insulin absorption. ACS Appl. Mater. Interfaces 7, 15430-15441.

Sheng, J., He, H., Han, L., Qin, J., Chen, S., Ru, G., Li, R., Yang, P., Wang, J., Yang, V.C., 2016. Enhancing insulin oral absorption by using mucoadhesive nanoparticles loaded with LMWP-linked insulin conjugates. J. Control. Release 233, 181-190.

Siddiqui, N.A., Billa, N., Roberts, C.J., 2017. Multiboronic acid-conjugated chitosan scaffolds with glucose selectivity to insulin release. J. Biomater. Sci. Polym. Ed. 28, 781-793.

Siddiqui, N.A., Billa, N., Roberts, C.J., Asantewaa Osei, Y., 2016. Cross-linked dependency of boronic acid-conjugated chitosan nanoparticles by diols for sustained insulin release. Pharmaceutics 8, 30.

Sonaje, K., Chen, Y.J., Chen, H.L., Wey, S.P., Juang, J.H., Nguyen, H.N., Hsu, C.W., Lin, K.J., Sung, H.W., 2010a. Enteric-coated capsules filled with freeze-dried chitosan/poly(gamma-glutamic acid) nanoparticles for oral insulin delivery. Biomaterials 31, 3384-3394.

Sonaje, K., Lin, K.J., Wey, S.P., Lin, C.K., Yeh, T.H., Nguyen, H.N., Hsu, C.W., Yen, T.C., Juang, J.H., Sung, H.W., 2010b. Biodistribution, pharmacodynamics and pharmacokinetics of insulin analogues in a rat model: Oral delivery using pH-responsive nanoparticles vs. subcutaneous injection. Biomaterials 31, 6849-6858.

Su, F.Y., Lin, K.J., Sonaje, K., Wey, S.P., Yen, T.C., Ho, Y.C., Panda, N., Chuang, E.Y., Maiti, B., Sung, H.W., 2012. Protease inhibition and absorption enhancement by functional nanoparticles for effective oral insulin delivery. Biomaterials 33, 2801-2811.

Sun, S., Liang, N., Kawashima, Y., Xia, D., Cui, F., 2011. Hydrophobic ion pairing of an insulin-sodium deoxycholate complex for oral delivery of insulin. Int J Nanomedicine 6, 3049-3056.

Sun, S., Liang, N., Piao, H., Yamamoto, H., Kawashima, Y., Cui, F., 2010. Insulin-S.O (sodium oleate) complex-loaded PLGA nanoparticles: Formulation, characterization and in vivo evaluation. J. Microencapsul. 27, 471-478.

Sun, S., Liang, N., Yamamoto, H., Kawashima, Y., Cui, F., Yan, P., 2015. pH-sensitive poly(lactide-co-glycolide) nanoparticle composite microcapsules for oral delivery of insulin. Int. J. Nanomedicine 10, 3489-3498.

Tahtat, D., Mahlous, M., Benamer, S., Khodja, A.N., Oussedik-Oumehdi, H., Laraba-Djebari, F., 2013. Oral delivery of insulin from alginate/chitosan crosslinked by glutaraldehyde. Int. J. Biol. Macromol. 58, 160-168.

Thompson, C.J., Tetley, L., Cheng, W.P., 2010. The influence of polymer architecture on the protective effect of novel comb shaped amphiphilic poly(allylamine) against in vitro enzymatic degradation of insulin--towards oral insulin delivery. Int. J. Pharm. 383, 216-227.

Thompson, C.J., Tetley, L., Uchegbu, I.F., Cheng, W.P., 2009. The complexation between novel comb shaped amphiphilic polyallylamine and insulin: towards oral insulin delivery. Int. J. Pharm. 376, 46-55.

Tiyaboonchai, W., Woiszwillo, J., Sims, R.C., Middaugh, C.R., 2003. Insulin containing polyethylenimine-dextran sulfate nanoparticles. Int. J. Pharm. 255, 139-151.

Verma, A., Sharma, S., Gupta, P.K., Singh, A., Teja, B.V., Dwivedi, P., Gupta, G.K., Trivedi, R., Mishra, P.R., 2016. Vitamin B12 functionalized layer by layer calcium phosphate

nanoparticles: A mucoadhesive and pH responsive carrier for improved oral delivery of insulin. Acta Biomater. 31, 288-300.
Viehof, A., Javot, L., Beduneau, A., Pellequer, Y., Lamprecht, A., 2013. Oral insulin delivery in rats by nanoparticles prepared with non-toxic solvents. Int. J. Pharm. 443, 169-174.
Wang, J., Kong, M., Zhou, Z., Yan, D., Yu, X., Cheng, X., Feng, C., Liu, Y., Chen, X., 2017a. Mechanism of surface charge triggered intestinal epithelial tight junction opening upon chitosan nanoparticles for insulin oral delivery. Carbohydr. Polym. 157, 596-602.
Wang, Y., Huang, F., Sun, Y., Gao, M., Chai, Z., 2017b. Development of shell cross-linked nanoparticles based on boronic acid-related reactions for self-regulated insulin delivery. J. Biomater. Sci. Polym. Ed. 28, 93-106.
Woitiski, C.B., Neufeld, R.J., Ribeiro, A.J., Veiga, F., 2009a. Colloidal carrier integrating biomaterials for oral insulin delivery: Influence of component formulation on physicochemical and biological parameters. Acta Biomater. 5, 2475-2484.
Woitiski, C.B., Neufeld, R.J., Veiga, F., Carvalho, R.A., Figueiredo, I.V., 2010. Pharmacological effect of orally delivered insulin facilitated by multilayered stable nanoparticles. Eur. J. Pharm. Sci. 41, 556-563.
Woitiski, C.B., Sarmento, B., Carvalho, R.A., Neufeld, R.J., Veiga, F., 2011. Facilitated nanoscale delivery of insulin across intestinal membrane models. Int. J. Pharm. 412, 123-131.
Woitiski, C.B., Veiga, F., Ribeiro, A., Neufeld, R., 2009b. Design for optimization of nanoparticles integrating biomaterials for orally dosed insulin. Eur. J. Pharm. Biopharm. 73, 25-33.
Wu, Z., Zhang, S., Zhang, X., Shu, S., Chu, T., Yu, D., 2011. Phenylboronic acid grafted chitosan as a glucose-sensitive vehicle for controlled insulin release. J. Pharm. Sci. 100, 2278-2286.
Wu, Z.M., Zhou, L., Guo, X.D., Jiang, W., Ling, L., Qian, Y., Luo, K.Q., Zhang, L.J., 2012. HP55-coated capsule containing PLGA/RS nanoparticles for oral delivery of insulin. Int. J. Pharm. 425, 1-8.
Yu, F., Li, Y., Liu, C.S., Chen, Q., Wang, G.H., Guo, W., Wu, X.E., Li, D.H., Wu, W.D., Chen, X.D., 2015. Enteric-coated capsules filled with mono-disperse micro-particles containing PLGA-lipid-PEG nanoparticles for oral delivery of insulin. Int. J. Pharm. 484, 181-191.
Zhang, N., Li, J., Jiang, W., Ren, C., Li, J., Xin, J., Li, K., 2010. Effective protection and controlled release of insulin by cationic beta-cyclodextrin polymers from alginate/chitosan nanoparticles. Int. J. Pharm. 393, 212-218.
Zhang, N., Ping, Q., Huang, G., Xu, W., Cheng, Y., Han, X., 2006. Lectin-modified solid lipid nanoparticles as carriers for oral administration of insulin. Int. J. Pharm. 327, 153-159.
Zhang, P., Xu, Y., Zhu, X., Huang, Y., 2015. Goblet cell targeting nanoparticle containing drug-loaded micelle cores for oral delivery of insulin. Int. J. Pharm. 496, 993-1005.
Zhang, X., Sun, M., Zheng, A., Cao, D., Bi, Y., Sun, J., 2012a. Preparation and characterization of insulin-loaded bioadhesive PLGA nanoparticles for oral administration. Eur. J. Pharm. Sci. 45, 632-638.
Zhang, Y., Du, X., Zhang, Y., Li, G., Cai, C., Xu, J., Tang, X., 2014. Thiolated eudragit-based nanoparticles for oral insulin delivery: preparation, characterization, and evaluation using intestinal epithelial cells in vitro. Macromol. Biosci. 14, 842-852.
Zhang, Y., Wu, X., Meng, L., Zhang, Y., Ai, R., Qi, N., He, H., Xu, H., Tang, X., 2012b. Thiolated Eudragit nanoparticles for oral insulin delivery: preparation, characterization and in vivo evaluation. Int. J. Pharm. 436, 341-350.
Zhang, Z., Cai, H., Liu, Z., Yao, P., 2016. Effective enhancement of hypoglycemic effect of insulin by liver-targeted nanoparticles containing cholic acid-modified chitosan derivative. Mol. Pharm. 13, 2433-2442.
Zhang, Z.H., Lv, H.X., Zhou, J.P., 2009. Novel solid lipid nanoparticles as carriers for oral administration of insulin. Pharmazie 64, 574-578.
Zhang, Z.H., Zhang, Y.L., Zhou, J.P., Lv, H.X., 2012c. Solid lipid nanoparticles modified with stearic acid-octaarginine for oral administration of insulin. Int. J. Nanomedicine 7, 3333-3339.

Zhao, X., Shan, C., Zu, Y., Zhang, Y., Wang, W., Wang, K., Sui, X., Li, R., 2013. Preparation, characterization, and evaluation in vivo of Ins-SiO(2)-HP55 (insulin-loaded silica coating HP55) for oral delivery of insulin. Int. J. Pharm. 454, 278-284.

Zhu, X., Shan, W., Zhang, P., Jin, Y., Guan, S., Fan, T., Yang, Y., Zhou, Z., Huang, Y., 2014. Penetratin derivative-based nanocomplexes for enhanced intestinal insulin delivery. Mol. Pharm. 11, 317-328.

Appendix B4.2: Publisher agreement and permission for chapter 5

Wong CY et al 2019. "Bio-nanotechnological advancement of orally administered insulin nanoparticles: Comprehensive review of experimental design for physicochemical characterization." International Journal of Pharmaceutics 572: 118720.

Appendix B5.1: Supplementary data for chapter 6 - Cellular assays and applied technologies for characterization of orally administered protein nanoparticles: A systematic review.

Wong CY et al 2020. "Cellular assays and applied technologies for characterization of orally administered protein nanoparticles: A systematic review." Journal of Drug Targeting 28 (6): 585-599.

The following supplementary data is available from https://doi.org/10.1080/1061186X.2020.1726356 and https://www.tandfonline.com/doi/abs/10.1080/1061186X.2020.1726356

Supplementary table 1. Cell culture conditions

Supplementary table 2. Experimental conditions for cellular uptake studies

Supplementary table 3. Experimental conditions for cytotoxicity assays

Supplementary table 4. Experimental conditions for TEER measurement and permeability study

Supplementary table 5. Experimental conditions to examine nanoparticle and protein integrity during intracellular trafficking

Supplementary table 6. Experimental conditions for endocytosis and exocytosis mechanisms

Supplementary table 1. Cell culture conditions

Cells	Medium	Medium change	FBS	Non-essential amino acids	Antibiotics	Incubator	Passage	Flask/ density/confluency	Year/ Ref
Caco-2	DMEM	n/a	10%	1% L-glutamine	1% penicillin, streptomycin (100 IU/mL)	37 °C, 5% CO_2, 90% humidity	n/a	n/a	2018: [1]
	MEM	Every 2 days	9%	1%	Penicillin-streptomycin (100 U/mL, 1%)	37 °C, 5% CO_2, 95% air	30-40	25 cm^2 Nunc plastic flask	2018: [2]
	MEM	n/a	10%	n/a	n/a	n/a	n/a	n/a	2018: [3]
	DMEM	n/a	20%	1%; 4.5 g/L glucose, L-glutamine	1% antibiotic–antimitotic solution	37 °C, 5% CO_2, 21 days	30-60	73,000 cells/cm^2	2018: [4]
	DMEM	n/a	10%	1%	1% penicillin, streptomycin (100 IU/mL)	37 °C, 5% CO_2, 90% humidity	n/a	n/a	2018: [5]
	DMEM	n/a	20%	1%; 4.5 g/L glucose	1% penicillin, streptomycin (100 IU/mL)	37 °C, 5% CO_2, 90% humidity	n/a	n/a	2018: [6]
	MEM	n/a	20%	1%	Penicillin (100 IU/mL), streptomycin (10000 µg/mL)	37 °C, 5% CO_2	n/a	T-75 flasks, 80-90%	2018: [7]
	DMEM	n/a	10%	1%	1% penicillin, streptomycin (100 IU/mL)	5% CO_2, 95% humidity	n/a	75 cm^2 culture flasks	2018: [8]
	DMEM	n/a	10%	1%; 4.5 g/L glucose, 1% L-glutamine	1% penicillin, streptomycin (100 IU/mL)	37 °C, 5% CO_2	n/a	n/a	2018: [9]
	DMEM	n/a	10%	1%	Penicillin (100 U/mL), streptomycin (100 U/mL)	37 °C, 5% CO_2	n/a	n/a	2018: [10]
	DMEM	n/a	10%	1%; 4.5 g/L glucose, 1% L-glutamine	1% penicillin, streptomycin (100 IU/mL)	37 °C, 5% CO_2	n/a	n/a	2018: [11]
	DMEM	Every 2 days	10%	1%; 4.5 g/L glucose, 1% L-glutamine	1% penicillin, streptomycin (100 IU/mL)	37 °C, 5% CO_2, 95% humidity	n/a	n/a	2018: [12]
	DMEM	n/a	20%	1%; 4.5 g/L glucose	Penicillin (100 U/mL), streptomycin (100 mg/mL)	37 °C, 5% CO_2, 90% humidity	n/a	80%	2018: [13]
	RPMI-1640	Every other day	10%	n/a	Penicillin (100 U/mL), streptomycin (100 mg/mL)	37 °C, 5% CO_2	28-35	25 cm^2 culture dishes, 80-90%	2017: [14]
	DMEM	n/a	20%	1%; 2 mM glutamine	Penicillin (100 U/mL), streptomycin (100 mg/mL)	37 °C, 5% CO_2, 95% humidity	40-50	80%	2016: [15]
	DMEM	n/a	10%	1%; 1% L-glutamine	1% of penicillin (100 IU/mL) and streptomycin (100 mg/mL)	n/a	n/a	n/a	2016: [16]
	DMEM	n/a	10%	1%; 4.5 g/L glucose, 1% L-glutamine	1% penicillin and streptomycin (100 IU/mL)	37 °C, 5% CO_2, 95% humidity	n/a	n/a	2016: [17]
	DMEM	n/a	10%	1%; 1% L-glutamine	Penicillin (100 U/mL), streptomycin (100 IU/mL)	37 °C, 5% CO_2, 95% humidity	31-39	n/a	2016: [18]

	RPMI-1640	n/a	10%	n/a	1% penicillin-streptomycin (100 U/mL)	37 °C, 5% CO_2	5-30	85-90%	2016: [19]
	DMEM	n/a	10%	1%	n/a	37 °C, 5% CO_2, 95% humidity	n/a	n/a	2015: [20]
	DMEM			1%	1% penicillin–streptomycin	37 °C, 5% CO_2	n/a	n/a	2015: [21]
	DMEM	Every other day		10%; 10% L-glutamine	1% penicillin (100 IU/mL) and streptomycin (100 µg/mL)	37 °C, 5% CO_2, 95% humidity	n/a	75 cm^2 culture flasks, 60-80%	2015: [22]
	RPMI-1640	n/a	10%	n/a	1% penicillin-streptomycin (100 U/mL)	37 °C, 5% CO_2	5-30	85-90%	2015: [23]
	DMEM	n/a	20%	1%; 4.5 g/L glucose,	1% antibiotic–antimycotic solution	37 °C	n/a	60000 cells/cm^2	2015: [24]
	DMEM	n/a	10%	1%; 1% L-glutamine	n/a	37 °C, 5% CO_2	n/a	25 cm^2 Nunc plastic flask	2014: [25]
	RPMI-1640	n/a	15%	1%	1% penicillin-streptomycin (100 U/mL)	37 °C, 5% CO_2, 95% air	30-45	n/a	2014: [26]
	DMEM	n/a	10%	n/a	Penicillin (100 U/mL), streptomycin (100 µg/mL)	37 °C, 5% CO_2, 95% humidity	n/a	n/a	2014: [27]
	DMEM	n/a	10%	1%; 1% L-glutamine	1% penicillin and streptomycin	37 °C, 5% CO_2	n/a	75 cm^2 culture flasks, $5x10^4$ cell/cm^2, 80%	2014: [28]
	DMEM	n/a	10%	n/a	n/a	n/a	n/a	75 cm^2 culture flasks	2012: [29]
	DMEM	Every 2 days		1%; 25 mM D-glucose, 25 mM HEPES, 44 mM $NaHCO_3$, 1% L-glutamine	1% penicillin–streptomycin	37 °C, 5% CO_2, 90% humidity	32-38	80-85%	2012: [30]
	DMEM	n/a	20%	1%; 4.5 g/L glucose, L-glutamine	1% antibacterial–antimycotic solution	37 °C, 5% CO_2	50-70	60,000 cells/cm^2	2012: [31]
	EMEM	n/a	10%	1%; 1% L-glutamine	n/a	37 °C, 5% CO_2, 95% humidity	45-60		2011: [32]
	DMEM	Every other day	10%	1%; 2 mM L-glutamine	1% penicillin–streptomycin	37 °C, 5% CO_2, 90% humidity, 95% air	70–75	75 cm^2 culture flasks, 4×10^5 cells/flask	2011: [33]
	DMEM	n/a	n/a	n/a	n/a	37 °C, 5% CO_2, 90% humidity, 95% O_2	n/a	n/a	2011: [34]
	EMEM	Every 2 days	10%	1%; 1% L-glutamine	Penicillin (100 IU/mL), streptomycin (100 µg/mL)	37 °C, 5% CO_2, 95% humidity	45-60	75 cm^2 culture flasks, 4×10^5 cells/flask	2010: [35]
	DMEM	Every other day	10%	1%; 4.5 g/L glucose, L-glutamine and sodium pyruvate	Penicillin (100 IU/mL), streptomycin (100 µg/mL), Amphotericin B (25 µg/mL)	T-75 flask	60-80	T-75 flasks, 3×10^3 cells/cm^2, 80-90%	2010: [36]

HT29-MTX or HT29-MTX-E12	DMEM	n/a	10%	1%; 4.5 g/L glucose, 1% L-glutamine	1% penicillin, streptomycin (100 IU/mL)	37 °C, 5% CO_2	n/a	n/a	2018: [9]
	DMEM	n/a	10%	1%	Penicillin (100 U/mL), streptomycin (100 U/mL)	37 °C, 5% CO_2	n/a	n/a	2018: [10]
	DMEM	n/a	10%	1%	1% penicillin, streptomycin (100 IU/mL)	5% CO_2, 95% humidity,	n/a	75 cm^2 culture flasks	2018: [8]
	DMEM	n/a	10%	1%; 1% L-glutamine	1% penicillin, streptomycin (100 IU/mL)	37 °C, 5% CO_2	n/a	n/a	2018: [11]
	DMEM	n/a	10%	1% L-glutamine, 1% NEAA	Penicillin (100 U/mL), streptomycin (100 U/mL)	37 °C, 5% CO_2, 95% humidity	30-39	n/a	2016: [18]
	DMEM	n/a	10%	1%; 1% L-glutamine	Penicillin (100 U/mL), streptomycin (100 mg/mL)		n/a	n/a	2016: [16]
	DMEM	n/a	10%	1%	1% penicillin, streptomycin (100 IU/mL)	37 °C, 5% CO_2, 95% humidity	n/a	75 cm^2 culture flasks	2016: [37]
	DMEM	n/a	10%	1%; 4.5 g/L glucose, 1% L-glutamine	1% penicillin, streptomycin (100 IU/mL)	37 °C, 5% CO_2, 95% humidity	n/a	n/a	2016: [17]
	DMEM	n/a	10%	1%; 4.5 g/L glucose, 1% L-glutamine	1% penicillin, streptomycin (100 IU/mL)	37 °C, 5% CO_2	n/a	n/a	2015: [38]
	DMEM	n/a	10%	1%	n/a	37 °C, 5% CO_2, 95% humidity	n/a	n/a	2015: [20]
	DMEM	n/a	10%	1%; 1% L-glutamine	n/a	37 °C, 5% CO_2	n/a	n/a	2014: [25]
	DMEM	n/a	10%	1%; 1% L-glutamine	1% penicillin, streptomycin	37 °C, 5% CO_2	n/a	75 cm^2 culture flasks, $5x10^4$ cells/cm^2, 80%	2014: [28]
	DMEM	Every other day	10%	1%; 4.5 g/L glucose, L-glutamine, sodium pyruvate	Penicillin (100 IU/mL), streptomycin (100 µg/mL), Amphotericin B (25 µg/mL)	n/a	8-20	T-75 flasks, $2×10^4$ cells/cm^2, 80-90%	2010: [36]
	DMEM	Every 2 days	10%	1%; 1% L-glutamine	n/a	10% CO_2, 95% humidity	43-50	24-well plates or 6-well uncoated polycarbonate Transwell filter inserts (0.4 mm pore size, 4.71 cm^2), $6x10^4$ cell/cm^2	2009: [39]
HT-29	MEM		10%	1.5 g/L sodium bicarbonate	1% penicillin/ streptomycin solution	37 °C, 5% CO_2, 95% humidity	n/a	n/a	2017: [40]
	DMEM	Every 2 days	10%	1%; 2 mM L-glutamine	Penicillin (100 U/mL), streptomycin (100 mg/mL)	37 °C, 5% CO_2, 90% humidity, 95% air	12-25	75 cm^2 culture flasks, $4x10^5$ cells/cm^2, 80%	2011: [34]

	DMEM	Every other day	10%	1%; 2 mM L-glutamine	Penicillin (100 U/mL), streptomycin (100 mg/mL)	37 °C, 5% CO_2, 90% humidity, 95% air	25–18	5 cm^2 culture flasks, 4×10^5 cells/flask	2011: [33]
Caco-2/ HT-29	n/a	n/a	n/a	n/a	n/a	n/a	n/a	7:3 on 96-well plates	2015: [20]
	DMEM	Every 2 days	10%	1%; 2mM L-glutamine	Penicillin (100 IU/mL), streptomycin (100 mg/mL)	n/a	n/a	90:10 on transwell diffusion cells (3 µm pore size, 1 cm^2 growth area), 100000 cells/cm^2	2011: [34]
	DMEM	Every other day	10%	1%; 2mM L-glutamine	Penicillin (100 IU/mL), streptomycin (100 mg/mL)	n/a	n/a	90:10 on Transwell plates, 300000 cells/cm^2	2011: [33]
Caco-2/ HT29-MTX	DMEM	Every 2 days	10%	1%; 4.5 g/L glucose, 1% L-glutamine	1% penicillin, streptomycin (100 IU/mL)	37 °C, 5% CO_2, 95% humidity	n/a	7:3 in 96-well plates, $1x10^4$ cells/well	2018: [12]
	DMEM	n/a	10%	1%; 1% L-glutamine	Penicillin (100 IU/mL), streptomycin (100 mg/mL)	n/a	n/a	1:1 on 96-well plates, 80–90%	2015: [41]
	DMEM	n/a	20%	1%	1% antibiotic–antimycotic solution	5% CO_2	30-60	73000 cells/cm^2	2015: [42]

Notes:

Dulbecco's modified Eagle's medium (DMEM), modified eagle medium (MEM), N-2-hydroxyethyl piperazine-N0-2-ethane sulfonate buffer (HEPES), Roswell Park Memorial Institute-1640 medium (RPMI-1640)

Supplementary table 2. Experimental conditions for cellular uptake studies

Method	System	Cell line	Cell culture	Objective	Sample	Incubation	Visualization and labelling materials	Year/ Ref
CLSM	Zeiss LSM 780	Caco-2	6-well plates, 3 hr, $4x10^5$ cells/well, cover slip	Tight junction opening	CS/Ins/HS NPs (1 mg/mL) in artificial intestinal fluid (pH 6.8)	0, 15, 30, 60 and 120 min (with sample)	PBS wash (remove extracellular residues), 3.7% paraformaldehyde (15 min), DAPI (nucleus), Alexa Fluor 488 phalloidin (F-actin), Alexa Fluor 647 ZO-1 monoclonal antibody (ZO-1)	2018: [3]
	Leica SP5 II	Caco-2	Glass-bottom cell culture dishes	NPs penetration into GI cells, cell morphology	LBL4, LBL4-Alg NPs, free insulin (250 mg/mL)	4 hr (with sample)	PBS wash (3 times), 4 % paraformaldehyde, Cy5-anti-insulin (insulin), DAPI (nucleus)	2018: [13]
	Leica TCS SP8	HT29-MTX-E12	8-well chamber cover glass, $1x10^4$ cells/well	NPs mucus penetration	Cy5-INS, RITC–HTCC, R123-HA, R123-HA-SH	2 hr (with sample)	PBS wash (3 times), 4 % paraformaldehyde, DAPI (nucleus)	2018: [11]
	Leica TCS SP8	Caco-2	n/a	Tight junction opening	n/a	n/a	PBS wash (3 times), 4 % cold paraformaldehyde (15 min), anti-occludin antibody (15 min), anti-rabbit IgG Fab2 Alexa Fluor 488 Molecular Probe (1 hr)	2018: [11]
	n/a	Caco-2	Glass-bottom cell culture dish, 24 hr	NPs penetration into GI cells	FITC-insulin/CMCD-g-CS NPs (50 µg/mL)	2, 4 hr (with sample)	PBS wash (3 times), 4 % cold paraformaldehyde (30 min), Hoechst 33342 solution (nucleus)	2018: [43]
	n/a	Caco-2	n/a	Tight junction opening	CMCD-gCS NPs	2 hr (with sample) 0-48 hr (before CLSM)	4% paraformaldehyde (30 min), 0.2% Triton X-100 (15 min), PBS with 1% BSA and 1% Tween-20 (30 min), PBS wash (3 times), anti-occludin (5 mg/mL; 24 hr), anti-rabbit IgG Fab2 Alexa Fluor 488 Molecular Probes (1:100; 30 min)	2018: [43]

n/a	Caco-2, Caco-2/HT29-MTX/Raji B	Transwell® TM, glass slide with fluorescence mounting medium	NPs penetration into GI cells	n/a	n/a	2% paraformaldehyde (30 min), 0.2% Triton X-100 (7 min), PBS with 10% BSA and 0.05% Tween-20 (30 min), rabbit occludin primary antibody (1:50; 2 hr), rabbit occludin primary antibody (1:1000; nucleus), PBS wash (3 times)	2018: [10]
Olympus FV1000	Caco-2	Coverslip in 12 well plates, 4 days, 5×10^4 cells/mL	NPs penetration into GI cells	DiO NPs	3 hr (with sample)	PBS wash (3 times), 4% paraformaldehyde, DAPI (nucleus)	2018: [44]
n/a	Caco-2	24-well plates, 7 days, 5×10^4 cells/well	NPs penetration into GI cells	500 µL free F-insulin, insulin NPs (0.2 mg/mL)	2 hr (with sample)	PBS wash, heparin (0.5 mg/mL; 3min; remove extracellular residues)	2018: [7]
Beckman Coulter FCS	Caco-2	24-well plates	NPs penetration into GI cells	NPs in SFM (containing 600 µg/mL PLGA)	3 hr (with sample)	n/a	2018: [1]
Nikon	Hep G2	Special Petri dishes, 1×10^5 cells/well	Liver penetration	FITC-insulin, FITC-insulin NPs (25 µg/mL)	4 hr (with sample)	PBS wash (3 times), 4% paraformaldehyde	2018: [45]
Olympus FV1000	Caco-2	n/a	NPs penetration into GI cells	FITC-insulin NPs (200 mg/mL insulin) with free apo-TF, control (no free apo-Tf)	3 hr (with sample)	PBS wash, 4% paraformaldehyde	2018: [8]
Olympus FV1000	Caco-2/HT29-MTX-E12 (7:3)	n/a	NPs mucus penetration	FITC-insulin NPs (200 mg/mL insulin) with free apo-TF	3 hr (with sample)	3% formalin solution wash (3 times; remove mucus layer), PBS wash, 4% paraformaldehyde	2018: [8]
Olympus FV1000	Caco-2	n/a	Tight junction opening	FITC-insulin NPs (200 mg/mL insulin) with free apo-TF	3 hr (with sample)	4% paraformaldehyde, 0.1% Triton X-100, 5% goat serum, monoclonal antibody of claudin-4, Alexa Fluors 594-conjugated goat anti-mouse IgG (1:100)	2018: [8]
n/a	HT-29	FluoroDish, $1x10^5$ cells/dish, 70-80% confluence	NPs mucus penetration	FITC-insulin/alginate/stearic acid NPs, FITC-insulin/alginate-C18 NPs (1 mL, 2 mg/mL in PBS)	1 hr (with sample)	n/a	2017: [40]

Leica	Caco-2	6 well plate, $1x10^5$ cells/well	NPs penetration into GI cells	VitB12-Chi-CPNPs, Chi-CPNPs in either 20% FBS/intrinsic factor media or serum free/no intrinsic factor media	1 hr (with sample)	PBS wash (2 times), 10% formalin buffer (10 min), glycerol with DPAI (nucleus; 5 µg/ml)	2016: [15]
Cal Zeiss LSM 710	Caco-2	Glass-bottom cell culture dish	Tight junction opening	MNPs, insulin-LMWP MNPs (containing 2.5 µM insulin)	2 hr (with sample)	10% formalin, 1% BSA, 0.4% Triton-X, 5% goat serum, ZO-1 rabbit polyclonal antibody IgG (1:1000 in PBS; 12 hr; ZO-1 protein); Alexa Fluor 488-labeled goat anti-rabbit IgG (1:100 in PBS; 1 hr), 5% donkey serum, occludin goat polyclonal IgG (1:1000; occludin protein); Alexa Fluor 488-labeled donkey anti-goat IgG (1:100)	2016: [16]
Cal Zeiss LSM 710	Caco-2	Culture plates	NPs penetration into GI cells	Fluorescein-labeled MNPs conjugate (containing 2.5 µM insulin)	2 hr (with sample)	DAPI (nucleus; 5 µg/ml; 10 min)	2016: [16]
Cal Zeiss LSM 710	HT29-MTX	Culture plates	NPs mucus penetration	Insulin, insulin-LMWP MNPs (containing 2.5 µM insulin)	2 hr (with sample)	Rhodamine B (insulin), FPR648 (PLGA), Alexa Fluor 488-labeled WGA (mucus layer; 5 µg/mL), bis-benzimide H33342 trihydrochloride (nucleus; 5 µg/mL)	2016: [16]
Olympus FV1000	HT-29-MTX-E12	Coverslips, 24-well plates, 2 days, $5x10^4$ cells/mL	NPs penetration into GI cells	Dil-loaded NPs (containing 500 µg/mL PLA)	2 hr (with sample)	PBS wash (2 times), DAPI (nucleus)	2016: [17]
Leica SP5	Caco-2/HT-29-MTX (90:10)	Lab-Tek 8-chamber slides, 24 hr,	NPs penetration into GI cells/ mucus	Alexa 488®-loaded insulin NPs	n/a	HBSS–MES buffer (2 times), 200 µL Alexa Fluor® 488-loaded NPs (0.5 mg/mL; 3 hr), 200 µL CellMask™ DeepRed (plasma membrane; 3 min); 2.5% glutaraldehyde (20 min);	2016: [18]
Olympus FV1000	HT-29-MTX-E12	Cover slides	Tight junction opening	T-NPs, P-T-NPs	3 hr	4% paraformaldehyde, 0.1% Triton X-100, 5% goat serum, anti-claudin-4 antibody (claudin-4 protein), Alexa	2016: [37]

	Olympus FV1000	HT-29-MTX-E12	12-well plates with glass cover-slip bottoms, 1×10^5 cells/well	NPs mucus penetration	T-NPs, P-T-NPs	60 min	Fluor® 594-conjugated goat anti-mouse IgG (1:100; 30 min)	PBS wash (3 times), rhodamine-conjugated ulex europaeus agglutinin I lectin (mucus layer; 10 min)	2016: [37]
	n/a	Caco-2/ HT29-MTX-E12	Cover slips	Tight junction opening	Insulin NPs (50 µg/mL)	1 hr	4% paraformaldehyde, 0.2% Triton X-100, 5% BSA, anti-ZO1 monoclonal antibody (ZO-1 protein; 1 mg/mL), anti-rabbit IgG (30 min)		2015: [20]
	n/a		n/a	NPs mucus penetration	Insulin NPs (50 µg/mL)	1 hr	10 mM N-acetylcysteine in HBSS (30 min)		2015: [20]
	Leica TCS SP5	Caco-2	6-well plates, $1x10^5$ cells/well	NPs penetration into GI cells	100 µL FITC-INS-PLGA-lipid-PEG NPs	1, 2, 4, 6 hr	PBS (2 times), 4% paraformaldehyde, rhodamine-phalloidin, DAP		2015: [21]
	Cal Zeiss LSM 710	HT29-MTX	Glass-bottomed cell culture dish, 14 days, 5×10^4 cells/cm^2	NPs mucus penetration	500 µL RB-Ins loaded FPR648-PLGA NPs, TMC-FPR648-PLGA NPs in HBSS (containing 500 µg/mL RB-Ins)	2 hr	PBS (2 times), FPR648 (PLGA), rhodamine B (insulin), Alexa Fluor 488 labeled wheat germ agglutinin (5 µg/mL; 20 min)		2015: [22]
	Cal Zeiss LSM 710	Caco-2	Glass-bottomed cell culture dish, 14 days, 5×10^4 cells/cm^2	NPs penetration into GI cells	500 µL RB-Ins loaded FPR648-PLGA NPs, TMC-FPR648-PLGA NPs in HBSS (containing 500 µg/mL RB-Ins), control (RB-Ins)	2 hr	PBS (3 times), DAPI (5 µg/mL; 10 min)		2015: [22]
	Cal Zeiss LSM 710	Caco-2	Transwell (polyester membrane, pore size of 0.4 µm, 21 days	Tight junction opening	FPR648-PLGA NPs, TMC-FPR648-PLGA NPs	2 hr	10% formalin, 1% BSA, 0.4% Triton-X PBS, 5% donkey serum (1 hr), occludin goat polyclonal IgG (1:1000; 24 hr), Alexa Fluor 488 labeled donkey anti-goat IgG (1:100 in PBS; 1 hr)		2015: [22]
	Zeiss LSM 510	Caco-2	n/a	NPs penetration into GI cells	Nanocomplexes	n/a	10 µM endocytotic fluorescent marker FM464 (15 min)		2014: [25]
	Nikon C2 si	Caco-2/ HT29-MTX	Cover slips in 6-well plates, 6-7 days, $3x10^4$ cells/well	NPs penetration into GI cells and mucus	500 µL 6-AF-Eul-cys/GSH NPs (1 mg/mL)	0.5, 1, 2, 3 hr	PBS wash (3 times), 4% paraformaldehyde (30 min), DAPI (2 mg/mL), PI (5 mg/mL)		2014: [28]

		n/a	Tight junction opening	500 µL 6-AF-Eul-cys/GSH NPs (10 mg/mL), Eul-cys NPs (5mg/mL) with SC (1 mg/mL) in PBS	n/a	PBS wash (3 times), 4% paraformaldehyde (20 min), 0.2% Triton X-100 (20 min), 200 µL ZO-1 antibody (ZO-1; 1:50; 24 hr), FITC anti-rabbit IgG (1:100; 1 hr)	2014: [28]
Zeiss LSM 5 Pa	HT29-MTX-E12	Transwell filter inserts, 14-17 days, coverslips	NPs mucus penetration	Alexa 488 insulin NPs	n/a	PBS wash, Alexa Fluor 555 labeled wheat germ agglutinin (mucus; 10 mg/mL; 10 min)	2013: [46]
Leica Sp2MP	Caco-2	4-well Lab-Tek chamber slides	NPs penetration into GI cells	FITC-insulin NPs (containing 10 mg PLGA/cm^2), FITC-insulin NPs followed by 4 hr DMEM	2 hr	DMEM wash (3 times; 10 min), CellMask Deep Red (cell membrane; 5 µg/mL), Hoechst (nucleus; 10 µg/mL)	2012: [31]
TCS SL	Caco-2	n/a	NPs penetration into GI cells	Cy3-aspart-insulin NPs (0.2 mg/mL)	2 hr	PBS wash (2 times), 3.7% paraformaldehyde	2010: [47]
TCS SL	Caco-2	n/a	NPs penetration into GI cells	fluorescent insulin NPs (0.2 mg/mL) in pH 6.6, pH 7, pH 7.4	2 hr	PBS wash (2 times), 3.7% paraformaldehyde	2009: [48]
Zeiss LSM 510	HT-29-MTX-E12	Glass cover slides, 2 days	NPs mucus penetration	Insulin, polymer, insulin NPs (containing 250 mg/mL insulin)	2 hr	Transport buffer wash (3 times), 3.7% paraformaldehyde, DAPI (20 min), Oregon Green 488, FITC, TRITC	2009: [39]
TCS SL	Caco-2	n/a	NPs transportation across GI cells	Cy3-insulin NPs (containing 0.2 mg/mL NPs)	n/a	PBS wash (2 times), 3.7% paraformaldehyde	2008: [49]
TCS SL	Caco-2	Cover slides	Tight junction opening	Cy3-insulin NPs (containing 0.2 mg/mL NPs)	2 hr	PBS wash (3 times), 3.7% paraformaldehyde, 0.2% Triton X-100 and RNase (100 µg/mL; 15 min), 5% normal goat serum (1 hr), rabbit anti-ZO-1 mAb (1:50; 1 hr), Cy-5 conjugated goat antirabbit IgG (1:100), propidium iodide (nucleus)	2008: [49]
TCS SL	Caco-2	Transwell, 24-30 days,	NPs transportation across GI cells	FITC-insulin NPs (0.2 mg/mL)	1 hr	PBS wash, 3.7% paraformaldehyde	2007: [50]

	TCS SL	Caco-2	n/a	Tight junction opening	FITC-insulin NPs (0.2 mg/mL)	1 hr	PBS wash (3 times), 3.7% paraformaldehyde, 0.2% Triton X-100 and RNase (100 µg/mL; 15 min), 5% normal goat serum, rabbit anti-ZO-1 mAb (60 min)	2007: [50]
	TCS SL	Caco-2	n/a	Tight junction opening	FITC-insulin NPs (0.2 mg/mL)	n/a	PBS wash (3 times), 3.7% paraformaldehyde, 0.2% Triton X-100 and RNase (100 µg/mL; 15 min), 5% normal goat serum (60 min), rabbit anti-ZO-1 mAb (1:50; 60 min), Cy5 conjugated goat anti-rabbit IgG (1:100), 100 nM propidium iodide (nucleus; 10 min)	2007: [51]
Flow cytometry	Cytomics FC500	Caco-2	n/a	n/a	Insulin NPs	30 min	n/a	2018: [44]
	Beckman Coulter FCS	Caco-2	24-well plates	NPs penetration into GI cells	NPs in SFM (containing 600 µg/mL PLGA), negative control (HBSS medium with cells)	3 hr (with sample)	10 000 cells detection	2018: [1]
	Cytomics FC500	Caco-2	12-well plates, 5 days	NPs penetration into GI cells	SLNs (containing FITC-insulin 100 µg/mL)	3 hr (with sample)	PBS wash	2018: [52]
	BD LSR II	Caco-2/Rev-HT29-MTX	24-well plates, 21 days	NPs penetration into GI cells	Insulin NPs (containing 5 mg/well PLGA) in medium without FCS	4 hr (with sample)	HBSS wash (3 times), 10 000 cells detection	2018: [4]
	FACSCalibur	Hep G2	n/a	NPs penetration into liver	FITC-insulin, FITC-insulin NPs (25 µg/mL)	4 hr	PBS wash (3 times)	2018: [45]
	n/a	Caco-2	n/a	NPs penetration into GI cells	NPs (containing 200 mg/mL FITC-insulin)	3 hr	PBS wash (3 times), $1x10^4$ cells detection	2018: [8]
	Beckman Coulter Galios™	Caco-2/HT29-MTX (90:10)	6-well plates, 48 hr, $7x10^5$ cell/mL	NPs penetration into GI cells	Alexa Fluor®-insulin NPs (0.5 mg/mL)	3 hr	HBSS-MES buffer wash (3 times), 0.5 mL Versene, 5 mM ethylenediamine tetraacetic acid, 25 mM MES, 10 000 cells detection	2016: [18]

		HT29-MTX-E12	24-well plates, 7 days, $7x10^4$ cells/well	NPs mucus penetration	Dil-loaded NPs (containing 500 µg/mL PLA)	2 hr	PBS wash (3 times)	2016: [17]
	FACSCalibur	Caco-2	6-well plates, $2x10^5$ cells/mL		FITC-INS-PLGA-lipid-PEG NPs	2 hr	HBSS wash (2 times)	2015: [21]
	Guava EasyCyte	Caco-2	24-well plates	NPs penetration into GI cells	Empty NPs, FITC/insulin NPs (containing 10 mg PLGA/cm^2), FITC/insulin (0.22 mg/cm^2) in DMEM without FBS	0.5, 1, 2, 3, 4, 6 h	HBSS wash (3 times; 10 min), propidium iodure (6 mg/mL)	2012: [31]
	n/a	Caco-2	Transwell inserts with microporous membranes (1 µm pore size)	NPs penetration into GI cells and exocytosis	FITC/insulin NPs (containing 10 mg PLGA/cm^2) in DMEM without FCS	0.5, 1, 2 hr (with samples) 1, 2, 4, 19, 24 h (before exocytosis analysis)	n/a	2012: [31]
ELISA with BCA assay kit	R&D System	Caco-2	n/a	NPs penetration into GI cells	SLN suspensions (containing 100 µg/mL insulin)	3 hr	cell extracts obtained by freeze–thaw cycles	2018: [52]
Microplate reader with BCA assay kit	MultiMode and Scepter™ 2.0 handheld automated cell counter	Caco-2, HT29-MTX, Caco-2/ mucin	24-well plates, $5x10^4$ cells/well	NPs penetration into GI cells and mucus	RITC-insulin NPs	3 hr	Lysis buffer	2018: [9]
	n/a	Caco-2/ HT29-MTX-E12 (7:3)	96-well plates,	NPs penetration into GI cells and mucus	Dio-labeled NPs	3 hr	4% formalin solution in PBS (remove trapped NPs and mucus; 3 times), PBS wash (2 times)	2018: [12]
	n/a	Caco-2, HT29-MTX-E12	96-well plates, $1x10^4$ cells/well	n/a	Dio-labeled NPs, PLGA-PEG-R8-COOH NPs	3 hr	Lysis buffer, 4% formalin solution in PBS, intestinal alkaline phosphatase	2018: [12]
	Varioskan Flash multimode	Caco-2	24- or 96-well plates, $5x10^4$ cells/mL	n/a	FITC-insulin, FITC-insulin NPs (containing 200 µg/mL insulin), FITC-insulin NPs with apo-Tf (200 µg/mL)	3 hr	n/a	2018: [8]
	Infinite 200 PRO	HT29-MTX	NAC (N-acetyl cysteine),	NPs mucus penetration	Insulin NPs, free insulin	n/a	PBS wash (3 times) or 3% formalin solution wash in PBS,	2016: [16]

		formalin and control group				cell lysis by ultrasound sonication	
Varioskan Flash multimode	HT-29-MTX-E12		NPs mucus penetration	Fluorescent NPs (containing 200 µg/mL insulin)	3 hr	200 µl 3% formalin solution wash in PBS, PBS wash (2 times)	2016: [37]
Varioskan Flash multimode	HT29-MTX-E12	96-well plates, 5×10^4 cells/mL	NPs mucus penetration	Dil-loaded NPs (containing 500µg/mL PLA)	2 hr	N-acetyl cysteine, DMSO	2016: [17]
Varioskan Flash multimode	Caco-2/HT29-MTX	n/a	NPs penetration into GI cells and mucus	FITC-insulin NPs	3 hr	Lysis buffer, Ex/Em = 490/520 nm	2016: [18]
Varioskan Flash multimode	HT29-MTX-E12	96-well plates, 50000 cells/well	NPs mucus penetration	Insulin NPs (containing 0.25 mg/mL insulin)	2 hr	N-acetyl cysteine, lysis buffer, mild or thorough wash	2015: [38]
Varioskan Flash multimode	Caco-2/HT29-MTX	n/a	NPs penetration into GI cells and mucus	100 µl FITC-INS, T NPs, VB12-T NPs in HBSS (50, 100, 200, 300 and 400 µg/mL)	2 hr	PBS wash, lysis buffer (1% triton X-100, 50 mM HEPES, 150 mM NaCl, 2 mM Na_3VO_4, 100 mM NaF, 100 units/mL aprotinin, 20 mM leupeptin, 0.2 mg/mL phenylmethanesulfonyl fluoride), 10 mM N-acetyl-L-cysteine	2015: [41]
Varioskan Flash multimode	Caco-2, Caco-2/HT29-MTX	n/a	NPs penetration into GI cells and mucus	Insulin NPs	3 hr	Lysis buffer	2015: [20]
Infinite 200 PRO	HT29-MTX	n/a	NPs mucus penetration	RB-Ins PLGA NPs, TMC-PLGA NPs (containing 500 µg/mL of RB-Ins) in HBSS	n/a	10 mM N-acetyl cysteine (1 hr), HBSS wash (3 times), ultrasound sonication, Ex/Em = 566/590 nm	2015: [22]
Varioskan Flash multimode	Caco-2/HT29-MTX	n/a	NPs penetration into GI cells and mucus	100 µl FITC-INS, T NPs, VB12-T NPs in HBSS (containing 50, 100, 200, 300, 400 µg/mL insulin)	2 hr	PBS wash, lysis buffer (1% triton X-100, 50 mM HEPES, 150 mM NaCl, 2 mM Na_3VO_4, 100 mM NaF, 100 units/mL aprotinin, 20 mM leupeptin, 0.2 mg/mL phenylmethanesulfonyl fluoride)	2015: [41]
Varioskan Flash multimode	Caco-2, Caco-	24-well plates, 7 days, 5×10^4 cells/well	NPs penetration	500 µL free insulin, insulin NPs in HBSS	2 hr	PBS wash, heparin wash (0.5 mg/mL; 3 min), 10 mM N-	2014: [25]

		2/HT29-MTX (1:1)		into GI cells and mucus	(containing 0.2 mg/mL insulin)		acetyl-L-cysteine (60 min), lysis buffer	
	BioTek Synergy	Caco-2/HT29-MTX	n/a	NPs penetration into GI cells and mucus	n/a	n/a	Acetylcysteine, HBSS–HEPES wash (2 times), 3% formalin solution	2014: [28]
TEM	Philip's CM10	Caco-2	Polythene embedding capsule	Tight junction opening	n/a	n/a	2.5% glutaraldehyde in PBS, osmium oxide (1 hr), 30-100% ethanol (5.5 hr), ethanol:Spurr's resin (21 hr)	2011: [32]
Fluorescence microscopy	Photon Tech ASOC-10	Caco-2	n/a	NPs penetration into GI cells	RhoB-Ins/heparin/chitosan NPs in AIF (1 mg/mL NPs)	n/a	n/a	2018: [3]
	Olympus FV1000	Caco-2	n/a	NPs penetration into GI cells	FITC-INS NPs (containing 200μg/mL of insulin), FITC-INS NPs with free apo-Tf	3 hr	PBS wash, 4% paraformaldehyde	2018: [8]
	Olympus IX71	Caco-2	12-well transwell plates, 1×10^5 cells/cm^2, 85% confluence	NPs penetration into GI cells	0.5 mL NPs	1, 2, 3, 4 hr	HBSS wash (2 times), 100 μL RIPA cell lysate (20 min), acetone, 0.1 mol/L hydrochloric acid	2017: [14]
	Axiostar Plus epifluorescence	Caco-2	Sterile coverslips coated with poly-L-lysine, cell culture (35x10 mm), 24 hr	NPs penetration into GI cells	Rhodamine B-insulin NPs	4 hr	DRAQ5 nuclear dye, PBS wash (3 times)	2016: [19]
	Axiostar Plus epifluorescence	Caco-2	Sterile coverslips coated with poly-L-lysine, cell culture (35x10 mm), 24 hr	NPs penetration into GI cells	Rhodamine B-insulin NPs	4 hr	DRAQ5 nuclear dye, PBS wash (3 times)	2016: [23]
	n/a	Caco-2	21 days, 60000 cells/cm^2	NPs penetration into GI cells	FITC-PLGA, FITC PPC NPs	2, 5, 12 hr	PBS wash (3 times)	2015: [24]
	n/a	HT29-MTX-E12	n/a	NPs mucus penetration	Alexa 488 insulin	1 hr	300 μL formalin solution in PBS (4 %), lysis buffer	2013: [46]
	Leica DMI 4000B	n/a	24-well polyester plates, 3 days, 0.1×10^6 cells/mL		Pa2.5R, QPa2.5R, FITC-insulin	0.5, 1, 2 hr	DAPI (300 nM, 5 mins)	2011: [32]

	Perkin Elmer LS 50B	HT29-MTX-E12	n/a	NPs mucus penetration	Polymer (250 µg/mL), insulin NPs (containing 125 µg/mL insulin)	2 hr	2% sodium dodecyl sulfate, 50 mM EDTA, Ex/Em = 493/515 nm (polymer), 534/567 nm (insulin), 10 mM N-acetyl-L-cysteine	2009: [39]

Supplementary table 3. Experimental conditions for cytotoxicity assays

Assay	Cell	Flask/ seeding/ density	Medium change/ remove	Sample	Sample incubation	Reagent	System	Year/ Ref
MTT	Caco-2	96-well plates, 48 hr, 1×10^4 cells/well	Before sample treatment After treatment sample	n/a	3 hr (with sample) 24 hr (before MTT solution)	200 µL 0.05% MTT solution for 4 hr	Varioskan Flash multimode reader	2018: [5]
		96-well plates, 24 hr, $7x10^4$ cells/mL	non-FBS medium	LBL4 and LBL4-Alg NPs (0, 125, 250, 500, 1000 µg/mL)	24 hr (with sample)	20 µl MTT (5 mg/mL) for 4 hr, 100 µl DMSO		2018: [13]
		96-well plates, 24 hr, $2x10^3$ cells/mL	After sample treatment	Insulin, CMCD-g-CS NPs, insulin/CMCD-g-CS NPs (20-360 µg/mL)	24 hr (with sample)	100 µL MTT (0.5 mg/mL) for 3 hr, 150 µL DMSO	Microplate reader (570 nm)	2018: [43]
		96-well plates, 24 hr, $1x10^4$ cells/mL	After sample treatment (washed cells with PBS)	NPs containing polymers from 0.01 to 5 mM	24 hr (with sample)	20 µl MTT (5 mg/mL) for 4 hr, DMSO	Microplate reader (550 nm)	2018: [2]
		96-well plates, 24 hr, $2x10^4$ cells/mL	Before sample treatment (washed cells with 200 µL PBS) After sample treatment (washed cells twice with 200 µL PBS)	Insulin-loaded lipid-polymeric NPs, blank lipid-polymeric NPs and insulin (100, 50, 25, 12.5 and 5 µg/mL), negative control (1% Triton X-100), positive control (medium with cell incubation)	4 hr (with sample)	200 µL MTT (0.5 mg/mL) for 4 hr, 200 µL DMSO	Microplate spectrometer (570 and 630 nm)	2018: [10]
		96-well plates, 24 hr, $2x10^4$ cells/mL	Before sample treatment (replaced by serum-free medium)	Complex NPs (1000, 500, 250, and 125 µg/mL)	24 hr (with sample)	n/a	n/a	2018: [53]
		96-well plates, 24 hr, $1x10^4$ cells/mL	n/a	200 µL NPs (125-1000 µg/mL)	24 hr (with sample)	n/a	n/a	2018: [54]
		96-well plates, 24 hr, $1x10^4$ cells/mL	n/a	NPs solution (25-400 µg/mL)	n/a	n/a	n/a	2018: [6]
		96-well plates, 24 hr, $1x10^4$ cells/mL	After sample treatment	M-β-CD, CM-β-CD or R8-CM-β-CD (1 -120 µg/mL)	2 hr (with sample)	n/a	n/a	2018: [7]

	n/a	n/a	SLNs, control (HBSS medium)	3 hr (with sample)	n/a	n/a	2018: [52]
	96-well plates, 48 hr, $5x10^4$ cells/mL	n/a	Insulin-CMCS NPs (31.25, 62.5, 125, 250, 500 µg/mL)	24 48, 72 hr (before MTT solution)	n/a	n/a	2017: [55]
	96-well plates, 48 hr, $1x10^5$ cells/mL	After sample treatment	VEN suspensions, insulin, blank VEN, insulin-loaded VEN (1.25-40 mg/ml)	3 hr (with sample) 24 hr (before MTT solution)	20 µl MTT (5 mg/mL) for 2 hr, 150 µL DMSO	Microplate reader (560 nm)	2016: [19]
	n/a	n/a	PLGA-lipid-PEG NPs	6 hr (with sample)			2015: [21]
	n/a	n/a	100 µL of FITC-INS, T NPs and VB12-T NPs (50, 100, 200, 300 and 400 µg/mL, pH7.4), positive control (sodium dodecyl sulfate; 50 µg/mL)	4 hr (with sample)	200 µl medium containing MTT (0.5 mg/mL), 200 µL DMSO	Varioskan Flash multimode reader (570 nm)	2015: [41]
	96-well plates, 7 days, $1x10^4$ cells/well	n/a	100 µL PEN and P-bis-CD solution (1, 2, and 5 mg/mL), control (HBSS)	24 hr (with sample)	n/a	n/a	2014: [25]
	96-well plates, $5x10^4$ cells/well	Before sample treatment (washed cells with 200 µL PBS)	100 µL Eulcys NPs (0.1-20 mg/mL), Eul-cys NPs (5 mg/mL) + GSH and SC (0.1-8 mg/mL)	3 hr (with sample)	100 µl MTT (5 mg/mL), 200 µL DMSO	Microplate reader (590 nm)	2014: [28]
	96-well plates, $1x10^4$ cells/well	n/a	Amino-benzyl-, pyridinyl- and benzyl- chitosan, NPs containing polymer (0.01-5 mM), control (non-treated cells)	3, 24 hr (with sample)	n/a	n/a	2014: [26]
	96-well plates, 24 hr, 5000 cells per 0.2 mL	n/a	l/d-R8-modified NPs, blank NPs (0.5-10 mg/mL)	2 hr (with sample) 24 hr (before MTT solution)	n/a	n/a	2013: [56]
	96-well plates, 48 hr, $1x10^4$ cells/well	n/a	n/a	2 hr (with sample)	100 µl MTT (0.5 mg/mL in HBSS) for 3 hr, 150 µL DMSO	Microplate reader (490 nm)	2013: [46]
	96-well plates, 5 days, 10000 cells/well	n/a	PLGA, blank PLGA NPs, blank CS-PLGA-NPs (1, 5, 20 mg/mL)	3 hr (with sample)	100 µl MTT (5 mg/mL in HBSS) for 4 hr, 200 µL DMSO	Microplate reader (590 nm)	2012: [30]

	96-well plates, 24 hr, 10000 cells/well	n/a	Polymer (0.0001-1 mg/mL), negative control (untreated cells), positive control (Triton X in PBS)	24 hr (with sample)	50 µl MTT (5 mg/mL in PBS) for 4 hr, 200 µL DMSO	VERSAmax tunable microplate reader (570 nm)	2010: [35]
	96-well plates, 24 hr, 10000 cells/well	n/a	Polymer (0.0001-1 mg/mL), negative control (untreated cells), positive control (Triton X in PBS)	24 hr (with sample) 24 hr (before MTT solution)	50 µl MTT (5 mg/mL in PBS) for 4 hr, 200 µL DMSO	Microplate reader (570 nm)	2009: [57]
HT29-MTX	96-well plates, $1x10^4$ cells/well	n/a	n/a	n/a	n/a	n/a	2018: [9]
	96-well plates, 24 hr, $1x10^4$ cells/well	Before sample treatment (washed cells with 200 µL PBS) After sample treatment (washed cells with 200 µL PBS)	Empty lipid-polymeric NPs, insulin NPs (5, 12.5, 25, 50, 100 µg/mL), negative control (1% Triton X-100), positive control (medium with cell)	4 hr (with sample)	200 µl MTT (0.5 mg/mL) for 4 hr, 200 µL DMSO	Microplate spectrometer (570 and 630 nm)	2018: [10]
	96-well plates, 24 hr, $5x10^4$ cells/0.3 mL	Before sample treatment (washed cells with PBS)	100 µL Eulcys NPs (0.1-20 mg/mL), Eul-cys NPs (5 mg/mL) + GSH and SC (0.1-8 mg/mL)	3 hr (with sample)	100 µl MTT (5 mg/mL), 200 µL DMSO	Microplate reader (590 nm)	2014: [28]
HT-29	96-well plates, 24 hr, $5x10^4$ cells/well	Before sample treatment After sample treatment	Insulin ASAN NPs, insulin AC18N NPs (10 mg in 0.5 mL PBS), control (MEM medium with cells)	n/a	20 µl MTT (5 mg/mL) for 4 hr, 150 µL DMSO	Microplate reader (570 nm)	2017: [40]
HT-29-MTX-E12	96-well plates, 24 hr, $5x10^3$ cells/well	Before sample treatment	Insulin, insulin NPs	24 hr (with sample)	20 µl MTT (5 mg/mL) for 4 hr, 150 µL DMSO	Microplate reader (570 nm)	2018: [11]
	96-well plates, 7 days, $1x10^4$ cells/well	n/a	200 µl T-NPs, P-T-NPs (50-300 20 µg/mL)	24 hr (with sample)	n/a	n/a	2016: [37]
NIH 3T3	96-well plates, 10000 cells/well	Before sample treatment	100 µl PMAPBA2/chitosan-SH1, PMAPBA1/chitosan-SH1, PMAPBA1/chitosan-SH2 (60-500 µg/mL), negative control (untreated cells)	48 hr (with sample)	10 µl MTT for 4 hr, 100 µL isopropanol	Microplate reader (570 nm)	2017: [58]

		96-well plates, 24 hr, 10000 cells/well	Before sample treatment (replaced by medium-sample mixture)	CS, PBA-grafted CS (5-100 mg/mL)	48, 96 hr (with sample)	20 µl MTT for 4 hr, 100 µL isopropanol	Microplate reader (570 nm)	2011: [59]
	Caco-2/HT-29-MTX-E12	96-well plates, $1x10^4$ cells/well	After sample treatment	NPs containing PLGA, negative control (PBS)	3 hr (with sample) 24 hr (before MTT solution)	n/a	n/a	2018: [12]
		n/a	n/a	n/a	3 hr (with sample)	100 µl MTT (0.5 mg/mL in HBSS) for 3 hr, 150 µL DMSO	n/a	2015: [20]
LDH	Caco-2	96-well plates, $1x10^5$ cells/well	n/a	NPs containing polymer (0.01-3 mM), control (medium with cells)	24 hr (with sample)	n/a	Cytotoxicity detection kit	2014: [26]
Alamar Blue	Caco-2	96-well plates, 48 hr, $1x10^4$ cells/well	Before sample treatment (washed with HBSS) After sample treatment (replaced by medium)	Insulin NPs, negative control (HBSS with cells)	3 hr (with sample) 24 hr (before Alamar Blue solution)	n/a	n/a	2018: [1]
MTS	Caco-2/HT-29-MTX	96-well plates, 21 days, 19200 cells/well	After sample treatment (washed trice with calcium- and magnesium-free HBSS)	Insulin NPs containing PLGA (5 mg) and insulin (0.5 mg/mL), negative control (untreated cells)	4 hr (with sample)	20 µL MTS for 1 hr	Microplate reader (490 nm)	2018: [4]
	Caco-2	96-well plates, 24 hr, $1x10^4$ cells/well	n/a	AuNPs, AuNPs/INS (0-10 µg/mL)	24, 48, 72 hr (with sample)	MTS for 4 hr	EMax Precision microplate reader (490 nm)	2014: [27]
Cell counting kit-8	Caco-2	96-well plates, 24 hr, $5x10^3$ cells/well	n/a	10 µL ES-cNPs, ES-Tat-cNPs, positive control (5-fluorouracil), negative control (without treatment)	4 hr (with sample)	20 µL CCK-8 solution for 2 hr	Microplate reader (450 nm)	2017: [14]
Cell Titer-Glo® reagent	Caco-2	96-well plates, 24 hr, $1x10^5$ cells/mL	Before sample treatment (washed twice with HBSS)	100 µL NPs (1, 0.5, 0.25, 0.1 mg/mL), positive control (1% Triton X-100), negative control (HBSS)	6 hr (with sample)	50 µL Cell Titer-Glo® reagent	Varioskan Flash Multimode Reader	2016: [18]

	HT29-MTX	96-well plates, 24 hr, $1x10^5$ cells/mL	Before sample treatment (washed twice with HBSS)	100 µL NPs (1, 0.5, 0.25, 0.1 mg/mL), positive control (1% Triton X-100), negative control (HBSS)	6 hr (with sample)	50 µL Cell Titer-Glo® reagent	Varioskan Flash Multimode Reader	2016: [18]

Supplementary table 4. Experimental conditions for TEER measurement and permeability study

Cell line	Material	Cell culture	Donor chamber	Receiver chamber	Time/ sample amount	ERS/ insulin quantification	Year/ Ref
Caco-2	Costar Transwell 24-well plates (pore size 0.4 µm, polycarbonate membrane)	21 days, 3×10^5 cells/well	100 µL NPs dispersed in DI water (1 mg/mL) and chitosan solution (1 mg/mL) at pH 6, 6.8, 7.4, heparin sodium solution (1-20 mg/mL at pH 7.4)	600 µL fresh medium	2 hr	Millicell ERS-2 Millipore, initial TEER (180-220 $\Omega\cdot cm^2$)	2018: [3]
Caco-2/HT29-MTX-E12 (7:3)	n/a	n/a	Prewarmed HBSS medium for 30 min, 200 µL Dio-labeled NPs in HBSS	Prewarmed HBSS medium for 30 min	8 hr (withdrew 100 µL sample)	Millicell ERS-2 Millipore	2018: [12]
Caco-2 with or without 1% mucin	Costar Transwell (pore size 0.4 µm, 1.12 cm^2, polycarbonate membrane)	17-21 days, 1×10^4 cells/insert	Prewarmed HBSS medium for 30 min, 200 µL insulin NPs (containing 250 µg/mL RITC-insulin) in HBSS	Prewarmed HBSS medium for 30 min	2 hr (withdrew 100 µL sample)	Millicell ERS Millipore, initial TEER 700-800 $\Omega\cdot cm^2$, fluorescence spectrometer (RF-5301 PC)	2018: [11]
Caco-2, Caco-2/HT29-MTX/Raji B (90:10)	Transwell 6-well plates (pore size 3 µm, polycarbonate membrane)	21 days, $1x10^5$ cells/cm^2,	Insulin and insulin lipid-polymeric NPs (100 µg/mL in 1.5 mL) HBSS at pH 6.5	HEPES at pH 7.4	0.25, 0.5, 1, 2, 3, 4 hr, replace with fresh HBSS (pH 7.4)	HPLC (insulin quantification)	2018: [10]
Caco-2	Transwell (pore size 3 µm, 0.33 cm^2)	21 days	Prewarmed HBSS medium for 30 min, 200 µL insulin NPs (containing 200 µg/mL FITC-insulin)	Prewarmed HBSS medium for 30 min	Withdrew 200 µL sample	Millicell ERS Millipore, monitor TEER for 20 hr post-sample treatment	2018: [8]
Caco-2	Transwell (polycarbonate membranes)	21 days	Prewarmed HBSS medium (100 µL), 200 µL DiO NPs	n/a	0, 0.5, 1, 2, 4, 6 hr	Varioskan Flash Multimode Reader (insulin quantification)	2018: [44]
Caco-2	Costar Transwell 12-well plates (pore size 0.4 µm, 12mm, 1.1 cm^2, polycarbonate membrane)	14-21 days. 2.0×10^4 cells/well	Serum-free medium (200 µL), insulin NPs (containing 0.2 mg/mL RITC-insulin)	n/a	n/a	Millicell ERS-2 Millipore, initial TEER (600-800 $\Omega\cdot cm^2$)	2018: [9]
Caco-2, Caco-2/HT29-MTX (75:25)	Transwell (0.336 cm^2)	21 days	Insulin NPs, positive control (EGTA)	n/a	0, 1, 2, 3, 4 hr	Millicell ERS-2 Millipore, initial TEER > 900 $\Omega\cdot cm^2$, microplate reader (Cytation3; insulin quantification)	2018: [4]

Caco-2	Transwell	14-21 days, $5x10^3$ cells/well	0.6 mL DMEM, NPs (containing 50 µg/mL insulin and 100 µg/mL polymer)	0.2 mL DMEM	0, 0.5, 1, 2, 3, 4, 6, 8, 10 hr	Millicell ERS-2 Millipore	2018: [5]
Caco-2	Transwell 12-well plates (pore size 0.4 µm, 12 mm, 1.12 cm^2, polyester membrane)	14 days, $2x10^5$ cells/well	Prewarmed HBSS medium (0.5 mL) for 30 min, 0.05 mg insulin	Prewarmed HBSS medium (1 mL)	0, 0.5, 1, 1.5, 2, 3 hr (withdrew 50 µL sample)	Millicell ERS-2 Millipore, initial TEER > 800 $\Omega \cdot cm^2$	2018: [6]
Caco-2	Transwell	n/a	Insulin SLNs, insulin HA2-W-SLNs, insulin HA2-O SLNs, free insulin (containing 100 µg/mL insulin)	n/a	6 hr	ELISA kit (insulin quantification)	2018: [52]
Caco-2	12-well plate (pore size 0.4 µm, polyethylene terephthalate membrane)	2×10^4 cell/cm^2, passage number 30-45	Transparent MEM with HEPES (pH7.4; 1 mL) for 1 hr, 1 mL insulin NPs (0.4 mg/mL)	Transparent MEM with HEPES (pH7.4; 2 mL) for 1 hr	0, 30, 60, 90, 120, 180, 240 min (withdrew 50 µL sample)	EVOM2, initial TEER > 600-700 $\Omega \cdot cm^2$,	2018: [2]
Caco-2	Transwell (pore size 3 µm, 0.33 cm^2)	21 days	Prewarmed HBSS medium for 30 min, 200 µL insulin NPs (containing 200 µg/mL FITC-insulin)	Prewarmed HBSS medium	Withdrew 200 µL sample	Varioskan Flash multimode reader (insulin quantification)	2018: [8]
Caco-2	Polycarbonate membrane	21 days	Prewarmed HBSS medium for 30 min, 200 µL insulin NPs in SFM buffer with or without HA2 and metformin, control (free insulin 120 µg/mL)	Prewarmed HBSS medium for 30 min	0.5, 1, 2, 4, 6 hr	Initial TEER 500-600 $\Omega \cdot cm^2$, Varioskan Flash Multimode Reader (insulin quantification), transmission electron microscopy (H-600; cell morphology)	2018: [1]
Caco-2	Transwell 12-well plates (pore size 3 µm, polycarbonate membrane)	21-28 days, 1×10^5 cells/cm^2	Prewarmed HBSS medium for 30 min, 0.5 mL insulin NPs	Prewarmed HBSS medium (1.5 mL) for 30 min	0.5, 1, 2, 4 hr (withdrew 100 µL sample)	Initial TEER > 500 $\Omega \cdot cm^2$,	2017: [14]
Caco-2, Caco-2/HT29-MTX	n/a	10 mM NAC treatment	0.1 mL RB-Insulin-LMWP conjugates or RB-insulin (2.5 µM), 0.1 mL RB-insulin MNPs or RB-Insulin-LMWP MNPs (2.5 µM)	n/a	2 hr	Fluorescent assay (insulin quantification)	2016: [16]
Caco-2/HT29-MTX/Raji B	n/a	n/a	HBSS medium with MES (pH 5.5), 0.5 mL insulin or insulin NPs (0.5 mg/mL)	HBSS medium with HEPES (pH 7.4)	15, 30, 60, 120, 180 min (withdrew 100 µL sample)	Human insulin Elisa kit (insulin quantification)	2016: [18]
HT29-MTX-E12	Transwell permeable supports (pore size 0.4 µm, 0.33 cm^2)	21 days, 3×10^4 cells/well	Prewarmed HBSS medium for 30 min, 200 µL T-NPs or P-T-NPs (containing 200 µg/mL FITC-insulin)	Prewarmed HBSS medium for 30 min	Withdrew 200 µL sample)	Varioskan Flash multimode reader (insulin quantification)	2016: [37]

Caco-2	Corning Transwell (pore size 0.4 μm, 2.4 cm^2, polycarbonate membrane)	$1x10^6$ cells/well	Insulin, insulin CPNPs, insulin Chi-CPNPs, insulin VitB12-Chi-CPNPs (1 IU/well)	n/a	n/a	Millicell ERS Millipore, initial TEER 250 Ω·cm^2, ELISA kit (insulin quantification)	2016: [15]
Caco-2, Caco-2/HT29-MTX	n/a	10 mM NAC	0.1 mL RB-insulin-LMWP conjugates or RB-insulin (2.5 μM), 0.1 mL RB-insulin MNPs or RB-insulin-LMWP MNPs (2.5 μM)	n/a	n/a	Millicell ERS Millipore	2016: [16]
HT29-MTX-E12	Transwell 24-well plates (pore size 3 μm, polycarbonate membrane)	18-21 days, $5×10^4$ cells/mL	Prewarmed HBSS medium for 30 min, 200 μL NPs (containing 500 μg/mL PLA) in serum-free medium	Prewarmed HBSS medium for 30 min	10 hr	Millicell ERS-2 Millipore, initial TEER > 500 Ω·cm^2	2016: [17]
HT29-MTX-E12	n/a	10 mM NAC for 60 min	T-NPs, P-T-NPs	n/a	n/a	Millicell ERS Millipore, monitor TEER for 21 hr post-sample treatment	2016: [37]
HT29-MTX-E12	Costar Transwell 24-well plates (pore size 0.4 μm, 6.5 mm, 0.33 cm^2, polycarbonate membrane)	18-19 days, $10x10^4$ cells/mL, NAC treatment	Prewarmed HBSS medium (200 μL) for 30 min, F-insulin (0.25 mg/mL)	Prewarmed HBSS medium for 30 min	Withdrew 200 μL sample	Initial TEER > 500 Ω·cm^2	2015: [38]
Caco-2	n/a	14 days	Prewarmed HBSS medium with 10 mM HEPES for 20 min, 0.1 mL insulin PLGA NPs, insulin TMC-PLGA NPs (containing 500 μg/mL RB-insulin)	Prewarmed HBSS medium for 20 min	22 hr (withdrew 0.2 mL samples)	Millicell ERS Millipore	2015: [22]
Caco-2, HT29-MTX	Costar Transwell (pore size 0.4 μm, 0.33 cm^2, polycarbonate membrane)	21 days	Prewarmed HBSS medium for 30 min, 200 μl NPs (containing 300 μg/mL FITC-insulin) with or without vitamin B12 (5 mg/mL) and/or intrinsic factor (200 IU/mL)	Prewarmed HBSS medium for 30 min	0.5, 1, 2, 3 hr (withdrew 200 μl samples)	Millicell ERS Millipore, initial TEER > 550 Ω·cm^2, fluorospectrophotometer (insulin quantification)	2015: [41]
Caco-2/ HT29-MTX-E12 (7:3)	Transwell 24-well plates (pore size 0.4 μm, 0.33 cm^2, polycarbonate membrane)	NAC treatment, 17 days	Prewarmed HBSS medium, 100 μL insulin NPs (containing 50 μg/mL)	Prewarmed HBSS medium	Withdrew 200 μL sample	Varioskan Flash multimode reader (insulin quantification)	2015: [20]
Caco-2, Caco-2/ HT-29-MTX (1:1)	n/a	n/a	Prewarmed HBSS medium with 0.2 mg/mL BSA, 100 μL FITC-insulin (0.2 mg/mL), 100 μL Eul-cys NPs (2 mg/mL) with GSH and SC (2, 5 mg/mL)	Prewarmed HBSS medium with HEPES (600 μL)	0.5, 1, 2, 3, 4 hr, Withdrew 200 μL sample	Fluorescence microplate reader (insulin quantification)	2014: [28]

Caco-2, Caco-2/ HT-29-MTX (1:1)	Corning Transwell 24-well plates (pore size 0.3 µm, 0.33 cm^2, polycarbonate membrane)	21-23 days, $1x10^5$ cells/ mL	Prewarmed HBSS medium with 30x10^{-3} M HEPES (pH 7.2), 100 µL Eul-cys NPs (5 mg/mL) with SH and SC (0.5-2.5 mg/mL)	n/a	0.5, 1, 1.5, 2, 3, 4 hr (with sample) 6, 8, 10, 24 hr (post-sample treatment)	Millicell ERS-1 Millipore, initial TEER > 300 Ω·cm^2, monitor TEER for 20 hr post-sample treatment	2014: [28]
Caco-2	Costar Transwell 24-well plates (6.5 mm, 0.33 cm^2, polycarbonate membrane)	14-18 days, $1×10^4$ cells/well	Prewarmed HBSS medium for 30 min, 100 µL free insulin and insulin NPs (containing 0.2 mg/mL insulin)	Prewarmed HBSS medium for 30 min	0.5, 1, 1.5, 2, 3 hr (withdrew 0.1 mL samples)	Millicell ERS Millipore, initial TEER > 500 Ω·cm^2, Varioskan Flash (insulin quantification)	2014: [25]
Caco-2	Corning Transwell 24-well (polycarbonate membrane)	21 days, $3.9×10^4$ cells/cm^2	CS/γ-PGA-EGTA NPs (0.02% in 0.5 mL) at pH 6.6, 7, 7.4	pH 7.4 medium	n/a	Millicell ERS Millipore	2013: [60]
HT29-MTX-E12	n/a	10 mM NAC treatment	Insulin NPs (containing 40 µg/mL Alexa 488 insulin) in HBSS medium	n/a	0, 15, 30, 45, 60, 90 min (withdrew 200 µL sample)	Microplate fluorometer (insulin quantification at Ex/Em = 485/530 nm)	2013: [46]
Caco-2	n/a	n/a	CS/γ-PGA–EGTA NPs (0.2 mg/mL), CS/γ-PGA NPs	n/a	n/a	TEM and lanthanum nitrate staining (Ultra-structural changes in AJCs)	2013: [60]
Caco-2	6-well plates (polycarbonate membrane)	21 days, $2x10^5$ cells/well	2 mL free insulin, insulin SLNs or SA-R8-Ins-SLNs (0.25 mg/mL) in HBSS medium with HEPES	n/a	15, 30, 45, 60, 120 min (withdrew 200 µL sample)		2012: [29]
Caco-2, Caco-2/HT-29	Transwell (1 cm^2, polycarbonate membrane)	n/a	Insulin, insulin NPs (100 µg/mL)	4 mL HBSS (pH 7.4)	Withdrew 200 µL sample	HPLC (insulin quantification)	2011: [34]
Caco-2	n/a	n/a	Prewarmed HBSS medium for 30 min, insulin NPs and polymer in HBSS	Prewarmed HBSS medium for 30 min,	0.5, 1, 1.5, 2 hr (with sample) 1, 2 hr (post-sample treatment)	Millicell ERS Millipore, initial TEER 300-500 Ω·cm^2, ELISA kit (insulin quantification)	2011: [32]
Caco2, Caco-2/HT-29, rat intestinal mucosa	n/a	n/a	Insulin NPs, control (medium without cells or tissue)	n/a	every 15 min during 3 hr	Epithelial voltohmmeter	2011: [34]
Caco-2	Corning Transwell (pore size 3 µm, 1 cm^2, polycarbonate membrane)	21 days	n/a	n/a	n/a	Epithelial voltohmmeter	2011: [34]

Caco-2, HT-29, Caco-2/HT-29 (90:10)	Transwell	n/a	Free insulin and insulin NPs (100 µg/ml in 1.5 mL) in HBSS	n/a	n/a	EVOM, HPLC-UV (insulin quantification)	2011: [33]
Caco-2	n/a	n/a	Insulin NPs (0.2 mg/mL, 1 mL) at pH 6.6 and 7	pH 7.4	Withdrew 50 µL sample	Millicell ERS Millipore, ELISA kit (aspart-insulin quantification)	2010: [47]
Caco-2	n/a	n/a	Freeze-dried NPs (0.2 mg/mL,1 mL) at pH 6.6 and 7	pH 7.4	Withdrew 50 µL sample	Millicell ERS Millipore, ELISA kit (insulin quantification)	2010: [61]
Caco-2	Costar Transwell 6-well plates (pore size 0.4 µm, 4.7 cm^2, polycarbonate membrane)	21-24 days, 6.0×10^4 cells/cm^2	n/a	n/a	1 hr	EVOM	2010: [36]
Caco-2	Costar Transwell 6-well plates (24.5 mm, 4.7 cm^2, polycarbonate membrane)	21 days	Insulin NPs (0.2 mg/mL,1 mL) at pH 6.6, 7 and 7.4	pH 7.4	Withdrew 50 µL sample	ELISA kit (insulin quantification)	2009: [48]
HT29-MTX-E12	Filter inserts	21 days	Transport medium for 15 min, 1.5 mL insulin NPs (containing 250 µg/mL insulin)	n/a	Every 20 min during first 2 hr (withdrew 1 mL)	EVOM, initial TEER > 50 Vcm^2, fluorescence spectroscopy (insulin quantification)	2009: [39]
Caco-2	Costar Transwell 6 well-plates (24.5 mm, 4.7 cm^2, polycarbonate membrane)	21 days	Insulin NPs (0.2 mg/mL, 1 mL) at pH 6.6, 7, 7.4	pH 7.4	n/a	Millicell ERS Millipore, initial TEER 600-800 $\Omega\cdot cm^2$,	2008: [49]
Caco-2	Costar Transwell 6 well-plates (24.5 mm, 4.7 cm^2, polycarbonate membrane)	24-30 days	Insulin NPs at pH 6.6 and 7.4	n/a	n/a	Millicell ERS Millipore, initial TEER 600-800 $\Omega\cdot cm^2$,	2007: [50]
Caco-2	Costar Transwell 6 well-plates (24.5 mm, 4.7 cm^2, polycarbonate membrane)	24-30 days	NPs (0.2 mg/mL, 2 mL) at pH 6.6 and 7.4	n/a	n/a	Millicell ERS Millipore, initial TEER 600-800 $\Omega\cdot cm^2$,	2007: [51]

Supplementary table 5. Experimental conditions to examine nanoparticle and protein integrity during intracellular trafficking

Method	System	Objective	Sample	Materials	Year/ Ref
FRET	Varioskan Flash multimode reader (Ex/Em = 440/485-600 nm)	Nanoparticle integrity in mucus	DiO/DiI-NPs	PBS (pH 7.4 or 4.5)	2018: [44]
	Ex/Em = 474/587 nm	HPMA coating dissociation in mucus	Double-fluorescently labeled P-T-NP suspensions (containing 200μg/mL FITC-insulin)	Mucus or PBS (pH 7.4) at 37°C	2016: [37]
	Ex/Em = 474/587 nm	Nanoparticle integrity in mucus	TRTIC-labeled HPMA, FITC-insulin, insulin NPs (containing 0.25 mg/mL FITC-insulin)	Mucus at 37°C	2015: [38]
CLSM	n/a	Nanoparticle integrity in HT29-MTX cells (2×10^4 cells/well in glass-bottom dish)	Insulin NPs (containing Cy5- insulin, RITC-HA), DAPI (nucleus)	Mucus for 2 hr at 37°C	2018: [9]
	CLSM, FV1000	Nanoparticle trafficking in Caco-2 cells ($5x10^4$ cells/mL)	Insulin NPs	Enterocytes for 2 hr, 1 mM LY294002, 100 μM chloroquine, 4% paraformaldehyde, 0.1% Triton X-100, 5% normal goat serum, rabbit anti-Rab5, mouse anti-Rab7, rabbit anti-caveolin-1 antibodies, TRITC-labeled goat antirabbit/mouse IgG, DAPI (nucleus)	2018: [44]
	Leica TCS SP8 STED 3X	Nanoparticle colocalization with lysosomes in Caco-2 cells	Insulin NPs with lysosomes	Enterocytes for 3 hr, Lyso-Tracker prober (50 nM), DAPI (nucleus)	2018: [44]
	Leica TCS SP8 STED 3X	Nanoparticle colocalization with lysosomes in Caco-2 cells	Insulin SLNs with lysosomes	Enterocytes, Lyso-Tracker prober (50 nM), DAPI (nucleus)	2018: [52]
	Leica TCS SP8 STED 3X	Nanoparticle colocalization with endosomes in Caco-2 cells	Insulin SLNs with endosomes	Enterocytes for 1 hr, 4% paraformaldehyde (15 min), 1% Triton X-100 (10 min), 5% normal goat serum (1 hr), primary rabbit anti-Rab5, mouse anti-Rab7 antibodies, 594-labeled goat anti-rabbit (2 hr), anti-mouse IgG (2 hr)	2018: [52]
	Olympus Optical Co	Nanoparticle trafficking in Caco-2 cells	Insulin NPs	Paraformaldehyde, 0.1% Triton X-100 (in PBS), 5% normal goat serum buffer, rabbit anti-Rab5, rabbit anti-Rab7, rabbit anti-	2018: [1]

				Rab11 antibodies, IgG conjugated to TRITC Red, DAPI (nucleus)	
	n/a	Nanoparticle trafficking in Caco-2 cells (6-well plates)	FITC-labeled INS-SeNPs, INS-CsNPs	Enterocytes for 30 min, paraformaldehyde	2017: [62]
	FV1000, Olympus	Nanoparticle integrity in HT29-MTX-E12 cells	Double-fluorescently labeled P-T-NPs (TRITC-pHPMA/FITC-insulin or TRITC-TMC/FITC-insulin), DAPI (nucleus)	Mucus for 1 hr at 37°C	2016: [37]
	FV1000, Olympus	Nanoparticle trafficking in Caco-2 cells (6-well plates)	Insulin NPs (containing 0.25 mg/mL F-insulin)	Mucus for 1 hr at 37°C	2015: [38]
	FV1000, Olympus	Nanoparticle integrity in HT29-MTX-E12 cells	TRITC-labeled penetratin	Mucus for 1 hr at 37°C, Lyso-Tracker prober (50 nM), ER-Tracker probe (500 nM), Mito-Tracker probe (200 nM) and Golgi-Tracker (150 µg/mL)	2015: [38]
	TCS SL	Nanoparticle trafficking in Caco-2 cells	FITC-labeled NPs (0.2 mg/mL) at 6H 6.6 and 7.4	3.7% paraformaldehyde	2007: [51]
ELISA	BCA protein assay	Protein stability in Caco-2 cells	INS-C NPs, INS-EGP NPs in HBSS.	Enterocytes for 30 min	2018: [44]

Supplementary table 6. Experimental conditions for endocytosis and exocytosis mechanisms

Mechanism	Cell culture	Endocytic inhibitor	Samples	Incubation	Year Ref
Receptor-mediated endocytosis	Caco-2	1 mM free EGP	DiO NPs	3 hr	2018: [44]
	BMDMs (1×10^5 cells/well) in 6-well plates for 24 hr	Free HA (100 μg/mL)	2 mL HA-CA NPs or HA-PCL NPs (0.5, 1, or 5 mg/mL)	60 min	2018: [63]
	Caco-2	Methyl-β-cyclodextrin (1 μg/mL)	Insulin NPs (containing 200 μg/mL insulin)	3 hr	2018: [8]
	Caco-2	Methyl-β-cyclodextrin (5 mg/mL)	Insulin NPs	1 hr	2018: [7]
	Caco-2	CRT peptide (50, 100, 200, 400 μg/mL)	Insulin NPs (containing 200 μg/mL insulin)	3 hr	2018: [8]
	Caco-2	LDL (100 μg/mL)	Insulin NPs	3 hr	2018: [1]
	Caco-2	Cholesterol (80 μg/mL)	Insulin NPs	3 hr	2018: [1]
	Caco-2	Heparin (10 μg/mL)	Insulin NPs	3 hr	2018: [1]
	Caco-2 , HT29-MTX-E12	CSK peptide	Insulin NPs	n/a	2018: [20]
	Caco-2/HT29-MTX	Vitamin B12 (5 mg/mL)	Insulin NPs	3 hr	2015: [41]
	Caco-2 in 24-well plates	10 mM Methyl-β-cyclodextrin	FITC-insulin NPs (containing 10 mg PLGA/cm^2) at 4 °C, 37 °C	1 hr	2012: [31]
Heparan sulfate proteoglycans-mediated endocytosis	Caco-2	30 mM sodium chlorate	Insulin NPs	3 hr	2018: [44]
	Caco-2	Heparin (5 μg/mL)	Insulin NPs	3 hr	2018: [44]
Clathrin-mediated endocytosis	Hep G2	Chlorpromazine (10 μg/mL)	FITC-insulin or FITC-insulin NPs (containing 25 μg/mL insulin)	4 hr	2018: [45]
	Caco-2	Chlorpromazine (10 μg/mL)	Insulin NPs (containing 200 μg/mL insulin)	3 hr	2018: [8]
	Caco-2	30 μM chlorpromazine, 0.4 M hypertonic sucrose	Insulin NPs	3 hr	2018: [44]
	Caco-2	30 μM chlorpromazine, 0.4 M hypertonic sucrose	Insulin NPs	3 hr	2018: [1]
	Caco-2	Chlorpromazine (10 μg/mL)	Insulin NPs	1 hr	2018: [7]
	Caco-2	30 μM chlorpromazine	Insulin SLNs	3 hr	2018: [52]
	HT-29 (5000 cells/fluoro Dish with 80% confluence)	1 mL chlorpromazine (7 μg/mL)	Insulin NPs (1 mg/mL) in PBS	1 hr	2017: [40]
	Caco-2/HT29-MTX	Chlorpromazine (10 mg/mL)	Insulin NPs	3 hr	2016: [18]
	Caco-2, HT29-MTX-E12	Chlorpromazine (10 mg/mL)	Insulin NPs	n/a	2015: [20]
	Caco-2	Chlorpromazine (10 μg/mL)	RB-insulin NPs at 4 °C, 37 °C	2 hr	2015: [22]
	Caco-2/HT29-MTX	Chlorpromazine (10 μg/mL)	Insulin NPs	3 hr	2015: [41]

	Caco-2	Chlorpromazine (10 µg/mL)	Insulin NPs at 4 ºC, 16 ºC, 37 ºC	1 hr	2014: [25]
Caveolae-mediated endocytosis/ lipid-raft-mediated endocytosis	Hep G2	200 µg/mL genistein	FITC-insulin or FITC-insulin NPs (containing 25 µg/mL insulin)	4 hr	2018: [45]
	Caco-2	Lovastatin (10 µg/mL)	Insulin NPs (containing 200 µg/mL insulin)	3 hr	2018: [8]
	Caco-2	500 nM filipin, 0.2 mM genistin	Insulin NPs	3 hr	2018: [44]
	Caco-2	500 nM filipin, lovastatin (10 µg/mL)	Insulin NPs	3 hr	2018: [1]
	Caco-2	500 nM filipin	Insulin SLNs	3 hr	2018: [52]
	Caco-2	Methyl-β-cyclodextrin (5 mg/mL)	Insulin NPs	1 hr	2018: [7]
	HT-29 (5000 cells/fluoro Dish with 80% confluence)	1 mL genistein (200 µM)	Insulin NPs (1 mg/mL) in PBS	1 hr	2017: [40]
	Caco-2/HT29-MTX	Filipin (1 mg/mL)	Insulin NPs	3 hr	2016: [18]
	Caco-2 cells, HT29-MTX-E12	Filipin (1 µg/mL)	Insulin NPs	n/a	2015: [20]
	Caco-2	Filipin (5 µg/mL)	Insulin NPs at 4 ºC, 37 ºC	2 hr	2015: [22]
	Caco-2/HT29-MTX	Filipin (1 µg/mL)	Insulin NPs	3 hr	2015: [41]
	Caco-2	Filipin (1 µg/mL)	Insulin NPs at 4 ºC, 16 ºC, 37 ºC	1 hr	2014: [25]
Micropinocytosis and macropinocytosis	Hep G2	500 nM wortmannin	FITC-insulin or FITC-insulin NPs (containing 25 µg/mL insulin)	4 hr	2018: [45]
	Caco-2	Amiloride (12 µg/mL)	Insulin NPs (containing 200 µg/mL insulin)	3 hr	2018: [8]
	Caco-2	Amiloride (12 µg/mL), 10 µM Rottlerin	Insulin NPs	3 hr	2018: [44]
	Caco-2	Amiloride (12 µg/mL), 10 µM Rottlerin	Insulin NPs	3 hr	2018: [1]
	Caco-2	Amiloride (12 µg/mL)	Insulin SLNs	3 hr	2018: [52]
	Caco-2	Amiloride (0.3 mg/mL)	Insulin NPs	1 hr	2018: [7]
	HT-29 (5000 cells/fluoro Dish with 80% confluence)	500 nM wortmannin (1 mL)	Insulin NPs (1 mg/mL) in PBS	1 hr	2017: [40]
	Caco-2, HT29-MTX-E12	Amiloride (0.3 mg/mL)	Insulin NPs	n/a	2015: [20]
	Caco-2	Amiloride (0.3 mg/mL)	Insulin NPs at 4 ºC, 16 ºC, 37 ºC	1 hr	2014: [25]
	Caco-2 in 24-well plates	10 mM 5-(N,N-dimethyl)-amiloride hydrochloride	Insulin NPs (containing 10 mg PLGA/cm^2) at 4 ºC, 37 ºC	1 hr	2012: [31]
Comprehensive active transport	Caco-2	Sodium azide (1 mg/mL)	Insulin NPs	1 hr	2018: [7]
	Caco-2	100 mM sodium azide	Insulin NPs (containing 200 µg/mL insulin)	3 hr	2018: [8]
	Caco-2	5 mM sodium azide	Insulin SLNs	3 hr	2018: [52]
	Hep G2	100 mM sodium azide	FITC-insulin or FITC-insulin NPs (25 µg/mL)	4 hr	2018: [45]
	Caco-2/HT29-MTX	100 mM sodium azide	Insulin NPs	3 hr	2016: [18]
	Caco-2	100 mM sodium azide	RB-insulin NPs at 4 ºC, 37 ºC	2 hr	2015: [22]

	Caco-2	Sodium azide (1 mg/mL)	Insulin NPs at 4 ºC, 16 ºC, 37 ºC	1 hr	2014: [25]
	Caco-2 in 24-well plates	0.02% sodium azide, 50 mM 2-deoxyglucose	Insulin NPs (containing 10 mg PLGA/cm^2) at 4 ºC, 37 ºC	1 hr	2012: [31]
	Caco-2	10 mM sodium azide	100 mM sodium azide	0.5, 1, 2 hr	2011: [32]
Bile acid transporters	Caco-2	100 µM free CA molecules	Insulin NPs	n/a	2018: [5]
P-gp efflux pumps	Caco-2	Verapamil	Free Rh-123 (13.5 µg/mL)	2 hr	2018: [7]
Desulfurization	Caco-2	35 mM sodium chlorate	Insulin NPs	3 hr	2016: [18]
	Caco-2/HT29-MTX	35 mM sodium chlorate	Insulin NPs		2015: [41]
Interaction with cholesterol (lipid rafts)	HT-29 (5000 cells/fluoro Dish with 80% confluence)	Nystatin (25 µg/mL; 1 mL)	Insulin NPs (1 mg/mL) in PBS	1 hr	2017: [40]
	Caco-2, HT29-MTX-E12	Nystatin (25 µg/mL)	Insulin NPs	n/a	2015: [20]
	Caco-2 in 24-well plates	Nystatin (25 µg/mL)	FITC-insulin NPs (containing 10 mg PLGA/cm^2) at 4 ºC, 37 ºC	1 hr	2012: [31]
Lysosome-releasing activity	Caco-2	100 µM chloroquine	Insulin NPs	3 hr	2018: [1]
	Caco-2	100 µM hemagglutinin-2	Insulin NPs	3 hr	2018: [1]
Constitutive exocytosis of lipoproteins	Caco-2	1 mM metformin, 0.5 mM AICAR	Insulin NPs	3 hr (samples), 1 hr (exocytosis)	2018: [1]
Endocytosis inhibitors	Caco-2	Cytochalasin-D (10 µg/mL)	RB-insulin NPs at 4 ºC, 37 ºC	2 hr	2015: [22]
	Caco-2	Cytochalasin-D (10 µg/mL), nocodazole (1 mg/mL)	Polymer, free insulin, insulin NPs	0.5, 1, 2 hr	2011: [32]
Protein kinase C regulation	Caco-2 in 24-well plates	10 µM phorbol 12-myristate 13-acetate	Insulin NPs (containing 10 mg PLGA/cm^2) at 4 ºC, 37 ºC	1 hr	2012: [31]
Adsorptive endocytosis	Caco-2/HT29-MTX	1 mM protamine sulfate	Insulin NPs	3 hr	2016: [18]
	Caco-2	1 mM protamine sulfate	RB-insulin NPs at 4 ºC, 37 ºC	2 hr	2015: [22]
PEPT1 transporter	Caco-2	Glycylsarcosine	Insulin NPs	2 hr	2016: [17]
Intestinal alkaline phosphatase	Caco-2	Cocktail II	P-R8-Pho NPs	3 hr	2018: [12]

Reference list

1. Cui Y, Shan W, Zhou R, et al. The combination of endolysosomal escape and basolateral stimulation to overcome the difficulties of "easy uptake hard transcytosis" of ligand-modified nanoparticles in oral drug delivery. Nanoscale. 2018;10(3):1494-1507.
2. Shamsa ES, Mahjub R, Mansoorpour M, et al. Nanoparticles prepared from n,n-dimethyl-n-octyl chitosan as the novel approach for oral delivery of insulin: Preparation, statistical optimization and in-vitro characterization. Iran J Pharm Res. 2018;17(2):442-459.
3. Liu L, Zhang Y, Yu S, et al. Dual stimuli-responsive nanoparticle-incorporated hydrogels as an oral insulin carrier for intestine-targeted delivery and enhanced paracellular permeation. ACS Biomater Sci Eng. 2018;4:2889-2902.
4. Czuba E, Diop M, Mura C, et al. Oral insulin delivery, the challenge to increase insulin bioavailability: Influence of surface charge in nanoparticle system. Int J Pharm. 2018 6;542(1-2):47-55.
5. Zhang Z, Li H, Xu G, et al. Liver-targeted delivery of insulin-loaded nanoparticles via enterohepatic circulation of bile acids. Drug Deliv. 2018;25(1):1224-1233.
6. Zeng Z, Dong C, Zhao P, et al. Scalable production of therapeutic protein nanoparticles using flash nanoprecipitation. Adv Healthc Mater. 2018:e1801010.
7. Yang L, Li M, Sun Y, et al. A cell-penetrating peptide conjugated carboxymethyl-β-cyclodextrin to improve intestinal absorption of insulin. Int J Biol Macromol. 2018;111:685-695.
8. Liu M, Wu L, Shan W, et al. Iron-mimic peptide converts transferrin from foe to friend for orally targeting insulin delivery. J Mater Chem B. 2018;6(4):593-601.
9. Tan X, Liu X, Zhang Y, et al. Silica nanoparticles on the oral delivery of insulin. Expert Opin Drug Deliv. 2018;15(8):805-820.
10. Sgorla D, Lechanteur A, Almeida A, et al. Development and characterization of lipid-polymeric nanoparticles for oral insulin delivery. Expert Opin Drug Deliv. 2018;15(3):213-222.
11. Tian H, He Z, Sun C, et al. Uniform core-shell nanoparticles with thiolated hyaluronic acid coating to enhance oral delivery of insulin. Adv Healthc Mater. 2018:e1800285.
12. Wu J, Zheng Y, Liu M, et al. Biomimetic viruslike and charge reversible nanoparticles to sequentially overcome mucus and epithelial barriers for oral insulin delivery. ACS Appl Mater Interfaces. 2018;10(12):9916-9928.
13. Zhang L, Qin H, Li J, et al. Preparation and characterization of layer-by-layer hypoglycemic nanoparticles with ph-sensitivity for oral insulin delivery. J Mater Chem B. 2018;6(45):7451-7461.
14. Chen S, Guo F, Deng T, et al. Eudragit s100-coated chitosan nanoparticles co-loading tat for enhanced oral colon absorption of insulin. AAPS PharmSciTech. 2017;18(4):1277-1287.
15. Verma A, Sharma S, Gupta PK, et al. Vitamin b12 functionalized layer by layer calcium phosphate nanoparticles: A mucoadhesive and ph responsive carrier for improved oral delivery of insulin. Acta Biomater. 2016;31:288-300.
16. Sheng J, He H, Han L, et al. Enhancing insulin oral absorption by using mucoadhesive nanoparticles loaded with lmwp-linked insulin conjugates. J Control Release. 2016 10;233:181-190.
17. Shan W, Zhu X, Tao W, et al. Enhanced oral delivery of protein drugs using zwitterion-functionalized nanoparticles to overcome both the diffusion and absorption barriers. ACS Appl Mater Interfaces. 2016;8(38):25444-25453.
18. Lopes M, Shrestha N, Correia A, et al. Dual chitosan/albumin-coated alginate/dextran sulfate nanoparticles for enhanced oral delivery of insulin. J Control Release. 2016;232:29-41.
19. Boushra M, Tous S, Fetih G, et al. Development and evaluation of viscosity-enhanced nanocarrier (ven) for oral insulin delivery. Int J Pharm. 2016;511(1):462-472.

20. Zhang P, Xu Y, Zhu X, et al. Goblet cell targeting nanoparticle containing drug-loaded micelle cores for oral delivery of insulin. Int J Pharm. 2015;496(2):993-1005.
21. Yu F, Li Y, Liu CS, et al. Enteric-coated capsules filled with mono-disperse micro-particles containing plga-lipid-peg nanoparticles for oral delivery of insulin. Int J Pharm. 2015 30;484(1-2):181-91.
22. Sheng J, Han L, Qin J, et al. N-trimethyl chitosan chloride-coated plga nanoparticles overcoming multiple barriers to oral insulin absorption. ACS Appl Mater Interfaces. 2015 22;7(28):15430-41.
23. Boushra M, Tous S, Fetih G, et al. Methocel-lipid hybrid nanocarrier for efficient oral insulin delivery. J Pharm Sci. 2016;105(5):1733-1740.
24. Sharma R, Gupta U, Garg NK, et al. Surface engineered and ligand anchored nanobioconjugate: An effective therapeutic approach for oral insulin delivery in experimental diabetic rats. Colloids Surf B Biointerfaces. 2015;127:172-181.
25. Zhu X, Shan W, Zhang P, et al. Penetratin derivative-based nanocomplexes for enhanced intestinal insulin delivery. Mol Pharma. 2014;11(1):317-328.
26. Mahjub R, Radmehr M, Dorkoosh FA, et al. Lyophilized insulin nanoparticles prepared from quaternized n-aryl derivatives of chitosan as a new strategy for oral delivery of insulin: In vitro, ex vivo and in vivo characterizations. Drug Dev Ind Pharm. 2014;40(12):1645-1659.
27. Cho HJ, Oh J, Choo MK, et al. Chondroitin sulfate-capped gold nanoparticles for the oral delivery of insulin. Int J Biol Macromol. 2014;63:15-20.
28. Zhang Y, Du X, Zhang Y, et al. Thiolated eudragit-based nanoparticles for oral insulin delivery: Preparation, characterization, and evaluation using intestinal epithelial cells in vitro. Macromol Biosci. 2014;14(6):842-52.
29. Zhang ZH, Zhang YL, Zhou JP, et al. Solid lipid nanoparticles modified with stearic acid-octaarginine for oral administration of insulin. Int J Nanomedicine. 2012;7:3333-9.
30. Zhang X, Sun M, Zheng A, et al. Preparation and characterization of insulin-loaded bioadhesive plga nanoparticles for oral administration. Eur J Pharm Sci. 2012;45(5):632-638.
31. Reix N, Parat A, Seyfritz E, et al. In vitro uptake evaluation in caco-2 cells and in vivo results in diabetic rats of insulin-loaded plga nanoparticles. Int J Pharm. 2012;437(1-2):213-20.
32. Thompson C, Cheng WP, Gadad P, et al. Uptake and transport of novel amphiphilic polyelectrolyte-insulin nanocomplexes by caco-2 cells--towards oral insulin. Pharm Res. 2011;28(4):886-896.
33. Fonte P, Nogueira T, Gehm C, et al. Chitosan-coated solid lipid nanoparticles enhance the oral absorption of insulin. Drug Deliv Transl Res. 2011;1(4):299-308.
34. Woitiski CB, Sarmento B, Carvalho RA, et al. Facilitated nanoscale delivery of insulin across intestinal membrane models. Int J Pharm. 2011;412(1-2):123-31.
35. Thompson CJ, Tetley L, Cheng WP. The influence of polymer architecture on the protective effect of novel comb shaped amphiphilic poly(allylamine) against in vitro enzymatic degradation of insulin--towards oral insulin delivery. Int J Pharm. 2010;383(1-2):216-227.
36. Carr DA, Peppas NA. Assessment of poly (methacrylic acid-co-n-vinyl pyrrolidone) as a carrier for the oral delivery of therapeutic proteins using caco-2 and ht29-mtx cell lines. J Biomed Mater Res A. 2010;92(2):504-512.
37. Liu M, Zhang J, Zhu X, et al. Efficient mucus permeation and tight junction opening by dissociable "mucus-inert" agent coated trimethyl chitosan nanoparticles for oral insulin delivery. J Control Release. 2016;222:67-77.
38. Shan W, Zhu X, Liu M, et al. Overcoming the diffusion barrier of mucus and absorption barrier of epithelium by self-assembled nanoparticles for oral delivery of insulin. ACS Nano. 2015;9(3):2345-56.
39. Jintapattanakit A, Junyaprasert VB, Kissel T. The role of mucoadhesion of trimethyl chitosan and pegylated trimethyl chitosan nanocomplexes in insulin uptake. J Pharm Sci. 2009;98(12):4818-30.

40. Alfatama M, Lim LY, Wong TW. Alginate-c18 conjugate nanoparticles loaded in tripolyphosphate-cross-linked chitosan-oleic acid conjugate-coated calcium alginate beads as oral insulin carrier. Mol Pharm. 2018;15(8):3369-3382.
41. Ke Z, Guo H, Zhu X, et al. Efficient peroral delivery of insulin via vitamin b12 modified trimethyl chitosan nanoparticles. J Pharm Pharm Sci. 2015;18(2):155-70.
42. Diop M, Auberval N, Viciglio A, et al. Design, characterisation, and bioefficiency of insulin-chitosan nanoparticles after stabilisation by freeze-drying or cross-linking. Int J Pharm. 2015;491(1-2):402-8.
43. Song M, Wang H, Chen K, et al. Oral insulin delivery by carboxymethyl-β-cyclodextrin-grafted chitosan nanoparticles for improving diabetic treatment. Artif Cells Nanomed Biotechnol. 2018;46: S774-S782.
44. Zheng Y, Wu J, Shan W, et al. Multifunctional nanoparticles enable efficient oral delivery of biomacromolecules via improving payload stability and regulating the transcytosis pathway. Acs Appl Mater Inter. 2018;10(40):34039-34049.
45. Li H, Zhang Z, Bao X, et al. Fatty acid and quaternary ammonium modified chitosan nanoparticles for insulin delivery. Colloids Surf B Biointerfaces. 2018;170:136-143.
46. Li X, Guo S, Zhu C, et al. Intestinal mucosa permeability following oral insulin delivery using core shell corona nanolipoparticles. Biomaterials. 2013;34(37):9678-9687.
47. Sonaje K, Lin KJ, Wey SP, et al. Biodistribution, pharmacodynamics and pharmacokinetics of insulin analogues in a rat model: Oral delivery using ph-responsive nanoparticles vs. Subcutaneous injection. Biomaterials. 2010;31(26):6849-6858.
48. Sonaje K, Lin YH, Juang JH, et al. In vivo evaluation of safety and efficacy of self-assembled nanoparticles for oral insulin delivery. Biomaterials. 2009;30(12):2329-39.
49. Mi FL, Wu YY, Lin YH, et al. Oral delivery of peptide drugs using nanoparticles self-assembled by poly(gamma-glutamic acid) and a chitosan derivative functionalized by trimethylation. Bioconjug Chem. 2008;19(6):1248-1255.
50. Lin YH, Mi FL, Chen CT, et al. Preparation and characterization of nanoparticles shelled with chitosan for oral insulin delivery. Biomacromolecules. 2007;8(1):146-152.
51. Lin YH, Chen CT, Liang HF, et al. Novel nanoparticles for oral insulin delivery via the paracellular pathway. Nanotechnology. 2007;18(10).
52. Xu Y, Zheng Y, Wu L, et al. Novel solid lipid nanoparticle with endosomal escape function for oral delivery of insulin. ACS Appl Mater Interfaces. 2018;135:46365.
53. Kalantarian G, Ziamajidi N, Mahjub R, et al. Effect of insulin-coated trimethyl chitosan nanoparticles on igf-1, igf-2, and apoptosis in the hippocampus of diabetic male rats. Restor Neurol Neurosci. 2018;36(4):571-581.
54. Ji N, Hong Y, Gu Z, et al. Fabrication and characterization of complex nanoparticles based on carboxymethyl short chain amylose and chitosan by ionic gelation. Food Funct. 2018;9: 2902-2912.
55. Bai X, Kong M, Xia G, et al. Systematic investigation of fabrication conditions of nanocarrier based on carboxymethyl chitosan for sustained release of insulin. Int J Biol Macromol. 2017;102:468-474.
56. Liu X, Liu C, Zhang W, et al. Oligoarginine-modified biodegradable nanoparticles improve the intestinal absorption of insulin. Int J Pharm. 2013;448(1):159-167.
57. Thompson CJ, Tetley L, Uchegbu IF, et al. The complexation between novel comb shaped amphiphilic polyallylamine and insulin: Towards oral insulin delivery. Int J Pharm. 2009;376(1-2):46-55.
58. Wang Y, Huang F, Sun Y, et al. Development of shell cross-linked nanoparticles based on boronic acid-related reactions for self-regulated insulin delivery. J Biomater Sci Polym Ed. 2017;28(1):93-106.
59. Wu Z, Zhang S, Zhang X, et al. Phenylboronic acid grafted chitosan as a glucose-sensitive vehicle for controlled insulin release. J Pharmaceutical Sci. 2011;100(6):2278-2286.

60. Chuang EY, Lin KJ, Su FY, et al. Calcium depletion-mediated protease inhibition and apical-junctional-complex disassembly via an egta-conjugated carrier for oral insulin delivery. J Control Release. 2013;169(3):296-305.
61. Sonaje K, Chen YJ, Chen HL, et al. Enteric-coated capsules filled with freeze-dried chitosan/poly(gamma-glutamic acid) nanoparticles for oral insulin delivery. Biomaterials. 2010;31(12):3384-94.
62. Deng W, Xie Q, Wang H, et al. Selenium nanoparticles as versatile carriers for oral delivery of insulin: Insight into the synergic antidiabetic effect and mechanism. Nanomedicine. 2017;13(6):1965-1974.
63. Rho JG, Han HS, Han JH, et al. Self-assembled hyaluronic acid nanoparticles: Implications as a nanomedicine for treatment of type 2 diabetes. J Control Release. 2018;279:89-98.

Appendix B5.2: Publisher agreement and permission for chapter 6

Wong CY et al 2020. "Cellular assays and applied technologies for characterization of orally administered protein nanoparticles: A systematic review." Journal of Drug Targeting 28 (6): 585-599.

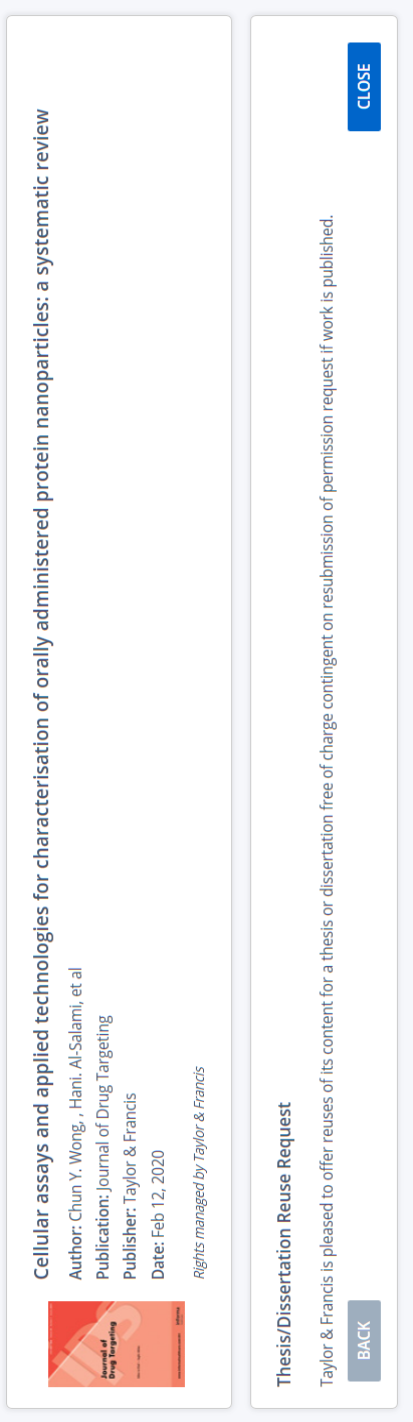

Appendix B6.1: Supplementary data for chapter 7 - Current status and applications of animal models in pre-clinical development of orally administered insulin-loaded nanoparticles.

Wong CY et al 2020. "Current status and applications of animal models in pre-clinical development of orally administered insulin-loaded nanoparticles." Journal of Drug Targeting 1-22.

The following supplementary data is available from https://doi.org/10.1080/1061186X.2020.1726356 and https://www.tandfonline.com/doi/abs/10.1080/1061186X.2020.1726356

Supplementary table 1. Experimental conditions for ex vivo intestinal absorption and mucoadhesive studies for insulin-loaded nanoparticles between 1999 and 2017

Supplementary table 2. Experimental conditions for examination of *in vivo* biocompatibility of insulin-loaded nanoparticles between 2009 and 2017

Supplementary table 3. Experimental conditions for *in vivo* pharmacological and pharmacokinetic studies of orally administered insulin-loaded nanoparticle between 2009 and 2017

Supplementary table 1. Experimental conditions for *ex vivo* intestinal absorption and mucoadhesive studies for insulin-loaded nanoparticles between 1999 and 2017

Animal model	Protocol name	Intestine segments	Treatment	Quantification	Year/ Ref
Diabetes rats	Permeation of NPs	5 cm jejunum in Kreb's-Ringer buffer	1 mL CMCS/CS NPs (Cy3-insulin) for 2 hr	Fluorescence microplate reader to obtain apparent permeability of protein. Intestinal loops were fixed with paraformaldehyde, and observed by CLSM	2017: [1]
Diabetes rats	Ultrastructural changes in tight junctions	Colon	1 mL CMCS/CS NPs (Cy3-insulin) for 4 hr before the rats were sacrificed	Intestinal loops were fixed with 4% paraformaldehyde	2017: [1]
Diabetes rats	Western blot analysis	Homogenized jejunum (100 mg)	1 mL CMCS/CS NPs (Cy3-insulin) for 2 and 4 hr	Bicinchoninic acid method	2017: [1]
Male Sprague-Dawley rats (200-250 g, fasted for 12 hr, sacrificed by cervical dislocation)	Mucus Penetration	1 cm duodenum	0.2 mg FITC-NPs in 20 µL water for 30 min	CLSM	2017: [2]
Goto-Kakizaki rats (sacrificed by cervical dislocation)	*Ex vivo* imaging of transepithelial transport	0.5 cm duodenum, jejunum and ileum	25 IU/kg SeNPs (FITC-chitosan) for 2 hr	Intestinal loops were fixed with 4% paraformaldehyde, cell nucleus labeled with DAPI and observed by CLSM	2017: [3]
Male Wistar rats	*In vivo* intestinal uptake	5-10 mm duodenum, jejunum and ileum	10 µg rhodamine B-VitB12-Chi-CPNPs for 4 hr before the rats were sacrificed	Intestinal loops were fixed with 20% formalin for 24 hr, observed by CLSM	2016: [4]
Male Sprague-Dawley rats (180-220 g, fasted overnight, free access to water, anesthetized)	*In situ* absorption study	3 cm jejunum	200 µL Dil-loaded NPs for 2 hr	Intestinal loops were fixed with 4% paraformaldehyde for 4 hr, dehydrated in 30% sucrose at 4 °C, cell nucleus labeled with DAPI and observed by CLSM. Fluorescence microplate reader to quantify amount of protein.	2016: [5]
Porcine intestine	Intestinal residence time test	3 cm porcine intestine in 250 mL of simulated intestinal fluid	250 mL ChS-PEG/CS NPs (0.8 mg/mL) for 12 hr	n/a	2016: [6]
Sprague-Dawley rats (180-220 g, 6 weeks, fasted for 24 hr, free access to water, raised at 23 °C and 55% humidity, anesthetized by intraperitoneal injection of 50 mg/kg pentobarbital sodium and	Intestinal absorption study	11 cm ileum	1 mL NPs (50 IU/kg) for 4 hr	Withdrew 0.25 mL from jugular vein to determine insulin concentration	2016: [7]

12.5 mg/kg was given every 1 hr to maintain the anaesthesia)					
Sprague-Dawley rats (sacrificed by cervical dislocation)	*Ex vivo* permeability studies with Ussing chamber	Ileum	NPs (50 mg/mL insulin) in Kreb's Ringer solution	Fluorescence microplate reader to obtain protein concentration, apparent permeability coefficient and absorption enhancement ratio	2015: [8]
Sprague-Dawley rats (fasted overnight)	Quantitative and qualitative intestinal analysis of proteins	Intestine	FITC-PPC and FITC-PLGA Ns for 3 hr before the rats were sacrificed	Fluorescence microscope	2015: [9]
Female Sprague-Dawley rats (100-120 g, anesthetized by phenobarbital)	*Ex vivo* permeability study of NPs	5 cm small intestine in Krebs–Ringer bicarbonate solution (95% O_2, 5% CO_2)	10 mL PPC NPs	UV-visible spectrophotometer	2015: [9]
Male Kunming mice (18-22 g, fasted overnight, free access to water, sacrificed by cervical dislocation)	*In vivo* intestinal mucoadhesion study	Small intestine and colon	^{125}I-Ins TMC-PLGA NPs	γ-radioactive counter	2015: [10]
Small intestine from local slaughterhouse	Barr and Riegelman method	5 cm small intestine in Krebs–Ringer solution	10 mL NPs	RP-HPLC	2015: [11]
Male Sprague-Dawley rats (180-220 g, fasted overnight, free access to water, anesthetized by intraperitoneal injection of 40 mg/kg pentobarbital sodium)	Absorption studies in the ligated intestinal loops	4 cm ileum	0.2 mL VB12-T NPs (300 μg/mL FITC-insulin) for 3 hr before the rats were sacrificed by cervical dislocation	Fluorospectrophotometer to quantify protein in PBS, mucus and intestine	2015: [12]
Male Sprague-Dawley rats (180-220 g, fasted overnight, free access to water, anesthetized by intraperitoneal injection of 40 mg/kg pentobarbital sodium)	*In situ* absorption study	10 cm ileum	NPs (1 mg/kg FITC-insulin) for 1 hr before the rats were sacrificed by cervical dislocation	Intestinal loops were fixed with 4% paraformaldehyde for 2 hr, dehydrated in 30% sucrose at 4 °C, cell nucleus and mucus labeled with DAPI and Rho-UEA-I, and observed by fluorescence microscope	2014: [13]
Male Wistar rats (anesthetized by pentobarbital sodium)	*Ex vivo* studies on excised rat jejunum by using Frantz diffusion cells	Jejunum	NPs in Hanks Balanced Salt Solution for 3 hr	HPLC	2014: [14]
Male Sprague-Dawley rats (180-220 g, fasted for 12 hr, anesthetized by intraperitoneal injection of 100 mg/kg pentobarbital sodium, restrained in a supine position)	*In situ* absorption experiment	10 cm ileum	1 mL CSO-DA insulin NPs (25 and 50 IU/kg)	Glucometer to measure blood glucose levels	2014: [15]
Rats	Estimation of *in situ* mucoadhesivity	10 cm small intestine	Twenty alginate/chitosan beads	n/a	2013: [16]

Rats (fasted for 24 hrs, anesthetized by intraperitoneal injection of 50 mg/kg pentobarbital sodium, restrained in a supine position)	*In situ* absorption experiment	15 cm ileum	1 mL l-R8-INS-NP or d-R8-INS-NP (10 IU/kg insulin)	n/a		2013: [17]
Male Sprague-Dawley rats (6-8 weeks old)	*Ex vivo* permeation studies	5 cm ileum in 10 mL Krebs–Ringer solution	0.5 mL Alexa 488 insulin CSC and NC NPs	Fluorescence spectroscopy		2013: [18]
Male Sprague-Dawley rats (6-8 weeks old, fasted overnight, free access to water, anesthetized by 0.04 mg/kg pentobarbital sodium)	*In vivo* absorption assay	5 cm ileum with or without 10% N-acetyl cysteine treatment	0.5 mL CSC and NC NPs (100 mg/mL of Alexa 488 insulin) for 0.5 or 2 hr before the rats were sacrificed	Intestinal loops were fixed with 4% paraformaldehyde for 2 hr, dehydrated in 30% sucrose at 4 °C, cell nucleus labeled with DAPI, and observed by CLSM		2013: [18]
Rat	*Ex vivo* drug release characteristics	Colon	NPs (0.75 mg insulin) in 50 mL sodium phosphate buffer	n/a		2013: [19]
Wistar rats (250 g, fasted overnight, anesthetized by intraperitoneal injection of 50 mg/kg Zoletil)	*In situ* absorption experiment	5 cm duodenum	0.5 mL NPs (2 mg/mL Cy3-insulin-Cy5) with or without γPGA-EGTA(40 mg)	IVIS		2013: [20]
Wistar rats (250 g, fasted overnight, anesthetized by intraperitoneal injection of 50 mg/kg Zoletil)	Ultra-structural examination of the permeability of epithelial tight junctions	Duodenum, jejunum and ileum	0.5 mL EGTA-conjugated NPs (2 mg/mL) for 3 hr before the rats were sacrificed	Intestinal loops were fixed with paraformaldehyde, incubated with 2% lanthanum for 2 hr, and observed by TEM		2013: [20]
Wistar rats (250 g, fasted overnight, anesthetized by intraperitoneal injection of 50 mg/kg Zoletil)	Structural reorganization of tight junctions and intestinal absorption of insulin	Duodenum, jejunum and ileum	EGTA-conjugated NPs for 2 hr before the rats were sacrificed	Intestinal loops were fixed with paraformaldehyde, treated with rabbit anti ZO-1 and Alexa-Fluor-conjugated secondary antibodies, cell nucleus labeled with propidium iodide, and observed by CLSM		2013: [20]
Male rat	*Ex vivo* intestinal transport study	5 cm ileum in Krebs-Ringer bicarbonate solution	NPs (2 mg insulin)	RP-HPLC		2012: [21]
Wistar rats (220-280 g)	Mucoadhesive study	5 cm intestine	10 mg Eul-cys NPs	Fluorescence microscope to quantify mucoadhesion		2012: [22]
Wistar rats (220-280 g, anesthetized with 500 mg/kg chloral hydrate)	*In situ* absorption experiment	jejunum and ileum	1 mL Eul-cys and Eul NPs (5 mg/mL) for 2 hr before the rats were sacrificed	Fluorescence microscope		2012: [22]
54 male Sprague-Dawley rats (237-263 g, fasted overnight, free access to water)	Bioadhesive studies	20 cm duodenum, jejunum, and ileum	2 mL NPs (0.5 mg insulin) for 7 hr before the rats were sacrificed by cervical dislocation	HPLC		2012: [23]

Wistar rats (250 g, fasted overnight, anesthetized by 50 mg/kg Zoletil)	*In situ* mucoadhesion and absorption enhancement study	5 cm duodenum, jejunum and ileum	0.5 mL Cy5-CS NPs (2 mg/mL Cy3-insulin) for 2 hr before the rats were sacrificed	Intestinal loops were fixed with paraformaldehyde, cell nucleus labeled with SYTOX blue, and observed by CLSM	2012: [24]
Male Wistar rats (12-13 weeks, fasted for 24 hr)	*In vivo* mucoadhesion studies	Duodenum, upper jejunum, lower jejunum, upper ileum, and lower ileum	NPs for 1 or 3 hr before the rats were sacrificed	Observed by fluorophotometry and CLSM	2011: [25]
Wistar diabetic rats (fasted overnight)	Prediction of absorption mechanism of insulin by confocal microscopy	Intestine	Chitosan-coated SLN NPs (FITC-insulin) for 3 hr before the rats were sacrificed	Intestinal epithelial cell membranes labeled with Alexa Fluor 594 solution for 1 hr, and observed by CLSM	2011: [26]
Wistar rats	Internalization of nanoencapsulated insulin in small intestinal cells	3-5cm duodenum, jejunum and ileum	FITC-insulin/RBITC-alginate NPs (5 IU/mL insulin)	Intestinal loops were fixed with 0% neutral buffered formalin solution for 24 hr, dehydrated in 30% sucrose for 12 hr, and observed by CLSM	2011: [27]
Male sheep (anesthetized by phenobarbital)	*Ex vivo* absorption studies	7 cm intestine in phosphate buffer solution	Chitosan/arabic gum NPs	HPLC	2011: [28]
Wistar rats	Permeation of insulin through rat intestinal mucosa	2-3cm jejunum	1 mL multilayered NPs (100 µg insulin) for 3 hr	HPLC to determine apparent permeability coefficient and enhancement ratios	2011: [27]
Wistar rats	Internalization of nanoencapsulated insulin in small intestinal cells	3-5cm duodenum, jejunum and ileum in Dulbecco's modified Eagle's medium	FITC-insulin/RBITC-alginate NPs (5 IU/mL insulin) for 2 hr	Dehydrated in 30% sucrose for 12 hr, and observed by CLSM	2010: [29]
Male Wistar rats (250 g, fasted overnight)	Mucoadhesion of NPs and permeation of their constituted components in the intestinal tract	Intestine	1 mL NPs (1 mg/mL) for 4 hr before the rats were sacrificed	Observed by CLSM	2009: [30]
Male rat (anesthetized by 50 mg/kg ketamine and 10 mg/kg chlorpromazine)	*Ex vivo* absorption study	5 cm ascending colon in Krebs-Ringer bicarbonate solution	INS-CS, INS-TEC or INS-DMEC NPs (10 mg insulin)	HPLC	2008: [31]
Wistar diabetic rats (fasted overnight)	Tracking FITC-labelled nanoparticles	Intestine	NPs (FITC-insulin 2 mg/mL) for 3 hr before the rats were sacrificed	Intestinal epithelial cell membranes labeled with Alexa Fluor 594 solution for 1 hr, and observed by CLSM	2007: [32]
Wistar diabetic rats (fasted overnight)	Tracking FITC-labeled nanoparticles	Intestine	150 mg NPs (FITC-insulin 2 mg/mL) in 1.0 mL of pH 4.5 phosphate buffer for 3 hr	Intestinal epithelial cell membranes labeled with Alexa Fluor 594 solution for 1 hr, and observed by CLSM	2007: [33]

			before the rats were sacrificed		
Male Wistar rats (212-238 g, fasted overnight, free access to water)	Gastrointestinal distribution, adhesion, and in vivo release	Small intestine, caecum and colon	2 mL NPs (0.5 mg FITC-insulin) for 6 hr before the rats were sacrificed by cervical dislocation	n/a	2007: [34]
Non-diabetic rats (fasted overnight, anesthetized by 100 mg/kg ketamine)	*In situ* absorption experiment	30 cm ileum	1 mL FITC-insulin NPs (50 IU/kg)	Fluorescence microscope and spectrofluorimetry	2007: [35]
Male Wistar rat (200-250 g)	Mucoadhesion study	Small intestine	PMCP NPs for 3 hr	n/a	2006: [36]
Wistar rats (fasted overnight, anesthetized by intraperitoneal injection of 80 mg/kg pentobarbitone sodium)	Association of NPs in the intestinal epithelium	1-2 cm ileum	2.5 mL NPs for 3 hr before the rats were sacrificed	Observed by CLSM	2005: [37]
Male Wistar adult rats (350 g, fasted overnight)	Gastrointestinal distribution of NPs	2 cm duodenum, jejunum and ileum	2 mL NPs (10 UI insulin/mL) for 4 hr before the rats were sacrificed	Spectrofluorometer	2000: [38]
Male Wistar rats (200-230 g, fasted for 24 hr, raised at 25 °C, anesthetized by intraperitoneal injection of 60 mg/kg sodium pentobarbital, restrained in a supine position)	*In situ* absorption	10 cm ileum	0.5 mL or 1 mL NPs (10 or 20 U/kg) in phosphate buffered saline	Glucometer to measure blood glucose levels	1999: [39]

Supplementary table 2. Experimental conditions for examination of *in vivo* biocompatibility of insulin-loaded nanoparticles between 2009 and 2017

Animal model	Protocol objective	Animal group	Treatment	Tissue staining	Quantification	Year/ Ref
Diabetic GK rats	Haematological examination on oxidative stress	n/a	Insulin selenium NPs (25 IU/kg/day) for 2 weeks	n/a	Measurement of reactive oxygen species, malondialdehyde, super oxide dismutase, glutathione and GSH-Px	2017: [3]
GK rats	Determination of pancreatic β-cell viability by TUNEL assay	n/a	Insulin selenium NPs (25 IU/kg/day) for 2 weeks	n/a	Fluorescence microscope to measure percentage of apoptotic cells	2017: [3]
KM mice (18-22 g)	*In vivo* toxicity	3 groups each contain 5 mice (negative control: without treatment)	Insulin trimethyl chitosan NPs, pHPMA-coated trimethyl chitosan NPs (50 IU/kg insulin) for 7 days	Hematoxylin-eosin staining of liver and kidney	Measurement of body weight	2016: [40]
Male Wistar rats (180-200 g, anesthetized with 50 mg/kg sodium pentobarbital)	*Ex vivo* biocompatibility assay by jejunum and colon segments	Positive control (insulin in 3% triton), negative control (insulin in pH 7.4 PBS)	Insulin-loaded Vit B12-Chi-CPNPs (10 IU/mL)	n/a	Analysis of intestinal membrane integrity by LDH assay	2016: [4]
Male Wistar rats (120-150 g g)	*In vivo* toxicity	2 groups each contain 5 rats (negative control: without treatment)	Empty VitB12Chi-CPNPs (100 mg/kg) for 28 days	n/a	Measurement of body weight	2016: [4]
Male Sprague-Dawley rats (6 weeks old)	Lactate dehydrogenase leakage by rat intestine	Positive control: 5% sodium taurodeoxycholate solution	β-cyclodextrin-grafted chitosan	n/a	Cytotoxicity assay kit to measure reduction of nicotinamide adenine dinucleotide	2016: [7]
Male KM mice	Histological analysis	Negative control: physiological saline	HTCC-CA (0.5 mg/kg) once daily for 7 and 15 days	Hematoxylin-eosin staining of heart, liver, spleen, lung and kidney	Microscopic observation	2016: [41]
Male KM mice (18-22 g)	*In vivo* toxicity study	4 groups each contain 5 rats (negative control: without treatment; positive control: 5 mg/kg LPS)	LPS (5 mg/kg) with or without bis-β-cyclodextrin NPs (50 IU/kg insulin) once daily for 7 days	Hematoxylin-eosin staining of liver	Measurement of ALT and AST	2014: [13]

Adult albino rats (150-250 g)	Determination of biochemical parameters	5 groups (negative control: distilled water)	Placebo NPs, oral insulin (5 IU/Kg), insulin NPs (10 IU/Kg), insulin injection (5 IU/Kg)	n/a	Measurement of total cholesterol, urea, creatinine, and protein levels in serum	2013: [42]
Male Sprague Dawley rats (180-220 g)	Lactate dehydrogenase leakage and by histological examination ileum	Positive control (1% sodium taurodeoxycholate), negative control (Kreb-Ringers buffer solution)	1 mL oligoarginine-modified NPs (5 mg/mL) for 2 hr	Hematoxylin-eosin staining of ileum	Measurement of lactate dehydrogenase in intestinal membrane by LDH assay kit and microscopic analysis of ileal segments	2013: [17]
ICR mice (25–30 g)	Toxicity of test NPs	2 groups each contain 5 mice (negative control: without treatment)	Empty NPs (100 mg/kg) for 14 days	Hematoxylin-eosin staining of intestine, liver and kidney	Observation of signs of toxicity, measurement of body weight, microscopic observation of organs	2013: [20]
10 embryos of zebrafish	Zebrafish toxicity studies	n/a	Various concentration of insulin carbon NPs for 4, 8, 24, 48 and 96 hrs	n/a	Measurement of hatching rate, survival rate, pericardial sac, heartbeat, pigmentation and facial oedema	2013: [19]
Wistar rats (220-280 g)	Histopathological examination	Negative control: physiological saline	Eul-cys NPs (100 mg/kg)	Hematoxylin-eosin staining of intestine	Observation of intestinal membrane damage	2012: [22]
Wistar rats	Histopathological study	3 groups each contain 5 mice (negative control: without treatment)	Con A NPs (2 mg/mL FITC) for 4 hr	n/a	Observation of NPs localization in Peyer's patches and enterocytes by fluorescence microscope	2012: [21]
Wistar rats	Integrity of intestinal mucosa	n/a	FITC-dextran (10 mg/mL)	n/a	Fluorescence spectroscopy	2011: [27]
Wistar rats	MTT assay	Positive control (2% Triton), negative control (untreated cells in HEPES buffer)	Insulin multilayered NPs, insulin, empty NPs, chitosan with albumin-free NPs, albumin-free NPs	n/a	Measurement of viability of intestinal tissue	2011: [27]
Adult male and female ICR mice (33-40 g)	*In vivo* toxicity	2 groups each contain 14 mice (negative control: without treatment)	Empty NPs (100 mg/kg) for 14 days	Hematoxylin-eosin staining of liver and kidney	Observation of signs of toxicity, measurement of body weight, measurement of complete blood count, lactate dehydrogenase, alkaline phosphatase, triglycerides, total cholesterol, ALT, AST, blood urea nitrogen and creatinine (haematology analyzer), microscopic observation of organs	2009: [30]

Normal rats	Biocompatibility of polymer in ileum	Positive control (1% sodium tauroglycocholate), negative control (PBS)	0.5 mL CCGN (1%) for 1 hr	n/a	Measurement of lactate dehydrogenase by LDH-UV kit	2009: [43]
Normal rats	Haemolysis Assay	Positive control (Water), negative control (normal saline)	100, 200 and 300 µL of CCGN (1%) with erythrocyte for 1 hr	n/a	Measurement of haemolysis	2009: [43]

Supplementary table 3. Experimental conditions for in vivo pharmacological and pharmacokinetic studies of orally administered insulin-loaded nanoparticle between 2009 and 2017

Animal model	Average fasting BSL	Animal numbers	Blood collection	Control/ treatment	Quantification	Year/ Ref
Streptozotocin-induced diabetic rats (free access to water)	n/a	3 groups each contain 5 rats	From tail vein	**Positive control:** 5 IU/kg subcutaneous insulin injection **Treatment:** insulin:CMCS/CS-NPs (−) solution, insulin:CMCS/CS-NPs (+) (50 IU/kg)	Radioimmunoassay method (blood insulin)	2017: [1]
Streptozotocin (60 mg/kg)-induced diabetic male Sprague-Dawley rats (200-250 g, 3 months old, free access to food and water)	13.89-16.67 mmol/L	7 groups each contain 6 rats	From retroorbital plexus	**Positive control:** 0.3 mL subcutaneous insulin injection (1 IU/kg) **Negative control:** 1 mL oral saline solution, blank AC18N, blank AC18N in CCAB **Treatment:** insulin-AC18N, insulin-AC18N in CCAB, 1 mL free insulin (15 IU/kg)	Glucometer (blood glucose), insulin ELISA kit (plasma insulin)	2017: [2]
Normal Sprague-Dawley, rats and type II diabetes GK rats (180-220 g, free access to food and water)	n/a	10 groups each contain 6 rats	From tail vein	**Positive control:** 1 IU/kg subcutaneous insulin injection **Negative control:** saline **Treatment:** INS-SeNPs (12.5, 25, 50 IU/kg in GK rats), free insulin (50 IU/kg)	Glucose assay kit (blood glucose)	2017: [3]
Streptozotocin (60 mg/kg)-induced diabetic male Wistar rats (180-220 g, 12 weeks old, free access to water)	> 16.7 mmol/L after 1 week	5 groups each contain 6 rats	20 μL from tail vein	**Positive control:** 1 IU/kg subcutaneous insulin injection **Negative control:** physiological saline **Treatment:** ES-c NPs, ES-Tat-c NPs, free insulin (20 IU/kg)	Roche glucose meter (blood glucose)	2017: [44]
Male Guangxi Bama minipigs (9.5-10.5 kg, 5-7 months old, free access to water)	n/a	2 groups each contain 6 pigs	1 mL from precaval vein (0, 0.5, 1, 2, 4, 6, 8, 10, 12, 16, 24, 30, 36 hr)	**Treatment:** ES-c NPs and ES-Tatc NPs (10 IU/kg)	Roche glucose meter (blood glucose), ELISA kit (plasma insulin)	2017: [44]
Alloxan (250 mg/kg)-induced male Sprague-Dawley rats (220-250 g, free access to water)	> 13 mM	Each group contain 5 rats	From caudal vein	**Positive control:** 1 IU/kg subcutaneous insulin injection **Treatment:** INS/HTCC, INS/HTCC-CA solutions injection (1 IU/kg)	ACCU-CHEK Active glucometer (blood glucose)	2016: [41]
Streptozotocin (65 mg/kg)-induced diabetic male Wistar rats (105-135 g, free access to water)	> 300 mg/dL after 1 week	5 groups each contain 15 rats	From caudal vain and retro orbital vein	**Positive control:** 5 IU/kg subcutaneous insulin injection **Negative control:** PBS (pH 7.4)	Glucose meter (blood glucose), ELISA (insulin concentration)	2016: [4]

				Treatment: VitB12-Chi-CPNPs, Chi-CPNPs (50 IU/kg)		
Streptozotocin (60 mg/kg)-induced diabetic male Wistar rats (180-220 g, free access to water)	n/a	7 groups each contain 6 rats	From caudal vein	**Positive control:** 2 IU/kg subcutaneous insulin injection, insulin-LMWP conjugates injection **Negative control:** PBS **Treatment:** insulin MNPs (20 IU/kg), insulin-LMWP conjugates (50 IU/kg), free insulin (20 IU/kg)	AccuChek glucose meter (blood glucose)	2016: [45]
Streptozotocin (65 mg/kg)-induced diabetic male Sprague-Dawley rats (180-220 g, free access to water)	> 300 mg/dL after 5 days	Each group contain 5 rats	From tail vein	**Positive control:** 5 IU/kg subcutaneous insulin injection, insulin-LMWP conjugates injection **Treatment:** insulin-loaded F127 NPs, PVA NPs, DLPC NPs, empty DLPC NPs, free insulin (50 IU/kg)	Glucose meter (blood glucose), porcine insulin ELISA kit (plasma insulin)	2016: [5]
Streptozotocin (60 mg/kg)-induced diabetic male Sprague Dawley rats (180-220 g)	> 16.7 mM	4 groups each contain 3 rats	From tail vein (0, 0.5, 1, 2, 4, 6, 8, 10, 12 hr)	**Positive control:** 2 IU/kg subcutaneous insulin injection **Treatment:** insulin-loaded L/C NPs (40, 60 IU/kg), free insulin (60 IU/kg)	Blood analyzer (blood glucose)	2016: [46]
Streptozotocin (70 mg/kg)-induced diabetic male Sprague-Dawley rats (200-220 g, free access to water)	> 16.0 mM after 1 week	n/a	From tail vein	**Positive control:** 5 IU/kg subcutaneous insulin injection **Treatment:** TNPs, P-T NPs, free insulin (50.0 IU/kg)	Glucose meter (blood glucose), insulin ELISA kit (serum insulin)	2016: [40]
Streptozotocin (60 mg/kg) – induced diabetic adult albino male rats (200-220 g, free access to water)	n/a	4 groups each contain 6 rats	From retroorbital plexus	**Positive control:** 1 IU/kg (0.036 mg/kg) subcutaneous insulin injection **Negative control:** 1 mL saline solution **Treatment:** MSN-PMV-INS, free insulin (15 IU/kg; 0.54 mg/kg)	Glucose test kit-GOD-POD method (blood glucose)	2016: [47]
New Zealand male albino rabbits (1.2 and 1.5 kg, free access to water)	n/a	4 groups each contain 6 rabbits	From marginal ear vein (5, 10, 30, 45, 60, 90, 120, 180 min up to 24 hr)	**Positive control:** 1 IU/kg subcutaneous insulin injection **Treatment:** 20 mg MSN-PMV-INS (15 IU/kg)	n/a	2016: [47]
Male Sprague-Dawley rats (225-275 g, free access to food and water)	n/a	3 groups	From tail vein	**Positive control:** 2 IU/kg subcutaneous insulin injection **Treatment:** 1 mL VEN NPs, free insulin (50 IU/kg)	Veterinarian glucometer (blood glucose)	2016: [48]
Streptozotocin (70 mg/mL) - induced diabetic Sprague-Dawley rats (200-240 g, free access to water)	> 16 mM.	5 groups each contain 4 rats	From tail vein	**Positive control:** 5 IU/kg subcutaneous insulin injection	Glucose meter (blood glucose), insulin ELISA kit (serum insulin)	2015: [8]

Streptozotocin (75mg/kg)-induced diabetic male Wistar rats (180-220 g)	n/a	4 groups each contain 5 rats	From tail vein	**Treatment:** 1 mL micelles, unmodified NPs, CSK NPs (50 IU/kg), free insulin (50 IU/kg) **Positive control:** subcutaneous insulin injection **Treatment:** enteric-coated capsules with free insulin (40 IU/kg) and PLGA-lipid PEG NPs; enteric-coated capsule with microparticles containing INS-PLGA-lipid-PEG NPs; enteric-coated capsule with INS-PLGA-lipid-PEG NPs	Glucose meter (blood glucose), porcine insulin ELISA kit (plasma insulin)	2015: [49]
Streptozotocin (60 mg/kg)-induce diabetic male Wistar rats(250-350 g, free access to water)	> 250 mg/dL with frequent urination, weight loss after 3 days	3 groups each contain 6 rats	From tail vein	**Positive control:** 2 IU/kg subcutaneous insulin injection **Negative control:** unloaded NPs **Treatment:** alginate-dextran NPs, free insulin	ACCU-CHEK Aviva device (blood glucose)	2015: [50]
Streptozotocin (60 mg/kg)-induced diabetic male Wistar rats (180-220 g, free access to water)	> 15 mmol/L after 1 week	n/a	From caudal vein	**Positive control:** 2 IU/kg subcutaneous insulin injection **Negative control:** PBS **Treatment:** insulin PLGA NPs (20 IU/kg), insulin TMC-PLGA NPs (20 IU/kg), free insulin (50 IU/kg)	n/a	2015: [10]
Streptozotocin (45 mg/kg)-induced diabetic female albino rats	> 20 mM/L	6 groups each contain 6 rats	From retroorbital sinus	**Positive control:** 0.4 IU/kg subcutaneous insulin injection **Treatment:** insulin PPC NPs, blank PPC NPs, free insulin (20 IU/kg)	Glucose-estimation kit (plasma glucose)	2015: [9]
Streptozotocin (65 mg/kg) – induced diabetic male Sprague Dawley rats weighting (180-220 g, free access to water)	> 16 mM after 1 week	Each group contain 5 rats	From tail vein	**Positive control:** 5 IU/kg subcutaneous insulin injection **Treatment:** NCs, NPs-1, free insulin (75 IU/kg)	Glucose meter (blood glucose), porcine insulin ELISA kit (plasma insulin)	2015: [51]
Streptozotocin (65 mg/kg)-induced diabetic male Wistar rats (180-220 g, 12-13 weeks old, free access to water)	> 16.67 mmol/dL after 7 days	5 groups each contain 6 rats	From retroorbital plexus	**Positive control:** 1 IU/kg subcutaneous insulin injection **Negative control:** saline **Treatment:** composite microcapsules, PLGA NPs, free insulin (20 IU/kg)	Mutarotase-GOD method (blood glucose)	2015: [52]
Streptozotocin (50 mg/kg)-induced diabetic Albino rabbits (2-2.5 kg, free access to water)	> 250 mg/dL after 8-10 days with frequent urination, weight loss	5 groups each contain 2 rabbits	1 mL from marginal ear vein	**Positive control:** 1\20 IU/kg subcutaneous insulin injection **Negative control:** plain water **Treatment:** insulin NPs, ligand-conjugated NPs, free insulin (20 IU/Kg)	Glucose oxidase-peroxidase (blood glucose), HPLC (insulin)	2015: [11]

Streptozotocin (65 mg/kg)-induced diabetic male Sprague-Dawley rats (180-220 g)	> 16.0 mM after 1 week	n/a	From tail vein	**Positive control:** 1 IU/kg subcutaneous insulin injection **Negative control:** physiological saline **Treatment:** PEN NC, P-bis-CD NC, free insulin (30 IU/kg)	Glucose meter (blood glucose), porcine insulin ELISA kit (plasma insulin)	2014: [13]
Streptozotocin (60 mg/mL) - induced diabetic male Sprague-Dawley rats (220-230 g, 7 weeks old, free access to water)	> 300 mg/dL of	n/a	From tail vein and femoral artery (0, 30, 60, 120, 180, 240 min)	**Treatment:** AuNPs/INS, free insulin (50 IU/kg)	Accu-Chek glucometer (blood glucose), human insulin ELISA assay (plasma insulin)	2014: [53]
Streptozotocin (60 mg/kg)-induced male Wistar rats (200-250 g, free access to water)	> 250 mg/dL after 4 days with frequent urination	Each group contain 6 rats	0.3 mL from tail vein	**Positive control:** 5 IU/kg subcutaneous insulin injection **Negative control:** free insulin (30 IU/kg) **Treatment:** enteric-coated capsules with lyophilized aminobenzyl chitosan NPs or trimethyl chitosan NPs (30 IU/kg)	Glucometer (plasma glucose), ELISA test kit (serum insulin)	2014: [14]
Streptozotocin (60 mg/kg)-induced diabetic male Sprague-Dawley rats (200-250 g)	> 16. 7 mmol/L	n/a	From eye-ground venous plexus (0.5, 1, 2, 3, 4, 6, 8, 12, 18, 24 hr)	**Negative control:** distilled water **Treatment:** insulin-SiO2, insulin-SiO2-HP55, free insulin (30 IU/kg)	Glucose GOD-PAD kit (blood glucose)	2013: [54]
Streptozotocin (60 mg/kg)-induced diabetic adult albino rats (150-250 g, free access to water)	> 250mg/dL after 16 hr with weight loss	6 groups each contain 6 rats	From tail tip	**Positive control:** 5 IU/kg subcutaneous insulin injection **Negative control:** distilled water **Treatment:** placebo NPs, insulin NPs (10 IU/Kg), free insulin (5 IU/Kg)	Glucose strip method (blood glucose), human insulin ELISA kit (serum insulin)	2013: [42]
Streptozotocin (65 mg/kg)-induced diabetic male Sprague-Dawley rats (180-200 g, free access to water)	> 250 mg/dL after one week	n/a	From tail vein (1, 2, 4, 6, 8, 10 hr)	**Positive control:** 5 IU/kg subcutaneous insulin injection **Treatment:** insulin NC, insulin CSC, free insulin (50 IU/kg)	Glucose meter (blood glucose), insulin ELISA kit (serum insulin)	2013: [18]
Streptozotocin-induced diabetic Wistar rats (250 g, free access to water)	n/a	Each group contain 6 rats	From tail vein	**Positive control:** 5 IU/kg subcutaneous insulin injection **Treatment:** enteric-coated capsule with CS/γPGA-EGTA NPs, enteric-coated capsule with free insulin powder (30 IU/kg) and trehalose	Glucose meter (blood glucose)	2013: [55]
Diabetic rats (administered 1 g/kg glucose at 2 hr after treatments)	n/a	4 groups each contain 6 rats	From tail vein	**Positive control:** 5 IU/kg subcutaneous insulin injection **Negative control:** distilled water **Treatment:** enteric-coated capsule with free insulin (30 IU/kg) and trehalose	Glucose meter (blood glucose), bovine insulin ELISA kit (plasma insulin)	2013: [20]

Streptozotocin (50 mg/kg)-induced diabetic male albino rats (150-250 g, free access to water)	n/a	2 groups each contain 6 rats	From tail vein (every hour up to 8 hr)	**Treatment:** insulin NPs, free insulin (50 IU/kg)	Glucometer (blood glucose)	2013: [19]
Alloxan (250 mg/kg)-induced male Swiss albino mice (28-30 g, free access to water)	> 250 mg/dL after 6 days	Each group contain 5 rats	From tail vein	**Positive control:** 5 IU/kg subcutaneous insulin injection **Treatment:** chitosan/insulin self-assembled NPs (50, 100 IU/kg)	Bayer's glucose meter (blood glucose)	2013: [56]
Male Sprague-Dawley rats (250-500 g)	n/a	9 groups each contain 4 rats	From tail vein	**Positive control:** 1 IU/kg subcutaneous insulin injection **Negative control:** water **Treatment:** insulin GLY NPs, insulin PEG-NPs, blank NPs, free insulin (50 IU/kg)	Blood glucose meter (blood glucose)	2013: [57]
Male Sprague Dawley rats (180-220 g, free access to water)	n/a	n/a	0.5 mL from tail tip (5, 10, 15, 30, 60, 120, 180, 240, 300, 360, 480 min)	**Positive control:** 1 IU/kg subcutaneous insulin injection (0.5 mL) **Treatment:** unmodified INS-NP, l-R8-INS-NP, d-R8-INS-NP (10 IU/kg)	Radioimmunoassay (plasma insulin), glucose oxidase method (blood glucose)	2013: [17]
Streptozotocin (65 mg/kg)-induced diabetic male Wistar rats (220-280 g, free access to water)	> 300 mg/dL two weeks	4 groups each contain 5 rats	From ocular vein plexus	**Positive control:** 5 IU/kg subcutaneous insulin injection **Negative control:** 50 IU/kg free insulin **Treatment:** enteric-coated capsules with lyophilized insulin Eul-cys NPs or lyophilized Eul NPs (50 IU/kg)	GOD-PAD kit (blood glucose)	2012: [22]
Streptozotocin (75 mg/ kg)-induced diabetic Wistar rats (250 g, free access to water)	> 300 mg/dL after 2 weeks	Each group contain 5 rats	From tail vein	**Positive control:** 5 IU/kg subcutaneous insulin injection **Treatment:** enteric-coated capsule with CS/gPGA-DTPA NPs, enteric-coated capsule with free insulin and trehalose, free insulin (30 IU/kg)	Glucose meter (blood glucose), bovine insulin ELISA kit (plasma insulin)	2012: [24]
Streptozotocin (50 mg/kg)-induced diabetic Wistar rats weighing (200-250 g, free access to water)	> 250 mg/dL after 2 weeks	4 groups each contain 6 rats	0.2 from retro orbital plexus	**Positive control:** 2.5 IU/kg subcutaneous insulin injection **Negative control:** healthy rat, untreated diabetic rats **Treatment:** insulin NPs, insulin Con A NPs, free insulin (20 IU/kg)	Glucometer (blood glucose)	2012: [21]
Streptozotocin (55 mg/kg)-induced diabetic adult male Sprague-Dawley rats (220-280 g, free access to water)	> 250 mg/dL	8 groups	200 µL from retro orbital plexus (0, 1, 2, 4, 6, 8, 12, 18, 24, 36 hr)	**Positive control:** 5 IU/kg subcutaneous insulin injection **Negative control:** untreated diabetic animals	Insulin ELISA kit (plasma insulin)	2012: [58]

				Treatment: insulin PLGA, NH2-PEG-PLGA, OCH3-PEG-PLGA, FA-PEG-PLGA NPs, free insulin (50 IU/kg)		
Streptozotocin (65 mg/kg)-induced diabetic male Wistar rats (200-300 g, free access to water)	> 3 g/L after 1 week	3 groups each contain 5-8 rats		**Negative control:** untreated diabetic animals **Treatment:** oral insulin NPs, insulin NPs injection to duodenum (50 IU/kg)	Accu-Chek® glucometer (blood glucose)	2012: [59]
Alloxan (40 mg/kg)- induced diabetic Sprague-Dawley male rats (190-210 g)	13.89-16.67 mmol/L	5 groups each contain 5 rats	From retro-orbital plexus	**Positive control:** 1 IU/kg subcutaneous insulin injection (0.036 mg/kg) **Negative control:** 1 mL saline solution **Treatment:** insulin PLGA NPs, insulin adhesive PLGA NPs, free insulin (15 IU/kg; 0.54 mg/kg)	Glucose-oxidase method (blood glucose)	2012: [23]
Streptozotocin (65 mg/kg)-induced diabetic male Wistar rats (180-220 g, 12-13 weeks, free access to water)	> 16.7 mmol/dL after 7 days	4 groups each contain 6 rats	From retro-orbital plexus	**Positive control:** 1 IU/kg subcutaneous insulin injection **Negative control:** saline **Treatment:** Ins-SD-Comp-PLGA NPs, free insulin (20 IU/kg)	Glucose oxidase method (plasma glucose)	2011: [60]
Streptozotocin (65 mg/kg)-induced diabetic male Sprague-Dawley rats (250 g, free access to water)	> 250 mg/dL after 2 weeks with urination, weight loss	n/a	From tail vein	**Positive control:** 5 IU/kg subcutaneous insulin injection **Negative control:** empty NPs (50 IU/kg) **Treatment:** HP55-coated capsules with insulin PLGA/RS NPs (50 IU/kg)	Roche Accu-check glucometer (blood glucose)	2011: [61]
Streptozotocin (50 mg/mL) - induced diabetic male Wistar rats (200-250 g, free access to water)	> 250 mg/dL after 2 weeks	n/a	From tail vein	**Positive control:** 2.5 IU/kg subcutaneous insulin injection **Negative control:** free insulin (25 IU/kg) **Treatment:** SLN, chitosan-coated SLN (25 IU/kg)	Medisense Precision Xceed Kit (blood glucose)	2011: [26]
Streptozotocin (60mg/kg)-induced diabetic male Wistar rats (200-250 g)	> 250mg/dL after 7-10 days with frequent urination, weight loss	4 groups each contain 6 rats	From tail vein (up to 24 hr)	**Positive control:** 5 IU/kg subcutaneous insulin injection **Treatment:** insulin NPs, empty NPs free insulin (50 IU/kg)	ACCU-CHEK Aviva (blood glucose), Iso-insulin ELISA (serum insulin)	2010: [29]
Streptozotocin (75 mg/kg)-induced diabetic male Wistar rats (180-200 g, free access to water)	> 300 mg/dL, after 2 weeks	Each group contain 5 rats	From tail vein	**Positive control:** 5 IU/kg subcutaneous insulin injection **Treatment:** aspart-insulin NPs (30 IU/kg)	Glucose meter (blood glucose), iso-insulin ELISA and ultrasensitive insulin ELISA (plasma insulin)	2010: [62]
Streptozotocin (75 mg/kg)-induced diabetic male Wistar	> 300 mg/dL after 2 weeks	Each group contain 5 rats	From tail vein	**Positive control:** 5 IU/kg subcutaneous insulin injection	Glucose meter (blood glucose), bovine	2010: [63]

rats (180-200 g, free access to water)				**Treatment:** Eudragit S100-coated capsule with freeze-dried NPs; Eudragit L100-55-coated capsule with freeze-dried NPs, Eudragit L100-55-coated capsule with the free insulin (30 IU/kg) and trehalose;	insulin ELISA kit (plasma insulin)	
Streptozotocin (65 mg/kg)-induced diabetic male Wistar rats (180-220 g, 12-13 weeks old, free access to water)	> 16.67 mmol/dL after 7 days	6 groups each contain 6 rats	From inferior ophthalmic vein (0, 1, 3, 4, 6, 8, 12, 24 hr)	**Positive control:** 1 IU/kg subcutaneous insulin injection **Negative control:** saline **Treatment with glucose (2 g/kg):** insulin-S.O NPs, free insulin (20 IU/kg)	Plasma glucose, pharmacological bioavailability.	2010: [64]
Streptozotocin (65 mg/kg)-induced diabetic adult male Wistar rats (220-280 g, free access to water)	> 300 mg/dL after 2 weeks	n/a	From tail vein	**Positive control:** 2.5 IU/kg subcutaneous insulin injection **Negative control:** empty NPs **Treatment:** insulin NPs (25, 50, 100 IU/kg)	Accu-check (blood glucose), insulin-CT kit (plasma insulin)	2010: [65]
Streptozotocin (75 mg/kg)-induced diabetic male Wistar rats (180-200 g, free access to water)	> 300 mg/dL after 2 weeks	3 groups each contain 5 rats	From tail vein	**Positive control:** 5 IU/kg subcutaneous insulin injection **Treatment:** insulin NPs, free insulin (30 IU/kg)	Glucose meter (blood glucose), bovine insulin ELISA kit (plasma insulin)	2009: [30]
Streptozotocin (80 mg/kg)-induced diabetic adult male Wistar rats (250-300 g, free access to water)	> 200 mg/dL	Each group contain 5 rats	From tail vein	**Positive control:** 1 IU/kg subcutaneous insulin injection **Negative control:** placebo NPs **Treatment:** fresh NPs, NPs stored for 1 month at 4 °C (50 IU/kg)	Blood glucose meter (blood glucose)	2009: [66]
Normal rats	n/a	Each group contain 4 rats	From tail vein	**Treatment:** insulin CCGN colloid (15, 25, 50, 100 IU/kg), free insulin (100 IU/kg)	Glucose-oxidase kit (blood glucose)	2009: [43]
Alloxan (40 mg/kg)-induced diabetic rats	> 16.67 mmol/L	n/a	From tail vein	**Treatment:** insulin CCGN colloid (25, 50 IU/kg),free insulin (50 IU/kg)	Glucose-oxidase kit (blood glucose)	2009: [43]
Male Sprague-Dawley rats (180-220 g, free access to water)	n/a	4 groups each contain 6 rats	0.25 mL from tail vein (0.25, 0.5, 1, 2, 3, 4, 5, 6, 8, 10, 12 hr)	**Positive control:** 1 IU/kg subcutaneous insulin injection **Treatment:** 0.5 mL R8-Ins-SLNs, Ins-SLNs, free insulin (20 IU/kg)	ACCUCHEK Active (plasma glucose)	2009: [67]
Streptozotocin (65 mg/kg)-induced diabetic male Wistar rats (246-294 g, free access to water)	> 300 mg/dL after 10 days with frequent urination, weight loss	3 groups	From tail vein	**Negative control:** water, empty NPs **Treatment:** insulin NPs (50 IU/kg)	Glucose oxidase/peroxidase method (blood glucose)	2008: [68]
Streptozotocin (80 mg/mL)-induced diabetic male Wistar	n/a	n/a	From tail vein	**Positive control:** 2.5 IU/kg subcutaneous insulin injection	Glucose meter (blood glucose)	2007: [69]

rats (180-200 g, free access to water)				**Treatment:** empty NPs, insulin NPs, free insulin (15, 30 IU/kg)		
Streptozotocin (75 mg/kg)-induced diabetic male Wistar rats (250 g, free access to water)	n/a	Each group contain 6 rats	From tail vein (1-10 hr)	**Positive control:** 5 IU/kg subcutaneous insulin injection **Negative control:** deionised water **Treatment:** 2mL insulin (0.8 mg; 30 IU/kg) NPs, free insulin (30 IU/kg)	Glucose meter (blood glucose)	2007: [70]
Streptozotocin (50 mg/mL)-induced diabetic male Wistar rats (250-300 g, free access to water)	> 250 mg/dL after 2 weeks	7 groups each contain 6 rats	0.2 mL from tail vein	**Positive control:** 2.5 IU/kg subcutaneous insulin injection **Treatment:** 1.0 mL insulin NPs (25, 50, 100 IU/kg), empty NPs, free insulin (50 IU/kg)	Medisense Precision Xceed Kit (plasma glucose), ELISA test kit (serum insulin)	2007: [32]
Streptozotocin (45 mg/kg)-induced diabetic female Wistar rats (150-200 g)	> 250%	3 groups each contain 6 rats	From orbital sinus	**Positive control:** 0.4 IU/kg subcutaneous insulin injection **Negative control:** blank NPs **Treatment:** lyophilized NPs (20 IU/kg)	Glucose estimation kit (blood glucose), insulin ELISA kits (human insulin)	2007: [71]
Streptozotocin-induced diabetic Wistar male rats (200-250 g)	n/a	Each group contain 6 rats	Measure within 24 hr	**Positive control:** 2.5 IU/kg subcutaneous insulin injection **Negative control:** free insulin (50 IU/kg) **Treatment:** insulin NPs (50, 100 IU/kg), empty NPs (50 IU/kg)	Medisense Precision Xceed Kit (plasma glucose), ELISA (serum insulin)	2007: [33]
Streptozotocin (65 mg/kg)-induced diabetic adult male Wistar rats (free access to water)	> 300 mg/dL after 2 weeks	n/a	From tail vein	**Positive control:** 10 IU/kg subcutaneous insulin injection **Negative control:** empty NPs **Treatment with 2 g/kg glucose:** insulin NPs (100 IU/kg)	Insulin-CT kit (plasma insulin)	2007: [35]
Streptozotocin (45 mg/kg)-induced diabetic female Wistar rats (150-200 g, free access to water)	> 20 mM/L	3 groups each contain 6 rats	From orbital sinus	**Positive control:** 0.4 IU/kg subcutaneous insulin injection **Negative control:** insulin NPs without VB12, blank NPs **Treatment:** lyophilized insulin VB12-dextran NPs (20 IU/kg)	Glucose estimation kit (blood glucose)	2007: [72]
Streptozotocin (60 mg/kg)-induced diabetic male Wistar rats (free access to water)	> 250 mg/dL after 2 weeks	3 groups each contain 10 rats	0.2 mL from retro-orbital plexus (0, 1, 2, 4, 6, 8, 12, 16, 24 hr)	**Positive control:** subcutaneous insulin injection (0.25, 0.5, 1, 2 IU/kg) **Negative control:** insulin NPs without VB12, blank NPs **Treatment:** PLGA NPs, PLGA-Hp55 NPs, free insulin (20 IU kg)	Glucose-oxidase method (serum glucose), radioimmunoassay method (serum insulin)	2007: [73]
Streptozotocin (250 mg/kg) - induced diabetic male mice	n/a	n/a	From tail vein	**Negative control:** oral insulin with saline (20 U/kg) **Treatment:** insulin PLGA NPs (20 U/kg)	ACCU-CHEKÒ Advantage (plasma glucose)	2007: [74]

(18-20 g, five weeks old, free access to water)						
Streptozotocin-induced male diabetic rats (180-220 g, free access to water)	> 16 mmol/L	3 groups each contain 6 rats	From retro-orbital plexus	**Positive control:** 1 IU/kg subcutaneous insulin injection **Treatment:** insulin NPs, free insulin (20 IU/kg)	Glucose oxidase method (plasma glucose), radioimmunoassay (serum insulin)	2006: [75]
Normal male Sprague-Dawley rats (200-220 g)	n/a	Each group contain 6 rats	From tail vein	**Positive control:** 1 IU/kg subcutaneous insulin injection **Treatment:** insulin CM NPs, insulin CDM NPs, insulin CTM NPs, free insulin (100 IU/kg)	Glucose-oxidase method (blood glucose)	2006: [76]
Sprague-Dawley rats (225-275 g, free access to food and water)	n/a	4 groups each contain 6 rats	0.5 mL from subclavian vein	**Positive control:** 2 IU/kg subcutaneous insulin injection **Negative control:** phosphate buffer **Treatment:** insulin SLNs, WGA-modified SLNs (50 IU/kg)	Glucose oxidase method (blood glucose), radioactive immunity analysis (serum insulin)	2006: [77]
Streptozotocin (40 mg/kg)-induced diabetic male Wistar rats (200-250 g, free access to water)	> 250 mg/dL	3-5 groups each contain 8 rats	0.2 mL from orbital sinus (0, 2, 4, 6, 8, 10, 12, 14, 16, 18, 20, 22, 24 hr)	**Treatment:** F5.3np, F6.1np (50, 100 U/kg), mixture of chitosan and insulin, empty chitosan NPs, free insulin	Trinder Diagnostic reagent Glucose (blood glucose), porcine insulin RIA kit (serum insulin)	2005: [37]
Alloxan (40 mg/kg)-induced diabetic Wistar male rats (220-280 g, 12-13 weeks old)	180-250 mg/dL	n/a	From retro-orbital plexus	**Positive control:** 1 IU/kg subcutaneous insulin injection **Treatment:** insulin CS NPs with 1% poloxamer 188 (7, 14, 21 IU/kg), free insulin (14 IU/kg)	Glucose-oxidase method (blood glucose)	2002: [78]
Alloxan-induced diabetic male Wistar rats (220-280 g, free access to water)	13.9-16.7 mmol/L	5 groups	From eye orbital vein	**Positive control:** 1 IU/kg subcutaneous insulin injection **Treatment:** insulin CS-MP, free insulin (10 U/kg)	Glucose-oxidase method (blood glucose)	2002: [79]

Reference list

1. Wang J, Kong M, Zhou Z, et al. Mechanism of surface charge triggered intestinal epithelial tight junction opening upon chitosan nanoparticles for insulin oral delivery. Carbohydr Polym. 2017 10;157:596-602.
2. Alfatama M, Lim LY, Wong TW. Alginate-c18 conjugate nanoparticles loaded in tripolyphosphate-cross-linked chitosan-oleic acid conjugate-coated calcium alginate beads as oral insulin carrier. Mol Pharm. 2018;15:3369-3382.
3. Deng W, Xie Q, Wang H, et al. Selenium nanoparticles as versatile carriers for oral delivery of insulin: Insight into the synergic antidiabetic effect and mechanism. Nanomedicine. 2017;13(6):1965-1974.
4. Verma A, Sharma S, Gupta PK, et al. Vitamin b12 functionalized layer by layer calcium phosphate nanoparticles: A mucoadhesive and ph responsive carrier for improved oral delivery of insulin. Acta Biomater. 2016;31:288-300.
5. Shan W, Zhu X, Tao W, et al. Enhanced oral delivery of protein drugs using zwitterion-functionalized nanoparticles to overcome both the diffusion and absorption barriers. ACS Appl Mater Interfaces. 2016;8(38):25444-25453.
6. Pereira de Sousa I, Moser T, Steiner C, et al. Insulin loaded mucus permeating nanoparticles: Addressing the surface characteristics as feature to improve mucus permeation. Int J Pharm. 2016;500(1-2):236-44.
7. Daimon Y, Kamei N, Kawakami K, et al. Dependence of intestinal absorption profile of insulin on carrier morphology composed of beta-cyclodextrin-grafted chitosan. Mol Pharm. 2016;13(12):4034-4042.
8. Zhang P, Xu Y, Zhu X, et al. Goblet cell targeting nanoparticle containing drug-loaded micelle cores for oral delivery of insulin. Int J Pharm. 2015;496(2):993-1005.
9. Sharma R, Gupta U, Garg NK, et al. Surface engineered and ligand anchored nanobioconjugate: An effective therapeutic approach for oral insulin delivery in experimental diabetic rats. Colloids Surf B Biointerfaces. 2015;127:172-181.
10. Sheng J, Han L, Qin J, et al. N-trimethyl chitosan chloride-coated plga nanoparticles overcoming multiple barriers to oral insulin absorption. ACS Appl Mater Interfaces. 2015;7(28):15430-15441.
11. Jain A, Jain SK. L-valine appended plga nanoparticles for oral insulin delivery. Acta Diabetol. 2015;52(4):663-676.
12. Ke Z, Guo H, Zhu X, et al. Efficient peroral delivery of insulin via vitamin b12 modified trimethyl chitosan nanoparticles. J Pharm Pharm Sci. 2015;18(2):155-170.
13. Zhu X, Shan W, Zhang P, et al. Penetratin derivative-based nanocomplexes for enhanced intestinal insulin delivery. Mol Pharm. 2014;11(1):317-328.
14. Mahjub R, Radmehr M, Dorkoosh FA, et al. Lyophilized insulin nanoparticles prepared from quaternized n-aryl derivatives of chitosan as a new strategy for oral delivery of insulin: In vitro, ex vivo and in vivo characterizations. Drug Dev Ind Pharm. 2014;40(12):1645-1659.
15. Du X, Zhang J, Zhang Y, et al. Decanoic acid grafted oligochitosan nanoparticles as a carrier for insulin transport in the gastrointestinal tract. Carbohydr Polym. 2014;111:433-441.
16. Tahtat D, Mahlous M, Benamer S, et al. Oral delivery of insulin from alginate/chitosan crosslinked by glutaraldehyde. Int J Biol Macromol. 2013;58:160-168.
17. Liu X, Liu C, Zhang W, et al. Oligoarginine-modified biodegradable nanoparticles improve the intestinal absorption of insulin. Int J Pharm. 2013;448(1):159-167.
18. Li X, Guo S, Zhu C, et al. Intestinal mucosa permeability following oral insulin delivery using core shell corona nanolipoparticles. Biomaterials. 2013;34(37):9678-9687.
19. Ganeshkumar M, Ponrasu T, Sathishkumar M, et al. Preparation of amphiphilic hollow carbon nanosphere loaded insulin for oral delivery. Colloids Surf B Biointerfaces. 2013;103:238-243.

20. Chuang EY, Lin KJ, Su FY, et al. Noninvasive imaging oral absorption of insulin delivered by nanoparticles and its stimulated glucose utilization in controlling postprandial hyperglycemia during ogtt in diabetic rats. J Control Release. 2013;172(2):513-522.
21. Hurkat P, Jain A, Jain A, et al. Concanavalin a conjugated biodegradable nanoparticles for oral insulin delivery. J Nanopart Res. 2012;14(11):1219.
22. Zhang Y, Wu X, Meng L, et al. Thiolated eudragit nanoparticles for oral insulin delivery: Preparation, characterization and in vivo evaluation. Int J Pharm. 2012 Oct 15;436(1-2):341-350.
23. Zhang X, Sun M, Zheng A, et al. Preparation and characterization of insulin-loaded bioadhesive plga nanoparticles for oral administration. Eur J Pharm Sci. 2012;45(5):632-638.
24. Su FY, Lin KJ, Sonaje K, et al. Protease inhibition and absorption enhancement by functional nanoparticles for effective oral insulin delivery. Biomaterials. 2012 Mar;33(9):2801-2811.
25. Makhlof A, Tozuka Y, Takeuchi H. Design and evaluation of novel ph-sensitive chitosan nanoparticles for oral insulin delivery. Eur J Pharm Sci. 2011;42(5):445-451.
26. Fonte P, Nogueira T, Gehm C, et al. Chitosan-coated solid lipid nanoparticles enhance the oral absorption of insulin. Drug Deliv Transl Res. 2011;1(4):299-308.
27. Woitiski CB, Sarmento B, Carvalho RA, et al. Facilitated nanoscale delivery of insulin across intestinal membrane models. Int J Pharm. 2011;412(1-2):123-131.
28. Avadi MR, Sadeghi AMM, Mohamadpour Dounighi N, et al. Ex vivo evaluation of insulin nanoparticles using chitosan and arabic gum. ISRN Pharm. 2011;2011:860109.
29. Woitiski CB, Neufeld RJ, Veiga F, et al. Pharmacological effect of orally delivered insulin facilitated by multilayered stable nanoparticles. Eur J Pharm Sci. 2010;41(3-4):556-563.
30. Sonaje K, Lin YH, Juang JH, et al. In vivo evaluation of safety and efficacy of self-assembled nanoparticles for oral insulin delivery. Biomaterials. 2009;30(12):2329-2339.
31. Bayat A, Dorkoosh FA, Dehpour AR, et al. Nanoparticles of quaternized chitosan derivatives as a carrier for colon delivery of insulin: Ex vivo and in vivo studies. Int J Pharm. 2008;356(1-2):259-266.
32. Sarmento B, Ribeiro A, Veiga F, et al. Alginate/chitosan nanoparticles are effective for oral insulin delivery. Pharm Res. 2007;24(12):2198-2206.
33. Sarmento B, Ribeiro A, Veiga F, et al. Oral bioavailability of insulin contained in polysaccharide nanoparticles. Biomacromolecules. 2007;8(10):3054-3060.
34. Li MG, Lu WL, Wang JC, et al. Distribution, transition, adhesion and release of insulin loaded nanoparticles in the gut of rats. Int J Pharm. 2007;329(1-2):182-191.
35. Damge C, Maincent P, Ubrich N. Oral delivery of insulin associated to polymeric nanoparticles in diabetic rats. J Control Release. 2007;117(2):163-170.
36. Sajeesh S, Sharma CP. Cyclodextrin-insulin complex encapsulated polymethacrylic acid based nanoparticles for oral insulin delivery. Int J Pharm. 2006;325(1-2):147-154.
37. Ma Z, Lim TM, Lim LY. Pharmacological activity of peroral chitosan-insulin nanoparticles in diabetic rats. Int J Pharm. 2005;293(1-2):271-280.
38. Aboubakar M, Couvreur P, Pinto-Alphandary H, et al. Insulin-loaded nanocapsules for oral administration: In vitro and in vivo investigation. Drug Develop Res. 2000;49(2):109-117.
39. Barichello JM, Morishita M, Takayama K, et al. Encapsulation of hydrophilic and lipophilic drugs in plga nanoparticles by the nanoprecipitation method. Drug Dev Ind Pharm. 1999;25(4):471-476.
40. Liu M, Zhang J, Zhu X, et al. Efficient mucus permeation and tight junction opening by dissociable "mucus-inert" agent coated trimethyl chitosan nanoparticles for oral insulin delivery. J Control Release. 2016;222:67-77.
41. Zhang Z, Cai H, Liu Z, et al. Effective enhancement of hypoglycemic effect of insulin by liver-targeted nanoparticles containing cholic acid-modified chitosan derivative. Mol Pharm. 2016;13(7):2433-42.
42. Prusty Ak, Sahu SK. Development and evaluation of insulin incorporated nanoparticles for oral administration. ISRN Nanotechnology. 2013;2013:1-6.

43. Cui F, Qian F, Zhao Z, et al. Preparation, characterization, and oral delivery of insulin loaded carboxylated chitosan grafted poly(methyl methacrylate) nanoparticles. Biomacromolecules. 2009;10(5):1253-1258.
44. Chen S, Guo F, Deng T, et al. Eudragit s100-coated chitosan nanoparticles co-loading tat for enhanced oral colon absorption of insulin. AAPS PharmSciTech. 2017;18(4):1277-1287.
45. Sheng J, He H, Han L, et al. Enhancing insulin oral absorption by using mucoadhesive nanoparticles loaded with lmwp-linked insulin conjugates. J Control Release. 2016;233:181-190.
46. Liu L, Zhou C, Xia X, et al. Self-assembled lecithin/chitosan nanoparticles for oral insulin delivery: Preparation and functional evaluation. Int J Nanomedicine. 2016;11:761-769.
47. Guha A, Biswas N, Bhattacharjee K, et al. Ph responsive cylindrical msn for oral delivery of insulin-design, fabrication and evaluation. Drug Deliv. 2016;23(9):3552-3561.
48. Boushra M, Tous S, Fetih G, et al. Development and evaluation of viscosity-enhanced nanocarrier (ven) for oral insulin delivery. Int J Pharm. 2016;511(1):462-472.
49. Yu F, Li Y, Liu CS, et al. Enteric-coated capsules filled with mono-disperse micro-particles containing plga-lipid-peg nanoparticles for oral delivery of insulin. Int J Pharm. 2015;484(1-2):181-191.
50. Lopes MA, Abrahim-Vieira B, Oliveira C, et al. Probing insulin bioactivity in oral nanoparticles produced by ultrasonication-assisted emulsification/internal gelation. Int J Nanomedicine. 2015;10:5865-80.
51. Shan W, Zhu X, Liu M, et al. Overcoming the diffusion barrier of mucus and absorption barrier of epithelium by self-assembled nanoparticles for oral delivery of insulin. Acs Nano. 2015;9(3):2345-2356.
52. Sun S, Liang N, Yamamoto H, et al. Ph-sensitive poly(lactide-co-glycolide) nanoparticle composite microcapsules for oral delivery of insulin. Int J Nanomedicine. 2015;10:3489-3498.
53. Cho HJ, Oh J, Choo MK, et al. Chondroitin sulfate-capped gold nanoparticles for the oral delivery of insulin. Int J Biol Macromol. 2014;63:15-20.
54. Zhao X, Shan C, Zu Y, et al. Preparation, characterization, and evaluation in vivo of ins-sio(2)-hp55 (insulin-loaded silica coating hp55) for oral delivery of insulin. Int J Pharm. 2013;454(1):278-284.
55. Chuang EY, Lin KJ, Su FY, et al. Calcium depletion-mediated protease inhibition and apical-junctional-complex disassembly via an egta-conjugated carrier for oral insulin delivery. J Control Release. 2013;169(3):296-305.
56. Mukhopadhyay P, Sarkar K, Chakraborty M, et al. Oral insulin delivery by self-assembled chitosan nanoparticles: In vitro and in vivo studies in diabetic animal model. Mater Sci Eng C Mater Biol Appl. 2013;33(1):376-382.
57. Viehof A, Javot L, Beduneau A, et al. Oral insulin delivery in rats by nanoparticles prepared with non-toxic solvents. Int J Pharm. 2013;443(1-2):169-174.
58. Jain S, Rathi VV, Jain AK, et al. Folate-decorated plga nanoparticles as a rationally designed vehicle for the oral delivery of insulin. Nanomedicine. 2012;7(9):1311-1337.
59. Reix N, Parat A, Seyfritz E, et al. In vitro uptake evaluation in caco-2 cells and in vivo results in diabetic rats of insulin-loaded plga nanoparticles. Int J Pharm. 2012;437(1-2):213-220.
60. Sun S, Liang N, Kawashima Y, et al. Hydrophobic ion pairing of an insulin-sodium deoxycholate complex for oral delivery of insulin. Int J Nanomedicine. 2011;6:3049-3056.
61. Wu ZM, Zhou L, Guo XD, et al. Hp55-coated capsule containing plga/rs nanoparticles for oral delivery of insulin. Int J Pharm. 2012;425(1-2):1-8.
62. Sonaje K, Lin KJ, Wey SP, et al. Biodistribution, pharmacodynamics and pharmacokinetics of insulin analogues in a rat model: Oral delivery using ph-responsive nanoparticles vs. Subcutaneous injection. Biomaterials. 2010;31(26):6849-6858.

63. Sonaje K, Chen YJ, Chen HL, et al. Enteric-coated capsules filled with freeze-dried chitosan/poly(gamma-glutamic acid) nanoparticles for oral insulin delivery. Biomaterials. 2010;31(12):3384-3394.
64. Sun S, Liang N, Piao H, et al. Insulin-s.O (sodium oleate) complex-loaded plga nanoparticles: Formulation, characterization and in vivo evaluation. J Microencapsul. 2010;27(6):471-478.
65. Damge C, Socha M, Ubrich N, et al. Poly(epsilon-caprolactone)/eudragit nanoparticles for oral delivery of aspart-insulin in the treatment of diabetes. J Pharm Sci. 2010;99(2):879-889.
66. Elsayed A, Remawi MA, Qinna N, et al. Formulation and characterization of an oily-based system for oral delivery of insulin. Eur J Pharm Biopharm. 2009;73(2):269-279.
67. Zhang ZH, Lv HX, Zhou JP. Novel solid lipid nanoparticles as carriers for oral administration of insulin. Pharmazie. 2009;64(9):574-578.
68. Reis CP, Ribeiro AJ, Veiga F, et al. Polyelectrolyte biomaterial interactions provide nanoparticulate carrier for oral insulin delivery. Drug Deliv. 2008;15(2):127-139.
69. Lin YH, Mi FL, Chen CT, et al. Preparation and characterization of nanoparticles shelled with chitosan for oral insulin delivery. Biomacromolecules. 2007;8(1):146-52.
70. Lin YH, Chen CT, Liang HF, et al. Novel nanoparticles for oral insulin delivery via the paracellular pathway. Nanotechnology. 2007;18(10).
71. Chalasani KB, Russell-Jones GJ, Jain AK, et al. Effective oral delivery of insulin in animal models using vitamin b12-coated dextran nanoparticles. J Control Release. 2007;122(2):141-150.
72. Chalasani KB, Russell-Jones GJ, Yandrapu SK, et al. A novel vitamin b12-nanosphere conjugate carrier system for peroral delivery of insulin. J Control Release. 2007;117(3):421-429.
73. Cui FD, Tao AJ, Cun DM, et al. Preparation of insulin loaded plga-hp55 nanoparticles for oral delivery. J Pharm Sci. 2007;96(2):421-427.
74. Liu J, Zhang SM, Chen PP, et al. Controlled release of insulin from plga nanoparticles embedded within pva hydrogels. J Mater Sci Mater Med. 2007;18(11):2205-2210.
75. Cui F, Shi K, Zhang L, et al. Biodegradable nanoparticles loaded with insulin-phospholipid complex for oral delivery: Preparation, in vitro characterization and in vivo evaluation. J Control Release. 2006;114(2):242-250.
76. Qian F, Cui F, Ding J, et al. Chitosan graft copolymer nanoparticles for oral protein drug delivery: Preparation and characterization. Biomacromolecules. 2006;7(10):2722-2727.
77. Zhang N, Ping Q, Huang G, et al. Lectin-modified solid lipid nanoparticles as carriers for oral administration of insulin. Int J Pharm. 2006;327(1-2):153-159.
78. Pan Y, Li YJ, Zhao HY, et al. Bioadhesive polysaccharide in protein delivery system: Chitosan nanoparticles improve the intestinal absorption of insulin in vivo. Int J Pharm. 2002;249(1-2):139-147.
79. Pan Y, Zheng JM, Zhao HY, et al. Relationship between drug effects and particle size of insulin-loaded bioadhesive microspheres. Acta Pharmacologica Sinica. 2002;23(11):1051-1056.

Appendix B6.2: Publisher agreement and permission for chapter 7

Wong CY et al 2020. "Current status and applications of animal models in pre-clinical development of orally administered insulin-loaded nanoparticles." Journal of Drug Targeting 1-22.

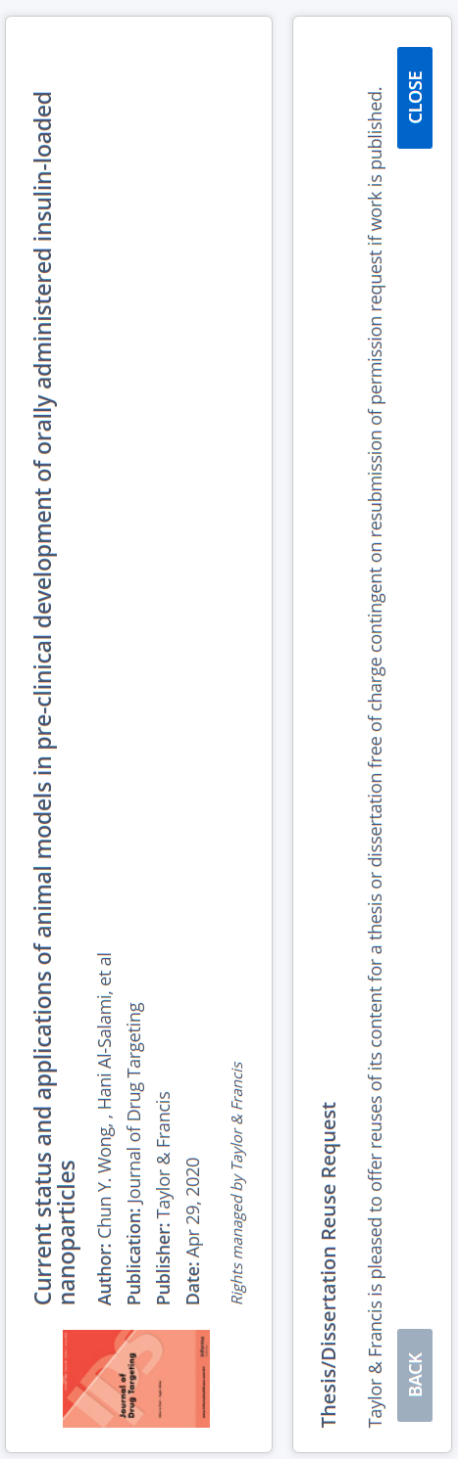

Appendix B7: Publisher agreement and permission for chapter 8 - Fabrication techniques for the preparation of orally administered insulin nanoparticles

Wong CY et al 2020. "Fabrication techniques for the preparation of orally administered insulin nanoparticles." Journal of Drug Targeting.

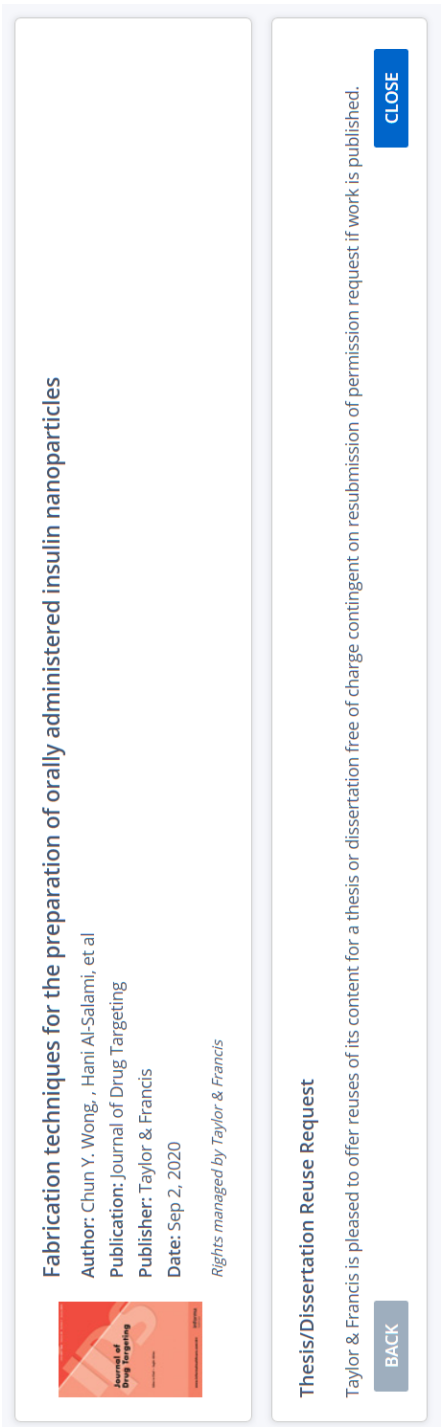

Appendix B8: Publisher agreement and permission for chapter 9 - The role of chitosan on oral delivery of peptide-loaded nanoparticle formulation

Wong CY et al 2018. "The role of chitosan on oral delivery of peptide-loaded nanoparticle formulation." Journal of Drug Targeting 26 (7): 551-562.

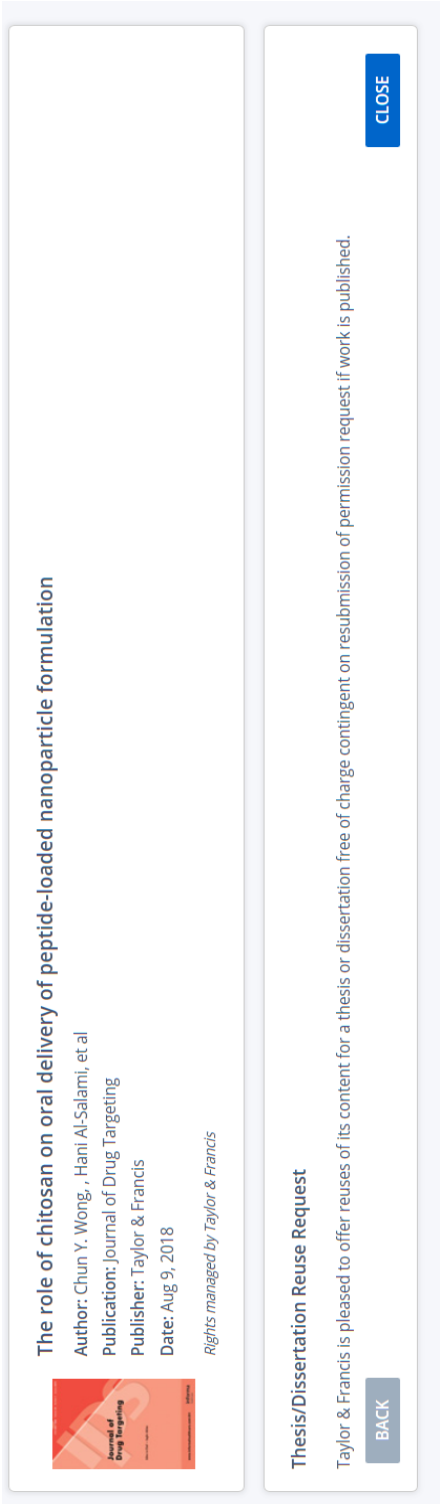

Appendix B9.1: Supplementary data for chapter 10 - C2C12 cell model: its role in understanding of insulin resistance at the molecular level and pharmaceutical development at the pre-clinical stage

Wong CY et al (2020). "C2C12 cell model: its role in understanding of insulin resistance at the molecular level and pharmaceutical development at the pre-clinical stage" Journal of Pharmacy and Pharmacology.

Supplementary table 1. C2C12 cellular culture conditions

Supplementary table 2. Cytotoxicity assay conditions

Supplementary table 3. Western blotting conditions

Supplementary table 4. Glucose uptake study conditions

Supplementary table 5. Real-time PCR

Supplementary table 6. Immunofluorescence assay

Table 1. C2C12 cellular culture conditions

C2C12 myoblasts							C2C12 myotubes (differentiation)				Others		
DMEM	**Glucose**	**FBS**	**Penicillin**	**Streptomycin**	**Amphotericin**	**Confluence**	**DMEM**	**Glucose**	**Horse serum**	**Antibiotics**	**Comments**	**Density**	**Year/ Ref**
✓	4.5 g/L	10%	1%; 100 U/mL	100 µg/mL	n/a	90-95%	✓	4.5 g/L	2%	Same	4 days fusion	n/a	2018: [1]
✓	n/a	10%	100 U/mL	100 µg/mL	250 ng/mL	n/a	✓	n/a	5%	Same	4 days fusion	0.5×10^5 cells/well	2018: [2]
✓	n/a	10%	50 U/mL	50 µg/mL	n/a	n/a	✓	n/a	2%	n/a	37 °C; 95% air and 5% CO_2	n/a	2018: [3]
✓	n/a	20%	1%	n/a	n/a	80-90%	n/a	n/a	n/a	n/a	n/a	150000 cells/ · cm^2	2018: [4]
✓	4.5 g/L	10%	100 U/mL	100 mg/mL	n/a	95%	✓	4.5 g/L	2%	Same	4 days fusion	n/a	2018: [5]
✓	n/a	10%	Unknown	n/a	Unknown	n/a	n/a	n/a	2%	n/a	4 days fusion; Subculture twice a week	5×10^3 cells/cm^2	2018: [6]
✓	4.5 g/L	10%	n/a (5 µg/mL blasticidin or 1 µg/mL puromycin)			n/a	n/a	4.5 g/L	5%	n/a	37 °C; air and 5% CO_2; EPS	n/a	2018: [7]
✓	High	10%	100 U/mL	100 µg/mL	n/a	95%	✓	High	2%	Same	37 °C; 5% CO_2	n/a	2018: [8]
✓	n/a	10%	1%			n/a	✓	n/a	2%		37 °C	n/a	2018: [9]
✓	n/a	10%	n/a	n/a	n/a	80-90%		n/a	n/a	n/a	37 °C; 5% CO_2	n/a	2018: [10]
✓	n/a	10%	100 U/mL	100 µg/mL	n/a	n/a		n/a	2%	n/a	37 °C; 5% CO_2	n/a	2018: [11]
✓	n/a	10%	n/a (5 µg/mL blasticidin)			n/a	✓	n/a	5%	n/a	37 °C; 5% CO_2	n/a	2018: [12]
✓	n/a	n/a	n/a	n/a	n/a	85-95%		n/a		n/a	37 °C; 5% CO_2	2×10^5 cells	2018: [13]
✓	n/a	10%	1%		n/a	70%	97%	n/a	2%	Same	37 °C; 5% CO_2; palmitate	2.2×10^6 cells	2018: [14]
✓	n/a	10%	100 U/mL	100 µg/mL	n/a	80%		n/a	n/a	n/a	37 °C; 5% CO_2; 4 mM glutamine	n/a	2017: [15]
✓	n/a	20%	1%		n/a	70%	✓	n/a	1%	Same	37 °C; 5% CO_2; 1 % L-glutamine	n/a	2017: [16]
✓	High	10%	1%		n/a	n/a		n/a	n/a	n/a	37 °C; 5% CO_2	n/a	2017: [17]
	n/a	n/a	n/a	n/a	n/a	n/a		n/a	n/a	n/a	37 °C; 5% CO_2	n/a	2016: [18]
✓	n/a	10%	1%		n/a	n/a	✓	n/a	2%	Same	37 °C; 95% air and 5% CO_2	n/a	2016: [19]
✓	n/a	10%	50 IU/mL	50 µg/mL	n/a (Gentamicin 20 µg/mL, Fungizone-Amphotericin B 1	70-80%	✓	n/a	2%	Same	37 °C; 95% air and 5% CO_2	n/a	2016: [20]

					µg/mL)								
✓	n/a	10%	10000 IU/mL	10 mg/mL	n/a	90%	✓	n/a	2%	n/a	4 days fusion; 37 °C; 5% CO_2	n/a	2016: [21]
✓	n/a	10%	Unknown	Unknown	n/a	n/a	✓	n/a	2%	n/a	4 days fusion; 37 °C; 5% CO_2	n/a	2016: [22]
✓	n/a	10%	100 U/mL	100 mg/mL	n/a	95%	✓	n/a	2%	n/a	4-6 days fusion; 37 °C; 5% CO_2	n/a	2016: [23]
✓	normal (5.5 mM)	10%	1%		n/a	80-90%		n/a	2%	Same	1% glutamine	n/a	2016: [24]
✓	n/a	n/a	100 U/mL	100 µg/mL	n/a	80-90%	✓	n/a	2%	n/a	6 days fusion; 5% CO_2; glutamine (2 mM)	n/a	2016: [25]
✓	n/a	10%	1% (5 U/mL penicillin; 50 µg/mL streptomycin)		n/a	80-90%	✓	n/a	2%	n/a	5 days fusion; 37 °C; 5% CO_2	n/a	2015: [26]
✓	n/a	10%	100 U/mL	100 mg/mL	n/a	n/a	n/a	n/a	n/a	n/a	37 °C; 5% CO_2	n/a	2015: [27]
	n/a	n/a	n/a	n/a	n/a	n/a	✓	11 mM glucose	2%	n/a		n/a	2014: [28]
✓	n/a	10%	Unknown	1%	n/a	80-90%	✓	Low (5.5mM)	5%	n/a	37 °C; 5% CO_2; 2 mM glutamine; palmitate	n/a	2014: [29]
✓	High	10%	1% (100 U/mL penicillin; 100 mg/mL streptomycin)		n/a	100%	✓	Low	2%	Same	4 days fusion; 37 °C; 5% CO_2	6 x 10^4 cells per well	2014: [30]
✓	n/a	10%	n/a	n/a	n/a	n/a		n/a	n/a	n/a	4 mM glutamine	n/a	2014: [31]
✓	n/a	10%	100 U/mL	100 mg/ml	n/a (Amphotericin B 2.5 mg/L)	n/a	✓	n/a	2%	Same	37 °C; 5% CO_2; 2-4 mM Glutamine; 110 mg/L sodium pyruvate, sodium bicarbonate (3.7 g/L)	n/a	2013: [32]
✓	At 40% confluence (15 mmol/L)	10%	n/a	n/a	n/a	40%	✓	n/a	2%	n/a	37 °C; 5% CO_2; high insulin (50 nmol/L) or IGF-I (30 nmol/L)	n/a	2013: [33]
✓	n/a	10%	n/a	n/a	n/a	n/a	✓	n/a	1%	n/a	6 days fusion	n/a	2013: [34]
✓	n/a	10%	n/a	n/a	n/a	90%	✓	High (15 mmol/L)	2%	n/a	37 °C; 5% CO_2; insulin (50 nmol/L)	n/a	2013: [35]

✓	High	10%	n/a (800 µg/ml gentamycin)		80%	✓	n/a	2%	Same	37 °C; 5% CO_2;	n/a	2012: [36]
✓	High	10%; 10% horse serum	Unknown		80%	✓	n/a	2%	Unknown	7 days fusion	n/a	2012: [37]
✓	n/a	10%	n/a	n/a	n/a	n/a	n/a	n/a	n/a	5% CO_2	n/a	2012: [38]
✓	4.5 mg/L	10%	100 IU/mL	100 µg/mL	70%	✓	n/a	2%	n/a	3-5 days fusion; 37 °C; 5% CO_2; 4.5 mM/L L-glutamine	2.0×10^5 cells/well	2012: [39]
✓	n/a	10%	50 U/mL	50 mg/mL	n/a	✓	n/a	2%	n/a	4 days fusion; palmitate	n/a	2011: [40]
✓	n/a	10%	n/a	n/a	n/a	✓	n/a	2%	n/a	0.1% gelatin-coated dishes	n/a	2011: [41]
✓	4.5 g/L	10%	n/a	n/a	n/a	✓	4.5 g/L	2%	n/a	4 days fusion; 4 mM glutamine	n/a	2011: [42]
✓	n/a	10% and 10% newborn calf serum	1%		n/a	✓	n/a	2%	Same	37 °C; 5% CO_2; 1% L-glutamine (2mM final)	n/a	2010: [43]
✓	n/a	10%	n/a	n/a	n/a	n/a	n/a	n/a	n/a	n/a	n/a	2008: [44]
✓	1 g/L	10%	30 µg/mL	100 µg/mL	n/a	✓	n/a	2% and 200 % amino acids	Same	37 °C; 5% CO_2; EPS	1×10^5 cells/well	2008: [45]
✓	4.5 g/L	10%	0.2%		n/a (5 µg/ml Fungizone)	✓	4.5 g/L	0.5% FBS	Same	9 days fusion; 2 mM glutamine	n/a	2005: [46]

Abbreviations:

Dulbecco's Modified Eagle Medium (DMEM), electric pulse stimulation (EPS); foetal bovine serum (FBS); reference (ref)

Table 2. Cytotoxicity assay conditions

Experiment	Cell type	Condition and medium	Treatment and incubation	Agent reaction time	Year/ Ref
CellTiter 96® aqueous one solution cell proliferation assay, MTS cell proliferation kit	C2C12 cells	96-well assay plate, hanks medium, 37°C in a humidified 5% CO_2 air	n/a	1 h	2018: [7]
Vybrant® MTT Cell proliferation assay kit	C2C12 cells	5×10^4 in a 96 well plate, 37°C	Sweet potato tuber and leaf extracts (10, 20, 50, 100, 200, 500, 1000 µg/mL) for 24 h	n/a	2018: [14]
Trypan blue assay	C2C12 myoblasts at 40 % confluence	60 × 15 mm culture dishes, DMEM medium	Ranolazine	n/a	2017: [16]
MTT assay	C2C12 cells	96-well plate, PBS wash, DMEM medium, 37°C in a humidified 5% CO_2 and 95% air in incubator	n/a	1 h	2016: [20]
Cell Counting Kit-8	C2C12 myotubes	37°C	Simvastatin (0-10 mM) with or without 100 mM mevalonolactone for 72 h	3 h	2016: [21]
MTT assay	C2C12 myotubes	96-well plate, DMEM medium in the presence or absence of 750 µM palmitic acid	Docosahexaenoic acid (50 µM), eicosapentaenoic acid (50 µM), arachidonic acid (50 µM)	3 h	2016: [25]
Alamar Blue® assay	C2C12 non-differentiated and differentiated cells	24-well plate ($6x10^4$ cells per well), low glucose DMEM, PBS wash	n/a	2 h	2014: [30]
Lactate dehydrogenase assay	C2C12 cells	96-well plate	Cinnamaldehyde (10, 20, 50, 100 µM) for 1 h	n/a	2013: [32]
MTT assay	C2C12 cells	96-well plate, 37°C	n/a	4 h	2013: [33]
Dichlorofluorescein assay	C2C12 differentiated myocytes	96-well plate, PBS wash, DMEM medium	Insulin-like growth factor 1	n/a	2011: [41]

Abbreviations:

Dulbecco's Modified Eagle Medium (DMEM), 3-(4,5-dimethylthiazol-2-yl)-2-5-diphenyltetrazolium bromide (MTT)

Table 3. Western blotting conditions

Cell lysis condition	Protein measurement	Western blot analyses	Antibodies	Year/ Ref
Centrifuge at 14,000g for 15 min	BioRad DC protein assay	nitrocellulose membranes	phospho-PERK, PERK, phospho-eIF2α, eIF2α, CHOP, spliced XBP1, phospho-p70S6K and p70S6K	2018: [1]
RIPA lysis buffer	Bicinchoninic acid protein assay	Sodium dodecyl sulfate-polyacrylamide gel, polyvinylidene difluoride membrane	horseradish peroxidase-conjugated secondary anti-rabbit antibody, anti-mouse antibody	2018: [3]
Lysis buffer (50 mM HEPES, 150 mM NaCl, 1.5 mM $MgCl_2$, 1 mM EGTA, 50 mM NaF, 50 mM β-Glycerophosphate, 1 mM Na_3VO_4, 1% Triton X 100, 2 mM PMSF)	Pierce 660 nm protein assay	Sodium dodecyl sulfate-polyacrylamide gel, nitrocellulose membranes	Akt, phosphor Akt (Ser473) and β-Actin, anti-rabbit horseradish peroxidase-conjugated secondary antibody	2018: [4]
Lysis buffer (50 mM HEPES, 137 mM NaCl, 1 mM $CaCl_2$, 10 mM sodium pyrophosphate, 10 mM NaF, 2 mM EDTA (pH 8.0), 10% glycerol, 10% NP-40, 2 mM Na3VO4, 10 mg/mL aprotinin, 5 mg/mL leupeptin, 10 mM benzamidine and 2 mM phenylmethylsulfonylfluoride)	DC protein assay	Sodium dodecyl sulfate-polyacrylamide gel, nitrocellulose membranes	phospho-CREB, phospho-Akt, CREB, Akt, GDF8/myostatin antibodies, β-actin antibodies	2018: [5]
Lysis buffer (50 mM Tris-HCl (pH 7.5), 150 mM NaCl, 2% Triton X-100, 2 mM EDTA, 50 mM NaF, 30mM $Na_4P_2O_7$, protease inhibitor cocktail)	Bicinchoninic acid protein assay	10% sodium dodecyl sulfate-polyacrylamide gel, polyvinylidene difluoride hybond-P membrane	n/a	2018: [6]
RIPA buffer (100 mM NaCl, 0.25% w/v sodium deoxycholate, 1.0% w/v NP40, 0.1% w/v SDS, 2 mM EDTA, 50 mM NaF, 10 nM okadaic acid, 1 mM sodium orthovanadate, protease inhibitor cocktail and 50 mM Tris-HCl pH 7.2)	Bicinchoninic acid protein assay	7.5% sodium dodecyl sulfate-polyacrylamide gel, polyvinylidene difluoride membrane	anti-rabbit horseradish peroxidase-conjugated secondary antibody	2018: [7]
RIPA buffer (50 mM Tris pH 8, 150 mM NaCl, 1% NP-40, 0.5% deoxycholic acid, 0.1% SDS supplemented with protease and phosphatase inhibitors (1 mM PMSF, 5 µg/mL leupeptin, 2 µg/mL aprotinin, 1 mM EDTA, 10 mM NaF, and 1 mM $NaVO_4$))	Bicinchoninic acid protein assay	n/a	anti-IRS-1, anti-phospho IRS-1, anti-SIRT1, anti-GLUT-4, primary antibody, horseradish peroxidase-conjugated secondary antibody	2018: [8]
CHAPS extraction solution (10 mol/L CHAPS, 2 mol/L EDTA, pH 8.0, and 4 mol/L iodoacetate in PBS) with protease and phosphatase inhibitors; centrifuged at 15,000 g for 10 min	n/a	sodium dodecyl sulfate-polyacrylamide gel, polyvinylidene difluoride membrane	primary antibodies, secondary horseradish peroxidase-linked donkey antimouse IgG	2018: [9]
Lysis buffer	n/a	12% sodium dodecyl sulfate-polyacrylamide gel, nitrocellulose membrane	primary antibody, horseradish peroxidase-conjugated secondary antibody	2018: [11]
Laemmli sample buffer supplemented with mercaptoethanol	n/a	Sodium dodecyl sulfate-polyacrylamide gel, polyvinylidene difluoride membranes	pan-Akt, phospho-Akt S473, phospho-Akt T308, phosphoPAK T423, anti-Rac1, pan-AMPKa, phospho-AMPKa T172, anti-GAPDH, a-actinin 1	2018: [12]
RIPA buffer	n/a	Sodium dodecyl sulfate-polyacrylamide gel, nitrocellulose membrane	primary antibodies, horseradish peroxidase-conjugated secondary antibody, anti-calnexin, GAPDH	2017: [16]
RIPA buffer (25 mM Tris, pH 7.4, 150 mM NaCl, 1 mM EDTA, and 1% Triton X-100 containing protease inhibitors)	Bicinchoninic acid protein assay	Sodium dodecyl sulfate-polyacrylamide gel, polyvinylidene difluoride membrane	primary antibody, horseradish peroxidase-conjugated secondary antibody	2017: [17]
Lysis buffer (20 mM Tris-HCl (pH 7.5), 150 mM NaCl, 1% Triton X, 2 mM EDTA, 10% glycerol, protease inhibitor cocktail)	n/a	Sodium dodecyl sulfate-polyacrylamide gel	Akt, phospho-Akt Ser473, phospho-IKK α/β, IKK α/β, JNK, phospsho-JNK, phospsho-p38, p38, phopsho-ERK, ERK, phospho-IRS-1 Ser636/639, IRS-1	2016: [19]
RIPA buffer (1x PBS, 10 mL/L Igepal CA-630, 5 g/L sodium deoxycholate, 1 g/L SDS) supplemented with 0.4 mM PMSF, 10 µg/mL of aprotinin and 10 µg/mL of sodium orthovanadate); centrifuge at 8000 g for 5 min	n/a	7.5, 10 or 12% acrylamide sodium dodecyl sulfate-polyacrylamide gel, polyvinylidene difluoride membrane	Antibodies against actin, myogenin, Mfn2, MyoD, AKT-1, P-S473-AKT-1, ERK1/2, P-T202/Y204-ERK1/2, GSK-3β, P-S9-GSK-3β, P-Y216-GSK-3β, cytochrome c oxidase subunit IV, horseradish peroxidase-conjugated secondary antibody	2016: [20]
n/a	Bicinchoninic acid protein	10% sodium dodecyl sulfate-polyacrylamide	rabbit anti-mouse GAPDH, mouse anti-mouse IR, rabbit	2016: [21]

	assay		gel, polyvinylidene difluoride membrane	anti-mouse IRS-1, rabbit anti-mouse AKT, rabbit anti-mouse phospho-IR on Tyr1361, rabbit antimouse phospho-IRS-1 on Tyr1222, rabbit anti-mouse phosphor-AKT on Ser473, Thr308, rabbit anti-mouse phospho-AKT on Ser473, horseradish peroxidase-conjugated secondary antibody	
n/a	Bicinchoninic acid protein assay		Sodium dodecyl sulfate-polyacrylamide gel	Antibodies against Akt, phospho-Akt Ser473, and GLUT-4	2016: [47]
RIPA buffer (50 mM NaCl, 10 mM Tris, 0.1 % sodium dodecyl sulfate, 1 % Triton X-100, 0.1 % sodium deoxycholate, 5 mM EDTA, and 1 mM Na_3VO_4 pH 7.4)	n/a		Sodium dodecyl sulfate-polyacrylamide gel, nitrocellulose membrane	Primary antibodies, horseradish peroxidase-conjugated secondary antibody	2016: [22]
Lysis buffer (20 mM Tris, pH 7.5, 5 mM EDTA, 10 mM Na_3PO_4, 100 mM NaF, 2 mM Na_3VO_4, 1% Nonidet P-40, and 1 mM PMSF, protease inhibitor cocktail); centrifuge at 12000 rpm for 20 min	n/a		Sodium dodecyl sulfate-polyacrylamide gel, polyvinylidene difluoride membrane	Primary antibody, secondary antibody	2016: [23]
n/a	n/a		Sodium dodecyl sulfate-polyacrylamide gel, polyvinylidene difluoride membrane	Primary antibodies, horseradish peroxidase-conjugated secondary antibody	2016: [24]
RIPA buffer	Plasma membrane extraction Kit	protein	Sodium dodecyl sulfate-polyacrylamide gel, polyvinylidene difluoride membrane	Primary antibodies, horseradish peroxidase-conjugated secondary antibody	2016: [25]
Lysis buffer (HEPES 50 mmol/L, NaCl 150 mmol/L, EDTA 10 mmol/L, NaPPi 10 mmol/L, β-glycerophosphate 25 mmol/L NaF 100 mmol/L, glycerol 10%, sodium orthovanadate 2 mmol/L, Triton X-100 1%; protease inhibitors)	n/a		Sodium dodecyl sulfate-polyacrylamide gel, nitrocellulose, membrane	Primary antibodies, horseradish peroxidase-conjugated secondary antibody	2015: [26]
RIPA buffer with protease and phosphatase inhibitor cocktail	Bicinchoninic acid protein assay		Sodium dodecyl sulfate-polyacrylamide gel, polyvinylidene difluoride membrane	Primary antibodies, secondary antibody	2013: [33]
n/a	n/a		Sodium dodecyl sulfate-polyacrylamide gel	Primary antibody, horseradish peroxidase-conjugated secondary antibody, oat polyclonal anti-actin antibody	2013: [35]
Lysis buffer (50 mM Tris, 150 mM NaCl, 10 mM EDTA, 1 % Triton X-100, 200 mM sodium fluoride, and 4 mM sodium orthovanadate, protease inhibitors, pH 7.5)	Bicinchoninic acid protein assay		10% sodium dodecyl sulfate-polyacrylamide gel, nitrocellulose membranes	Primary antibodies, horseradish peroxidase-conjugated secondary antibody	2012: [36]
RIPA buffer with protease inhibitor cocktails; centrifuged at 16,000 g for 10 min	Bicinchoninic acid protein assay		10% sodium dodecyl sulfate-polyacrylamide gel, nitrocellulose membranes	Primary antibodies, horseradish peroxidase-conjugated secondary antibody	2012: [39]
n/a	n/a		Sodium dodecyl sulfate-polyacrylamide gel	Anti-IkB, anti-p-IkB, anti-NF-kB, anti-tubulin	2011: [40]
Lysis buffer (50 mM Tris-HCl (pH 7.6), 150 mM NaCl, 1 mM dithiothreitol, 1% Nonidet P-40, protease inhibitor cocktail, phosphatase inhibitor cocktail)	Bio-Rad protein solution	assay	Sodium dodecyl sulfate-polyacrylamide gel, polyvinylidene difluoride membrane	Phospho-IGF-IR, IGF-IR, IR, phospho-Akt Ser473, Akt, phospho-specific anti-MAPK, ERK 1, phosphomTOR Ser2448, mTOR, phospho-p70S6K Thr389, p70S6K, phosphoFoxO1, FoxO1, Nox4, PTP-1B, horseradish peroxidase-conjugated secondary antibody	2011: [41]
Lysis buffer (50 mM Tris–HCl, 1 mM EDTA, 1 mM EGTA, 1% Triton X-100, protease inhibitor cocktail, 10 mM glycerophosphate, 50 mM NaF, 0.5 mM sodium orthovanadate pH 7.5); centrifuged at 13000 g for 10 min	Bicinchoninic acid protein assay		10% sodium dodecyl sulfate-polyacrylamide gel, nitrocellulose membranes	p-Akt Ser463, p-AMPK Thr172, β-actin, horseradish peroxidase-conjugated secondary antibody	2011: [42]
Lysis buffer (20 mM Tris-HCl (pH 7.6), 150 mM NaCl, 1 mM EDTA, 1% Nonidet P-40, 0.1% SDS, 5 mM NaF, 1 mM phenylmethylsulfonyl fluoride and aprotinin 10 µg/mL); centrifuged at 10000 g for 15 min	n/a		Sodium dodecyl sulfate-polyacrylamide gel	n/a	2008: [44]
n/a	Bicinchoninic acid protein assay		5 or 12% sodium dodecyl sulfate-polyacrylamide gel, polyvinylidene difluoride membrane	anti-LKB, anti-phospho-AMPK, anti-phospho-acetyl-CoA carboxylase, anti-phospho Erk5, anti-Erk5, anti-phospho Erk1/2, anti-Erk1/2, anti-phospho JNK, anti-JNK, anti-phospho p38, anti-p38, anti-phospho-activating transcription	2008: [45]

			factor 2, anti-ATF2, anti-phospho-Akt Ser473, anti-phospho-Akt Thr308, anti-Akt, anti-phospho-GSK-3, antiGSK3, anti-myocyte enhancer factor 2, anti-mouse IgG, anti-myosin heavy chain, anti-MHC, anti-sarcomeric-actinin, anti-myosin, anti-myogenin, anti-BD living colour antibody, antibodies against mouse Tbc1d1 and phospho-Tbc1d1 (Ser231), horseradish peroxidase-conjugated secondary antibody	
KRPH buffer	n/a	n/a	anti-mouse IgG antibody, anti-c-myc antibody, anti-BD living colour antibody	2008: [45]
n/a	n/a	Sodium dodecyl sulfate-polyacrylamide gel, nitrocellulose membranes	Primary antibodies, horseradish peroxidase-conjugated secondary antibody	2005: [46]
n/a	n/a	Sodium dodecyl sulfate-polyacrylamide gel	c-jun phospho-specific antibody	2005: [46]

Table 4. Glucose uptake study conditions

Glucose	Protein/ glucose measurement	Cell type/ density	Treatment	Treatment time	Year/ Ref
[^{3}H] 2-deoxy-D-glucose	Bicinchoninic acid assay	C2C12 myoblasts	100 mouse µg AGP/ml medium and 0 or 1 µM bovine insulin	24 h	2018: [2]
2-NBDG	n/a	C2C12 cells (5×10^4 cells/mL)	Atorvastatin (1 µM and 10 µM), pravastatin (1 µM and 10 µM), mevalonic acid (200 µM), MβCD (1 mg/mL), cholesterol (0.2 mg/mL)	24 h	2018: [3]
3H-Deoxy-D-Glucose (0.1 mM)	Liquid scintillation counting	C2C12 cells	100 nM insulin	30 min	2018: [4]
2-NBDG (50 µM)	Fluorescence intensity (Ex/Em = 485/535 nm).	C2C12 cells	100 nM insulin	30 min	2018: [6]
6-NBDG (20 µM)	Fluorescence intensity (Ex/Em = 466/540 nm).	C2C12 cells	serum free low-glucose medium	30 min	2018: [8]
Glucose (5 mM)	Cayman Chemical assay kit	C2C12 differentiating cells	100 nM insulin, myostatin	3 days	2018: [9]
2-NBDG	Flow cytometry at Ex/Em = 488/542 nm	C2C12 cells (80% confluence)	10 ng/ml recombinant mouse TNF- α, 100 nM insulin, *Ruellia tuberosa* L (0, 25, 50, 100, 200, 400, 800 µg/mL)	30 min	2018: [10]
2-Deoxyglucose	Fluorescence intensity (Ex/Em = 540/590 nm).	C2C12 myotubes	Electric pulse stimulation	1 h	2018: [13]
Glucose	Fluorescence intensity (Absorbance = 490 nm).	C2C12 cells	Simvastatin (20 mM), mevalonate (100 mM)		2016: [21]
2-NBDG (20 µM)	Fluorescence intensity (Ex/Em = 466/540 nm).	C2C12 myotubes	Balanced deep-sea water containing chitosan oligosaccharides, AICAR (1 mM), 100 nM insulin in serum-free low-glucose DMEM	1 h	2016: [22]
2-NBDG	Glucose Oxidase Method	C2C12 myotubes		6 h	2016: [23]
2-Deoxyglucose (100 mM)	Scintillation counter	C2C12 myotubes	100 nM insulin	1 h	2016: [25]
Glucose (5.5mM)	Glucose oxidase/peroxidase kit	C2C12 myotubes	*Eucalyptus tereticornis*	4 h	2014: [29]
Glucose	Glucose oxidase method	C2C12 myocytes (25000 cells/mL)	*Ficus lutea* acetone leaf extract (15, 31, 63, 125, 250 and 500 µg/ml), insulin (0.1 - 100 µM)	1 h	2014: [31]
2-deoxy-D-[1,2-^{3}H] glucose (100 µM)	Scintillation counter	C2C12 myotubes	AICAriboside (2 mM), insulin (100 nM)	120 min	2013: [34]
2-deoxy-D-[^{3}H] glucose	Scintillation counter	C2C12 cells	30 µmol/L LY294002, 100 nM insulin	30 min	2012: [36]
2-deoxyD-[1-^{3}H] glucose	Scintillation counter	C2C12 cells	Metformin (100 or 400 µM), phenformin (100 µM), 2,4-dinitrophenol (25, 50 or 100 µM), 100 nM insulin	15 h treatment followed by a 3 h repeat treatment	2012: [37]
^{3}H-2-deoxyglucose	n/a	C2C12 cells	10 nM insulin	60 min	2012: [38]
^{3}H-2-deoxyglucose	Bicinchoninic acid assay, scintillation counter	C2C12 myotubes (2×10^5 cells/well)	100 nM insulin	30 min	2012: [39]
2-NBDG (10 mM)	Flow cytometry	C2C12 cells	n/a	n/a	2011: [40]
[^{3}H] 2-deoxy-D-glucose	Scintillation counter	C2C12 myotubes	100 nM insulin, IL-8 (20 pg/ml), IL-8 (1 ng/ml), IL-6 (20 pg/ml), IL-6 (1 ng/ml), IL-15 (20 pg/ml), IL-15 (1 ng/ml), IL-8 (20 pg/ml) + IL-6 (20 pg/ml), IL-6 (20 pg/ml) + IL-15 (20 pg/ ml), IL-8 (20 pg/ml) + IL-15 (20 pg/ml), IL-8 (20 pg/ml) + IL-6 (20 pg/ml) + IL-15 (20 pg/ml), IL-8 (1 ng/ml) + IL-6 (1 ng/ml), IL-6 (1 ng/ml) + IL-15 (1 ng/ml), IL-8 (1 ng/ml) + IL-15 (1 ng/ml), and IL-8 (1 ng/ml) + IL-6 (1 ng/ml) + L-15 (1 ng/ml)	2 h	2011: [42]
2-deoxyglucose (10 µM)	Scintillation counter, bicinchoninic acid assay	C2C12 myotubes	30 or 100 nM insulin	30 min	2008: [48]
2-deoxyglucose	Scintillation counter	C2C12 cells	100 nM insulin	60 min	2005: [46]

Abbreviations:

2-[N-(7-Nitrobenz-2-oxa-1,3-diazol-4-yl) amino]−2-deoxy-D-glucose (2-NBDG), 6-[N-(7-nitrobenz-2-oxa-1,3-diazol-4-yl)amino]-2-deoxy-d-glucose (6-NBDG)

Table 5. Real-time PCR

RNA extraction	Reverse transcription	Sample/ primers	PCR System	Year/ Ref
TRIzol	Superscript III first-strand synthesis kit	ATF4, CHOP, XBP1s, MCP-1, TNF-α, IL-6, 18S rRNA	BioRad iCycler with iQ SYBR Green reagent	2018: [1]
TRIpure reagent	ReverTra Ace qPCR RT Master Mix	GLUT-4, hexokinase II, β-actin	LightCycler 96 real-time with SYBR green realtime PCR master mix	2018: [3]
TRI reagent	n/a	RNA polymerase II beta, myogeninn, peroxisome proliferator-activated coactivator, hexokinase II, GLUT-4	Stratagene Mx3005p thermocycler with Quantifast SYBR Green Mix	2018: [4]
TRIzol	Superscript III first-strand synthesis kit	GAPDH, myostatin	BioRad CFX96 with BioRadiQ SYBR Green supermix	2018: [5]
High-purity total RNA rapid extraction kit	TransStart® Top Green qPCR SuperMix	β-actin, MCP-1, E-selectin	LightCycler 96 system	2018: [7]
PureLink® RNA mini kit	SuperscriptTM VILOTM Mastermix	GLUT-4, nrf1, mef2a, cpt1, acc2, GAPDH	SteponeplusTM with PowerUpTM SYBRTM green master mix	2018: [14]
RNeasy mini kit	Reverse transcriptase kit	Glut-4, Bax, Bcl-2, GAPDH	SYBR green Master Mix in ABI StepOnePlus instrument	2017: [15]
Qiagen RNeasy mini extraction kit	Qiagen omniscript system	MAFbx, MuRF-1, mTOR, GAPDH	SYBR green	2016: [18]
Total RNA Maxi kit	Enhanced Avian HS RT-PCR-100 Kit	Mfn2, MtSSB, mtTFA, Cox-1, 18S rRNA	NanoDrop 1000 and SYBR green LightCycler1FastStart DNAMaster	2016: [20]
TRIzol	PrimeScript™ 1st Strand cDNA Synthesis Kit	Actin	FastStart SYBR Green Master in an Applied Biosystems StepOnePlus™ RealTime PCR System	2016: [22]
TriReagent™	M-MMLV reverse transcriptase	GLUT-4, IL-6, TNF-α, β-actin	StepOne System	2016: [25]
		GLUT-4, GAPDH	ABI step one plus instrument with Quantifast SYBR green kit	2013: [32]
TRIzol reagent	AMV reverse transcriptase kit	pGPU6NYGGF4-shRNA, pGPU6-NC-shRNA	Applied Biosystems 7300 Sequence Detection System	2012: [36]
RNeasy Mini RNA kit	Script cDNA synthesis kit	GAPDH	ABsolute SYBR Green ROX quantitative PCR mix on the Strategene Mx3005P	2012: [39]
RNeasy Mini Kit	Reverse-iTTM 1st Strand Synthesis Kit	GAPDH, Glut-4	ReddyMixTM PCR Master Mix on a Programmable Thermal Controller	2011: [40]
Trizol reagent	ReverTra Ace quantitative RT-PCR kit	Atrogin-1, MURF1, MyoD, MRF4, GAPDH, Nox1, Nox2, Nox4, IGF-I, MGF	SBYRmixExTaqTMII using an ABIPRISM 7500 Real-Time PCR System	2011: [41]
n/a	n/a	CXCL1/KC, CXCL5/LIX, IL-6, GLUT-1, GLUT-4	Light Cycler instrument and SYBR Green detection kit	2008: [45]

Table 6. Immunofluorescence assay

System	Fluorescence analysis	Materials	Staining	Year/ Ref
Confocal laser-scanning microscope (IX81, Olympus)	GLUT-4	4% formaldehyde, 10% normal goat serum, GLUT-4 mouse antibody, laminin rabbit antibody, 647 goat anti-mouse IgG (H+L), 488 goat antirabbit IgG (H+L)	DAPI (0.5 µg/mL)	2018: [3]
Fluorescence microscope (Olympus BX-60)	Myosin	1% formaldehyde, Triton X-100 solution (0.5% in PBS), primary mouse monoclonal anti-myosin IgG, Alexa Fluor1 488-conjugated AffiniPure	DAPI	2016: [20]
LSM510 META confocal microscope (Zeiss)	β actin	4% paraformaldehyde, anti-β actin antibody, Alexa Fluor 488 conjugated goat anti-mouse secondary antibody, RNase A	PI	2016: [23]
Confocal laser scanning microscope (FV-500 system, Olympus)	Cyclin A, cyclin B1, cyclin D1, p21, pRb, MyoD	3.7 % paraformaldehyde, 0.05 %Triton X-100, primary antibody anti-cyclin A, anti-cyclin B1, anti-cyclin D1, anti-p21, anti-pRb, anti-MyoD, Alexa Fluor 488 secondary antibodies	n/a	2013: [33]
Confocal microscope (Olympus)	Myc-positive fluorescence intensity (GLUT-4)	4% paraformaldehyde, anti-Myc antibodies, 1.5% saponin	n/a	2012: [38]
Microscope (Nikon Ti-E Eclipse, Nikon)	n/a	1% paraformaldehyde, 0.01% Tween-20, Alexa Fluor 568	300 nM DAPI	2012: [39]
n/a	GLUT-4-myc7-GFP	3% paraformaldehyde, 100 mM glycine, mAb, Myc, Texas Red-conjugated sheep antibodies, mouse IgG	n/a	2008: [44]

Reference list

1. Perry BD et al. Palmitate-induced ER stress and inhibition of protein synthesis in cultured myotubes does not require Toll-like receptor 4. *PLoS One* 2018; 13: e0191313.
2. Ramsay TG et al. alpha-1 acid glycoprotein inhibits insulin responses by glucose oxidation, protein synthesis and protein breakdown in mouse C2C12 myotubes. *Animal* 2019; 13: 771-776.
3. Sun B et al. Atorvastatin impaired glucose metabolism in C2C12 cells partly via inhibiting cholesterol-dependent glucose transporter 4 translocation. *Biochem Pharmacol* 2018; 150: 108-119.
4. Turner MC et al. The effect of chronic high insulin exposure upon metabolic and myogenic markers in C2C12 skeletal muscle cells and myotubes. *J Cell Biochem* 2018; 119: 5686-5695.
5. Xie Y et al. Glucocorticoid-induced CREB activation and myostatin expression in C2C12 myotubes involves phosphodiesterase-3/4 signaling. *Biochem Biophys Res Commun* 2018; 503: 1409-1414.
6. Yamasaki M et al. Vaccinium ashei leaves extract alleviates insulin resistance via AMPK independent pathway in C2C12 myotube model. *Biochem Biophys Rep* 2018; 14: 182-187.
7. Zhao Y et al. Conditioned medium from contracting skeletal muscle cells reverses insulin resistance and dysfunction of endothelial cells. *Metabolism* 2018; 82: 36-46.
8. Manna P et al. 1,25(OH)2-vitamin D3 upregulates glucose uptake mediated by SIRT1/IRS1/GLUT4 signaling cascade in C2C12 myotubes. *Mol Cell Biochem* 2018; 444: 103-108.
9. Liu XH et al. Myostatin inhibits glucose uptake via suppression of insulin-dependent and -independent signaling pathways in myoblasts. *Physiol Rep* 2018; 6: e13837.
10. Ko CY et al. Ameliorative effect of Ruellia tuberosa L. on hyperglycemia in type 2 diabetes mellitus and glucose uptake in mouse C2C12 myoblasts. *Food Sci Nutr* 2018; 6: 2414-2422.
11. Jung TW et al. WISP1 promotes non-alcoholic fatty liver disease and skeletal muscle insulin resistance via TLR4/JNK signaling. *J Cell Physiol* 2018; 233: 6077-6087.
12. Hu F et al. Electrical pulse stimulation induces GLUT4 translocation in a Rac-Akt-dependent manner in C2C12 myotubes. *FEBS Lett* 2018; 592: 644-654.
13. Barlow J, Solomon TPJ. Conditioned media from contracting skeletal muscle potentiates insulin secretion and enhances mitochondrial energy metabolism of pancreatic beta-cells. *Metabolism* 2019; 91: 1-9.
14. Ayeleso TB et al. Aqueous-methanol extracts of orange-fleshed sweet potato (Ipomoeabatatas) ameliorate oxidative stress and modulate type 2 diabetes associated genes in insulin resistant C2C12 cells. *Molecules* 2018; 23: 2058.
15. Ahangarpour A et al. Solid lipid nanoparticles of myricitrin have antioxidant and antidiabetic effects on streptozotocin-nicotinamide-induced diabetic model and myotube cell of male mouse. *Oxid Med Cell Longev* 2018; 2018: 7496936.
16. Terruzzi I et al. Ranolazine promotes muscle differentiation and reduces oxidative stress in C2C12 skeletal muscle cells. *Endocrine* 2017; 58: 33-45.
17. Li H et al. Rab8A regulates insulin-stimulated GLUT4 translocation in C2C12 myoblasts. *FEBS Lett* 2017; 591: 491-499.
18. Bonifacio A et al. IGF-1 prevents simvastatin-induced myotoxicity in C2C12 myotubes. *Arch Toxicol* 2017; 91: 2223-2234.
19. Matsugi K et al. Thrombospondin 1 suppresses insulin signaling in C2C12 myotubes. *Kobe J Med Sci* 2016; 62: 13-18.
20. Litwiniuk A et al. FOXO1 and GSK-3beta are main targets of insulin-Mediated myogenesis in C2C12 muscle cells. *PLoS One* 2016; 11: e0146726.

21. Li W et al. Simvastatin inhibits glucose uptake activity and GLUT4 translocation through suppression of the IR/IRS-1/Akt signaling in C2C12 myotubes. *Biomed Pharmacother* 2016; 83: 194-200.
22. Ha BG et al. Stimulatory effect of balanced deep-sea water containing chitosan oligosaccharides on glucose uptake in C2C12 myotubes. *Mar Biotechnol* 2016; 18: 475-484.
23. Ding H et al. Chronic reactive oxygen species exposure inhibits glucose uptake and causes insulin resistance in C2C12 myotubes. *Biochem Biophys Res Commun* 2016; 478: 798-803.
24. Coughlan KA et al. PKD1 inhibits AMPKalpha2 through phosphorylation of serine 491 and impairs insulin signaling in skeletal muscle cells. *J Biol Chem* 2016; 291: 5664-5675.
25. Chen SC et al. Long-chain polyunsaturated fatty acids amend palmitate-induced inflammation and insulin resistance in mouse C2C12 myotubes. *Food Funct* 2016; 7: 270-278.
26. Capel F et al. Oleate dose-dependently regulates palmitate metabolism and insulin signaling in C2C12 myotubes. *Biochim Biophys Acta* 2016; 1861: 2000-2010.
27. Yu J et al. Phosphorylation and function of DGAT1 in skeletal muscle cells. *Biophys Rep* 2015; 1: 41-50.
28. Paula FM et al. Exercise increases pancreatic beta-cell viability in a model of type 1 diabetes through IL-6 signaling. *FASEB J* 2015; 29: 1805-1816.
29. Guillen A et al. Antihyperglycemic Activity of Eucalyptus tereticornis in Insulin-Resistant Cells and a Nutritional Model of Diabetic Mice. *Adv Pharmacol Sci* 2015; 2015: 418673.
30. Yeh YC et al. nsulin-based regulation of glucose-functionalized nanoparticle uptake in muscle cells. *J Mater Chem B* 2014.
31. Olaokun OO et al. The potential role of GLUT4 transporters and insulin receptors in the hypoglycaemic activity of Ficus lutea acetone leaf extract. *BMC Complement Altern Med* 2014; 14: 269.
32. Nikzamir A et al. Expression of glucose transporter 4 (GLUT4) is increased by cinnamaldehyde in C2C12 mouse muscle cells. *Iran Red Crescent Med J* 2014; 16: 13426.
33. Grabiec K et al. The influence of high glucose and high insulin on mechanisms controlling cell cycle progression and arrest in mouse C2C12 myoblasts: The comparison with IGF-I effect. *J Endocrinol Invest* 2014; 37: 233-245.
34. Liu Y et al. Phosphatidylinositol 3-phosphate 5-kinase (PIKfyve) is an AMPK target participating in contraction-stimulated glucose uptake in skeletal muscle. *Biochem J* 2013; 455: 195-206.
35. Grzelkowska-Kowalczyk K et al. High glucose-mediated alterations of mechanisms important in myogenesis of mouse C2C12 myoblasts. *Cell Biol Int* 2013; 37: 29-35.
36. Zeng XQ et al. Knockdown of NYGGF4 increases glucose transport in C2C12 mice skeletal myocytes by activation IRS-1/PI3K/AKT insulin pathway. *J Bioenerg Biomembr* 2012; 44: 351-355.
37. Martineau LC. Large enhancement of skeletal muscle cell glucose uptake and suppression of hepatocyte glucose-6-phosphatase activity by weak uncouplers of oxidative phosphorylation. *Biochim Biophys Acta* 2012; 1820: 133-150.
38. Ijuin T, Takenawa T. Regulation of insulin signaling and glucose transporter 4 (GLUT4) exocytosis by phosphatidylinositol 3,4,5-trisphosphate (PIP3) phosphatase, skeletal muscle, and kidney enriched inositol polyphosphate phosphatase (SKIP). *J Biol Chem* 2012; 287: 6991-6999.
39. Hurst SE et al. Transient Silencing of a Type IV P-Type ATPase, Atp10c, Results in Decreased Glucose Uptake in C2C12 Myotubes. *J Nutr Metab* 2012; 2012: 152902.
40. Mor A et al. Ras inhibition induces insulin sensitivity and glucose uptake. *PLoS One* 2011; 6: e21712.
41. Handayaningsih AE et al. Reactive oxygen species play an essential role in IGF-I signaling and IGF-I-induced myocyte hypertrophy in C2C12 myocytes. *Endocrinology* 2011; 152: 912-921.

42. Gray SR, Kamolrat T. The effect of exercise induced cytokines on insulin stimulated glucose transport in C2C12 cells. *Cytokine* 2011; 55: 221-228.
43. Sharples AP et al. C2 and C2C12 murine skeletal myoblast models of atrophic and hypertrophic potential: Relevance to disease and ageing? *J Cell Physiol* 2010; 225: 240-250.
44. Takazawa K et al. Insulin-induced GLUT4 movements in C2C12 myoblasts: Evidence against a role of conventional kinesin motor proteins. *Kobe J Med Sci* 2008; 54: 14-22.
45. Nedachi T et al. Contractile C2C12 myotube model for studying exercise-inducible responses in skeletal muscle. *Am J Physiol Endocrinol Metab* 2008; 295: 1191-1204.
46. Mussig K et al. Insulin-induced stimulation of JNK and the PI 3-kinase/mTOR pathway leads to phosphorylation of serine 318 of IRS-1 in C2C12 myotubes. *Biochem Biophys Res Commun* 2005; 335: 819-825.
47. Kuo YH et al. Antcin K, a triterpenoid vompound from antrodia camphorata, displays antidiabetic and antihyperlipidemic effects via glucose transporter 4 and AMP-activated protein kinase phosphorylation in muscles. *Evid Based Complement Alternat Med* 2016; 2016: 4867092.
48. Kobayashi T et al. Irbesartan enhances GLUT4 translocation and glucose transport in skeletal muscle cells. *Eur J Pharmacol* 2010; 649: 23-28.

Appendix B9.2: Publisher agreement and permission for chapter 10

Wong CY et al 2020. "**C2C12 cell model: its role in understanding of insulin resistance at the molecular level and pharmaceutical development at the pre-clinical stage.**" Journal of Pharmacy and Pharmacology.

License Number	4893461297496
License date	Aug 21, 2020

Printable Details

Licensed Content

Licensed Content Publisher	John Wiley and Sons
Licensed Content Publication	JOURNAL OF PHARMACY AND PHARMACOLOGY
Licensed Content Title	C2C12 cell model: its role in understanding of insulin resistance at the molecular level and pharmaceutical development at the preclinical stage
Licensed Content Author	Chun Y. Wong, Hani Al-Salami, Crispin R. Dass
Licensed Content Date	Aug 18, 2020
Licensed Content Volume	0
Licensed Content Issue	0
Licensed Content Pages	27

Order Details

Type of use	Dissertation/Thesis
Requestor type	Author of this Wiley article
Format	Print and electronic
Portion	Full article
Will you be translating?	No

About Your Work

Title	Evaluation of Chitosan-Based Nanoparticles in Oral Delivery of Insulin
Institution name	Curtin University
Expected presentation date	Sep 2020

Additional Data

Requestor Location

Requestor Location	Curtin University School of Pharmacy 56A Manning Road Perth, WA 6107 Australia Attn: Curtin University School of Pharmacy

Tax Details

Publisher Tax ID	EU826007151

Appendix B10: Publisher agreement and permission for chapter 11

Wong CY et al 2020. "Development of orally administered insulin-loaded polymeric-oligonucleotide nanoparticles: statistical optimization and physicochemical characterization." Drug Development and Industrial Pharmacy, 46 (8): 1238-1252.

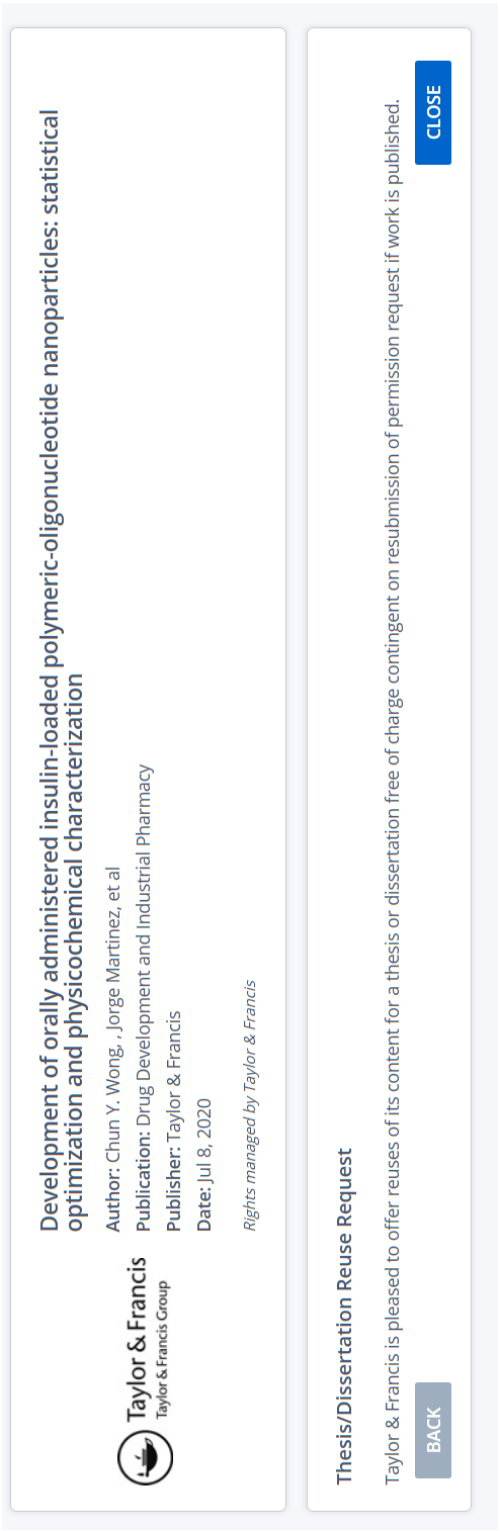

Appendix B11: Publisher agreement and permission for chapter 12

Wong CY et al 2020. "Formulation and characterisation of insulin-loaded chitosan nanoparticles capable of inducing glucose uptake in skeletal muscle cells *in vitro*." Journal of Drug Delivery Science and Technology, 57: 101738.

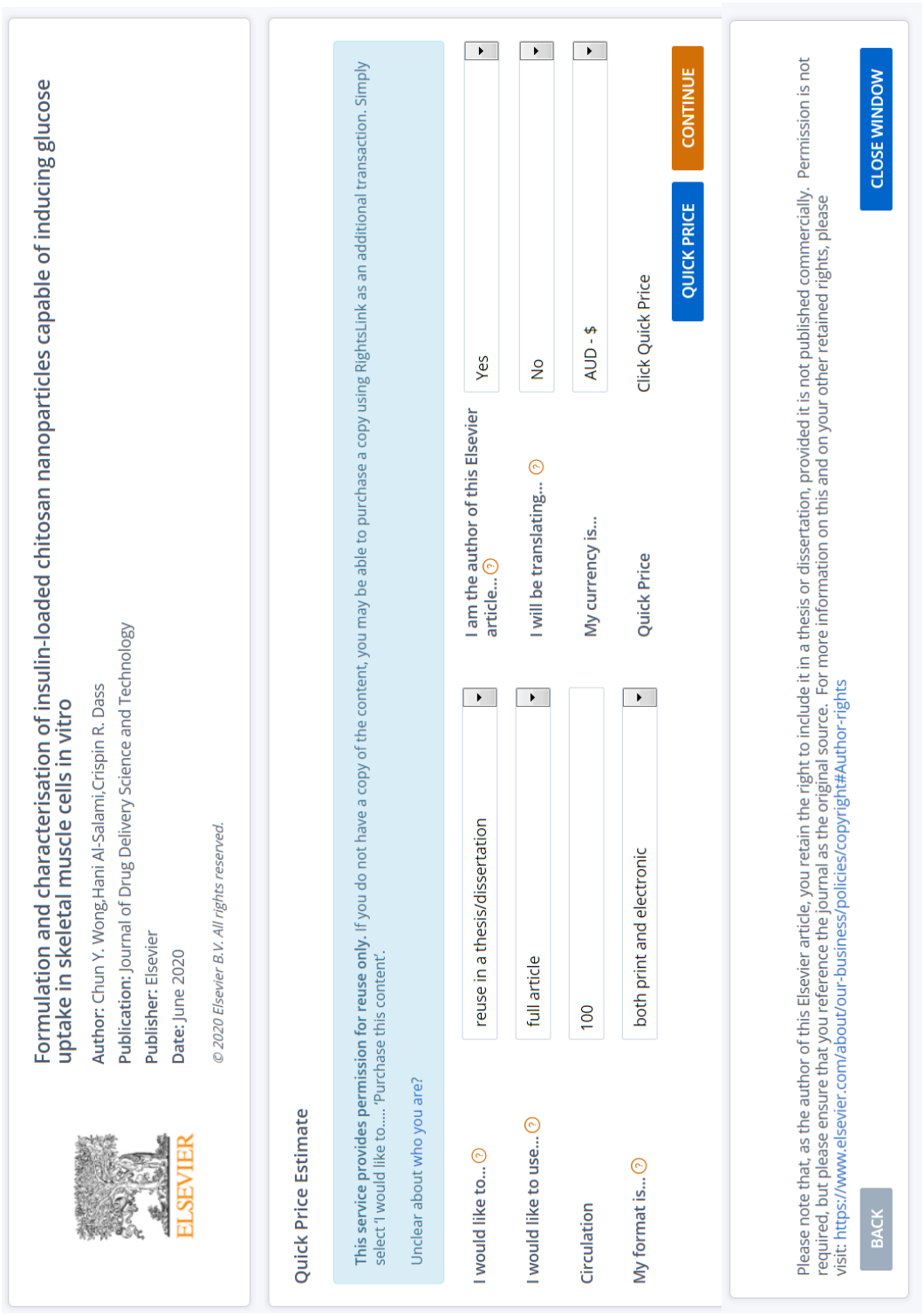

Appendix B12: Publisher agreement and permission for chapter 13

Wong CY et al 2020. "Lyophilisation improves bioactivity and stability of insulin-loaded polymeric-oligonucleotide nanoparticles for diabetes treatment." AAPS PharmSciTech 21 (3): 1-20.

Printable Details

Your confirmation email will contain your order number for future reference.

License Number 4820611335513

License date May 02, 2020

Licensed Content

Licensed Content Publisher	Springer Nature
Licensed Content Publication	AAPS PharmSciTech
Licensed Content Title	Lyophilisation Improves Bioactivity and Stability of Insulin-Loaded Polymeric-Oligonucleotide Nanoparticles for Diabetes Treatment
Licensed Content Author	Chun Y. Wong et al
Licensed Content Date	Mar 25, 2020

Order Details

Type of Use	Thesis/Dissertation
Requestor type	academic/university or research institute
Format	print and electronic
Portion	full article/chapter
Will you be translating?	no
Circulation/distribution	200 - 499
Author of this Springer Nature content	yes

Additional Data

About Your Work

Title	Evaluation of Chitosan-Based Nanoparticles in Oral Delivery of Insulin
Institution name	Curtin University
Expected presentation date	Sep 2020

Tax Details

Requestor Location

Curtin University School of Pharmacy
56A Manning Road

Perth, WA 6107
Australia
Attn: Curtin University School of Pharmacy

Price

Total 0.00 AUD